



Department of AERONAUTICS and ASTRONAUTICS
STANFORD UNIVERSITY

W. H. BOYKIN, JR.

I. FLÜGGE-LOTZ

ON THE HIGH-ACCURACY ATTITUDE CONTROL OF SATELLITES IN ELLIPTIC ORBITS

FACILITY FORM 602

(ACCESSION NUMBER)	N79-37316	(THRU)
(PAGES)	22	(CODE)
(NASA CR OR TMX OR AD NUMBER)	CR-112359	(CATEGORY)
		31



JULY
1967

Prepared for the National Aeronautics and Space Administration
Under Grant NsG 133-61

SUDAAR
NO 322

Department of Aeronautics and Astronautics
Stanford University
Stanford, California

ON THE HIGH-ACCURACY ATTITUDE CONTROL OF SATELLITES IN
ELLIPTIC ORBITS

by

W H Boykin, Jr

and

I Flugge-Lotz

SUDAAR NO 322

July 1967

This work was performed in association with research sponsored by
the National Aeronautics and Space Administration
under Research Grant NSG-133-61

ABSTRACT

The goal of the investigation was the development of a class of control systems which efficiently results in high-accuracy ($\leq 10^{-4}$ radian) earth-pointing attitude motions of satellites of different configurations in elliptic orbits. The earth-pointing orientation, i.e., the orientation such that one body-fixed axis is parallel to the local vertical and another is normal to the orbit plane, is required for the lifetimes of the satellites. Gas jets provide the control torque.

Linear differential equations with time-varying coefficients, which include terms for the gravity torque due to an oblate earth and terms for the aerodynamic torque, are used to describe the attitude motion when a satellite is practically earth-pointing. Nonlinear equations with time-varying coefficients are used to describe the attitude motion when acquisition of the earth-pointing motion from large deviation angles ($\approx 80^\circ$) is considered.

Pontryagin's Maximum Principle, the necessary conditions for exact solutions of optimal bounded-phase-coordinate problems and guidelines obtained from the minimum-fuel station-keeping controls devised for single-axis systems are used in the development of the station-keeping part of the control system. The acquisition part of the control system, developed here, results in acquisition of the earth-pointing motion from large angles in the time of one-quarter orbit with comparatively little fuel expenditures.

The motions of the satellites with the developed station-keeping control systems are simulated on an analog computer, and, the performances of the systems are evaluated. The nonlinear differential equations which include the developed acquisition control systems with time delays are integrated by using a digital computer. The fuel expenditures and the times of acquisition obtained from these digital computer runs are compared with those for the satellite motions described approximately by linear differential equations with the optimal controls obtained from the maximum principle.

The simulation studies together with the performance evaluations showed that the control systems are quite efficient as well as reliable (The acquisition system is a back-up system to the station-keeping system) The overall control system, which is very simple to realize, is given in diagram form

TABLE OF CONTENTS

	Page
LIST OF ILLUSTRATIONS	vii
LIST OF TABLES	xii
LIST OF SYMBOLS	xiii
CHAPTER	Page
I INTRODUCTION	1
A STATEMENT OF THE PROBLEM	1
B SATELLITE CONFIGURATIONS	1
C CONTROLLERS AND PERFORMANCE CRITERIA	2
D PREVIOUS CONTRIBUTIONS	3
E. CONTRIBUTIONS	3
II THE EQUATIONS OF CONTROLLED SATELLITE ATTITUDE MOTION	5
A THE INERTIA TORQUE	5
B THE (ACTIVE) TORQUE	8
C THE FULL NONLINEAR DIFFERENTIAL EQUATIONS OF CONTROLLED MOTION	8
D PARAMETERS OF THE SATELLITES AND THE SIMPLIFICATION OF THE MOTION EQUATIONS	11
1 The Simplified Acquisition Equations of Motion	13
2 The Simplified Steady-State Equation of Motion	16
E THE ERROR IN THE MOTION DUE TO THE SIMPLIFICATIONS	18
F DISTURBANCES	20
III THEORY OF THE CONTROL OF THE SATELLITES' ATTITUDES	24
A THE MOTION REQUIREMENTS IN TERMS OF THE STATE OF THE PLANT	24
B SATISFACTORY PERFORMANCE AND THE COST	24
C THE OBJECTIVE	27
D MATHEMATICAL TOOLS USED FOR DETERMINING A CONTROL LAW	27
1 Pontryagin's Maximum Principle for Nonautonomous Systems	28
2 Application to the Acquisition Problem	31
3 Application to Approximate Station-Keeping Problems	31
4 Necessary Conditions for an Exact Solution (NCES) of the Station-Keeping Problem	36
IV DERIVATION OF STATION-KEEPING CONTROLS LAWS	39
A THE APPROXIMATE SOLUTIONS - SPECIAL ORBITS	40
1 A Station-Keeping Control Law Obtained From PMP with $J = \int_{\tau_0}^{\tau_f} [f_1(\underline{x}) + \sum_{l=1}^3 \underline{v}_l] d\tau$	41
2 The Steady-State Motion Obtained from PMP for $\underline{x}'' = \underline{v}$	53

CHAPTER		Page
	3 The Steady-State Motion Obtained from PMP for $x'' + a^2x = v, a^2 > 0$	71
	4 The Steady-State Motion Obtained from PMP for $x'' + a^2x = v, a^2 < 0$	78
B	THE STATION-KEEPING CONTROLS — GENERAL ORBITS	83
	1 Station-Keeping Control of Satellites in a Maximum Gravitational Torque Orbit	83
	2 Improvement of the Control Law of Part 1, Section A	89
	3 The Controls — Approximate Motions	89
	4 The Controls — Station-Keeping Motions of the Satellites	91
V	DERIVATION OF ACQUISITION CONTROL LAWS	104
A	EXTENSIONS OF BUSCH'S SOLUTION	104
	1 Via Phase Plane Techniques	104
	2 Via Pontryagin's Maximum Principle	108
B	ACQUISITION CONTROL LAWS WHICH PERFORM SATISFACTORILY	110
VI	COMPLETE ATTITUDE CONTROL AND PERFORMANCE EVALUATION	134
A	ACQUISITION CONTROL COMPARED TO OPTIMAL (LINEAR) ACQUISITION CONTROL	134
B	STATION-KEEPING CONTROL	137
	1 Comparison with Busch's Solution	137
	2. Fuel Expenditure Per Orbit for Values of Various Parameters	139
C	IMPERFECTIONS IN THE MODEL AND THE ULTIMATE ABILITY TO EARTH-POINT	145
	1 Nonrigidity of the Satellites	145
	2 Gas Jet Misalignment	145
	3 Sensors and Error	146
	4 Others	146
VII	CONCLUSION	148
	REFERENCES	149
APPENDIX		Page
A	THE GRAVITATIONAL TORQUE	153
B	THE AERODYNAMIC TORQUE	159
C	THE PARAMETERS OF THE ORBIT AS FUNCTIONS OF TIME	164
D	THE STATE-SPACE REGION OF STATION-KEEPING	170
E	AN APPROXIMATE SOLUTION OF THE ADJOINT EQUATIONS	172
F	DIGITAL AND ANALOG COMPUTER PROGRAMS	176

LIST OF ILLUSTRATIONS

Figure		Page
2.1	Principal Axes of Inertia, L_1 , $i = 1,2,3$, the Unit Vectors \underline{n}_1 , $i = 1,2,3$, the Satellite B and the Earth E	6
3 1	A Simplified Diagram of the Controlled Attitude System.	25
3.2	The Functions f_1, f_2, f_e and f_s for $s_1 = 10^{-4}$.	34
4 1	Solution of Equations (4.3)-(4.6) for Satellite (2) .	45
a	Yaw Trajectory for $N_1 = 2.1 \times 10^{-4}$	45
b	Yaw Adjoint Variables for $n_1 = 1.0, n_2 = 2.0$.	45
c	Roll Trajectory for $N_2 = 7.1 \times 10^{-4}$	46
d.	Roll Adjoint Variables for $n_3 = 1.0, n_4 = 2.0$.	46
e	Pitch Trajectory for $N_3 = 2.06 \times 10^{-2}$	47
f.	Pitch Adjoint Variables for $n_1 = 2.0, n_2 = 4.0$	48
4 2	Solution of Equations (4.3)-(4.6) for Satellite (2) .	54
a	Yaw Trajectory for $N_1 = 2.1 \times 10^{-4}$	54
b.	Yaw Adjoint Variables for $n_1 = 2.1, n_2 = 1.0$	54
c.	Roll Trajectory for $N_2 = 7.1 \times 10^{-4}$	55
d.	Roll Adjoint Variables for $n_3 = 2.1, n_4 = 1.6$	55
e	Pitch Trajectory for $N_3 = 2.06 \times 10^{-2}$	56
f	Pitch Adjoint Variables for $n_1 = 2.1, n_2 = 3.3$.	57
4 3	Typical Minimum Fuel Trajectories for System (4.13), $N_2 = 5 \times 10^{-4}$	59
4 4	Nearly Minimum Fuel Boundary Encounter Trajectories for $x'' = v, N_2 = 5.0 \times 10^{-4}$	63
4.5	Adjoint Variable in Backwards Time Note: $p_4(\tau_a^*) > 1.0$	63
4 6	A Free End Point Solution for J with $f_2(\underline{x})$	68
a	Phase Plane Trajectory	68
b	Adjoint Variable	68

Figure		Page
4 7	Typical Minimum Fuel Solutions for Systems (4.34), $a^2 = 1$, $N = 2 \times 10^{-4}$	73
	a Minimum Fuel Trajectories	73
	b Adjoint Variables	73
4.8	A Minimum Fuel Boundary Encounter Solution for System (4.34)	74
	a Phase Plane Trajectories, $N = 2 \times 10^{-4}$, $a^2 = 1$	74
	b Adjoint Plane Trajectory	74
4 9	A Worst-Case Adjoint Solution Corresponding to Trajectory of Figure (4 8a), $n_1 = 1.03$, $n_2 = -1$	77
4 10	Adjoint Solutions	77
4 11	Some Phase Plots of Solutions of Maximum Principle Equations for $x'' + a^2 x = v$, $a^2 = -1$	79
	a Phase Plane Trajectories of (4 34), $N = 2 \times 10^{-4}$	79
	b. Phase Plane Plots of Adjoint Variables	79
4 12	Regions of Increase in Cost with Increase in N	80
4.13	Low Cost Control Laws and Trajectories, $N = 0.05$, Time Delay = 0.1 sec	82
	a A Low Cost Control Law and Trajectory for a Realistic Case	82
	b A Low Cost Control Law which Results in Limit Cycle Motion	82
4 14	A Single-Axis Station-Keeping Control Law	88
4.15	The Control of Figure 4 14 Applied to $x'' + a^2 = v$, $a^2 = 1.0$, $N = 0.1$, $d = 0$	90
4.16	The Control of Figure 4 14 Applied to $x'' + a^2 x = v$, $a^2 = -0.95$, $N = 0.05$, $d = 10^{-5}$	92
4 17	Station-Keeping Motion of Satellite (1)	93
	a. Yaw Trajectory, $N_1 = 0.01$, $t_d^- = 0.5$ sec, $t_d^+ = 1.25$ sec, $d = 4 \times 10^{-5}$	93

Figure		Page
4.17	b. Roll Trajectory, $N_2 = 0.01$, $t_d^- = 0.5$ sec., $t_d^+ = 1.0$ sec., $d = 4.0 \times 10^{-5}$	93
	c. Pitch Trajectory, $N_3 = 0.2$, $t_d^- = 0.05$ sec., $t_d^+ = 0.01$ sec., $d = 2.5 \times 10^{-5}$	94
4.18	Station-Keeping Motion of Satellite (2)	95
	a. Yaw Trajectory, $N_1 = 0.02$, $t_d^- = 0.5$ sec., $t_d^+ = 1.25$ sec., $d = 4 \times 10^{-5}$	95
	b. Roll Trajectory, $N_2 = 0.02$, $t_d^- = 0.5$ sec., $t_d^+ = 1.0$ sec., $d = 4 \times 10^{-5}$	95
	c. Pitch Trajectory, $N_3 = 0.03$, $t_d^- = 0.2$ sec., $t_d^+ = 0.04$ sec., $d = 2.5 \times 10^{-5}$	96
4.19	Station-Keeping Motion of Satellite (3)	97
	a. Yaw Trajectory, $N_1 = 0.001$, $t_d^- = 0.5$ sec., $t_d^+ = 1.25$ sec., $d = 2 \times 10^{-5}$	97
	b. Roll Trajectory, $N_2 = 0.001$, $t_d^- = 0.5$ sec., $t_d^+ = 1.25$ sec., $d = 2 \times 10^{-5}$	97
	c. Pitch Trajectory, $N_3 = 0.03$, $t_d^- = 0.2$ sec., $t_d^+ = 0.04$ sec., $d = 2.5 \times 10^{-5}$	98
4.20	Station-Keeping Motion of Satellite (4)	99
	a. Yaw Trajectory, $N_1 = 0.01$, $t_d^- = 0.5$ sec., $t_d^+ = 1.25$ sec., $d = 4 \times 10^{-5}$	99
	b. Roll Trajectory, $N_2 = 0.01$, $t_d^- = 0.5$ sec., $t_d^+ = 1.0$ sec., $d = 4 \times 10^{-5}$	99
	c. Pitch Trajectory, $N_3 = 0.12$, $t_d^- = 0.2$ sec., $t_d^+ = 0.04$ sec., $d = 2.5 \times 10^{-5}$	100
5.1	Switching Curves of the Busch Control Law in the Yaw and Pitch Planes	106
5.2	Optimal (Linear) Acquisition Solutions	111
	a. Satellite (1), $J = 8.19$, $\tau_f - \tau_o = 1.42$, $\theta_o = \pi/4$	111
	b. Satellite (2), $J = 8.92$, $\tau_f - \tau_o = 1.32$, $\theta_o = \pi/4$	112
	c. Satellite (3), $J = 6.03$, $\tau_f - \tau_o = 1.32$, $\theta_o = \pi/4$	113
	d. Satellite (4), $J = 8.73$, $\tau_f - \tau_o = 1.42$, $\theta_o = 5\pi/4$	114

Figure		Page
5.3	Suboptimally Controlled Acquisition Motion of Satellite (1), $J = 12.66$, $\tau_f - \tau_o = 1.42$, $\theta_o = \pi/4$.	121
a.	Large Yaw Angles .	121
b.	Small Yaw Angles .	121
c.	Large Roll Angles	122
d.	Small Roll Angles	122
e.	Large Pitch Angles	123
f.	Small Pitch Angles	123
5.4	Suboptimally Controlled Acquisition Motion of Satellite (2), $J = 9.07$, $\tau_f - \tau_o = 1.69$, $\theta_o = \pi/4$.	124
a.	Large Yaw Angles	124
b.	Small Yaw Angles	124
c.	Large Roll Angles	125
d.	Small Roll Angles	125
e.	Large Pitch Angles	126
f.	Small Pitch Angles	126
5.5	Suboptimally Controlled Acquisition Motion of Satellite (3), $J = 9.75$, $\tau_f - \tau_o = 1.63$, $\theta_o = \pi/4$	127
a.	Large Yaw Angles	127
b.	Small Yaw Angles	127
c.	Large Roll Angles	128
d.	Small Roll Angles	128
e.	Large Pitch Angles	129
f.	Small Pitch Angles	129
5.6	Suboptimally Controlled Acquisition Motion of Satellite (4), $J = 8.37$, $\tau_f - \tau_o = 1.69$, $\theta_o = 7\pi/4$	130
a.	Large Yaw Angles	130
b.	Small Yaw Angles	130
c.	Large Roll Angles	131
d.	Small Roll Angles	131
e.	Large Pitch Angles	132
f.	Small Pitch Angles	132

Figure		Page
6 1	Block Diagram of the Complete Attitude Control System	135
6.2	Pitch Fuel Cost Per Orbit vs Eccentricity, $N_3 = 0.035$, $k_3 = 0.99$, $d = 0$	140
6 3	Roll-Yaw Fuel Cost for Various Values of k_1 and k_2 , $N_1 = N_2 = 0.01$, $e = 0.05$, $d = 3 \times 10^{-5}$	141
6 4	Fuel Cost Per Orbit vs. Control Strength	143
	a Roll-Yaw of Satellites (2) and (3)	143
	b Pitch of Satellite (3)	143
6 5	Fuel Cost Per Orbit vs Size of the Region S - Satellite (2), $d = 2.0 \times 10^{-5}$, $N_1 = N_2 = 0.01$, $N_3 = 0.1$	144
A.1	Unit Vectors and Parameters of the Orbit	155
F 1	Solution of Approximate, Minimum-Fuel Optimal, Station- Keeping Equations ((4 3) and (4 4)) for Roll-Yaw	177
F 2	Solution of Approximate, Minimum-Fuel Optimal, Station- Keeping Equations ((4 5) and (4 6)) for Pitch	180
F 3	Analog Program for Steady-State Roll-Yaw Motion (Aero term added as required)	183
F 4	Analog Program for Steady-State Pitch Motion (Aero- dynamic torque term is added as required)	185
F.5	Solution of Nonlinear Suboptimal Acquisition Equations ((2 14)-(5 2))	187
F 6	Solution of Optimal Linear Acquisition Equation in Backward Time	190

LIST OF TABLES

TABLE		Page
2 1	Parameters of the Satellites and of Their Orbits	11
2.2	The Significant Torque Terms for Various Earth-Pointing Accuracies	23
4 1	Fuel Expenditure for the Simulation Runs of Figure 4 17- Figure 4 20	102
5 1	Modified Versions of Busch's Switching Curves	109
5 2	Slopes for the Straight Line Switching Curves as Obtained from the Optimal (Linear) Solutions	115
5 3	The Parameters of the Control Law for the Initial Test	118

LIST OF SYMBOLS

<u>SYMBOL</u>	<u>MEANING</u>	<u>PAGE OF FIRST OCCURANCE</u>
a	Semi-major axis of elliptic orbit	10
A_1	See equations (2.15)	15
B	Rigid body satellite	5
B^*	Center of mass of B	5
C_D	Drag coefficient	10
c_δ	Cosine function of δ	9
c_1	Cosine function θ_1 , $1 = 1, 2, 3$	7
C_1	Components of control torque	8
CST	"Coast function" (see equation (4.2))	41
c_θ	Cosine function of $\theta + \theta_o$	9
$c\theta$	Cosine function of $\theta + \theta_p$	10
d	Distance between control switching lines (see Figure 4.14)	87
δ	Angle between earth's polar axis and the normal to orbit plane (see Figure A.1)	9
$\Delta \tau_1^+$	See equation (E.7)	49
e	Eccentricity of orbit	10
E	Earth	5
E^*	Center of mass of E	5
f^1	Functions representing right sides of equation of motion (see equation (3.1))	28
f_j	Functions of state which appear in some cost functionals	32
$F(x_1)$	Derivative of f_1 with respect to x_1	42
G	Universal gravity constant	153
h	$h = r^2 \dot{\theta}$ for kepler orbit	10
H	Hamiltonian function	29
I_1	Principal moments of inertia, $1 = 1, 2, 3$	5

<u>SYMBOL</u>	<u>MEANING</u>	<u>PAGE OF FIRST OCCURANCE</u>
J	{ Oblateness coefficient (see Appendix A) Cost functional or nondimensional fuel cost	9 28
K	Constant in exponential atmospheric density law	10
k_1	Nondimensional inertia parameters, $i = 1, 2, 3$	7
ℓ_1	Components of distance vector from B^* to center of aerodynamic pressure for \underline{n}_1	10
μ	{ Mass of earth times G Coefficient in transversality condition	9 33
n	Mean orbital rate	14
NCES	"Necessary conditions for exact solution"	36
n_1	Parameters in f_1	32
\underline{n}_1	Unit vectors, $i = 1, 2, 3$, parallel to principal axes	5
N_1	Maximum absolute value of v_1	41
N'_1	Maximum absolute value of u_1	104
ω_1	Components of the satellite's angular velocity	5
Ω	See Figure A 1	11
p	Adjoint vector ($n+1$ - dimensional)	29
\underline{p}	Adjoint vector (n - dimensional)	33
r	Distance from E^* to B^*	9
r_E	Equatorial radius of earth	9
r_p	Value of r at perigee	10
ρ	Atmospheric density	10
ρ_a	Value of ρ at apogee	11
ρ_p	Value of ρ at perigee	10
S	{ Effective cross-sectional area of satellite Region of state space	10 24
s_δ	Sine function of δ	9

<u>SYMBOL</u>	<u>MEANING</u>	<u>PAGE OF FIRST OCCURANCE</u>
s_1	$\left\{ \begin{array}{l} \text{Sine function of } \theta_1, \quad 1 = 1, 2, 3 \\ \text{Constants in definition of region } S, \quad 1 = 1, \dots, 6 \end{array} \right.$	 7 24
S^+	Region of state space which contains the region S	91
S_Y	Yaw phase plane projection of the region S , others are roll (R) and pitch (P)	72
$s\theta$	Sine function of $\theta + \theta_p$ (see Figure A 1)	9
s_θ	Sine function of $\theta + \theta_o$	9
T_{a1}	Components of aerodynamic torque	8
τ	Nondimensional time ($= nt$)	14
\underline{T}	Active torque for B^*	8
\underline{T}_I	Inertia torque for B^*	5
T_{g1}	Components of gravity torque	8
T_1	Components of \underline{T} for $\underline{n}_1, \quad 1 = 1, 2, 3$	8
T_{I1}	Components of \underline{T}_I for \underline{n}_1	7
θ	Orbital angle measured from perigee	7
$\dot{\theta}_E$	Magnitude of earth's angular velocity	10
θ_1	Three-axes Euler angles, $1 = 1, 2, 3$	7
u_1	Nondimensional components of acquisition control torque	104
v	Single-axis nondimensional control	53
V	Magnitude of velocity of B^* relative to the local atmosphere	10
\underline{v}	Nondimensional station-keeping control vector	28
v_1	Components of \underline{v} for $\underline{n}_1, \quad 1 = 1, 2, 3$	15
W_1	See equations (2.15)	15
\underline{x}	State vector	24
\underline{x}_f	Final state considered	28

<u>SYMBOL</u>	<u>MEANING</u>	<u>PAGE OF FIRST OCCURANCE</u>
\underline{x}_0	Initial state considered	28
x_1	See equations (2.13)	14
y_1	x_1 scaled for analog computer to give one volt when $x_1 = 10^{-4}$	183

I INTRODUCTION

A. STATEMENT OF THE PROBLEM

At this time there are many planned artificial earth satellites which must perform tasks which require a given satellite-fixed line to be (nearly) parallel to the local vertical while the angles between every satellite-fixed line and the orbit plane are (nearly) constant. This required orientation is called (near) earth-pointing. Earth-pointing is not a natural satellite orientation so that control effort must be spent to keep the orientation (called station-keeping) once it has been acquired. The time interval of station-keeping for practical satellites ranges from minutes to years. In any case the controller, which causes the satellite to acquire the earth pointing attitude and keep it, must be efficient as well as reliable.

The problem considered in this investigation is how to efficiently and reliably control a satellite's attitude motion so that it is very accurately earth-pointing for a given interval of time.

B. SATELLITE CONFIGURATIONS

Since attitude motion characteristics vary widely with satellite configuration and since the efficiency of a given control varies with the characteristics of attitude motion, it, at first, seems necessary to consider an almost infinite variety of satellite configurations. However, upon further investigation it is found that a few satellite configurations exhibit a wide variety of attitude motions whose characteristics are basic characteristics of a whole range of satellite configurations.

Four configurations of satellites and their orbits are considered here. These four configurations were chosen since they exhibit a wide variety of natural attitude motions and since they are similar to some future as well as some recent earth satellites.

Satellites (1) and (4) are similar to some of today's "stable" scientific satellites e.g., satellites of the Orbiting Geophysical Observatory and the Tiros series. Satellite (4) is such that aerodynamic forces significantly affect its attitude motion. Satellite (2) is

similar to "unstable" manned and unmanned spacecraft which will be inserted into (nearly) circular earth parking orbits for transfer to orbits about other celestial bodies. Examples of such spacecraft are Apollo and Unmanned Mars Excursion Vehicle. Satellite (3) is similar to future "unstable" military applications satellites.

The orbits of the satellites are elliptic, although for satellites (2) and (3) the eccentricity is assumed to be only 0.01. The orbits are not considered circular since such an assumption is generally a gross oversimplification and since the number of orbits a satellite will complete before the aerodynamic forces cause it to move on a trajectory back to earth increases with eccentricity. (Breakwell and Koehler [4] have derived an expression for the number of orbits before decay. This expression, which gives a lifetime of about 10,000 orbits (about 1.7 years) for an initial perigee height of 200 miles and an initial eccentricity of 0.03, has been experimentally verified.)

C CONTROLLERS AND PERFORMANCE CRITERIA

In recent years many devices which showed promise of controlling the attitude motion of satellites have been constructed, analyzed and to some extent applied with success. These controllers are categorized according to their subsystems which supply the control torques. Control torques are obtained by devices such as gas jets, ion propulsion units, three-axes-gyroscopes, v-gyroscopes, reaction wheels, reaction spheres, extendable booms and magnetic devices.

Several investigators have considered such devices in solving various acquisition and station-keeping problems. For example, Horwitz [19] has considered pulse width modulation for fairly high accuracy control of highly idealized attitude motion. Huston [20] considered the feasibility of employing twin-gyroscopes for control, and, Schwartz [32] considered minimum energy acquisition using reaction wheel control. Asymptotic stabilization of the spin axis of a satellite in a circular orbit by magnetic control was considered by Wheeler [34]. Haefner [15] and Nichol [28] each considered some of the general aspects of attitude control. Although these solutions contribute to the solution of the problem at hand, none result in sufficient guidelines for the construction

of a device which will efficiently and reliably control the attitude motion for high accuracy earth-pointing

Because of their simplicity and reliability, gas jets are considered in this investigation as the suppliers of control torque

The error in orientation for the high accuracy earth-pointing orientation is considered* to have priority over all other performances measures. However, for efficiency, the weight of the fuel spent for control must be as near minimal as is practicable (See Section B, Chapter III) Another criterion used in the present investigation is the time limit for acquisition of the high accuracy earth-pointing orientation Since some satellites require rapid acquisition (e g , the acquisition of the Gemini-Agena to earth-pointing before firing the agena rocket for changing orbit), the time of acquisition is limited to the time of one-fourth of an orbit

D PREVIOUS CONTRIBUTIONS

The present investigation is a continuation of the work at Stanford on the attitude control of satellites Busch** [6] has developed a sub-optimal minimum-fuel acquisition control law for a "stable" satellite in an elliptic orbit The use of this control law does not consistently result in acquisition to high accuracy earth-pointing unless the eccentricity of the orbit is very small However, Busch has included a reaction wheel for improving the accuracy when the eccentricity is not small Although the reaction wheel must be slowed periodically by applying gas jet torque, Busch's controller performs quite well in station-keeping. The controller gives fairly high accuracy in earth-pointing, but the controller is not efficient while station-keeping

*After completing this work it came to our attention that A E Pearson in his presentation on "Performance Maintainability in Precision Attitude Control Systems" in J A C C preprints (Philadelphia, 1967) discussed generalized performance measures for practical attitude control systems

**Also, see SUDAAR No 261 or R E Busch and I. Flügge-Lotz, "Attitude Control of a Satellite in an Elliptic Orbit", Journal of Spacecraft and Rockets, Vol 4, No 4, 1967.

Others who have investigated certain aspects of minimum-fuel attitude control are Flugge-Lotz and Marbach [13], Foy [14], Meditch [27], Athans [1], Craig and Flugge-Lotz [10] and Hales [16]

E. CONTRIBUTIONS

In Chapter II the equations of motions of rigid satellites in elliptic orbits about an oblate body with atmosphere are derived in terms of the "three-axes Euler angles" which for small angles are nearly the yaw, roll and pitch angles. The effects of disturbances such as those due to solar radiation pressure, meteoroids, etc. are discussed. A means of determining an upper bounds on the error due to simplifying the full nonlinear equations of controlled motion is given.

In Chapter III the theory of the control of satellite attitude motion is discussed and its application justified.

In Chapter IV a high-accuracy station-keeping feedback control law is developed. The application of this control law to "unstable" as well as "stable" satellites results in very little fuel expenditure. The reliability and efficiency of the station-keeping controller under adverse circumstances is investigated in Chapter VI where the overall system is discussed.

Suboptimal acquisition control laws for the four satellites are developed in Chapter V by extending Busch's results with the aid of phase-plane methods and Pontryagin's Maximum Principle.

It is assumed that sensors of attitude angles and their rates for such high accuracy will be available in the very near future.

II. THE EQUATIONS OF CONTROLLED SATELLITE ATTITUDE MOTION

Satellite attitude motion is suitably described by a system of differential equations in which the dependent variables are the generalized coordinates of the satellite. Three of the generalized coordinates completely determine the attitude of a rigid satellite in some reference frame. The time-history of these three coordinates and their rates for some interval of time is called the attitude motion in that time interval or more simply the motion

A THE INERTIA TORQUE

For a rigid* satellite, B, the inertia torque for the mass center of B, B*, is well known. (See, for example, Kane [22].) If \underline{n}_1 , $1 = 1, 2, 3$, are elements of a right-handed set of mutually perpendicular unit vectors which are parallel to principal axes of inertia of B for B*, say I_1 , $1 = 1, 2, 3$, (see Figure 2 1) and if I_1 , $1 = 1, 2, 3$, are the associated principal moments of inertia, then the inertia torque of B for B* is given by

$$\begin{aligned} \underline{T}_I = & [\omega_2 \omega_3 (I_2 - I_3) - \dot{\omega}_1 I_1] \underline{n}_1 \\ & + [\omega_3 \omega_1 (I_3 - I_1) - \dot{\omega}_2 I_2] \underline{n}_2 \\ & + [\omega_1 \omega_2 (I_1 - I_2) - \omega_3 I_3] \underline{n}_3, \end{aligned} \quad (2\ 1)$$

where ω_1 , $1 = 1, 2, 3$, are the measure numbers of the angular velocity of B in an inertial reference frame for the basis, \underline{n}_1 , $1 = 1, 2, 3$, and where the symbol $(\dot{}) \equiv d()/dt$

One orbit of the satellites considered very nearly lies in a plane in an inertial space. (See King-Hele [23].) This plane, which contains the mass center, E*, of the earth, E, (together with the plane's normal) determines a suitable inertial reference frame

* Causes of non-rigidity of the satellite and their effects on the controlled motion of the satellite and on the fuel cost are discussed in Section C of Chapter VI.

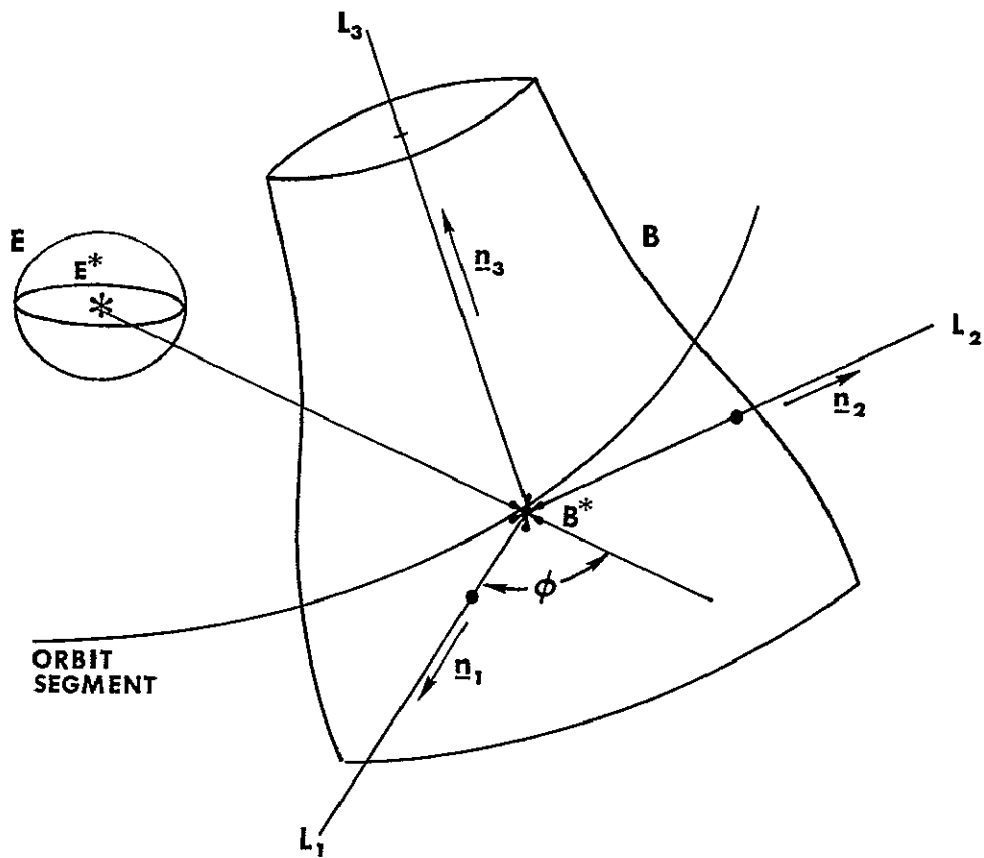


Figure 2 1 Principal Axes of Inertia, L_i , $i = 1, 2, 3$, the Unit Vectors \underline{n}_i , $i = 1, 2, 3$, the Satellite B and the Earth E

In terms of the "three-axes Euler angles", θ_1 , $1 = 1, 2, 3$,* (see Busch [6]) the measure numbers of \underline{T}_1 , (2 1), for the basis \underline{n}_1 , $1 = 1, 2, 3$, are

$$\begin{aligned} T_{11} = & \{-\theta_1 c_2 c_3 - \theta_2 s_3 + \theta_1 \theta_2 s_2 c_3 - \theta_2 \theta_3 c_3 + \theta_1 \theta_3 c_2 s_3 \\ & - \dot{\theta} [\theta_1 (c_1 s_3 + s_1 s_2 c_3) - \theta_2 c_1 c_2 c_3 + \theta_3 (s_1 c_3 + c_1 s_2 s_3)] \\ & - \ddot{\theta} (s_1 s_3 - c_1 s_2 c_3) - k_1 \omega_2 \omega_3\} \times I_1 \end{aligned} \quad (2.2a)$$

$$\begin{aligned} T_{12} = & \{-\theta_2 c_3 + \theta_1 c_2 s_3 - \theta_1 \theta_2 s_2 s_3 + \theta_2 \theta_3 s_3 + \theta_1 \theta_3 c_2 c_3 \\ & - \theta [\theta_1 (c_1 c_3 - s_1 s_2 s_3) + \theta_2 c_1 c_2 s_3 + \theta_3 (c_1 s_2 c_3 - s_1 s_3)] \\ & - \theta (s_1 c_3 + c_1 s_2 s_3) - k_2 \omega_3 \omega_1\} \times I_2 \end{aligned} \quad (2.2b)$$

$$\begin{aligned} T_{13} = & \{-\dot{\theta}_3 - \theta_1 s_3 - \dot{\theta}_1 \theta_2 c_2 + \dot{\theta} (\theta_1 s_1 c_2 + \theta_2 c_1 s_2) \\ & - \dot{\theta} c_1 c_2 - k_3 \omega_1 \omega_2\} \times I_3 \end{aligned} \quad (2.2c)$$

where $c_1 = \cos \theta_1$, $s_1 = \sin \theta_1$, $1 = 1, 2, 3$, and where

$$\begin{aligned} \omega_1 = & (\theta s_1 + \theta_2) s_3 - (\theta c_1 s_2 - \theta_1 c_2) c_3 \\ \omega_2 = & (\theta s_1 + \theta_2) c_3 + (\theta c_1 s_2 - \theta_1 c_2) s_3 \\ \omega_3 = & \theta c_1 c_2 + \theta_1 s_2 + \theta_3 \end{aligned} \quad (2.3)$$

The angle θ is defined in Appendix A (see Figure A 1) and the inertia parameters k_1, k_2, k_3 are defined by

$$k_1 = \frac{I_3 - I_2}{I_1}, \quad k_2 = \frac{I_1 - I_3}{I_2}, \quad k_3 = \frac{I_2 - I_1}{I_3}. \quad (2.4)$$

*When θ_1 , $1 = 1, 2, 3$, are small, they can be considered as the yaw, roll and pitch angles, respectively

B THE (ACTIVE) TORQUE

The torque for B^* is due to all contact and body forces acting on B . The body forces are due primarily to the gravitational attraction of the earth and other celestial bodies and the interaction of the satellite with the earth's magnetic field. The contact forces are due primarily to the interaction of the satellite with the earth's atmosphere and emissions from the sun, to collisions of the satellite with meteoroids and to the controls, for example gas jets.

All of these forces were considered in the derivation of the torque for B^* (See Section F of this chapter.) However, the torque expression used in the derivation of the equations of motion is a result of considering only aerodynamic, control and earth gravitational forces. This torque expression can be written as

$$\underline{T} = \sum_{i=1}^3 T_{i\underline{n}_1} = \sum_{i=1}^3 (T_{g1} + T_{a1} + C_1) \underline{n}_1 \quad (2.5)$$

where for the basis \underline{n}_1 , $i = 1, 2, 3$, the measure numbers C_1 , $i = 1, 2, 3$, are for the control torque vector, the measure numbers T_{g1} , $i = 1, 2, 3$, are for the gravitational torque vector and the measure numbers T_{a1} , $i = 1, 2, 3$, are for the aerodynamic torque vector.

C. THE FULL NONLINEAR DIFFERENTIAL EQUATIONS OF CONTROLLED MOTION

If for each \underline{n}_1 , $i = 1, 2, 3$, the corresponding measure numbers of \underline{T}_i and \underline{T} are divided by I_1 , $i = 1, 2, 3$, respectively, and summed to zero, then from (2.2a)-(2.2c) and (2.5) the result is represented by three equations in θ_1 , $i = 1, 2, 3$. If these three equations are solved for θ_1 , $i = 1, 2, 3$, they give

$$\begin{aligned} \theta_1 = & (\dot{\theta}_1 \theta_2 s_2 - \theta_2 \dot{\theta}_3 - \theta \dot{\theta}_1 s_1 s_2 + \theta \theta_2 c_1 c_2 \\ & - \dot{\theta} \dot{\theta}_3 s_1 + \theta c_1 s_2 + s_3 k \omega_3 \omega_1 - c_3 k \omega_2 \omega_3 \\ & + c_3 T_1 / I_1 - s_3 T_2 / I_2) / c_2 \end{aligned} \quad (2.6a)$$

$$\begin{aligned}
\dot{\theta}_2 &= \theta_1 \theta_3 c_2 - \theta \theta_1 c_1 - \theta \theta_3 c_1 s_2 - \dot{\theta} s_1 \\
&- c_3 k_2 \omega_3 \omega_1 - s_3 k_1 \omega_2 \omega_3 \\
&+ c_3 T_2 / I_2 - s_3 T_1 / I_1
\end{aligned} \tag{2.6b}$$

$$\begin{aligned}
\dot{\theta}_3 &= - \dot{\theta}_1 s_2 - \dot{\theta}_1 \theta_2 c_2 + \theta \theta_1 s_1 c_2 + \theta \theta_2 c_1 s_2 \\
&- \theta c_1 c_2 - k_3 \omega_1 \omega_2 + T_3 / I_3
\end{aligned} \tag{2.6c}$$

Equations (2.6a)-(2.6c) are the desired differential equations of motion in the dependent variables θ_1 , $1 = 1, 2, 3$, and the independent variable t if $\dot{\theta}$ and θ are known functions of t and T_1 , $1 = 1, 2, 3$, are known functions of θ_1 , $\dot{\theta}_1$, $1 = 1, 2, 3$, and t . Except for G_1 , $1 = 1, 2, 3$, which are to be determined in the following chapters as functions of θ_1 , $\dot{\theta}_1$, $1 = 1, 2, 3$, and t , the measure numbers T_1 , $1 = 1, 2, 3$, are known functions of θ_1 , $\dot{\theta}_1$, $1 = 1, 2, 3$, and t . Equations (B.11) with (B.3) and (B.10) give the desired relationships for T_{a1} , $1 = 1, 2, 3$, and Equations (A.8) with (A.9) and (A.10) give the desired relationships for T_{g1} , $1 = 1, 2, 3$, if r , r^{-2} , μ/r^3 , c_θ and s_θ are known functions of time. Equations (C.23)-(C.29) give r , μ/r^3 , θ , r^{-2} , $\dot{\theta}$, s_θ and c_θ^* as functions of time.

The measure numbers of the torque as given by (2.5) can be written with the aid of Equations (A.8)-(A.10), (B.3), (B.10) and (B.11) as

$$\begin{aligned}
T_1 &= G_1 + \mu/r^3 (I_3 - I_2) \{-3c_2 s_2 s_3 \\
&+ J(r_E/r)^2 [5(7s_\delta^2 s_\theta^2 - 1)c_2 s_2 s_3 - 2s_\delta c_\delta c_\theta c_1^2 c_2 c_3 \\
&- 2s_\delta^2 c_\theta s_\theta c_1 s_2 c_3 + 2s_\delta^2 c_\theta c_1 s_1 c_2 c_3 \\
&- 2c_\delta^2 c_1 s_1 c_2 c_3 + 8c_\delta s_\delta c_\theta c_1 c_2^2 s_3 \\
&+ 10s_\delta c_\delta c_\theta c_1 c_2 s_2 + (\text{TERMS IN } s_1^2, \dots, s_1^4)]\}
\end{aligned} \tag{continued}$$

* If, of course, θ_o is replaced with θ_p .

$$\begin{aligned}
& - (C_D/2) \text{Sp} V \{ \dot{r} (\ell_2 s_2 + \ell_3 c_2 s_3) \\
& - r (\dot{\theta} - \theta_E c_\delta) [\ell_2 s_1 c_2 + \ell_3 (c_1 c_3 - s_1 s_2 s_3)] \\
& + r \dot{\theta}_E s_\delta c_\theta [\ell_2 c_1 c_3 - \ell_3 (s_1 c_3 + c_1 s_2 s_3)] \} \quad (2.7a)
\end{aligned}$$

$$\begin{aligned}
T_2 = & C_2 + \mu/r^3 (I_1 - I_3) \{ 3c_2 s_2 c_3 + J(r_E/r)^2 [5(1 - 7s_\delta^2 s_\theta^2) c_2 s_2 c_3 \\
& - 2s_\delta c_\delta c_\theta c_1^2 c_2 s_3 + 2c_\delta^2 c_1 c_2 s_2 c_3 + 8s_\delta c_\delta s_\theta c_1 c_2^2 c_3 - 8s_\delta^2 s_\theta c_\theta s_1 c_2^2 c_3 \\
& + 18s_\delta^2 s_\theta^2 c_2 s_2 c_3 + (\text{TERMS IN } s_1^2, s_1^3)] \} - (C_D/2) \text{Sp} V \{ r(\ell_3 c_2 c_3 - \ell_1 s_2) \\
& + r(\dot{\theta} - \theta_E c_\delta) [\ell_3 (s_1 s_2 c_3 + c_1 s_3) + \ell_1 s_1 c_2] \\
& + r \theta_E c_\theta s_\delta [\ell_3 (s_1 s_3 - c_1 s_2 c_3) - \ell_1 c_1 c_2] \} \quad (2.7b)
\end{aligned}$$

$$\begin{aligned}
T_3 = & C_3 + \mu/r^3 (I_2 - I_1) \{ -3c_2^2 c_3 s_3 + J(r_E/r)^2 [5(7s_\delta^2 s_\theta^2 - 1) c_2^2 c_3 s_3 \\
& + 8s_\delta^2 s_\theta c_\theta c_1 c_2 c_3^2 + 8s_\delta c_\delta s_\theta s_1 c_2 c_3^2 - 18s_\delta^2 s_\theta^2 c_2^2 c_3 s_3 \\
& - 2s_\delta^2 c_\theta^2 c_1^2 c_3 s_3 + 2s_\delta c_\delta c_\theta c_1^2 s_2 c_3^2 + (\text{TERMS IN } s_1^2, s_1^5)] \} \\
& - (C_D/2) \text{Sp} V \{ -r(\ell_1 c_2 s_3 + \ell_2 c_2 c_3) \\
& + r(\theta - \theta_E c_\delta) [\ell_1 (c_1 c_3 - s_1 s_2 s_3) - \ell_2 (s_1 s_2 c_3 + c_1 s_3)] \\
& + r \theta_E c_\theta s_\delta [\ell_1 (s_1 c_3 + c_1 s_2 s_3) - \ell_2 (s_1 s_3 - c_1 s_2 c_3)] \} \quad (2.7c)
\end{aligned}$$

where

$$\rho = \rho_p \exp[K(r - r_p)] \quad (2.8)$$

$$V = (h/a)(1 + 2ec\theta)^{1/2} \quad (2.9)$$

Equations (2.6a)-(2.6c) with Equations (2.3), (2.4), (2.7a)-(2.9) and with Equations (C.23)-(C.29) are the desired nonlinear differential

equations of controlled motion This model of the controlled motion can be simplified without introducing significant error The simplifications strongly depend on the parameters of the satellite and on the mode (steady-state or acquisition) of motion

D PARAMETERS OF THE SATELLITES AND THE SIMPLICATION OF THE MOTION EQUATIONS

In the Introduction, Chapter I, the general configurations and the altitudes of the four satellites to be considered were discussed Here this discussion is translated into numbers for $I_1, I_2, I_3, k_1, k_2, k_3, e, a, \delta, \theta_p, \rho_p$, the height of perigee (ph) and the height of apogee (ah) These numbers for the four satellites are given in Table (2 1) together with the air density at apogee, ρ_a

TABLE 2 1 PARAMETERS OF THE SATELLITES AND OF THEIR ORBITS

Satellite No	(1)	(2)	(3)	(4)
I_1	2.30×10^5	1.15×10^5	7.00×10^3	1.43×10^4
I_2	2.33×10^5	7.00×10^3	1.21×10^5	1.44×10^4
I_3	2.36×10^5	1.21×10^5	1.15×10^5	1.45×10^4
(slug-ft ²)				
k_1	0.01	0.99	-0.86	0.01
k_2	-0.03	-0.86	-0.89	-0.01
k_3	0.01	-0.89	0.99	0.01
e	0.05	0.01	0.01	0.03
a(miles)	4480	4500	4500	4260
ph(miles)	300	500	500	200
ah(miles)	745	585	585	460
θ_p (radians)	variable from 0 to 2π			
δ (radians)	variable from 0 to π if $0 \leq \Omega \leq \pi$			
ρ_p	6.2×10^{-15}	1.6×10^{-16}	1.6×10^{-16}	4.0×10^{-14}
ρ_a	3.4×10^{-18}	4.7×10^{-17}	4.7×10^{-17}	3.7×10^{-16}
(slugs/ft ³)				

The orbits of the satellites are fixed by the values given for a, e, θ_p, Ω and δ . The shapes and compositions of the satellites are not completely fixed by the values given for I_1, I_2 and I_3 and are even less fixed if values are only given for $k_1, 1 = 1, 2, 3$, (since common multiples of $I_1, 1 = 1, 2, 3$, result in the same values of $k_1, 1 = 1, 2, 3$) Typical configurations of the four satellites are as follows

- (1) Nearly spherical with a weight of 60,000 lbs , a maximum dimension of 14 ft and a specific weight of 40 lbs/ft³
- (2) Nearly circular cylindrical with a weight of 50,000 lbs , a height of 30 ft., a mean diameter of 6 ft. and a specific weight of 60 lbs/ft³. The axis of minimum moment of inertia is nearly tangent to the orbital path when in the earth-pointing mode.
- (3) Similar to (2) except that its axis of minimum moment of inertia is nearly coincident with the local vertical when in the earth-pointing mode
- (4) Nearly spherical with a weight of 10,000 lbs , a maximum dimension of 9 ft. and a specific weight of 30 lbs./ft³

The simplifications of the equations of motion are naturally divided by the regimes of $|\theta_1|, 1 = 1, 2, 3$, and the magnitudes of their compatible rates. In the acquisition mode $|\theta_1|, 1 = 1, 2, 3$, vary from about one radian down to 10^{-3} radians or less with most of the time of acquisition spent with $|\theta_1|, 1 = 1, 2, 3$, assuming the larger values. In the steady-state mode the motion will be controlled in a manner such that $|\theta_1|, 1 = 1, 2, 3$, will be less than 10^{-3} radians. In the following two parts of this section, Parts 1 and 2, the equations of controlled motion are simplified for the two modes of motion. The reasons for the simplifications are the solution of the full nonlinear equations of controlled motion with the aid of a digital computer is extremely costly, the analog simulation of these equations (even after they have been linearized in $\theta_1, \dot{\theta}_1, 1 = 1, 2, 3$) requires a greater number of operational amplifiers than is available on the analog computer used (two pax TR-48 computers slaved together), and, finally, the error due to the simplifications is insignificant in the final results (see Chapter VI)

1 The Simplified Acquisition Equations of Motion

For some satellites certain terms in the nonlinear equations of controlled motion are insignificantly small when the controlled satellite is in the acquisition mode. These terms are less than one-one hundredth of the other terms in magnitude for all but about the last one-tenth of the time of acquisition, which is assumed to be the time of one-quarter of an orbit or less. During the last one-tenth of the acquisition time all of the terms are of the order of 10^{-9} or less.

For satellites (1), (2) and (3) the insignificant terms are those in equations (2.7a)-(2.7c) with C_D and J as coefficients and some of those in equations (2.6a)-(2.6c) and (2.7a)-(2.7c) which are products of two or three of s_1, θ_1 , $1 = 1, 2, 3$, and $\dot{\theta}$. The cost of the digital computer solution of the equations with the latter of the above insignificant terms included is not significantly greater than the cost of the solution without these terms. If only those terms with C_D and J as coefficients are omitted, then the simplified acquisition equations of motion for satellites (1), (2) and (3) are

$$\begin{aligned}\theta_1 = & (\theta_1 \theta_2 s_2 - \theta_2 \theta_3 - \theta \theta_1 s_1 s_2 + \theta \theta_2 c_1 c_2 - \theta \theta_3 s_1 + \dot{\theta} c_1 s_2 \\ & + k_2 s_3 \omega_3 \omega_1 - k_1 c_3 \omega_2 \omega_3 + c_3 C_1 / I_1 - 3k_1 (\mu/r^3) c_2 s_2 c_3 s_3 \\ & - s_3 C_2 / I_2 - 3k_2 (\mu/r^3) c_2 s_2 c_3 s_3) / c_2\end{aligned}\quad (2.10a)$$

$$\begin{aligned}\theta_2 = & \theta_1 \theta_3 c_2 - \theta \theta_1 c_1 - \theta \theta_3 c_1 s_2 - \theta s_1 - k_2 c_3 \omega_3 \omega_1 - k_1 s_3 \omega_2 \omega_3 \\ & + c_3 C_2 / I_2 + 3k_2 (\mu/r^3) c_2 s_2 c_3^2 \\ & - s_3 C_1 / I_1 + 3k_1 (\mu/r^3) c_2 s_2 s_3^2\end{aligned}\quad (2.10b)$$

$$\begin{aligned}\theta_3 = & -\theta_1 s_2 - \dot{\theta}_1 \theta_2 c_2 + \dot{\theta} \theta_1 s_1 c_2 + \theta \theta_2 c_1 s_2 - \dot{\theta} c_1 c_2 - k_3 \omega_1 \omega_2 \\ & + C_3 / I_3 - 3k_3 (\mu/r^3) c_2^2 c_3 s_3\end{aligned}\quad (2.10c)$$

where $\omega_1, 1 = 1, 2, 3$, are given by (2.3) and $\mu/r^3, \dot{\theta}$ and θ are given by (C 24), (C 25) and (C 27) with θ_0 , the angle from perigee at $t = 0$, added to nt

For satellite (4) the terms which are insignificant and will be omitted in the acquisition equations of motion are those which contain one of $J, C_D \dot{r}, C_D r \dot{\theta}$ and $r \theta \ell_1 s_{j k}, 1, j, k = 1, 2, 3$, as factors. In this case, if $Vr \dot{\theta}$ is replaced by $(h^2/a^2)(1 + 2e \cos \theta) \approx (h^2/a^2)[1 + 2e \cos (nt + \theta_0)]$ (see equations (B.10) and (C.29)), the simplified equations of motion are the same as (2 10a)-(2 10c) except that the terms

$$\begin{aligned} \text{rhs}_1 &= (C_D/2) S_p (h^2/a^2) [1 + 2e \cos(nt + \theta_0)] \\ &\quad \times (c_3/I_1 c_2) (\ell_2 s_1 c_2 + \ell_3 c_1 c_3) \end{aligned} \quad (2.11a)$$

$$\text{rhs}_2 = 0, \quad (2.11b)$$

$$\begin{aligned} \text{rhs}_3 &= (C_D/2 I_3) S_p (h^2/a^2) [1 + 2e \cos(nt + \theta_0)] \\ &\quad \times (\ell_2 c_1 s_3 - \ell_1 c_1 c_3) \end{aligned} \quad (2.11c)$$

are added to the right-hand sides of equations (2 10a), (2.10b) and (2 10c), respectively

If (C 23) is substituted into (B 2) and θ is assumed to be θ_0 at $t = 0$, then

$$\rho = \rho_p \exp\{K e [\cos(nt + \theta_0)]\} \quad (2.12)$$

A more convenient form of the simplified acquisition equations of motion is obtained by letting $\tau = nt$, $()' = d()/d\tau$

$$x_{2x1-1} = \theta_1, \quad x_{2x1} = \theta_1' \quad \text{for } 1 = 1, 2, 3 \quad (2.13)$$

With these substitutions and the substitution of (C 24), (C 25) and (C 27) into (2 10a)-(2 10c) the equations of motion for satellites (1), (2) and (3) becomes

$$x_1' = x_2$$

(continued)

$$x_2' = \{x_2 x_4 s_2 - x_4 x_6 + A_1(x_4 c_1 c_2 - x_2 s_1 s_2 - x_6 s_1) + A_2 c_1 s_2 \\ + k_2 s_3 W_3 W_1 - k_1 c_3 W_2 W_3 + c_3 v_1 - s_3 v_2 \\ - 3A_3(k_1 + k_2)c_2 s_2 c_3 s_3\}/c_2$$

$$x_3' = x_4$$

$$x_4' = x_2 x_6 c_2 - A_1(x_2 c_1 + x_6 c_1 s_2) - A_2 s_1 - k_2 c_3 W_1 W_1 - k_1 s_3 W_2 W_3 \\ + c_3 v_2 - s_3 v_1 + 3A_3(k_2 c_3^2 - k_1 s_3^2)c_2 s_2$$

$$x_5' = x_6$$

$$x_6' = -x_2 x_4 c_2 - x_2' s_2 + A_1(x_2 s_1 c_2 + x_4 c_1 s_2) \\ - A_2 c_1 c_2 - k_3 W_1 W_3 + v_3 - 3k_3 A_3 c_2^2 c_3 s_3 \quad (2.14)$$

where $v_1 = C_1/n^2 I_1$, $1 = 1, 2, 3$,

$$A_1 = \dot{\theta}/n = [1 + 2e \cos(\tau + \theta_0)]$$

$$A_2 = \dot{\theta}/n^2 = -2e[\sin(\tau + \theta_0) + 5e \cos(\tau + \theta_0)\sin(\tau + \theta_0)]$$

$$A_3 = (\mu/r^3 n^2) = [1 + 3e \cos(\tau + \theta_0)]$$

$$W_1 = \omega_1/n = x_2 c_2 c_3 + x_4 s_3 + A_1(s_1 s_3 - c_1 s_2 c_3)$$

$$W_2 = \omega_2/n = x_4 c_3 - x_2 c_2 s_3 + A_1(s_1 c_3 + c_1 s_2 s_3)$$

$$W_3 = \omega_3/n = x_6 + x_2 s_2 + A_1 c_1 c_2 \quad (2.15)$$

The acquisition equations of motion for satellite (4) are obtained by adding

$$RHS_1 = rhs_1/n^2 = A_4(\ell_2 s_1 c_2 + \ell_3 c_1 c_3)(c_3/I_1 c_2)$$

(continued)

$$\text{RHS}_2 = \text{rhs}_2/n^2 = 0$$

$$\text{RHS}_3 = \text{rhs}_3/n^2 = A_4(\ell_2 c_1 s_3 - \ell_1 c_1 c_3)(I_3^{-1}) \quad (2.16)$$

where $A_4 = (C_D \rho_p Sh^2/2a^2)[1 + 2e \cos(\tau + \theta_0)] \exp\{Ke[\cos(\tau + \theta_0) - 1]\}$ to the right-hand side of the second, fourth and sixth of equations (2.13), respectively. Equations (2.16) are obtained from equations (2.11a)-(2.11c) and (2.12)

2 The Simplified Steady-State Equation of Motion

High-accuracy earth-pointing motion or steady-state motion is defined to be motion such that $|x_1| < 10^{-3}$ radians, $i = 1, \dots, 6$ (see equations (2.13)) (In the search for a steady-state control law, i.e., for the functions $v_1 = v_1(x_1, \dots, x_6, \tau)$, $i = 1, 2, 3$, it is required that $|x_1| \leq 1.1 \times 10^{-4}$ radians) In the steady-state mode the terms in the nonlinear equations of motion which contain products of some of x_1 , $i = 1, \dots, 6$, are insignificantly small and can be omitted The terms in the earth oblateness part of the gravitation torque (terms with J as a coefficient) cannot in general be neglected as was done in the acquisition equations. However, in the equation corresponding to the T_{3-3} component of the torque the oblateness terms can be neglected since for an entire orbit these terms are about one one-hundredth of the inertia torque term, $\dot{\theta}$ In the two equations corresponding to the T_{1-1} and T_{2-2} components of the torque the oblateness terms which are significant are of the same order of magnitude as the largest of the other terms for some orbits, but, these oblateness terms which are significant for some orbits are insignificant for other orbits (These significant oblateness terms are periodic with zero occurring at the time of coincidence of B^* with a point of the earth's equatorial plane except in the case where the orbit is in the earth's equatorial plane and all of the oblateness terms are zero.) It should be remarked that for greater earth-pointing accuracy, say an order of magnitude greater, some of the oblateness terms are the most significant terms in the equations corresponding to T_{1-1} and T_{2-2} for most orbits if the aerodynamic torque is insignificant.

In the simplified steady-state equations of motion, which are written below, the significant oblateness terms are included; although, in some of the control law analysis the orbits are chosen so that these terms are zero. Before the equations are written it should be remarked that the "best" functions $v_1 = v_1(x_1, \dots, x_6, \tau)$, $i = 1, 2, 3$, are such that v_1 are of the same order of magnitude as x_1 , $i = 1, \dots, 6$, so that terms in the equations which are products of v_1 and x_1 are insignificant.

If s_1 and c_1 are replaced by x_1 and 1 , respectively, then for satellites (1), (2) and (3) the simplified steady-state equations of motion are

$$\dot{x}_1 = x_2$$

$$\dot{x}_2 = -k_1 A_1^2 x_1 + A_2 x_3 + K_1 A_1 x_4 - 2k_1 A_3 J(r_E/r)^2 s_\delta c_\delta c_\theta + v_1$$

$$\dot{x}_3 = x_4$$

$$\begin{aligned} \dot{x}_4 = & -A_2 x_1 - K_2 A_1 x_2 + k_2 (3A_3 + A_1^2) x_3 \\ & + 8k_2 A_3 J(r_E/r)^2 s_\delta c_\delta s_\theta + v_2 \end{aligned}$$

$$\dot{x}_5 = x_6$$

$$\dot{x}_6 = -3k_3 A_3 x_5 - A_2 + v_3 \quad (2.17)$$

where $K_1 = 1 - k_1$, $K_2 = 1 + k_2$ and A_i , $i = 1, 2, 3$, are given in (2.15).

For satellite (4) the simplified steady-state equations of motion are

$$\dot{x}_1 = x_2$$

$$\dot{x}_2 = K_1 A_1 x_4 + (A_4/I_1) l_3 + v_1$$

$$\dot{x}_3 = x_4$$

(continued)

$$\dot{x}_4' = -K_2 A_1 x_2 + 8k_2 A_3 J(r_E/r)^2 s_\delta^c s_\theta + v_2 ,$$

$$\dot{x}_5' = x_6$$

$$\dot{x}_6' = -A_2 - A_4 \ell_1 / I_3 + v_3 \quad (2.18)$$

where A_4 is the same as in (2.16)

E. THE ERROR IN THE MOTION DUE TO THE SIMPLIFICATIONS

An upper bound on the motion error due to the simplifications made in the equations of motion can be easily obtained for satellites which are stable in the sense of DeBra [11]. Suppose that the full nonlinear equations of motion are written in matrix form as

$$\dot{\underline{x}}' = A(\tau)\underline{x} + B\underline{v}(\tau) + \underline{g}_1[\underline{x}, \underline{v}(\tau), \tau] + \underline{g}_2[\underline{x}, \underline{v}(\tau), \tau] \quad (2.19)$$

where the transpose of \underline{x} is given by $\underline{x}^t = (x_1, x_2, \dots, x_6)$, $A(\tau)$ is a six-by-six periodically time-varying matrix, B is a six-by-three constant matrix, $\underline{v}^t(\tau) = [v_1(\tau), v_2(\tau), v_3(\tau)]$ is the control vector which is a known function of τ and the steady-state (or acquisition) solutions of (2.19), say $\underline{\varphi}(\tau)$, for given initial conditions, $\underline{\varphi}_0$, corresponding to τ_0 , $\underline{g}_1[\underline{x}, \underline{v}(\tau), \tau]$ is a vector function which contains all of the forcing function (or nonlinear) terms retained in the simplified steady-state (or acquisition) equations, and, $\underline{g}_2[\underline{x}, \underline{v}(\tau)]$ is a vector function which contains all of the terms omitted in the simplification. Then the solution of (2.19) can be written as

$$\begin{aligned} \underline{\varphi}(\tau) = & \Phi(\tau, \tau_0) \underline{\varphi}_0 + \int_{\tau_0}^{\tau} \Phi(\tau, \lambda) B \underline{v}(\lambda) d\lambda \\ & + \int_{\tau_0}^{\tau} \Phi(\tau, \lambda) \underline{g}_1[\underline{\varphi}(\lambda), \underline{v}(\lambda), \lambda] d\lambda \\ & + \int_{\tau_0}^{\tau} \Phi(\tau, \lambda) \underline{g}_2[\underline{\varphi}(\lambda), \underline{v}(\lambda), \lambda] d\lambda \end{aligned} \quad (2.20)$$

where $\Phi(\tau, \tau_0)$ is the fundamental matrix of $\dot{\underline{x}} = A(\tau)\underline{x}$.

If the norm is defined by

$$|\underline{x}| = \sum_{i=1}^6 |x_i| \quad \text{and} \quad |\Phi| = \sum_{i,j=1}^6 |\phi_{ij}|$$

where ϕ_{ij} are elements of Φ and if $\underline{\phi}_s(\tau)$ is defined to be the solution of the simplified equations, then

$$|\underline{\phi}(\tau) - \underline{\phi}_s(\tau)| \leq \int_{\tau_0}^{\tau} |\Phi(\tau, \lambda)| |g_2[\underline{\phi}(\lambda), \underline{v}(\lambda), \lambda]| d\lambda \quad (2.21)$$

in the steady-state case since g_1 is a function of τ only in this case

DeBra has investigated the motion of satellites in elliptic orbits about an oblate earth and has found for certain satellite configurations that the motion is "stable". Satellites which have such "stable" motion have the characteristic that $\max_{\lambda} |\Phi(\tau_f, \lambda)| \approx 20$ for $\tau_0 \leq \lambda \leq \tau_f$. In the steady-state case, since $\underline{v}(\tau)$ is such that $|\phi_{ij}(\tau)| \leq 1.1 \times 10^{-4}$ for all τ , the maximum value of $|g_2[\underline{\phi}(\tau), \underline{v}(\tau), \tau]|$ is less than 10^{-8} . Since the equations are periodic with period 2π , the equations for the steady-state case need be integrated only over the interval $\tau_f - \tau_0 = 2\pi$. Thus, in this case $|\underline{\phi}(\tau_f) - \underline{\phi}_s(\tau_f)| < 1.26 \times 10^{-6}$. Since $|\phi_{s1}(\tau_f)| \approx 10^{-4}$, $i = 1, \dots, 6$, for most solutions obtained (see Chapters IV and VI), the error in $\phi_{s1}(\tau)$ is generally less than 2% for satellites which are stable in the sense of DeBra. Satellites (1) and (4), the roll and yaw motions of satellite (2) and the roll and pitch motions of satellite (3) are "stable".

Since the vector function g_1 is a function of $\underline{\phi}(\tau)$ as well as of τ in the acquisition case, no meaningful upper bound on the error due to simplifying the acquisition equations can be found with the above method. However, Busch [6] found that there was little detectable error in his acquisition motion obtained from his simplified equations, which were completely linearized.

^xBusch compared the linear acquisition solutions with the nonlinear solutions

F. DISTURBANCES

Those influences of the motion (or those torques) which are not taken account of by the equations of motion are called disturbances. The primary sources of possible disturbances are the sun, the earth's magnetic field and meteoroids. (Other disturbances, e g , misalignment of gas jets, are discussed in Chapter VI)

The torque for B^* due to the sun's gravitational attraction of the satellite is no larger than 10^{-4} times the torque, \underline{T}_g , due to the gravitational attraction of the earth when the satellite is in the high-accuracy earth-pointing mode of motion. This torque is, of course, very insignificant when studying the motion for one orbit or less.

Emissions from the sun exert a pressure on the exposed part of the satellite's surface area. A torque for B^* due to this pressure (usually called solar radiation pressure) can be quite significant. Expressions for this torque have been derived by McElvain [26] and Wheeler [34]. From these expressions it is concluded for the satellites considered here that the solar pressure torque is no larger than 10^{-3} times $|\underline{T}_g|$ when the satellite has large motion and a distance, d_s , between B^* and the center of solar pressure of 1 ft. For high-accuracy earth-pointing motion the solar pressure torque can be as large as $|\underline{T}_g|$ if d_s is of the order of 1 ft. This torque can affect the form of the required steady-state control law and the cost of the control. However, since the solar torque is very similar to the aerodynamic torque in effect and since the aerodynamic torque is accounted for, the solar pressure torque per se is not considered further.

The torque for B^* due to the interaction of a satellite with the earth's magnetic field can have a significant effect on the motion. Bandeen and Manger [2] have considered a model of the Tiros I satellite for correlating data on the precession of the nearly earth-pointing spin axis. The model included the effect of the interaction with the earth's magnetic field. To model this satellite Bandeen and Manger assumed that a circular conductor with a one meter diameter was on board and carrying a current of one ampere. This model correlated well with the data received. The magnetic torque of this model was of the same order of

magnitude as the earth's gravitational torque for an inaccuracy in earth-pointing of 0.1 radians. However, since Tiros I was much less massive and extensive than the satellites considered here (with about the same asymmetry), the same magnetic torque is only about 10^{-2} times $|T_g|$ for the same earth-pointing accuracy. If this same current-carrying coil were placed on the satellites considered here, the magnetic torque would be of the same order of magnitude as T_g when the satellites are in the high-accuracy earth-pointing mode of motion.

For actual satellites in general it is difficult to say what effect the torque due to the interaction of a satellite with the earth's magnetic field will have on the motion. Part of this torque results from a residual component due to magnetization of some parts of the satellite. Since the magnetic torque is considered to be no larger than the other torques and since by properly designing the satellite this torque can be made quite small, it is considered hereafter only as an unknown disturbance of a certain maximum amplitude which must be overcome by the control.

The forces and their torques due to collisions with meteoroids are considered to be extremely insignificant for nearly the entire lifetime of the satellite. Christman and McMillan [8] have concluded from measurements obtained by the Explorer, Mariner and Pegasus satellites that the probability of no impact by a meteoroid with momentum of 6.67×10^{-3} lb-ft/sec is 0.99 and that for meteoroids with greater momentum impact it is even less. Using experimentally available data, Whipple [35] has estimated that meteoroids with speeds of 20,000 ft/sec and masses of 2×10^{-12} lb. will impact a satellite with a cross-sectional area of twenty square feet about every 20 seconds at an altitude of 200 miles. Whipple has also concluded that the frequency of impact decreases log arithmetically with altitude and with increase in the mass of the meteoroid.

Cloutier [9] has found that the torque due to the forces exerted on a satellite by meteoroid impact can be as great or greater than the torque due to the earth's gravitational attraction but that this is generally a rarity. A provision must be made for such rare occurrences; and, this is done in Chapter IV.

A summary of the most significant torques, which can be predicted with some certainty, is found in Table (2 2) In this table for various ranges of $|\theta_1|$, $1 = 1,2,3$, the satellite numbers ((1) thru (4)) are placed under the torques and beside the component designation if for a particular satellite the component of the torque is significant A component of a torque is insignificant if it is at least one order of magnitude less than corresponding components of other torques For satellite (1) some components of the totality of the torques in the table are shown as insignificant for some ranges of $|\theta_1|$, $1 = 1,2,3$. The reason for this is that these components are insignificant compared to the corresponding components of the inertia torque, which is not included in the table.

The model used for determining the magnetic torque in Table 2.2 was the same as Bandeen and Manger used for Tiros I The expression used for the solar pressure torque of Table 2 2 was derived by Wheeler.

TABLE 2 2 THE SIGNIFICANT TORQUE TERMS FOR VARIOUS EARTH-POINTING ACCURACIES

$ \theta_1 $ 1=1,2,3 RADIANS	GRAVITATIONAL SPHERICAL EARTH	TORQUE OBLATE EARTH	AERODYNAMIC TORQUE	SOLAR PRESSURE TORQUE	MAGNETIC TORQUE	COMPONENT
≥ 0.1	(1) (2) (3) (4)	- - - -	- - - (4)	- - - -	- - - -	n_1
	(1) (2) (3) (4)	- - - -	- - - -	- - - -	- - - -	n_2
	(1) (2) (3) (4)	- - - -	- - - (4)	- - - -	- - - -	n_3
0.01- 0.1	- (2) (3) -	- - - -	- - - (4)	- - - -	- - - -	n_1
	(1) (2) (3) (4)	- - - -	- - - -	- - - -	- - - -	n_2
	(1) (2) (3) (4)	- - - -	- - - (4)	- - - -	- - - -	n_3
0.001- 0.01	- (2) (3) -	- (2) (3) -	- - - (4)	- - (3) -	- - - -	n_1
	(1) (2) (3) (4)	- (2) (3) -	- - - -	- (2) - -	- - - -	n_2
	- (2) (3) -	- - - -	- - - (4)	- - - -	- - - -	n_3
0.0001- 0.001	- (2) (3) -	- (2) (3) -	- - - (4)	- - (3) -	- - - -	n_1
	(1) (2) (3) -	(1) (2) (3) -	- - - -	- (2) - (4)	- - - -	n_2
	- (2) (3) -	- (2) (3) -	- - - (4)	- - - -	- - - -	n_3
1.0×10^{-5} -0.0001	- (2) (3) -	- (2) (3) -	- - - (4)	(1) (2) (3) -	- - (3) -	n_1
	- (2) (3) -	(1) (2) (3) -	- - - -	(1) (2) - (4)	- (2) - (4)	n_2
	- (2) (3) -	- (2) (3) -	- - - (4)	- - - -	- - - -	n_3

III THEORY OF THE CONTROL OF THE SATELLITES' ATTITUDES

A THE MOTION REQUIREMENTS IN TERMS OF THE STATE OF THE PLANT

In Chapter I, Section A, the attitude motion requirements of the satellites were given in geometric terms. Here, they will be given in an algebraic form.

In Chapter II the differential equations of attitude motion were derived in terms of the three-axes Euler angles, $\theta_1, \theta_2, \theta_3$, which define the orientation of the satellite with respect to the orbiting earth-pointing reference frame. On page 14 of Chapter II the three second-order differential equations of attitude motion were replaced with six first-order differential equations by defining the vector $\underline{x} = (x_1, x_2, \dots, x_6)^t$. The state of the plant at some time, τ , is defined to be the six-dimensional vector $\underline{x}(\tau) = [x_1(\tau), x_2(\tau), \dots, x_6(\tau)]^t$. The state space is the six-dimensional euclidian vector space, X , of which $\underline{x}(\tau)$ is an element.

High accuracy earth-pointing requires that $x_i, i = 1, 2, \dots, 6$, be kept less than or equal to given small positive numbers for the lifetime of the satellite. (See Appendix D.) Let $s_i, i = 1, 2, \dots, 6$, be these given* small positive numbers. Then it is required that $x_i \leq s_i, i = 1, 2, \dots, 6$. These inequalities define a closed and bounded region, S , of the vector space X which contains the origin or zero vector.

B SATISFACTORY PERFORMANCE AND THE COST

A satellite attitude controller (see Figure 3.1) will be said to have satisfactory performance if acquisition to the region S from $x_i \approx 1.50 < \pi/2, i = 1, 2, \dots, 6$, can be accomplished with near minimum cost in less than the time of one quarter orbit and if the station-keeping part of the controller with near minimum cost for the lifetime of the satellite can keep the state space trajectory from departing the region S by a significant amount (except when large unaccounted for disturbances overpower the station-keeping part of the controller).

* See Chapter IV

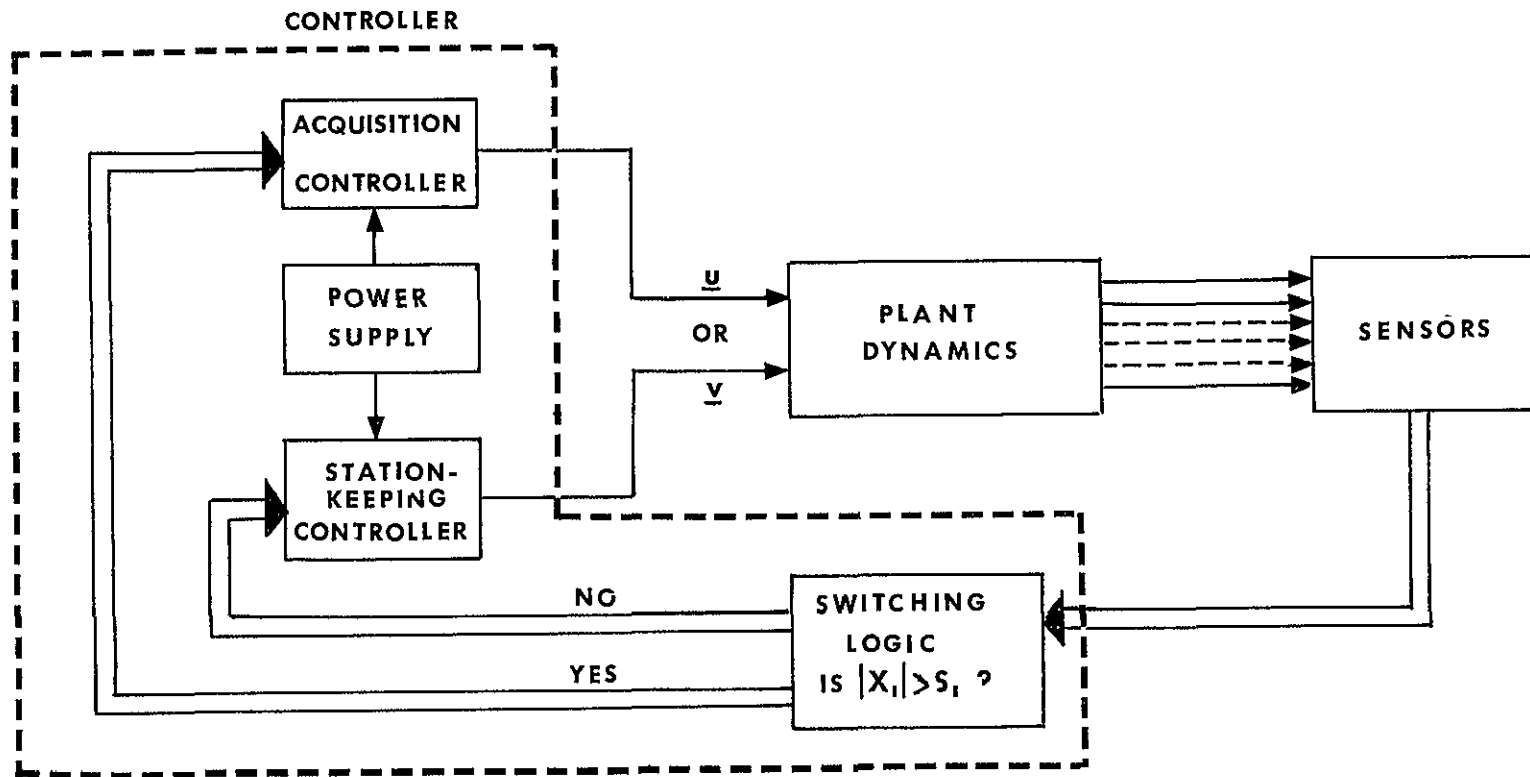


Figure 3.1 A Simplified Diagram of the Controlled Attitude System

The cost of a satisfactorily performing satellite is ultimately a combination of the monetary cost and time costs of producing the satellite which performs the required mission. In this presentation it is assumed that except for the attitude controller the satellite is of a given configuration and cost, so that, reductions in cost are obtainable only by reducing the cost of the controller

The cost of the controller is not just the cost of constructing the controller and operating it in orbit but includes the cost of placing the controller in orbit with the satellite. A heavy controller will require more power from the vehicle which orbits the satellite than a light controller

When the controller uses gas jets to provide the control torque, the weight of the fuel for the gas jets can increase the cost even if increases in the cost of orbiting the satellite are not considered. For example, the increase in cost due to an increase in the weight of the fuel can result from expensive packaging caused by the increase in volume of the fuel container or from the increase in the cost of constructing the fuel container which must withstand higher pressures if the volume is kept small

The feedback attitude controller will contain electronic computing elements and gas jet thrusters. The number, sizes, weights and complexities of these should be kept at a minimum for minimum overall cost. It is true that the use of off-the-shelf hardware components will reduce the cost if the weights and complexities of these components are not prohibitive.

Thus, to reduce the cost of the attitude controller the weight of the controller should be reduced as much as possible compatible with inexpensive off-the-shelf components and with the simplicity of the overall system

The power supply for a year or more of control is the heaviest component of the controller so that the weight of the power supply should be at the focus of attention. Other components are nearly fixed in weight by the state of the art except for the thrusters which generally decrease in size and weight with decrease in thrust magnitudes. It should be

pointed out, however, that for very small thrust requirements hot gas or ion thrusters are used and they require a weightly power supply for supplying heat

For a controller which utilizes gas jets for control the power supply consists of the fuel, which is usually an inert gas, the fuel container, tubes for carrying the fuel to the thrusters and pressure regulating devices. Except for the fuel, the components of the power supply are nearly standard in weight for all but high gas pressures. By reducing the weight of the fuel, the gas pressure and/or volume will be reduced. Thus, the weight of the fuel will be at the focus of further attention.

C THE OBJECTIVE

In summary, the objective is to determine a controller which will acquire the region S of the state space within the one quarter orbit time limit from values of x_1 , $i = 1, 2, \dots, 6$, of about 1.5 radians and which will keep the state of the system within S for the remaining lifetime of the satellite while using as little fuel as possible compatible with costs due to the complexity of components and the development of new components.

D. MATHEMATICAL TOOLS USED FOR DETERMINING A CONTROL LAW

Two basic approaches to solving the problem of determining a control law are

- 1) The application of mathematical results based on fundamental principles which apply to the minimization problem
- 2) The simulation on an analog or digital computer of the plant with various controllers which are determined by theoretical knowledge of the behavior of the plant under the action of the controllers

In the mathematical theory the problem to be solved is one in the field of optimal control with inequality constraints on the state variables (the station-keeping part) and without such constraints (the acquisition part).

Pontryagin's Maximum Principle [29] and extensions of it will be used as a mathematical aid in obtaining solutions to both the acquisition problem and the station-keeping problem. For future use Pontryagin's Maximum Principle is stated below in the form which is applicable to both problems.

1. Pontryagin's Maximum Principle for Nonautonomous Systems

The maximum principle gives necessary conditions for the solution of the optimal problem

Suppose the following are given

- 1) The differential equations of motion

$$\underline{x}' = \underline{f}(\underline{x}, \underline{v}, \tau) \quad (3.1)$$

where $\underline{x} = (x_1, \dots, x_n)^t$ and $\underline{f} = (f^1, \dots, f^n)^t$. (For example, equation (3.1) can represent equations (2.14).)

- 2) An initial point in the state space, say \underline{x}_0 , which describes the motion at an initial time, τ_0 , after which the motion is considered to be under the influence of the control, \underline{v}
- 3) A final point in the state space, say \underline{x}_f , which describes the motion at the final instant of consideration, τ_f
- 4) The cost functional

$$J = \int_{\tau_0}^{\tau_f} f^0[\underline{x}(\tau), \underline{v}(\tau)] d\tau \quad (3.2)$$

Then the optimal problem is to find the control $\underline{v} = \underline{v}(\tau)$, which is at least as smooth as piecewise continuous, that causes the motion to be given by \underline{x}_f at τ_f and results in the minimization of J

It should be pointed out that the maximum principle applies to problems in which the control is much less smooth than piecewise continuous. However, there is no need to consider a more general class of control since the control devices considered here are adequately described by piecewise continuous functions.

The set V is defined as the set of all bounded piecewise continuous vector functions $\underline{v} = \underline{v}(\tau)$. The function $H[p(\tau), \underline{x}(\tau), \tau,$

$\underline{v}(\tau)]$, the Hamiltonian, is defined by

$$H(\underline{p}, \underline{x}, \tau, \underline{v}) = \sum_{i=0}^n p_i f^i(\underline{x}, \underline{v}, \tau) \quad (3.3)$$

where $\underline{p} = (p_0, p_1, \dots, p_n)^t$ is defined in detail below $H_{\max}(\underline{p}, \underline{x}, \tau)$ is given by

$$H_{\max}[\underline{p}(\tau), \underline{x}(\tau), \tau] = \max_{\underline{v}(\tau) \in V} H[\underline{p}(\tau), \underline{x}(\tau), \tau, \underline{v}(\tau)] \quad (3.4)$$

where the maximization of H on $\underline{v}(\tau)$ is with respect to $\underline{p}(\tau)$, $\underline{x}(\tau)$ and τ

In order that $\underline{v}(\tau)$ yield a solution of the given optimal problem it is necessary that there exist a nonzero continuous vector function $\underline{p}(\tau) = [p_0(\tau), p_1(\tau), \dots, p_n(\tau)]^t$ corresponding to the functions $\underline{v}(\tau)$ and $\underline{x}(\tau)$ through equation (3.1) and

$$p_1' = -\partial H / \partial x_1, \quad i = 1, \dots, n \quad (3.5)$$

such that

(1) for all τ , $\tau_0 \leq \tau \leq \tau_f$, the function $H[\underline{p}(\tau), \underline{x}(\tau), \tau, \underline{v}]$ of the variable $\underline{v} \in V$ attains its maximum value at $\underline{v} = \underline{v}(\tau)$, $i \in$,

$$H[\underline{p}(\tau), \underline{x}(\tau), \tau, \underline{v}(\tau)] = H_{\max}[\underline{p}(\tau), \underline{x}(\tau), \tau]$$

where H is given by equation (3.3) and H_{\max} is given by equation (3.4),

(11) the function $p_0(\tau)$ is a nonpositive constant

This is a statement of Pontryagin's Maximum Principle (PMP) for nonautonomous systems. Pontryagin, et al [29] assume that $f^0(\underline{x}, \underline{v})$ and $\underline{f}(\underline{x}, \underline{v}, \tau)$ have continuous first derivatives in \underline{x} in their proof of the maximum principle. This restriction in the proof can be weakened so that the maximum principle applies to problems in which $\partial f^0(\underline{x}(\tau), \underline{v}(\tau)) / \partial x_1$ is only continuous almost everywhere. Breakwell [3] gives a derivation in this case for autonomous systems in an early paper. A slight extension of Halkin's work [17] results in a proof. Rozoner [30] gives a proof for optimal problems in which both $f^0(\underline{x}, \underline{v})$ and $\underline{f}(\underline{x}, \underline{v}, \tau)$ have continuous second derivatives in \underline{x}_1 . This proof can be modified so that

it is clear that PMP applies to problems which have $f^0(\underline{x}, \underline{v})$ smooth only almost everywhere along $\underline{x}(\tau)$, $\tau_0 \leq \tau \leq \tau_f$

The maximum principle as stated above can be extended to apply to the optimal station-keeping problem and to the optimal acquisition problem in the case acquisition to the region S is required rather than the case were acquisition to the origin of the state space, X , is required. The applications of the maximum principle to these problems differ primarily in the boundary conditions

Before the maximum principle is applied to an optimal problem there should be some certainty that the results of the application will give correct information about the solution of the problem. The maximum principle gives conditions which, if they are not satisfied, imply that the control is not optimal.

Suppose that there are many controls $\underline{v} \in V$ which take \underline{x}_0 to \underline{x}_f and suppose that only one of these satisfies the maximum principle. Then this one control is the optimal control if an optimal control exists. An optimal solution does not exist if the functional J for the control $\underline{v} \in V$ which takes \underline{x}_0 to \underline{x}_f while satisfying the maximum principle is not a minimum. Otherwise, a solution to the optimal problem exists.

In the present investigation Pontryagin's Maximum Principle gives a complete set of relations for the determination of a control. Even so and even if a solution exists, there is no guarantee that the control obtained from the maximum principle does not give a local minimum of J .

In the linearized acquisition problem an optimal solution exists for $\underline{v} \in V$ and the functional J does not have local minima, so that for a solution of the optimal linearized acquisition problem, Pontryagin's Maximum Principle gives sufficiency conditions. A proof of this can be found in Rozonoer [30] for the case when $f(\underline{x}, \underline{v}, \tau)$ and $f^0(\underline{x}, \underline{v})$ have continuous first derivatives in \underline{x} which is true in the acquisition problem.

In the application of the maximum principle to the approximate station-keeping problems, the function $f^0(\underline{x}, \underline{v})$ is either nonlinear or has derivatives in \underline{x}_1 which are only almost everywhere continuous in $\underline{x}(\tau)$. In this case Rozonoer's proof of the sufficiency of the conditions

of the maximum principle does not hold. However, since the conditions of the maximum principle are necessary conditions and since they are sufficient to determine a unique motion, then they are sufficiency conditions for the optimal solution if an optimal solution exists. In the case of the approximate station-keeping problems, the existence is concluded by direct reasoning.

2. Application to the Acquisition Problem

Busch [6] has found a nearly optimal feedback control which will cause the motion to proceed from \underline{x}_0 to near zero for a "stable" satellite configuration. For simplicity and reliability Busch's control law is a function of the state only. The method Busch uses for determining a control law from the maximum principle is reverse-time integration, i.e., once $\underline{v} = \chi(p, \underline{x}, \tau)$ has been found from the maximization of the Hamiltonian H (see equation (3.4)), the equations (3.1) and (3.5) are integrated backwards from $p(\tau_f)$ and \underline{x}_f to \underline{x}_0 and $p(\tau_0)$. The solutions $\underline{x}(\tau)$ and $p(\tau)$, $\tau_0 \leq \tau \leq \tau_f$, are then analyzed in order that characteristics of the solutions $\underline{x}(\tau)$ and $p(\tau)$ can be found which enable the control to be written as

$$\underline{v} = \underline{v}(\underline{x}, \tau) \quad (3.6)$$

In the reverse time integration procedure τ is replaced with $\tau^* = \tau_f - \tau$ and \underline{x}_0 is determined by the choice of p_f and the interval of integration, $\tau_f - \tau$ (when \underline{x}_f is given).

In Chapter V a solution to the problem of the optimal acquisition control of unstable satellites is given. This solution is based on Busch's solution, the maximum principle and the imposed time limit of acquisition.

3. Application to Approximate Station-Keeping Problems

Approximate solutions of the station-keeping problem can be obtained from PMP by taking the cost functional to be of the form

$$J = \int_{\tau_0}^{\tau_f} [f(\underline{x}) + g(\underline{v})] d\tau \quad (3.7)$$

where $g(\underline{v})$ is scalar function of the control vector and $f(\underline{x})$, a "penalty function", is a scalar function of the state vector.

Since the minimization of the weight of the fuel is required, $g(\underline{v})$ is chosen as

$$g(\underline{v}) = \sum_{i=1}^3 |v_i| \quad (3.8)$$

The optimal control for the problem with the cost functional given by (3.7) with (3.8) and any $f(\underline{x})$ corresponds to the use of simple gas jets

The "penalty function" is chosen such that the control keeps \underline{x} in or very near S while using the least possible amount of fuel. If $f(\underline{x})$ is chosen so that it is zero when \underline{x} is in S , the functional (3.8) to be minimized becomes the minimum fuel functional while \underline{x} is in S . Thus, it seems that the fuel expenditure should be a minimum at least for those period when \underline{x} is in S .

Possible nonnegative functions which are zero when \underline{x} is in S are

$$f_1(\underline{x}) = \sum_{i=1}^6 \begin{cases} 0 & \text{if } |x_i| \leq s_i \\ 10^{n_i}(x_i - s_i) & \text{if } x_i > s_i \\ -10^{n_i}(x_i + s_i) & \text{if } x_i < -s_i \end{cases} \quad (3.9)$$

$$f_2(\underline{x}) = \sum_{i=1}^6 \begin{cases} 0 & \text{if } |x_i| \leq s_i \\ \frac{1}{2} 10^{n_i}(x_i - s_i)^2 & \text{if } x_i > s_i \\ \frac{1}{2} 10^{n_i}(x_i + s_i)^2 & \text{if } x_i < -s_i \end{cases} \quad (3.10)$$

⋮

(continued)

$$f_e(\underline{x}) = \sum_{i=1}^6 \begin{cases} 0 & \text{if } |\underline{x}_1| \leq s_1 \\ \exp[10^{-n_1}(\underline{x}_1 - s_1)] - 1 & \text{if } \underline{x}_1 > s_1 \\ \exp[-10^{-n_1}(\underline{x}_1 + s_1)] - 1 & \text{if } \underline{x}_1 < -s_1 \end{cases} \quad (3.11)$$

where $n_1, i = 1, \dots, 6$, are numbers chosen so that \underline{x} stays in or near S .

Functions similar to

$$f_s(\underline{x}) = \sum_{i=1}^6 k_1 |\underline{x}_1| / (\ell_1 \cdot s_1 - |\underline{x}_1|) \quad (3.12)$$

where k_1 and ℓ_1 (a number slightly greater than one) are chosen to keep \underline{x} near S , are possible choices. Since they exhibit singular behavior as $|\underline{x}_1| \rightarrow \ell_1 \cdot s_1$, they result in the state staying very near the boundary of S or in S (depending on ℓ_1), but, since they are not zero for \underline{x} in S , fuel is wasted.

For an idea of the relative values of the functions given by equations (3.9), (3.10), (3.11) and (3.12) for values of \underline{x}_1 see Figure 3.2.

Since in the station-keeping problem \underline{x}_0 and \underline{x}_f are arbitrary to within being in S or on the boundary of S , the boundary conditions on the variable $p(\tau)$ are somewhat better known in advance in the station-keeping problem than in the acquisition problem.

In Pontryagin, et al. [29] and in Rozonoer [30] it is shown that a necessary condition for an optimal solution is

$$\underline{p}(\tau_f) = [p_1(\tau_f), \dots, p_n(\tau_f)]^t = (0, \dots, 0)^t \quad (3.13)$$

if $\underline{x}(\tau_f)$ is (free) in the interior of S or

$$\underline{p}(\tau_f) = [p_1(\tau_f), \dots, p_n(\tau_f)]^t = -\mu \underline{b}(\underline{x}_f) \quad (3.14)$$

if $\underline{x}(\tau_f)$ is (free) on the boundary of S . The vector $\underline{b}(\underline{x}_f)$ is the outer normal to the boundary of S at $\underline{x}(\tau_f)$, μ is a nonnegative constant.

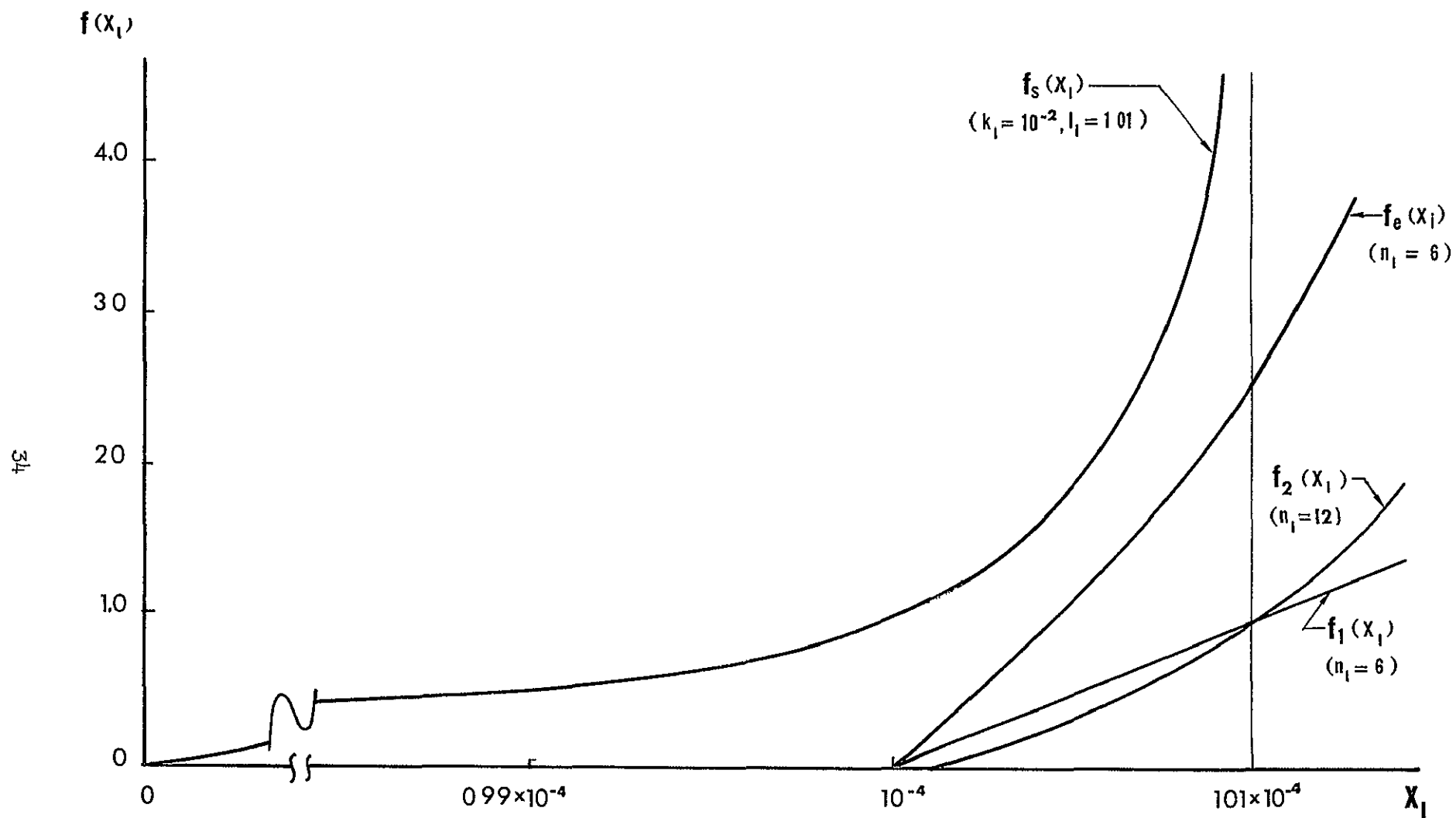


Figure 3.2. The Functions f_1, f_2, f_e and f_s for $s_1 = 10^{-4}$

and $n = 6$ in the present investigation

The relation expressed by equation (3 14) is called the transversality condition. Since S is defined by $|x_i| \leq s_i, i = 1, \dots, 6$, equation (3 14) can be written as

$$p_i(\tau_f) = -\mu \operatorname{sgn} [x_i(\tau_f)], i = 1, \dots, 6 \quad (3 14')$$

The maximum principle requires that p_0 be a nonpositive constant. Rozonoer has shown that if $p_0 = -\lambda$, then a necessary condition is $\lambda > 0$. Since H is homogeneous in $p_i, i = 1, \dots, 6$, the maximization of H is independent of λ . For convenience choose $\lambda = 1$.

The initial value $\underline{p}(\tau_0)$ is in general not known. If $\underline{x}(\tau_0)$ is required to be on the boundary of S , then $\underline{p}(\tau_0)$ must satisfy a condition similar to that given in equation (3 14). Otherwise, $\underline{p}(\tau_0)$ is unknown. Since $\underline{x}(\tau_0)$ is not required to be on the boundary of S , the transversality condition for $\underline{x}(\tau_0)$ is not applied.

It should be noted that the boundary conditions given by equation (3 14) do not apply when \underline{x} is on a "corner" of S , i.e., a point on the boundary of S at which two of $|x_i|, i = 1, \dots, 6$, or both of $|x_5|$ and $|x_6|$ are equal to the corresponding numbers s_i . This follows from the fact that the normal to the boundary of S is not defined at a "corner". If this should present a problem, the "corner" can be smoothed out by constructing a suitably smooth "surface" in the "corner" between the faces of the polyhedron in the six dimensional space. (If these surfaces are small enough, no physically measurable changes in the boundary will occur.)

The above boundary conditions and the cost functionals given by (3 7)-(3 11) are used in Chapter IV with the maximum principle to determine approximate solutions of the steady-state problem.

Similar approximate methods of solution for linear, minimum time problems with restricted phase coordinates has been developed by Lee [24] and by Russell [31]. Lee applies the method to the minimum time acquisition problem of a $1/s^2$ plant with bounded phase coordinates.

4 Necessary Conditions for an Exact Solution (NCES) of the Station-Keeping Problem

Several investigators have to some extent developed exact solutions to the bounded phase coordinate optimal control problem. Bryson, Denham and Dreyfus [5] have found necessary conditions for solving problems in which the control is a scalar and certain smoothness assumptions must hold. Chang [7] and Russell [31] are concerned with sufficiency conditions for solving the linear, minimum time acquisition problem with bounded phase coordinates. Pontryagin, et al [29] devote their Chapter VI to obtaining necessary conditions for the solution of the optimal control problem with restricted phase coordinates. These necessary conditions, which are discussed in this section, will be used in the derivation of the station-keeping control law in Chapter IV.

Since the control function $\underline{v}(\tau)$ is piecewise smooth (discontinuities of the first kind) and since the other terms in the right hand side of the differential equations of motion are smooth, there exists only a finite number of points in time at which the trajectory, $\underline{x}(\tau)$, is on the boundary and either $\underline{x}(\tau^-)$ or $\underline{x}(\tau^+)$ or both are not on the boundary. If $\underline{x}(\tau)$ is the state at such a point in time τ and if both $\underline{x}(\tau^-)$ and $\underline{x}(\tau^+)$ are in the interior of S or one is on the boundary of S , then the point $\underline{x}(\tau)$ is called a junction point of the trajectory. Of course, there are only a finite number of junction points.

In the derivation of the necessary conditions for an optimal trajectory with restricted states it is assumed that: (1) the optimal trajectory has only a finite number of junction points, (2) the optimal trajectory lies either entirely in S or on the boundary of S , and, (3) the parts of the optimal trajectory which lie on the boundary of S for a finite interval of time must be "regular".

The boundary of the region S must be somewhat "regular" or smooth, i.e., if $s(\underline{x}) = 0$ describes the boundary of S , then $\text{grad } s(\underline{x})$ must be continuous and not vanish for any \underline{x} in the boundary of S . In the station-keeping problem with S defined by $|x_1| \leq s_1$, $i = 1, 2, \dots, 6$, this is not the case unless the "corners" of S are avoided when the trajectory coincides with the boundary of S . By

suitably "smoothing" the "corners" (see p 35 of this section) this mathematical difficulty is overcome. In Chapter IV the NCEs are applied to several approximate single-axis satellite motions by replacing the "non-regular" boundaries of a phase-plane projection of S with appropriate "regular" boundaries. These "regular" boundaries are sections of known optimal trajectories which must exist and deviate from the phase-plane projection of S (for bounded \underline{v}) by some small allowable amount.

In Chapter VI of Pontryagin, et al., the concept of regularity is used in the derivation of necessary conditions for optimality of those parts of the trajectory (if any) which lie entirely on the boundary of S . It should be noted that Pontryagin, et al., derived these necessary conditions under the assumption that each of $f^0(\underline{x}, \underline{v})$ and $\underline{f}(\underline{x}, \underline{v}, \tau)$ have continuous first derivatives in both \underline{x} and \underline{v} . If it is assumed that $f^0(\underline{x}, \underline{v})$ has only continuous first derivatives in \underline{x} and not in \underline{v} , then a weaker set of necessary conditions are obtained. These weaker conditions are the same as Theorem 22 of Pontryagin, et al., except that $\partial H / \partial \underline{v}$ does not exist everywhere along the trajectory which coincides with the boundary.

If there exists an optimal trajectory which lies in the region S , it is possible that part of this trajectory lies entirely in the interior of S . These parts of the optimal trajectory must satisfy the conditions of the maximum principle.

If the regular optimal trajectory contains only a finite number of junction points, then an additional condition on the function $\underline{p}(\tau)$ at the junction time can be derived. Pontryagin, et al., call this condition the jump condition. The jump condition is satisfied if one of the two following conditions is satisfied:

$$\underline{p}(\tau^+) = \underline{p}(\tau^-) + \mu \text{ grad } s[\underline{x}(\tau)]$$

$$\underline{p}(\tau^+) = \underline{p}(\tau^-) + \mu \text{ grad } s[\underline{x}(\tau)] = 0, \quad \mu \neq 0 \quad (3.15)$$

where μ is a number to be determined.

(In the station-keeping problem the region S has corners. In a note in Chapter VI of Pontryagin, et al., (page 310) it is pointed out that jump conditions completely analogous to those of equations (3.15)

must be satisfied at the transition point from one smooth part of the boundary of S to another)

The necessary conditions for an exact solution of the station-keeping problem can be summarized as follows. The conditions of the maximum principle must be satisfied by each part of the regular optimal trajectory which lies in the interior of the region S . The conditions of Theorem 22 of Pontryagin, et al , must be satisfied by those parts of the optimal trajectory which lie entirely on the boundary of S . The jump condition must be satisfied at a junction point

The above necessary conditions are, generally, insufficient to determine the optimal control. Without any conditions other than those above the search for the optimal control must, usually, be carried out in a large dimension parameter space. Parameters of this space include the number of junction points, the number of the parts of the trajectory which lie on the boundary, the boundary conditions $p(\tau_0)$ and $p(\tau_f)$ and the number μ

In the next chapter the above necessary conditions will be used in a search for a control law for the station-keeping problem. This search will also be aided by the optimal solutions to the several approximate station-keeping problems

IV DERIVATION OF STATION-KEEPING CONTROLS LAWS

The attitude motion of a satellite in the steady-state mode of controlled motion is to be such that

- 1) The initial instant of station-keeping, τ_0 , is arbitrary, i.e., τ_0 is the time at which the satellite is at an arbitrary point in its orbit,
- 2) The motion at time τ_0 is arbitrary to within $\underline{x}(\tau_0)$ being in the region S of the state space,
- 3) The motion after τ_0 and until some given final time τ_f must be the result of a control $\underline{v}(\tau)$, $\tau_0 \leq \tau \leq \tau_f$, which keeps $\underline{x}(\tau)$, $\tau_0 < \tau \leq \tau_f$ from departing the region S and which uses as little fuel as possible

In the application of the theory of the previous chapter to the search for station-keeping control laws, it is convenient to take $\tau_0 = 0$, $\tau_f = 2\pi$ and (in either (2.17) or (2.18)) $\theta_0 = 0$. This can be done without loss of generality since (1) $\underline{x}(\tau_0)$ and $\underline{x}(\tau_f)$ are arbitrary to within their being in S ($\underline{x}(\tau_0)$ can be the final state of an acquisition trajectory or the final state of a previously considered station-keeping trajectory), (2) The equations of motion are periodic with a period of 2π radians, and, (3) In the lifetime of a typical satellite the boundary of S is encountered many thousands of times and the region S is nearly covered by the state-space trajectory (see Part 1 of Section A)

The region S was defined to within the numbers $s_1, 1 = 1, \dots, 6$, in Section A of Chapter III. If $s_1, 1 = 1, \dots, 6$, are greater than about 10^{-2} , the simplified steady-state equations of motion do not give a suitable description of the motion. The lower limits on $s_1, 1 = 1, \dots, 6$, are fixed by the state-of-the-art in the construction of sensors and controllers which have very small gas jet thrust and/or time delays. Hereafter, the numbers $s_1, 1 = 1, \dots, 6$, are assumed to be 10^{-4} unless otherwise specified.

A THE APPROXIMATE SOLUTIONS - SPECIAL ORBITS

In this section several approximate solutions will be presented. They are approximate solutions to the problem of determining a control which will keep the state of a satellite's attitude motion in the region S while minimizing the fuel used.

The approximate solutions are approximations in the sense that the state space trajectories are allowed to exist the region S by a small distance (compared to the maximum dimension of S) and in the sense that integral constraints on the states are used to limit the motion. If the integral constraint is given by

$$0 \leq \int_{\tau_0}^{\tau_f} f[\underline{x}(\tau)] d\tau \leq A$$

where A is a given (perhaps small) positive number and $f(\underline{x})$ is given by (3.9) or (3.10) or (3.11), then this optimal problem is equivalent to the optimal problem of Part 3, Section D of Chapter III. The problems are equivalent in the sense that their solutions (as obtained from the maximum principle) are the same.

In this section the equations of motion are assumed to be given by (2.17) with the angle δ either zero or $\pi/2$ radians. These values correspond to satellites in nearly equatorial or nearly polar orbits, respectively. They are used initially (Part 1) to simplify the analysis although the results do not depend on δ . In Parts 2-4 these orbits, i.e., these values of δ are assumed so that equilibrium points exist.

In Parts 2, 3 and 4 of this section the equations of motion are approximated further. The "stable" single-axis motions of the satellites are approximated by $\ddot{x} + a^2 x = v$, and, the "unstable" single-axis motions are approximated by $\ddot{x} = v$ and $\ddot{x} + a^2 x = v$ with $a^2 < 0$. The study of these simple motions results in characteristics of a suboptimal minimum-fuel station-keeping control as well as a check on the methods of Part 1.

1 A Station-Keeping Control Law Obtained From PMP with

$$J = \int_{\tau_0}^{\tau_f} [f_1(\underline{x}) + \sum_{i=1}^3 |v_i|] d\tau$$

The Hamiltonian for the system of equations (2.17) with $\delta = 0$ or $\delta = \pi/2$ can be written as

$$H = p_2 v_1 + p_4 v_2 + p_6 v_3 - |v_1| - |v_2| - |v_3| + (\text{terms which do not contain } v_i, i = 1, 2, 3) \quad (4.1)$$

since as was seen in Chapter III p_0 can be taken as -1

The control \underline{v} cannot be optimal unless it maximizes H for all values of \underline{p} , \underline{x} and τ . Thus, from (4.1) the optimal control for bounded v_i must be the "coast function" of \underline{p} given by

$$v_i = \text{CST}(p_{2xi}) = \begin{cases} 0 & , \text{ if } |p_{2xi}| < 1 \\ N_i \text{SGN}(p_{2xi}) & , \text{ if } |p_{2xi}| \geq 1 \end{cases} \quad i = 1, 2, 3$$

where $N_i, i = 1, 2, 3$, are given positive numbers and $\text{SGN}(g) = (g)/|(g)|$

Since the last two equations of (2.17), the pitch equations, are not coupled to the first four of (2.17), the yaw-roll equations, the controlled pitch motion can be solved for independently of the yaw-roll motion. These equations (for the cases when $\delta \approx 0$ or $\delta \approx \pi/2$) with the corresponding equations for the adjoint variables as determined from (3.5) can be written in backwards times by letting $\tau^* = 2\pi - \tau$ as follows

yaw-roll

$$\dot{x}_1 = -x_2$$

$$\dot{x}_2 = k_1 A_1^2 x_1 + A_2 x_3 - K_1 A_1 x_4 - v_1$$

$$\dot{x}_3 = -x_4$$

$$\dot{x}_4 = -A_2 x_1 + K_2 A_1 x_2 - k_2 (3A_3 + A_1^2) x_3 - v_2 \quad (4.3)$$

$$\begin{aligned}
\dot{p}_1 &= -F(x_1) - k_1 A_1^2 p_2 + A_2 p_4 \\
\dot{p}_2 &= F(x_2) + p_1 - K_2 A_1 p_4 \\
\dot{p}_3 &= -F(x_3) - A_2 p_2 + k_2 (3A_3 + A_1^2) p_4 \\
\dot{p}_4 &= F(x_4) + K_1 A_1 p_2 + p_3
\end{aligned} \tag{4.4}$$

pitch

$$\begin{aligned}
\dot{x}_5 &= -x_6 \\
\dot{x}_6 &= 3k_3 A_3 x_5 - A_2 - v_3 \\
\dot{p}_5 &= -F(x_5) - 3k_3 A_3 p_6 \\
\dot{p}_6 &= F(x_6) + p_5
\end{aligned} \tag{4.5}$$

$$\tag{4.6}$$

where $\dot{(\cdot)} = d(\cdot)/d\tau^*$, the functions A_1 , A_2 and A_3 are the same as in (2.15) but with τ replaced by τ^* and

$$F(x_1) = \partial f_1(\underline{x}) / \partial x_1 = \begin{cases} 0, & \text{if } |x_1| \leq 10^{-4} \\ 10^{n_1}, & \text{if } x_1 > 10^{-4} \\ -10^{n_1}, & \text{if } x_1 < -10^{-4} \end{cases}, \quad i = 1, \dots, 6 \tag{4.7}$$

Equations (4.3)-(4.6) with (4.2) and the boundary conditions given by (3.13), (3.14') and $\underline{x}(\tau_0^*) = \underline{x}(\tau_f^*)$ are sufficient for determining the controlled motion, $\underline{x}(\tau^*)$, the adjoint variables $\underline{p}(\tau^*)$ and, hence the control $\underline{v}(\tau^*)$ for $\tau_0^* \leq \tau^* \leq \tau_f^*$. These solutions can be used to determine the optimal feedback control law for this problem or at least characteristics of the optimal feedback control law which can be used in the construction of a minimum-fuel suboptimal feedback control law.

Although the differential equations are piecewise linear, it is not practical to invest a great deal of time in a search for their exact solution since the coefficients are time-varying. To determine the feedback control law it is only necessary to determine the values of $\underline{x}(\tau^*)$ and τ^* at which the adjoint variables assume the values of $+1$ or -1 .

Thus, the solution of the equations with the aid of a high-speed computer is perhaps the most logical approach to determining the feedback control law

After a thorough investigation the hope of using the analog computer for solving the above equations was abandoned. The reason for this was that some of the computer variables, i.e., the scaled dependent variables, are generally 10^4 times the other computer variables, so that, it was impossible to obtain an accurate and therefore meaningful solution with this computer.

The equations can be solved accurately enough with a digital computer. A Kutta-Merson integration routine was programmed as an AIGOL procedure on the Burroughs B5500 computer. The Kutta-Merson procedure used was a modified version of the Stanford Computation Center Kutta-Merson procedure. These modifications, the additions of an absolute error bound and a stepsize-cutting limiter, were made to the procedure to reduce the computation time. The modifications did not affect the accuracy in less than the fifth significant figure in the test runs made. A further reduction in the computation time is accomplished by scaling the equations so that the dependent variables are more nearly the same size. A listing of the program used for integrating the equations is given in Appendix F.

Several computer solutions of the yaw-roll equations and of the pitch equations were needed to determine the "best" values of n_1 , $i = 1, \dots, 6$, in the penalty function and N_1 , $i = 1, 2, 3$. (These "best" values are the values which result in the fuel cost being as small as possible while the control keeps $|x_1| \leq 1.1 \times 10^{-4}$, $i = 1, \dots, 6$.)

The initial choice of values for n_1 and N_1 was made in the following way. The possible choices on N_1 lie in a range from the smallest values with which control will be maintained at all times up to the largest values which cause changes in the motion to occur too rapidly. In practice the smaller values are the logical ones to choose since with large N_1 the inherent imperfections in the controller can cause unsatisfactory motion and wasted fuel. The smallest possible values of N_1 such that control could always be maintained, even if $|x_1|$, $i = 1, \dots, 6$, grew to values as large as 2.0×10^{-4} , were chosen. For satellite (2),

for example, these values are $N_1 = 2.1 \times 10^{-4}$, $N_2 = 7.1 \times 10^{-4}$ and $N_3 = 2.06 \times 10^{-2}$

The possible values of n_1 are the real numbers. From the cost functional for this problem it can be seen that its minimum for intervals of time when \underline{x} is not in S is the result of minimizing the part which is a functional of \underline{x} if

$$\sum_{i=1}^4 \pm 10^{n_i} (x_i \mp 10^{-4}) > \sum_{i=1}^2 N_i$$

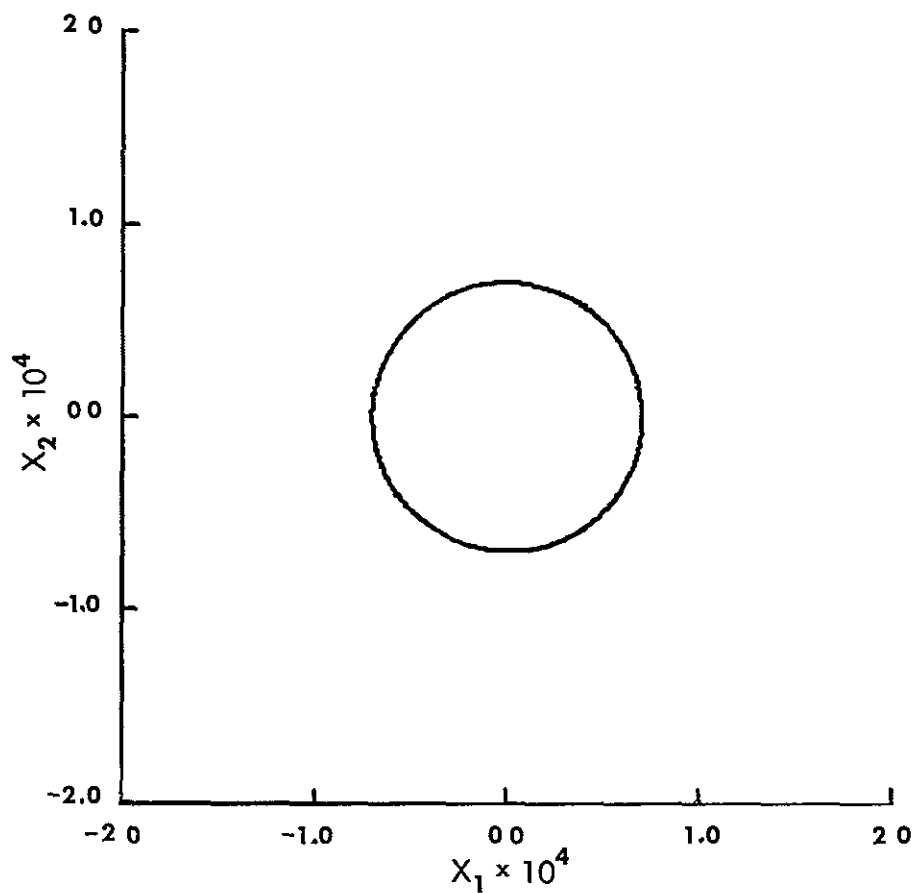
and

$$\sum_{i=5}^6 \pm 10^{n_i} (x_i \mp 10^{-4}) > N_3$$

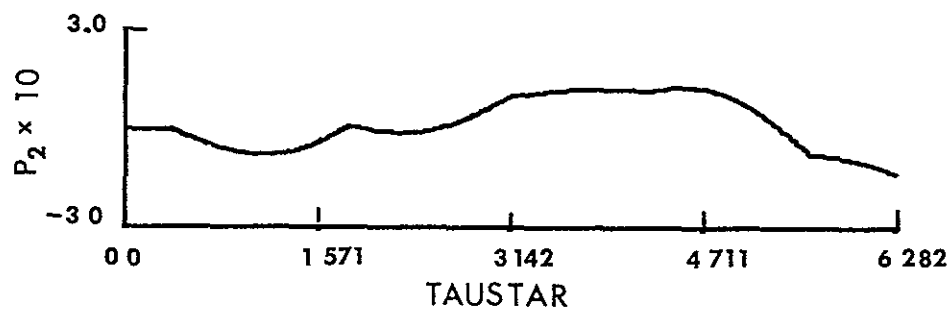
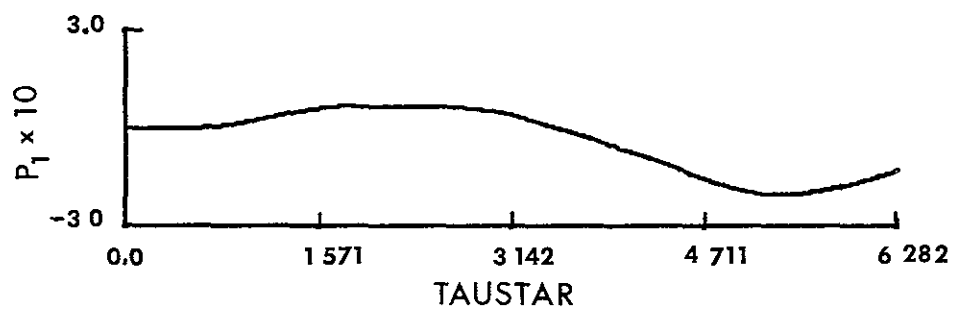
If it is desired to keep $|x_1| \leq 1.1 \times 10^{-4}$, then possible "best" values of n_1 for satellite (2) are $n_1 = 1.0$, $n_2 = 2.0$, $n_3 = 1.0$, $n_4 = 2.0$, $n_5 = 2.0$ and $n_6 = 4.0$. In the choice of these numbers nearly twice the weight was placed on the parts for x_2 , x_4 and x_6 since these variables change more rapidly than x_1 , x_3 and x_5 .

The results of a computer solution of the equations for satellite (2) with the above values of n_1 and N_1 are given in graphical form in Figure 4.1. From this solution it is obvious that the above values of n_1 and N_1 are not the "best" values. Even though this solution exhibits characteristics which aid both the search for the "best" values of n_1 and N_1 and the search for the feedback control law, the cost (in computer time) of continuing this method without other aids is prohibitive.

An approximate solution of the adjoint equations of this problem for arbitrary $\underline{x}(\tau^*)$ can be obtained so that an optimal feedback control law for this problem can be written in terms of n_1 . This approximate solution can be used as an aid in the search for the "best" values of n_1 and N_1 and as a guideline in the search for nearly optimal and practical feedback controllers of the attitude motions of satellites. The approximate solution, which is derived in Appendix E, is

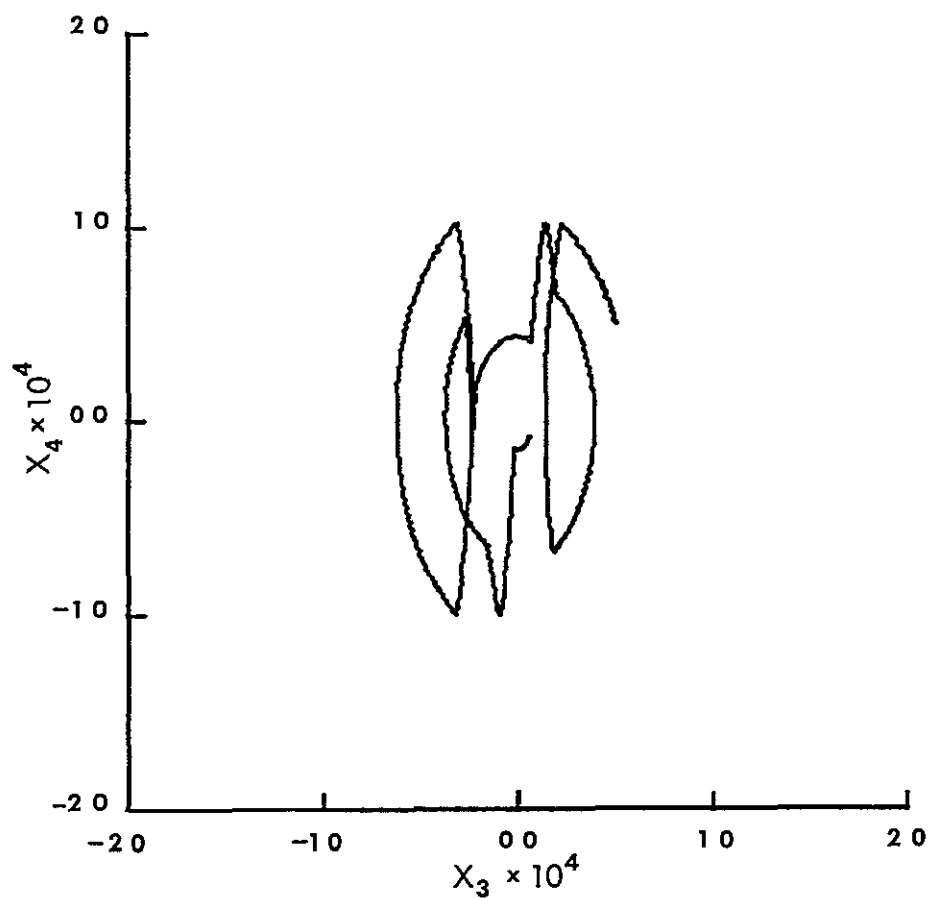


a Yaw Trajectory for $N_1 = 2.1 \times 10^{-4}$

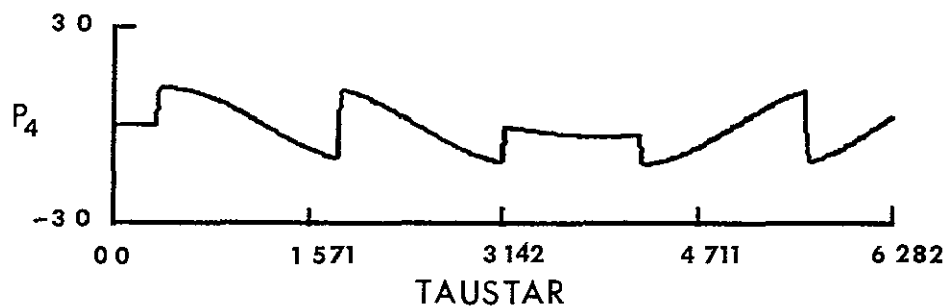
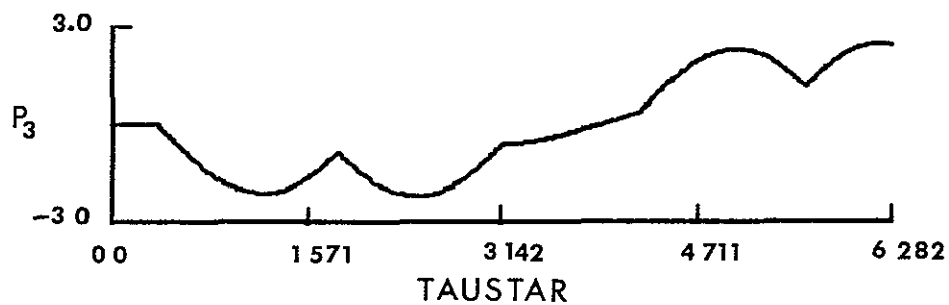


b. Yaw Adjoint Variables for $n_1 = 1.0$, $n_2 = 2.0$

Figure 4.1 Solution of Equations (4.3)-(4.6) for Satellite (2)

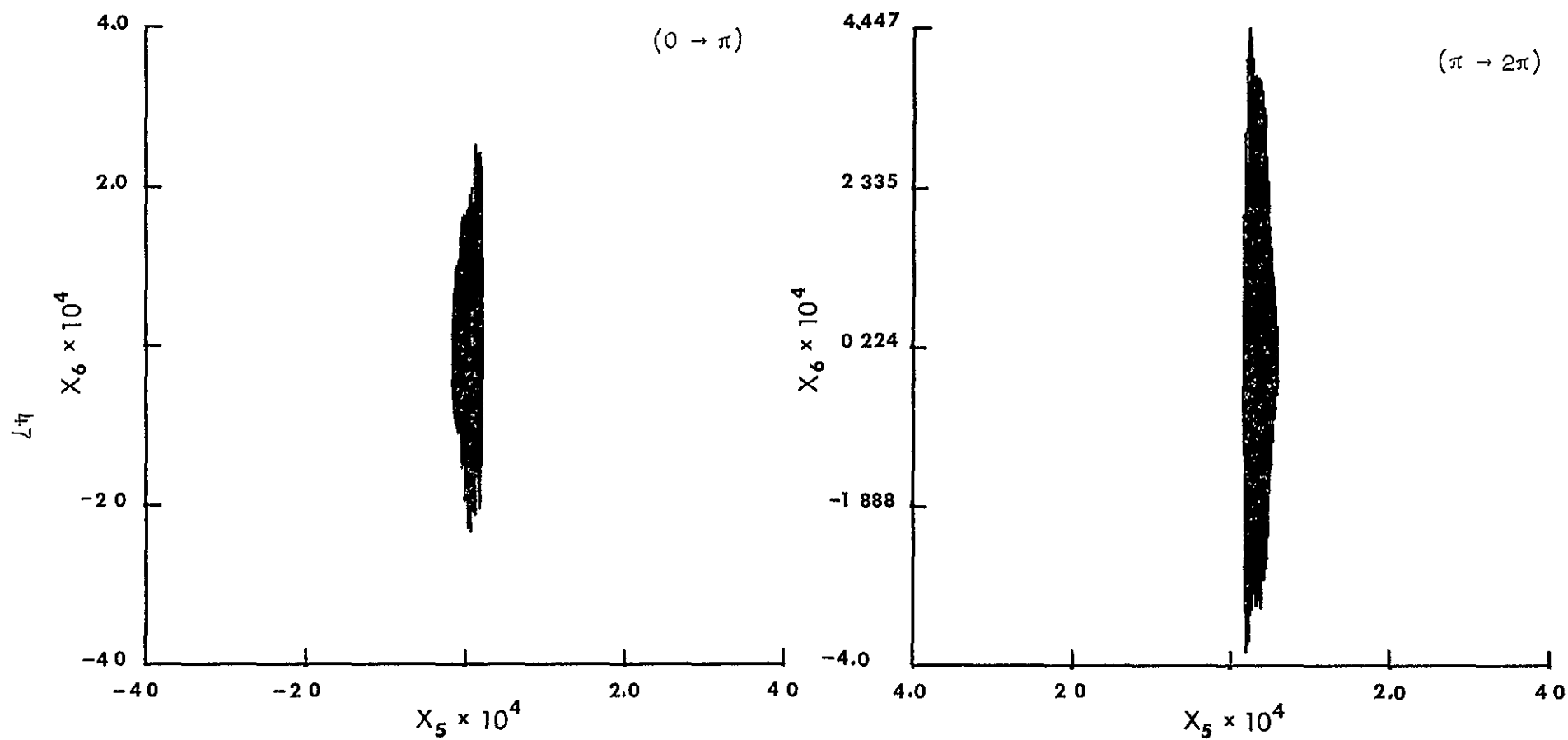


c Roll Trajectory for $N_2 = 7.1 \times 10^{-4}$



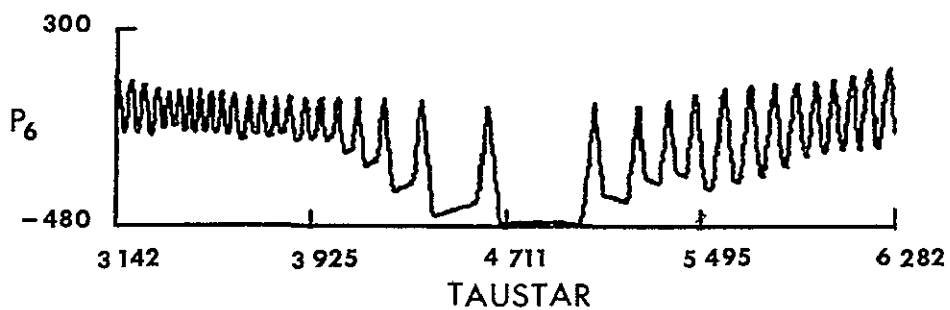
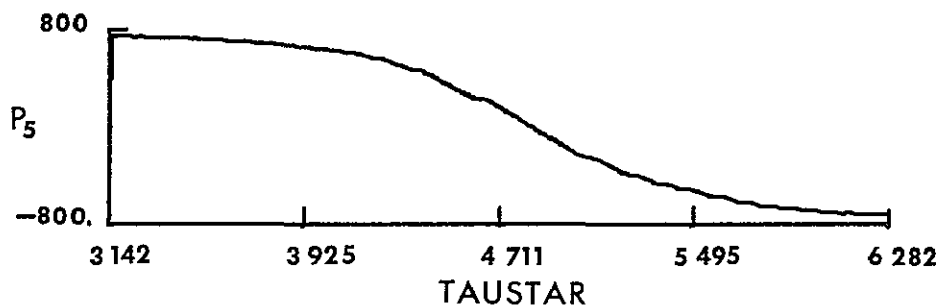
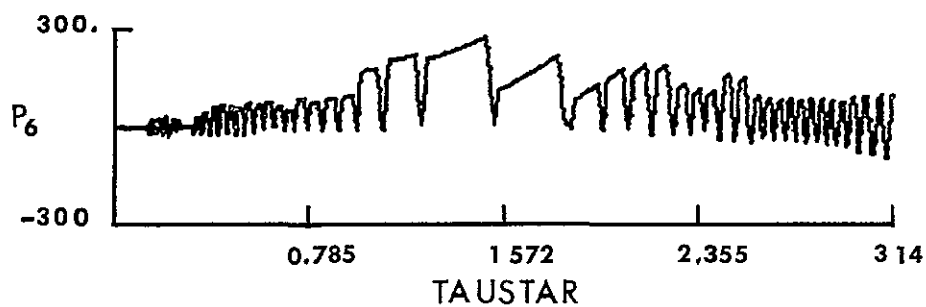
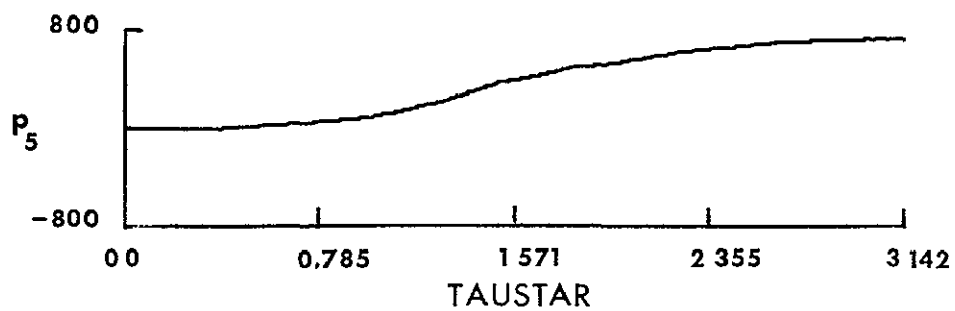
d Roll Adjoint Variables for $n_3 = 1.0$, $n_4 = 2.0$

Figure 4.1 Continued



e Pitch Trajectory for $N_3 = 2.06 \times 10^{-2}$

Figure 4.1 Continued



f Pitch Adjoint Variables for $n_1 = 2.0$, $n_2 = 4.0$

Figure 4.1 Continued

$$\begin{aligned}
p_1(\tau^*) &= p_{1e} \{1 - [(B_3 - B_4) + (\omega_1^2 + \omega_2^2)](\Delta\tau^*)^2\} \\
&\quad - p_{2e} [B_1 \Delta\tau^* + B_4 B_5 (\Delta\tau^*)^2] - p_{3e} B_5 (\Delta\tau^*)^2 - p_{4e} [B_5 \Delta\tau^* \\
&\quad - B_1 B_2 (\Delta\tau^*)^2] - F(x_1) \Delta\tau_1^* - F(x_2) B_1 (\Delta\tau_2^*)^2 - F(x_4) B_5 (\Delta\tau_4^*)^2 \\
p_2(\tau^*) &= p_{1e} \Delta\tau^* + p_{2e} \{1 - [(\omega_1^2 + \omega_2^2) + B_3](\Delta\tau^*)^2\} - p_{3e} B_2 (\Delta\tau^*)^2 \\
&\quad - p_{4e} [B_2 \Delta\tau^* + B_5 (\Delta\tau^*)^2] - F(x_1) (\Delta\tau_1^*)^2 - F(x_4) B_2 (\Delta\tau_4^*)^2 + F(x_2) \Delta\tau_2^* \\
p_3(\tau^*) &= p_{1e} B_5 (\Delta\tau^*)^2 + p_{2e} [B_5 \Delta\tau^* + B_3 B_4 (\Delta\tau^*)^2] + p_{3e} \{1 - [(\omega_1^2 - \omega_2^2) \\
&\quad + (B_1 + B_2)](\Delta\tau^*)^2\} - p_{4e} [B_3 \Delta\tau^* + B_2 B_5 (\Delta\tau^*)^2] \\
&\quad + F(x_2) B_5 (\Delta\tau_2^*)^2 - F(x_3) \Delta\tau_3^* - F(x_4) B_3 (\Delta\tau_4^*)^2 \\
p_4(\tau^*) &= p_{1e} B_4 (\Delta\tau^*)^2 + p_{2e} [B_4 \Delta\tau^* + B_5 (\Delta\tau^*)^2] \\
&\quad + p_{3e} \Delta\tau^* + p_{4e} \{1 - [(\omega_1^2 + \omega_2^2) + B_1](\Delta\tau^*)^2\} + F(x_2) B_4 (\Delta\tau_2^*)^2 \\
&\quad - F(x_3) (\Delta\tau_3^*)^2 + F(x_4) \Delta\tau_4^* \tag{4.8}
\end{aligned}$$

$$\begin{aligned}
p_5(\tau^*) &= p_{5e} [1 - B_6 (\Delta\tau^*)^2] - p_{6e} B_6 \Delta\tau^* - F(x_5) \Delta\tau_5^* - F(x_6) B_6 (\Delta\tau_6^*)^2 \\
p_6(\tau^*) &= p_{5e} \Delta\tau^* + p_{6e} [1 - B_6 (\Delta\tau^*)^2] - F(x_5) (\Delta\tau_5^*)^2 + F(x_6) \Delta\tau_6^* \tag{4.9}
\end{aligned}$$

where $\omega_1, \omega_2, \Delta\tau^*, \Delta\tau_1^*, B_1$ and $p_{1e}, 1 = 1, \dots, 6$, are as defined in Appendix E

In equations (4.8) and (4.9) all of $B_1, 1 = 1, \dots, 6$, are periodic (with a period of 2π) and except for B_5 they are nearly constant. The averages (over the time of one orbit) of $B_1, 1 = 1, \dots, 4, 6$, were substituted into the above equations. B_5 was considered constant in the time between boundary encounters with its value taken as the value

at the time of the previous boundary encounter (Its average value was not used since its average over the time of one orbit is zero) The approximate values for $p_1(\tau^*)$, $i = 1, 2, 6$, which are given by equations (4.8) and (4.9) were compared with the "exact" values obtained from digital computer solutions

Equations (4.3)-(4.6) were solved with the aid of the digital computer for several sets of values of n_i , $i = 1, 2, 6$, and several initial conditions (some of $\underline{x}(\tau_0)$ in the interior of S and some on the boundary of S) The time of solution was $\tau_f^* - \tau_0^* = 6.28 \approx 2\pi$ and the solution was printed out at intervals of τ^* of 0.01 The motions considered were the roll-yaw motions of satellites (1) and (2) and the pitch motions of satellite (3) The control strength used was $N_1 = 2.1 \times 10^{-4}$, $N_2 = 7.1 \times 10^{-4}$ and $N_3 = 2.06 \times 10^{-2}$ These "exact" solutions for $p_1(\tau^*)$, $i = 1, 2, 6$, were compared with the approximate values given by equations (4.8) and (4.9) for as many as ten intervals of time per solution as follows Each solution of $x_1(\tau^*)$, $i = 1, 2, 6$, was applied through $F(x_1)$ to equations (4.8) and (4.9) The initial conditions on p_{1e} , $i = 1, 2, 6$, were the same as $p_1(\tau_0^*)$, $i = 1, 2, 6$ After the initial time τ_0^* the values of p_{1e} , $i = 1, 2, 6$, were taken to be the values of $p_1(\tau^*)$, $i = 1, 2, 6$, at the time the proper (yaw, roll or pitch) trajectory projection reentered the proper projection of S . These new values of p_{1e} were retained until the trajectory exited and reentered S again

In most cases the comparison of the approximate solutions with the "exact" solutions showed that the approximate solutions differed from the exact solutions only in the third significant figure In other cases the difference was only in the fourth significant figure Therefore, if (4.8) and (4.9) are substituted into (4.2), the result is a time-varying feedback control law which is considered optimal for the present problem This control law can be implemented in a controller, but, the devices needed to determine if x_1 is exiting S or entering S when $|x_1| = 10^{-4}$ may be complicated and can be unreliable Timers, which are activated when x_1 , $i = 1, 2, 6$, exit S and reenter S are also needed to generate $\Delta\tau_1^*$, $i = 1, 2, 6$, and $\Delta\tau^*$ Thus, even if this

control law is the optimal minimum fuel control law with best values of n_1 and N_1 for the above satellites, it might not be the least costly control law to implement in practice. More is said about this in Section B.

Estimates of the "best" values of n_1 and N_1 for the satellites can be obtained with the aid of (4.8) and (4.9). If the control is off and $\underline{x}(\tau^*)$ is exiting S, the time it takes for $|\underline{x}_1(\tau^*)|$, $i = 1, \dots, 6$, to increase from 10^{-4} to 1.1×10^{-4} is generally small enough, so that, if NRS_1 , $i = 1, \dots, 6$, is the no-control right hand side of the equations, (4.3) and (4.5), for $\dot{\underline{x}}_1$, $i = 1, \dots, 6$, then

$$\Delta \underline{x}_1 \approx (NRS_1) \Delta \tau_1^* \quad i = 1, \dots, 6 \quad (4.10)$$

is a satisfactory approximation

During those periods of time when the control is off, $|p_1(\tau^*)|$, $i = 2, 4, 6$, must be less than unity. For the control to turn on so that $|\underline{x}_1(\tau^*)|$, $i = 1, \dots, 6$, do not increase to values greater than 1.1×10^{-4} , the values of the corresponding $|p_1(\tau^*)|$, $i = 2, 4, 6$, must be unity or greater at the time when $|\underline{x}_1(\tau^*)| = 1.1 \times 10^{-4}$. Since in (4.8) and (4.9) p_{1e} , $i = 1, \dots, 6$, are nearly periodic with an average over one orbit of nearly zero (see Figure 4.1b, for example) a first approximation is

$$p_2(\tau^*) \approx F(x_2) \Delta \tau_2^* - F(x_1) (\Delta \tau_1^*)^2$$

$$p_4(\tau^*) \approx F(x_4) \Delta \tau_4^* - F(x_3) (\Delta \tau_3^*)^2$$

$$p_6(\tau^*) \approx F(x_6) \Delta \tau_6^* - F(x_5) (\Delta \tau_5^*)^2 \quad (4.11)$$

so that for $|p_1(\tau^*)|$ to grow to unity in the time interval $\Delta \tau_1^*$ in which $|\Delta \underline{x}_1|$ grows to 10^{-5} , i.e., $|\underline{x}_1(\tau^*)|$ increases from 10^{-4} to 1.1×10^{-4} , it must be true (as seen from (4.10) and (4.11)) that

$$10^{-1} = F(x_1) \approx (\Delta \tau_1^*)^{-1} \approx NRS_1 / 10^{-5}, \quad i = 2, 4, 6$$

$$10^{-1} = F(x_1) \approx (\Delta \tau_1^*)^{-2} \approx (NRS_1 / 10^{-5})^2, \quad i = 1, 3, 5 \quad (4.12)$$

Equations (4.12) can be used to determine an estimate of the "best" values for n_1 , $i = 1, \dots, 6$. In (4.12) the largest possible values for NRS_1 should be used since smaller values result in n_1 which are too small to keep $|x_1| \leq 1.1 \times 10^{-4}$. For satellite (2), for example, the largest possible values of NRS_1 for $|x_1| \leq 1.1 \times 10^{-4}$ are $NRS_1 = 1.1 \times 10^{-4}$, $NRS_2 = 1.13 \times 10^{-4}$, $NRS_3 = 1.1 \times 10^{-4}$, $NRS_4 = 3.69 \times 10^{-4}$, $NRS_5 = 1.1 \times 10^{-4}$ and $NRS_6 = 2.06 \times 10^{-1}$. With these values it is found from (4.12) that $n_1 = 2.1$, $n_2 = 1.0$, $n_3 = 2.1$, $n_4 = 1.6$, $n_5 = 2.1$ and $n_6 = 3.3$.

From several digital computer solutions obtained with the above estimates of the best values of n_1 and with several sets of values of N_1 , it was found that some of $|x_1|$, $i = 1, \dots, 6$, grew to values as large as 6.0×10^{-4} , which, of course, is too large. Also, from the solutions it was found that for N_1 and N_2 neither the largest nor the smallest of the values tried were best and for N_3 the smallest value was best. A detailed examination of this result with the aid of (4.2), (4.3), (4.5), (4.8) and (4.9) proved to explain the effects of n_1 and N_1 on the solutions and offered new values of n_1 and N_1 to be tested. (This detailed examination is not given here since it is long and tedious with many numbers and since similar examinations are given in Parts 2 and 3.) With the newly offered values of n_1 and N_1 digital computer solutions were obtained. It was found that the requirement for the "best" values was satisfied by increasing n_1 , $i = 2, 4, 6$, by about one over the above estimated values. As expected, the accuracy of earth-pointing improved and the fuel cost increased to the maximum value, which was for no control-off intervals, with increasing n_1 . Also, it was found that both the fuel cost and the earth-pointing accuracy generally increased with increases in N_1 above their "best" values for values of N_1 less than about 0.1. For values of N_1 of 0.1 or more the fuel cost still increased with increases in N_1 but the accuracy of earth-pointing dropped off sharply. Values of N_1 which were smaller than the "best" values resulted in the control being on so much longer that the fuel cost was generally higher. The "best" values of n_1 and N_1 resulted in the pitch axis control staying on about 95% of the time while the roll-yaw control was on about 33% of the time.

In summary the main result of this part is the time-varying feedback control law given by (4.2) together with (4.8) and (4.9). The control law is optimal in the sense that it was obtained from the sufficient conditions of the maximum principle for the cost functional

$$J = \int_{\tau_0}^{\tau_f} \sum_{i=1}^3 |v_i| d\tau$$

and the integral constraint on the states

$$\int_{\tau_0}^{\tau_f} f_1[\underline{x}(\tau)] d\tau \leq A$$

Other results of this part are (a) a not-too-expensive method has been devised for determining the "best" values of the control law parameters n_1 and N_1 , (b) the effects of varying the parameters n_1 and N_1 from their "best" values was given, and, (c) satellite (2) has the smallest unit fuel cost with the above control. Figure (4.2) shows yaw, roll and pitch projections of a state space trajectory of satellite (2) for the time of one orbit with the above control and the "best" values of n_1 and N_1 .

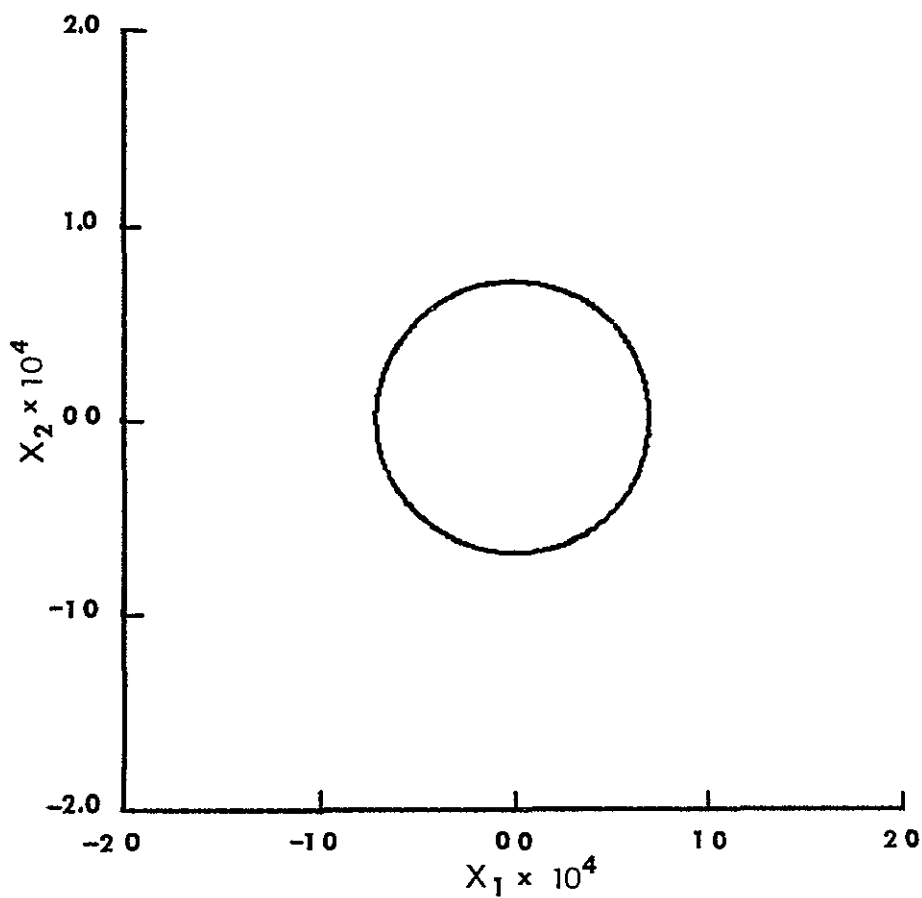
The optimal control of this part is not necessarily minimum fuel optimal. Indeed, it is not difficult to exhibit several controls which keep \underline{x} in S and use less fuel. Since it is very difficult and expensive computer-time to apply the NCES to the full three-axes satellite control problem and since a basis for fuel cost comparison is needed, simple single-axis control problems are now investigated.

2 The Steady-State Motion Obtained From PMP for $\underline{x}'' = \underline{v}$

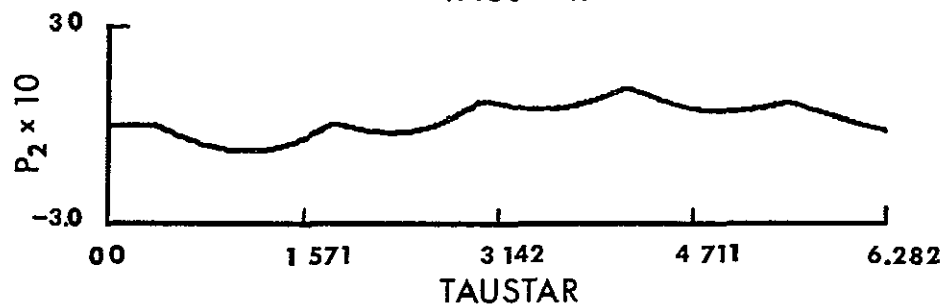
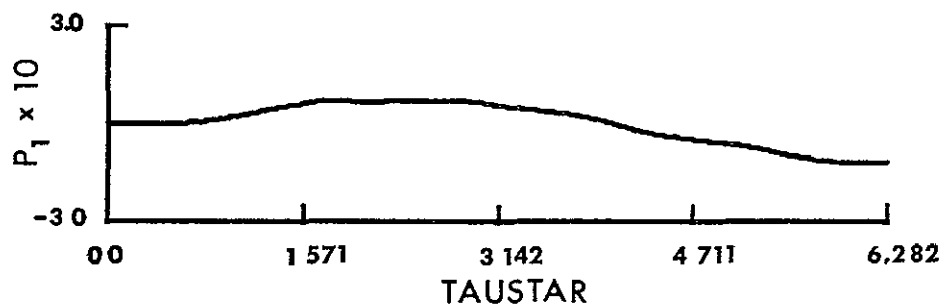
In $\underline{x}'' = \underline{v}$ let $x = x_3$, $x' = x_4$ and $\underline{v} = \underline{v}_2$. Then

$$x_3' = x_4$$

$$x_4' = v_2 \tag{4.13}$$

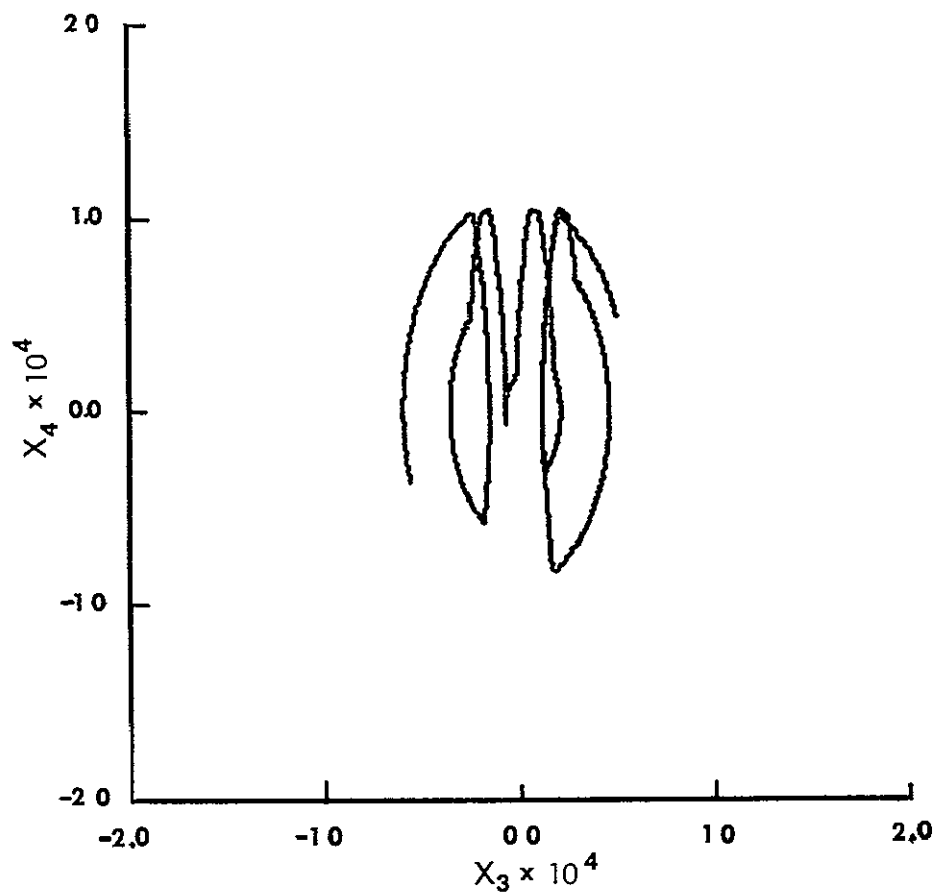


a Yaw Trajectory for $N_1 = 2.1 \times 10^{-4}$

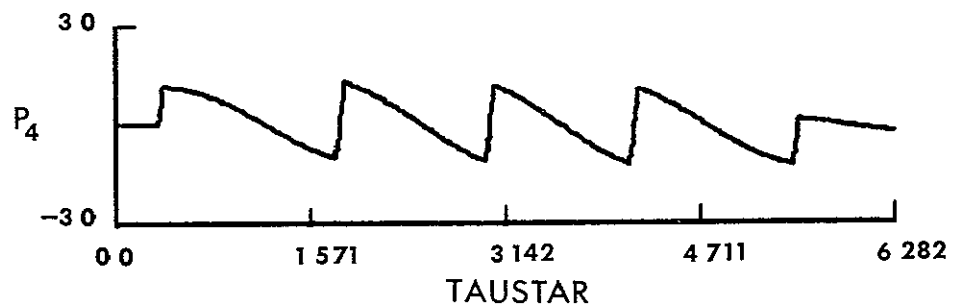
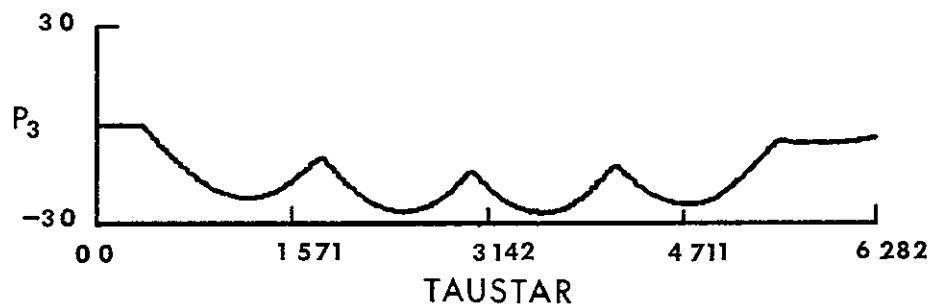


b Yaw Adjoint Variables for $n_1 = 2.1$, $n_2 = 1.0$

Figure 4.2 Solution of Equations (4.3)-(4.6) for Satellite (2)

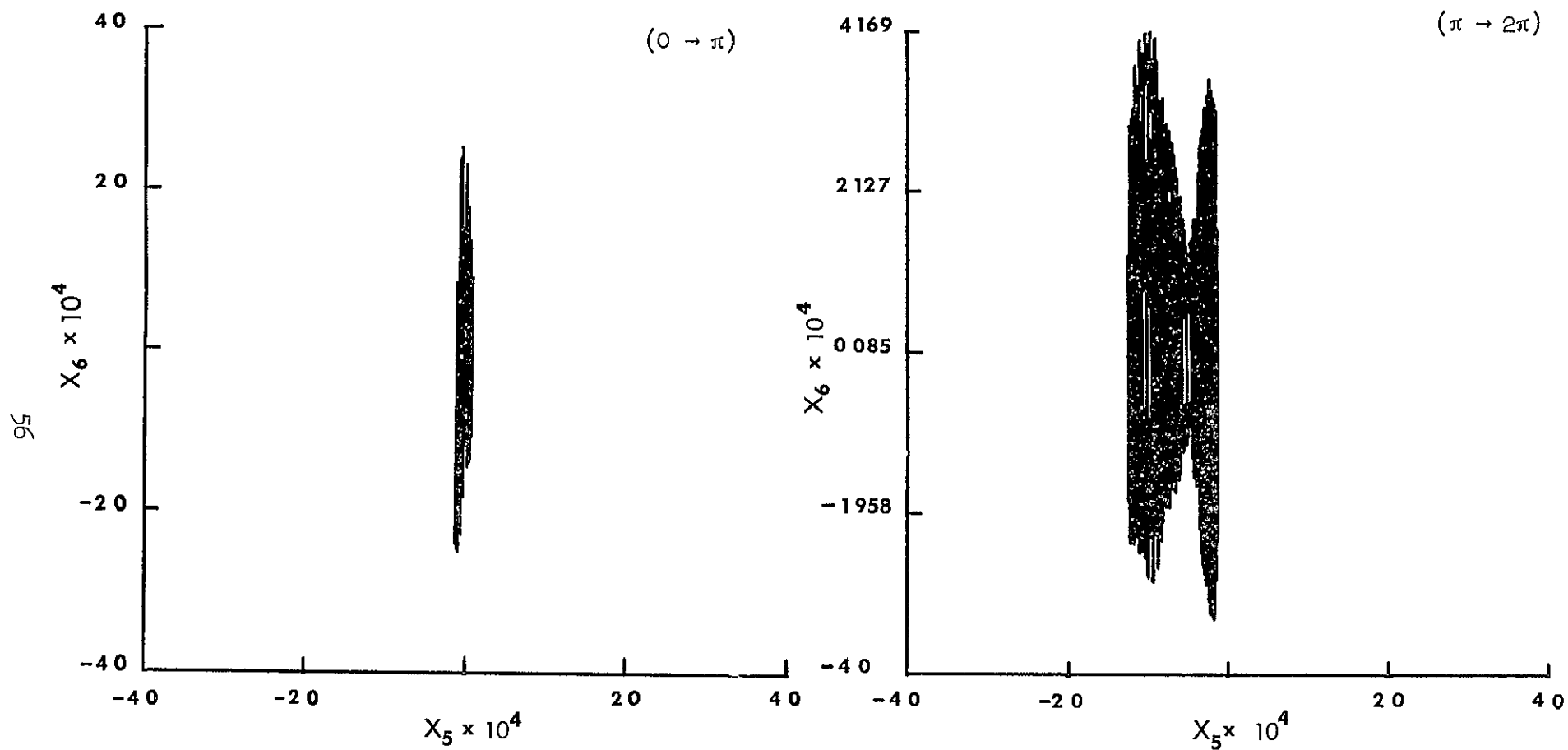


c Roll Trajectory for $N_2 = 7.1 \times 10^{-4}$



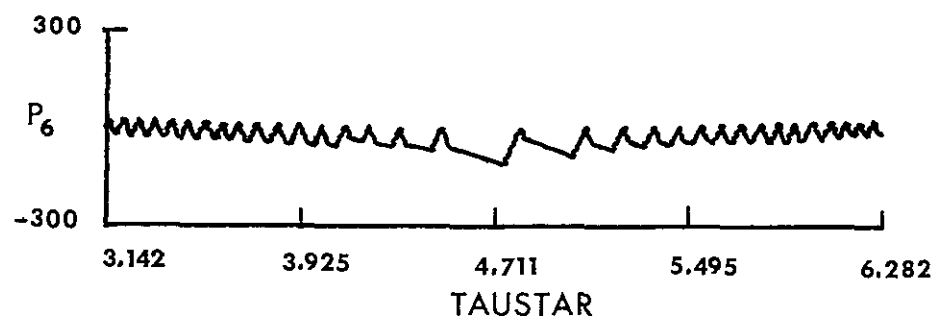
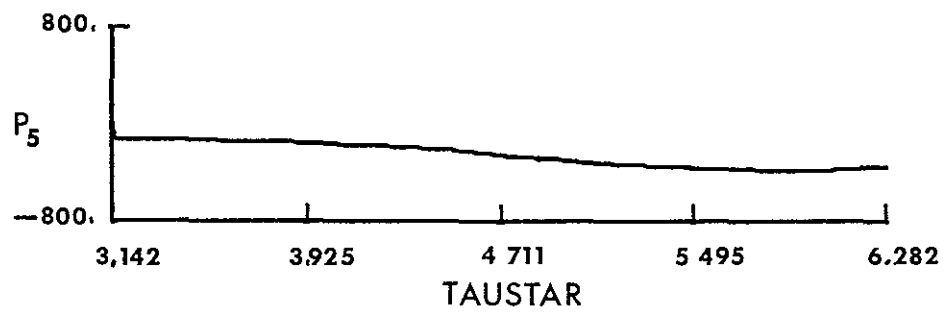
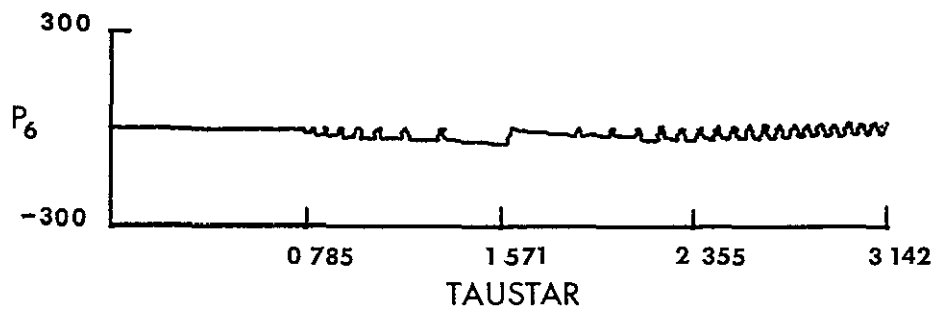
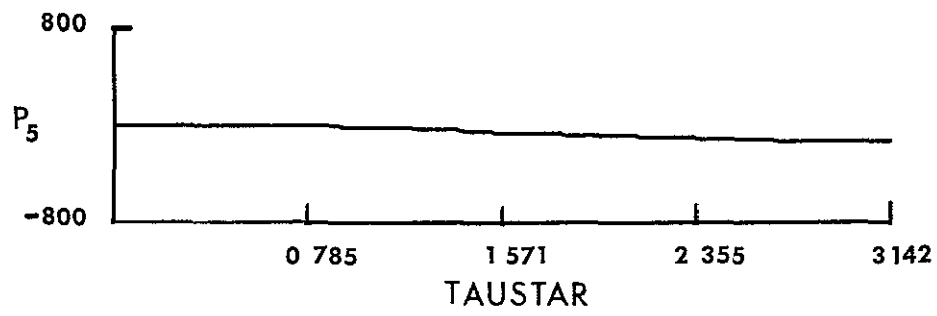
d. Roll Adjoint Variables for $n_3 = 2.1$, $n_4 = 1.6$

Figure 4.2 Continued



e Pitch Trajectory for $N_3 = 2.06 \times 10^{-2}$

Figure 4.2 Continued



f Pitch Adjoint Variables for $n_1 = 21$, $n_2 = 33$

Figure 4.2 Continued

is equivalent to $\ddot{x} = v$. For some intervals of time, equations (4.13) approximately describe the roll motion of satellites if they are nearly symmetric (such that $k_2 \approx 0$), if they are not significantly affected either by the earth's atmosphere or the disturbances mentioned in Chapter II and if they are controlled such that $x_1 = 0$, $i = 1, 2, 5, 6$. Of course, no such controlling of a satellite's motion is practicable at this time. However, if v_2 is a "coast function" with magnitude $N_2 \geq 0.01$, equation (4.13) adequately describes both the roll and yaw motions during those time intervals when the control is $\pm N_2$. In any case, for the purpose of comparing the two mathematical methods (approximate and exact), it is worthwhile to study the controlled motion of the simple plant described by (4.13).

By studying the possible controls and motions which satisfy the NCES (see Part 4, Section D, Chapter III), controls which perform satisfactorily are obtained and given below. (These controls are compared later to the controls obtained from PMP with

$$J = \int_{\tau_0}^{\tau_f} [f_1(\underline{x}) + |v|] d\tau$$

for the motion described by (4.13), i.e., the approximate method.)

While the phase-plane trajectory is in the interior of S_R , the roll phase-plane projection of S , the conditions of PMP must be satisfied. They are (4.13) and

$$p_3' = 0$$

$$p_4' = -p_3 \quad (4.14)$$

$$v_2 = N_2 \text{CST}(p_4) \quad (4.15)$$

The parts of the trajectories which coincide with the parts of the boundary of S_R given by $x_4 = \pm 10^{-4}$ are "regular". For a given value of $N_2 (< \infty)$, trajectories which begin in the shaded regions of S_R in Figure (4.3) must exit S_R in acquiring equilibrium points, namely those points such that $x_4 = 0$. These trajectories do not satisfy the

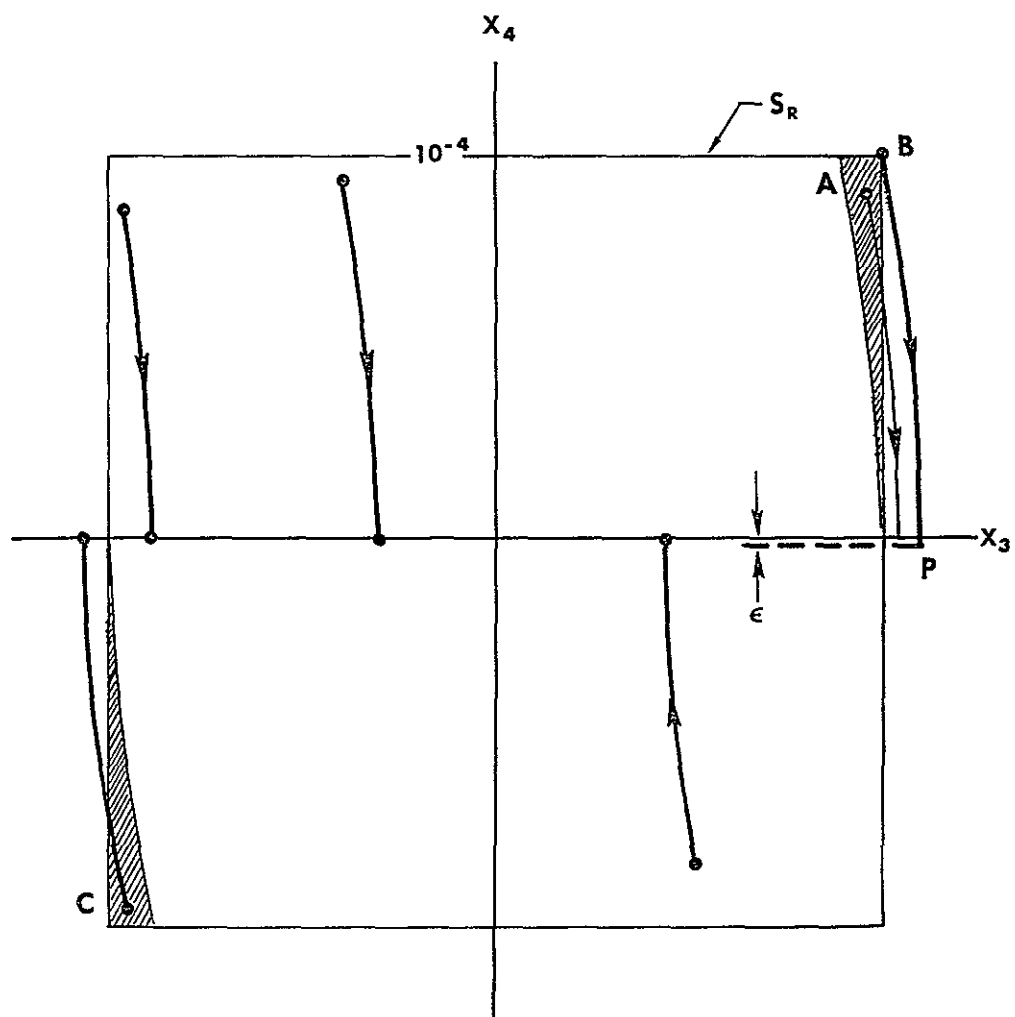


Figure 4 3 Typical Minimum Fuel Trajectories for System (4 13),
 $N_2 = 5 \times 10^{-4}$

NCES unless the vertical parts of the boundary of S_R are replaced by segments of parabolic curves (control-on trajectories). The control-on parts of the trajectories "A", "B" and "C" in Figure (4.3) are such curves. The trajectories are "regular". All trajectories in Figure (4.3) except "B" acquire the part of the line $x_4 = 0$ in or sufficiently near S_R . In this case the transversality condition (3.14) with $\underline{b}(\underline{x}_f)$ perpendicular to the x_3 -axis is applied. Trajectory "B" is not precisely a minimum fuel trajectory except in the limit as $\epsilon \rightarrow 0$. However, $\epsilon \neq 0$ is more practical since imperfections such as time delays, thresholds, etc., (see Flugge-Lotz [12]) are always present in the controller, and, for comparison of the NCES with the approximate method, this is an interesting case when \underline{x}_f is free in the interior of S . The value of N_2 used in Figure 4.3 is the smallest value which results in $|x_1| \leq 1.1 \times 10^{-4}$, $i = 3, 4$, (a 10% error in the maximum error) regardless of the initial point in S_R . The "jump condition" (3.15) is applied at "P".

Since the time required to reach $x_4(\tau_f) = 0$ in S_R (or a point suitably near so that no future control effort is required for the remaining part of the satellite's lifetime) is not important, the usual "bang-cost-bang" control, i.e., $\pm N_2 \rightarrow 0 \rightarrow \mp N_2$, does not result in a minimum fuel expenditure (see, for example, Marbach [25] wherein the acquisition time is given).

Now consider the controls and resulting motions obtained from PMP with

$$J = \int_{\tau_f}^{\tau_0} [f_1(\underline{x}) + |v|] d\tau$$

for $\underline{x}'' = v$ and for various times of consideration and compare them with the controls and resulting motions obtained from the NCES.

As in Part 1 of this section, the equations of the maximum principle for this problem can be written in backwards time as

$$\begin{aligned} \dot{x}_3 &= -x_4 \\ \dot{x}_4 &= -v \end{aligned} \tag{4.16}$$

$$p_3 = -F(x_3)$$

$$p_4 = F(x_4) + p_3 \quad (4.17)$$

$$v = N \text{CST}(p_3) \quad (4.18)$$

These equations can be solved in a piecewise manner.

The piecewise solution of (4.16) for intervals of τ^* over which $v(\tau^*)$ is constant is given by

$$x_3(\tau^*) = \begin{Bmatrix} +N \\ 0 \\ -N \end{Bmatrix} \tau^{*2} - x_{40} \tau^* + x_{30}$$

$$x_4(\tau^*) = \begin{Bmatrix} -N \\ 0 \\ +N \end{Bmatrix} \tau^* + x_{40} \quad (4.19)$$

where τ^* is measured from the last time of control switching, τ_s^* , or from the initial time, τ_0^* , and $x_{30} = x_3(\tau_1^*)$, $x_{40} = x_4(\tau^*)$, $i = 0, s$

If equations (4.17) are solved for the same intervals of τ^* as the piecewise solution of the adjoint variables given in Part I and in Appendix E, the result is

$$p_3(\tau^*) = p_{3e} - F(x_3) \Delta \tau_3^*$$

$$p_4(\tau^*) = p_{4e} + p_{3e} \Delta \tau^* + F(x_4) \Delta \tau_4^* - F(x_3) (\Delta \tau_3^*)^2 / 2 \quad (4.20)$$

(Notice that when $\underline{x} \in S$ equations (4.20) are just the backwards time solution of (4.14) and that (4.18) and (4.15) are the same for any $f_1(\underline{x})$)

With the proper initial conditions equations (4.19) and (4.20) can be used together with (4.18) to construct optimal controls and optimal trajectories. If the boundary of S is not encountered by the trajectory, which in forward time goes from a free initial point to a fixed final point on the x_3 -axis ($|x_4(\tau_f)| \leq 10^{-4}$), the optimal control results in a trajectory which is typically any of those in Figure 4.3 except the ones which cross the boundary of S_R . This is easily verified

with (4.18)-(4.20), since $F(x_1) \equiv 0$, $p_{1e} = p_1(\tau_0^*) = p_1(\tau_f)$, $i = 3, 4$, and $p_1(\tau_f)$ is either completely arbitrary (if $x(\tau_f)$ is a given point and $x(\tau_0)$ is freely chosen) or such that the transversality condition is satisfied (if $x(\tau_f)$ is any point of $x_4(\tau_f) = 0$ and $|x_3(\tau_f)| \leq 10^{-4}$)

If the initial point of the trajectory is so near the parts of the boundary of S_R given by $x_3 = \pm 10^{-4}$ that an exceedingly large control is needed to keep the trajectory in the interior of S_R , the trajectory is allowed to exit S_R by a suitably small amount. As before the trajectories are limited by $|x_1| \leq 1.1 \times 10^{-4}$, $i = 3, 4$. The value of N_2 used in applying the NCES, namely $N_2 = 5.0 \times 10^{-4}$, is used here.

If the proper final conditions (initial conditions in backwards time) are imposed by the adjoint variables and if the "best" value of n_3 is used, equations (4.18)-(4.20) give boundary encounter trajectories which are precisely the same as trajectory "B" of Figure 4.3 which was obtained from the NCES, see Part 4, Section D, Chapter III. Figure 4.4 shows two such phase-plane trajectories. Figure 4.5 shows a plot of $p_4(\tau^*)$ for one of the trajectories as obtained from both the NCES and (4.20). The curve in Figure 4.5 which is obtained from (4.20) is unique only for given $p_3(\tau_0^*)$ and $p_4(\tau_0^*)$. This curve is only required to pass through the points $(\tau_b^*, +1)$ and $(\tau_d^*, -1)$. Thus, the parameters, $p_3(\tau_0^*)$, $p_4(\tau_0^*)$ and n_3 , can be varied somewhat without affecting the control, $v_2(\tau^*)$, or the resulting trajectory. The values of these parameters used in constructing Figure 4.5 are $p_3(\tau_0^*) = -0.20$, $p_4(\tau_0^*) = 1.004$ and $n_3 = 0.42$. For convenience $p_4(\tau_c^*)$ was chosen to be zero so that the "best" value of n_3 was the same as obtained from the method of estimation of Part 1.

From the above investigation it is apparent that the approximate solution, equations (4.18)-(4.20), gives the same results as the exact solution, if it is required that the final point of the trajectory be a point of the x_3 -axis in S_R . It is not difficult to see that the two solutions also agree precisely in the case that the final point, $[x_3(\tau_f), x_4(\tau_f)]$, is free in S_R if S_R is exited only once. (As in Part 1 the free (in S_R) final point requires $p_3(\tau_f) = p_4(\tau_f) = 0$.)

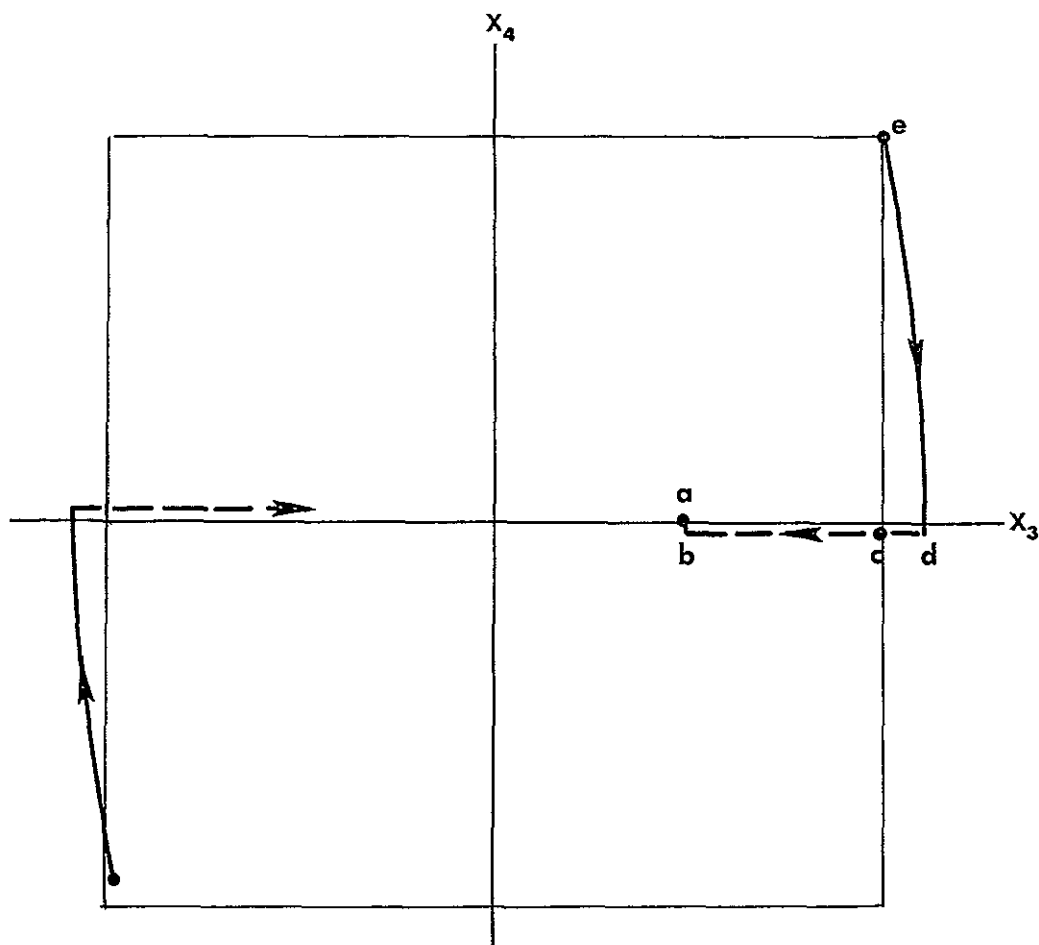


Figure 4.4 Nearly Minimum Fuel Boundary Encounter Trajectories for $x'' = v$, $N_2 = 5.0 \times 10^{-4}$

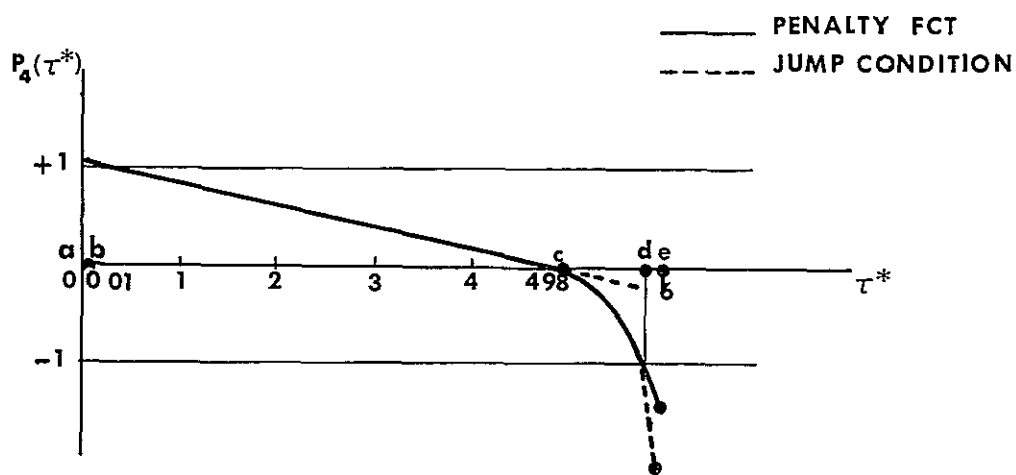


Figure 4.5 Adjoint Variable in Backwards Time. Note $p_4(\tau_a^*) > 1.0$

If the approximate solution is carried out for $\tau_f^* - \tau_0^*$ which is sufficiently large for two or more exits of S_R , it becomes clear that regardless of the values of n_3 , n_4 and N used the approximate solution has a fuel cost which is larger than the fuel cost of the exact minimum fuel solution. The approximate solution can be made better by changing the values of n_3 and n_4 before each exit of S_R or by applying the solution in a piecewise manner with the jump condition. These methods of improving the approximate solutions with more than one exit of S_R are, generally, not satisfactory since they make the conditions of the approximate solution as difficult to apply correctly as the NCES. An alternative to these methods is the use of functions other than $f_1(\underline{x})$ in the integral constraint on the states. The functions $f_2(\underline{x})$ and $f_e(\underline{x})$ given by (3.10) and (3.11) are the same as $f_1(\underline{x})$ when $\underline{x} \in S$ so that they result in the same satisfactory solutions if the trajectory remains in the interior of S . If the trajectory exits the region S more than once in the time interval of consideration, the use of $f_2(\underline{x})$ instead of $f_1(\underline{x})$ results in a reduction in fuel cost. This is true since the derivative of $f_2(\underline{x})$ (which appears in the adjoint solution) is smaller near the boundary of S than the derivative of $f_1(\underline{x})$ so that the fuel cost carries more weight over the trajectory when $f_2(\underline{x})$ is used than when $f_1(\underline{x})$ is used.

A free final point solution of the approximate problem with $f_2(\underline{x})$ used in the integral constraint is given below. The steps leading to this solution are very similar to steps leading to the solutions (with $f_1(\underline{x})$ used) given above with the several types of boundary conditions. For completeness these steps are given in detail.

The equations of the maximum principle for this problem in backwards time are

$$\begin{aligned} \dot{x}_3 &= -x_4 \\ \dot{x}_4 &= -v \end{aligned} \tag{4.21}$$

$$\dot{p}_3 = - \left\{ \begin{array}{ll} 10^{n_3}(x_3 - 10^{-4}), & \text{if } x_3 > 10^{-4} \\ 0 & , \text{ if } |x_3| \leq 10^{-4} \end{array} \right\} \tag{continued}$$

$$p_4 = p_3 + \begin{cases} 10^{n_3}(x_3 + 10^{-4}), & \text{if } x_3 < -10^{-4} \\ 0, & \text{if } |x_4| \leq 10^{-4} \\ 10^{n_4}(x_4 + 10^{-4}), & \text{if } x_4 < -10^{-4} \end{cases} \quad (4.22)$$

$$v = N \text{ CST}(p_4) \quad (4.23)$$

Equations (4.21) are the same as (4.16) and their solution is the same as (4.19). Equation (4.23) is identical to (4.18). If the "if" parts of the statements which define the functions in brackets in (4.22) are assumed but not written, the solution of (4.22) can be written as

$$p_3(\tau^*) = -\frac{10^{n_3}}{2} \begin{cases} 2(x_{30} - 10^{-4})\tau^* - x_{40}\tau^{*2} + v\tau^{*3}/3 \\ 0 \\ 2(x_{30} + 10^{-4})\tau^* - x_{40}\tau^{*2} + v\tau^{*3}/3 \end{cases} + p_{3e} \quad (4.24)$$

$$p_4(\tau^*) = -\frac{10^{n_3}}{2} \begin{cases} (x_{30} - 10^{-4})\tau^{*2} - x_{40}\tau^{*3}/3 + v\tau^{*4}/12 \\ 0 \\ (x_{30} + 10^{-4})\tau^{*2} - x_{40}\tau^{*3}/3 + v\tau^{*4}/12 \end{cases} + p_{4e} + p_{3e}\tau^* + 10^{n_4}\tau^* \begin{cases} x_{40} - 10^{-4} - v\tau^*/2 \\ 0 \\ x_{40} + 10^{-4} - v\tau^*/2 \end{cases} \quad (4.25)$$

where τ^* , x_{30} and x_{40} are initialized at each time of encounter with the boundary as well as at each time a switch in control occurs

Suppose that the initial point is given by $[x_3(\tau_0^*), x_4(\tau_0^*)] = (-5 \times 10^{-5}, 10^{-5})$ and in forward time is a free final point. In this

case $p_{3e} = p_3(\tau_0^*) = 0$ and $p_{4e} = p_4(\tau_0^*) = 0$ Until the boundary of S is encountered (point "1" in Figure 4.6a), say at τ_1^* , the solutions (4.19), (4.23), (4.24) and (4.25) give

$$x_3(\tau^*) = x_{30} - x_{40}\tau^* - 5 \times 10^{-5} - 10^{-5}\tau^*$$

$$x_4(\tau^*) = x_{40} = 10^{-5}$$

$$v = 0$$

$$p_3(\tau^*) = 0$$

$$p_4(\tau^*) = 0 \quad (4.26)$$

From the first equation of (4.26) the time of encounter with $x_3(\tau^*) = -10^{-4}$ is found to be $\tau_1^* = 5$. Since x_3, x_4, p_3 and p_4 are continuous, they have the same values at $(\tau_1^*)^+$ as at $(\tau_1^*)^-$. Thus, until the control turns on, say at τ_2^* , the solution is

$$x_3(\tau^*) = x_{30} - x_{40}\tau^* = -10^{-4} - 10^{-5}\tau^*$$

$$x_4(\tau^*) = x_{40} = 10^{-5}$$

$$v(\tau^*) = 0$$

$$p_3(\tau^*) = -10^{n_3}/2\{-x_{40}\tau^{*2}\} = 10^{n_3-5}\tau^{*2}/2$$

$$p_4(\tau^*) = -10^{n_3}/2\{-x_{40}\tau^{*3}/4\} = 10^{n_3-5}\tau^{*3}/8 \quad (4.27)$$

With $N = 5 \times 10^{-4}$ the allowable error will not be exceeded, i.e., $|x_3| \leq 1.1 \times 10^{-4}$, if the control turns on when $x_3 = -1.08 \times 10^{-4}$. From the first equation of (4.27) with $x_3(\tau_2^*) = -1.08 \times 10^{-4}$ it is found that $\tau_2^* = 0.8$ (measured from τ_1^*). For the control to turn on at τ_2^* , p_4 must grow to unity at τ_2^* . Thus, from the last equation of (4.27) the "best" value of n_3 is found to be $n_3 = 6.2$. From the fourth equation of (4.27) it is found that $p_3(\tau_2^*) = 5.0$. Thus, for the next part (from point "2" in Figure 4.6a), of the calculation $x_{30} = -1.08 \times 10^{-4}$, $x_{40} = 10^{-5}$, $p_{3e} = 5.0$, $p_{4e} = 1.0$ and $v = N = 5 \times 10^{-4}$. Until the boundary of S is again encountered (point "3" in Figure 4.6a), say at τ_3^* , the solution is

$$x_3(\tau^*) = N\tau^{*2} - x_{40}\tau^* + x_{30} = 5 \times 10^{-4}\tau^{*2} + 10^{-5}\tau^* - 1.08 \times 10^{-4}$$

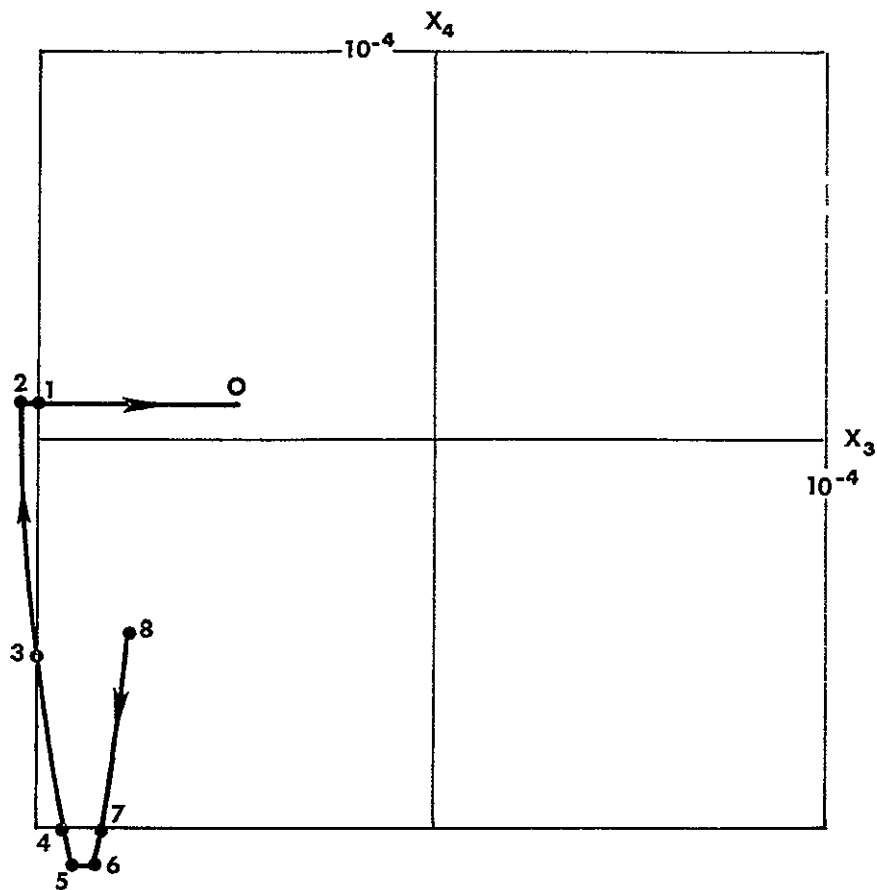
$$x_4(\tau^*) = -N\tau^* + x_{40} = -5 \times 10^{-4}\tau^* + 10^{-5}$$

$$v(\tau^*) = N$$

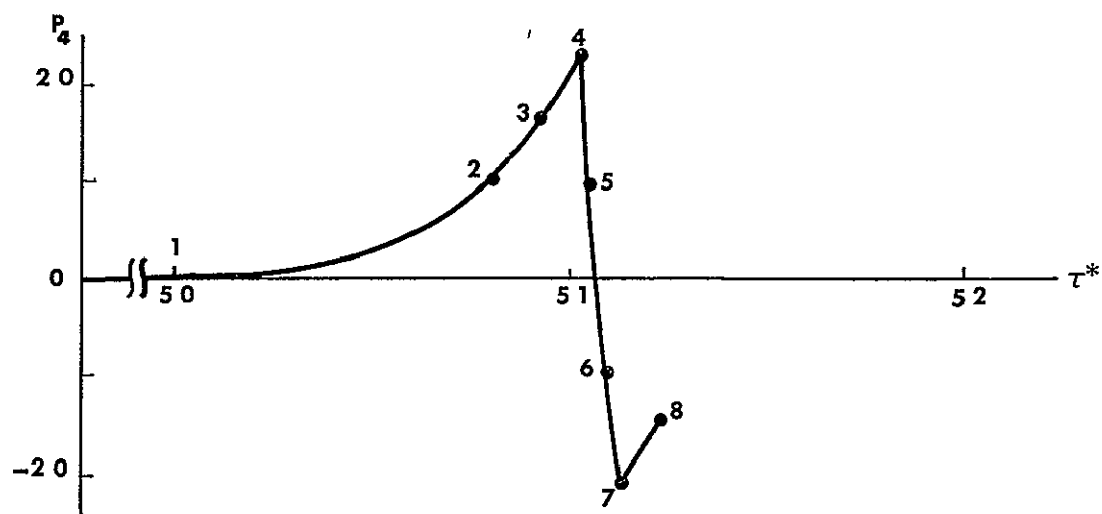
$$\begin{aligned} p_3(\tau^*) &= -10^3/2\{2(x_{30} + 10^{-4})\tau^* - x_{40}\tau^{*2} + v\tau^{*2}/2\} + p_{3e} \\ &= 5.0 + 12.5\tau^* + 7.8\tau^{*2} - 130.0\tau^{*3} \end{aligned}$$

$$\begin{aligned} p_4(\tau^*) &= -10^3/2\{(x_{30} + 10^{-4})\tau^{*2} - x_{40}\tau^{*3}/3 + v\tau^{*4}/12\} + p_{4e} + p_{3e}\tau^* \\ &= 1.0 + 5.0\tau^* + 6.25\tau^{*2} + 2.6\tau^{*3} - 32.5\tau^{*4} \end{aligned} \quad (4.28)$$

The time of reentry is found from the first equation of (4.28) to be $\tau_3^* = 0.126$, since $x_3(\tau_3^*) = -10^{-4}$. From (4.28) with $\tau_3^* = 0.126$, the initial values for the next part of the calculation are found to be $x_{40} = -5.30 \times 10^{-5}$, $p_{3e} = 6.43$, $p_{4e} = 1.73$ and $v = N$. The next part of the solution is such that $p_4(\tau^*)$ continues to increase so that the control stays on and drives the trajectory to the boundary again. Thus, until the boundary is encountered again (point "4" in Figure 4.6a), say at τ_4^* , the solution is



a. Phase Plane Trajectory



b Adjoint Variable

Figure 4.6 A Free End Point Solution for J with $f_2(\underline{x})$

$$x_3(\tau^*) = N\tau^{*2} - x_{40}\tau^* + x_{30}$$

$$= 5 \times 10^{-4}\tau^{*2} + 5.3 \times 10^{-5}\tau^* - 10^{-4}$$

$$x_4(\tau^*) = -N\tau^* + x_{40} = -5 \times 10^{-4}\tau^* - 5.3 \times 10^{-5}$$

$$v = N$$

$$p_3(\tau^*) = p_{3e} = 6.43$$

$$p_4(\tau^*) = p_{4e} + p_{3e}\tau^* = 1.73 + 6.43\tau^* \quad (4.29)$$

The time of exit, τ_4^* , is found from the second of (4.29) to be $\tau_4^* = 0.094$ since $x_4(\tau_4^*) = -10^{-4}$. From (4.29) with $\tau_4^* = 0.094$ the initial values for the next part are found to be $x_{30} = -9.1 \times 10^{-5}$, $p_{3e} = 6.43$, $p_{4e} = 2.33$ and $v = N$. The next part of the solution continues until the control switches, say at τ_5^* , and is

$$x_3(\tau^*) = 5 \times 10^{-4}\tau^{*2} + 10^{-4}\tau^* - 9.1 \times 10^{-5}$$

$$x_4(\tau^*) = -5 \times 10^{-4}\tau^* - 10^{-4}$$

$$p_3(\tau^*) = p_{3e}$$

$$p_4(\tau^*) = p_{4e} + p_{3e}\tau^* + 10^{n_4}\tau^{\tau}\{x_{40} + 10^{-4} - v\tau^*/2\}$$

$$= 2.33 + 6.43\tau^* + 10^{n_4}\tau^*\{-5 \times 10^{-4}\tau^*/2\} \quad (4.30)$$

The control switches to zero when $p_4(\tau_5^*) = 1.0$ and the trajectory becomes parallel to the x_3 -axis. Since it is required that $|x_4(\tau^*)| \leq 1.1 \times 10^{-4}$, the control switch must occur no later than $\tau_5^* = 0.02$. Thus, from the last equation of (4.30), it is found that $n_4 \geq 7.1$ is required. If $n_4 = 7.1$ and $\tau_5^* = 0.02$ are used in (4.30), the initial values for the next step are found to be $x_{30} = -8.88 \times 10^{-5}$, $x_{40} = -1.1 \times 10^{-4}$, $p_{3e} = 6.43$, $p_{4e} = 1.0$ and $v = 0$. The solution for the next part (from the point "5" in Figure 4.6a), is

$$x_3(\tau^*) = x_{30} - x_{40}\tau^* = -8.80 \times 10^{-5} + 1.1 \times 10^{-4}\tau^*$$

$$x_4(\tau^*) = x_{40} = -1.1 \times 10^{-4}$$

$$p_3(\tau^*) = p_{3e} = 6.43$$

$$p_4(\tau^*) = p_{4e} + p_{3e}\tau^* + 10^{-4}\tau^*\{x_{40} + 10^{-4}\} = 1.0 - 118.6\tau^* \quad (4.31)$$

This solution is for the time interval $(\tau_5^*, \tau_6^*]$ where τ_6^* is the time when the control switches from zero to $V = -N$. This switch in the control occurs when $p_4(\tau_6^*) = -1$. Thus, from the last equation of (4.31) it is found that $\tau_6^* = 0.017$. The initial values for the next step can be found from (4.31) with $\tau_6^* = 0.017$. They are $x_{30} = -8.69 \times 10^{-5}$, $x_{40} = -1.1 \times 10^{-4}$, $p_{3e} = 6.43$, $p_{4e} = -1.0$ and $v = -N$. Thus, the solution for the next step, which is until τ_7^* at which time the trajectory reenters S , is

$$x_3(\tau^*) = -N\tau^{*2} - x_{40}\tau^* + x_{30} = -5 \times 10^{-4}\tau^{*2} + 1.1 \times 10^{-4}\tau^* - 8.69 \times 10^{-5}$$

$$x_4(\tau^*) = N\tau^* + x_{40} = 5 \times 10^{-4}\tau^* - 1.1 \times 10^{-4}$$

$$p_3(\tau^*) = p_{3e} = 6.43$$

$$p_4(\tau^*) = p_{4e} + p_{3e}\tau^* + 10^{-4}\tau^*\{x_{40} + 10^{-4} + N\tau^*/2\} = -1.0 - 118\tau^* + 3120\tau^{*2} \quad (4.32)$$

The time τ_7^* can be found from the second equation of (4.32) since $x_4(\tau_7^*) = -10^{-4}$. It is $\tau_7^* = 0.02$. The initial values of the next (and final) step can be found from (4.32) with $\tau_7^* = 0.02$. They are $x_{30} = -8.4 \times 10^{-5}$, $x_{40} = -10^{-4}$, $p_{3e} = 6.43$, $p_{4e} = -2.12$ and $v = -N$. The solution for the last step which is until τ_8^* is

$$x_3(\tau^*) = -5 \times 10^{-4}\tau^{*2} + 10^{-4}\tau^* - 8.4 \times 10^{-5}$$

(continued)

$$x_4(\tau^*) = 5 \times 10^{-4} \tau^* - 10^{-4}$$

$$p_3(\tau^*) = 6.43$$

$$p_4(\tau^*) = -2.12 + 6.43\tau^* \quad (4.33)$$

The final time $\tau_f^* = \tau_1^* + \dots + \tau_8^*$ is chosen so that the trajectory begins (in forward time) in S . The solution is given in graphical form in Figure 4.6

In summary the main results of this part are (1) minimum fuel controls for the single-axis motion of satellites if the motion is described by $\dot{x} = v$, (2) the demonstration of the fact that the solutions obtained from PMP with

$$J = \int_{\tau_0}^{\tau_0} (f(\underline{x}) + |v|) d\tau$$

$(f(\underline{x}) = f_1(\underline{x}), f_2(\underline{x}), \dots, f_e(\underline{x}))$ are minimum fuel solutions if the boundary of S is exited no more than once, (3) the use of smooth functions like $f_2(\underline{x})$ results in less control effort than the piecewise smooth function $f_1(\underline{x})$ if more than one exit of S occurs

3 The Steady-State Motion Obtained from PMP for $\ddot{x} + a^2 x = v$, $a^2 > 0$

The equation $\ddot{x} + a^2 x = v$ describes a stable system if $a^2 > 0$. If the pitch motion is controlled so that $|x_1(\tau)| \leq 1.1 \times 10^{-4}$, $i = 5, 6$, and if the satellite has inertia properties such that $k_1 \approx 1$ and $k_2 \approx -1$ (like satellite (2), for example), then both the roll motion and the yaw motion are very nearly described by $\ddot{x} + a^2 x = v$ with $a^2 > 0$. If the eccentricity of orbit is less than 5×10^{-6} , $k_3 \approx 1$ and the yaw-roll motion is controlled so that $|x_1(\tau)| \leq 1.1 \times 10^{-4}$, $i = 1, 4$, then the pitch motion is also very nearly described by $\ddot{x} + a^2 x = v$. Thus, the application of the theory of Chapter III to

$$\dot{x}_1' = x_2$$

$$\dot{x}_2' = -a^2 x_1 + v \quad (4.34)$$

leads to useful information about the theory and the required control. In this part of Section A, the requirements on the control and the methods of analysis are the same as in Part 2 of Section A.

First consider the necessary conditions for exact solutions (NCES) of Part 4, Section D of Chapter III. While the state-space trajectory is in the interior of S the conditions of PMP, i.e., (4.34) and

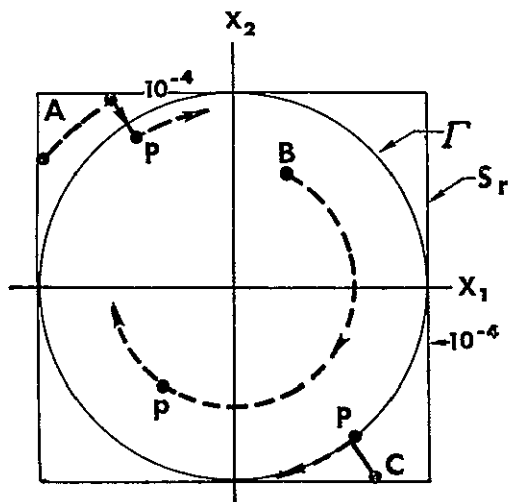
$$\begin{aligned} p_1' &= a^2 p_2 \\ p_2' &= -p_1 \end{aligned} \tag{4.35}$$

$$v = N \text{CST}(p_2) \tag{4.36}$$

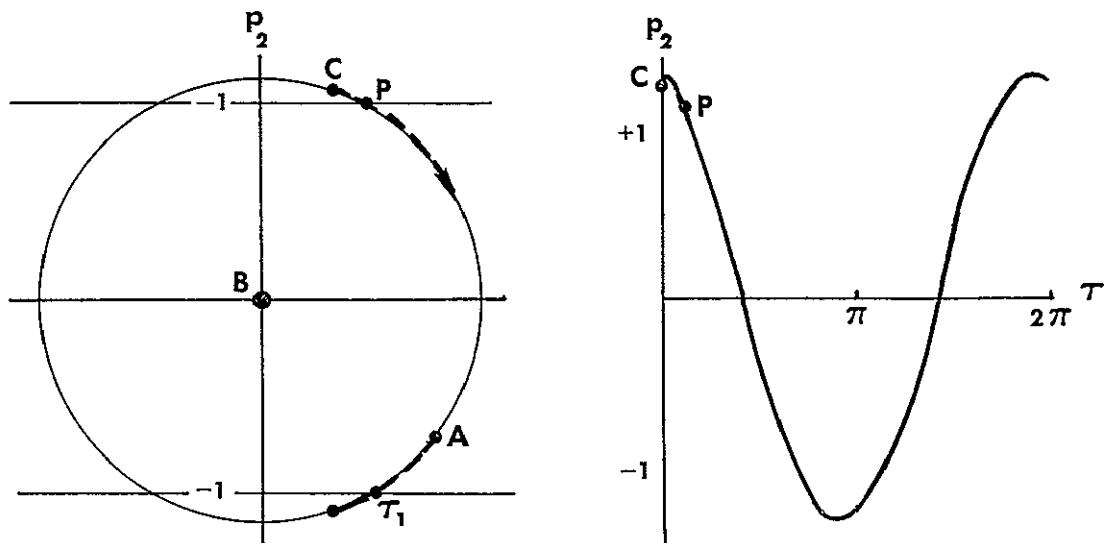
must be satisfied with the proper boundary conditions.

Three representative minimum fuel phase plane trajectories which do not encounter the boundary are shown in Figure 4.7a. These trajectories, denoted by A, B and C, are the results of applying PMP with three different sets of initial conditions on (x_1, x_2) and (p_1, p_2) . The circular region, Γ , which is just inside the yaw projection of S , S_Y , is the region to be acquired if initially (after acquisition to S) the trajectory is not already in Γ . The region Γ was chosen to be acquired since once it is acquired no future control effort is needed to keep the trajectory in S_Y (in the absence of detrimental disturbances). Also, less fuel is needed to acquire Γ (from within S_Y) than any other circular region in S_Y . The final points, P , of the trajectories, A, B and C, correspond to the final time of consideration, namely τ_f . For trajectory A the final point is fixed. The final point of trajectory B is free so that $p_1(\tau_f) = p_2(\tau_f) = 0$. The trajectory C acquires the boundary of Γ so that the transversality condition applies.

There are points in S_Y from which Γ cannot be acquired without encountering the boundary of S_Y . A typical case is shown in Figure 4.8. The final point of the trajectory is fixed so that $p_1(\tau_f)$, $i = 1, 2$, are entirely unknown a priori. The jump condition is applied at the junction point denoted by the number "3". (Those parts of the boundary of S_Y which are vertical lines are replaced by arcs of circles about $(\pm N, 0)$.) In Figure 4.8a the normal to the boundary at the junction point makes an

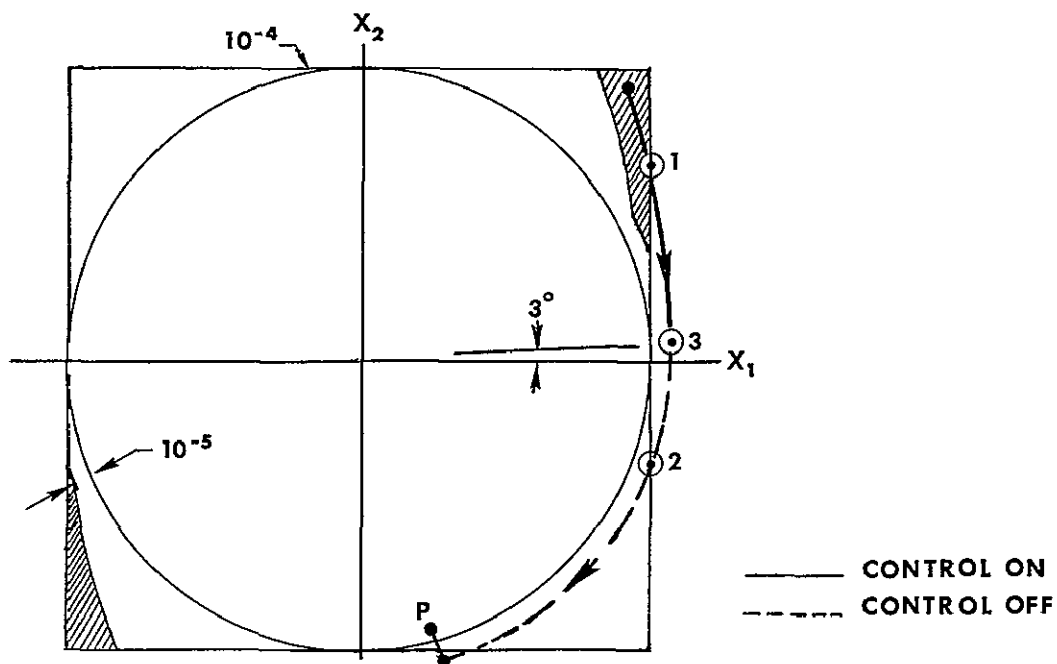


a Minimum Fuel Trajectories

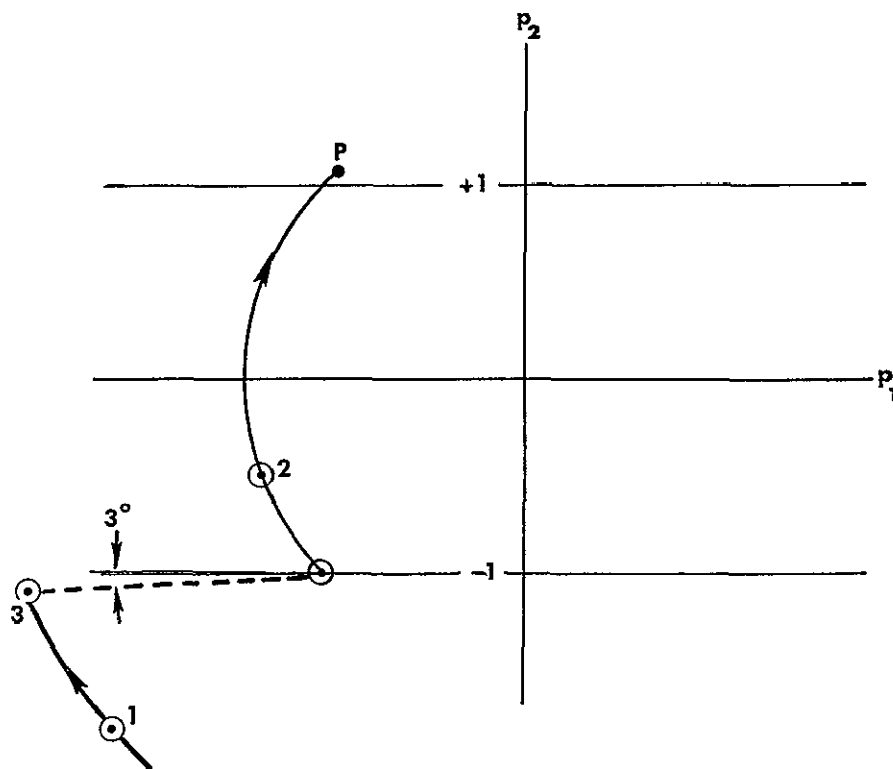


b Adjoint Variables

Figure 4.7 Typical Minimum Fuel Solutions for System (4.34), $a^2 = 1$,
 $N = 2 \times 10^{-4}$



a Phase Plane Trajectory, $N = 2 \times 10^{-4}$, $a^2 = 1$



b Adjoint Plane Trajectory

Figure 4 8 A Minimum Fuel Boundary Encounter Solution for System (4 34)

angle of 3° with the x_1 -axis, so that, in Figure 4 8b the "jump" in (p_1, p_2) at "3" is at an angle of 3° with the p_1 -axis. In this application the jump condition constant is negative. The normals to the vertical boundary lines at the boundary points "1" and "2" are parallel to the x_1 -axis.

The part of the trajectory in Figure 4 8a which begins at the junction point "3" and ends at the fixed final point P is part of the optimal trajectory from "3" to the origin for acquisition times greater than $5\pi/8$ (See Marbach [25], Fig 2 11.) This part of the trajectory is minimum-fuel optimal since it is part of an optimal trajectory. The time of acquisition ($> 5\pi/8$) is taken as large as possible since the fuel cost decreases with increase in acquisition time (See Marbach's Fig 2 15)

For $x'' + a^2 x = v$ as for $x'' = v$ in Part 2 it can easily be seen that the optimal (minimum fuel) controls obtained from the NCES with the jump conditions applied at boundary encounter points are the same as the optimal controls obtained from PMP with

$$J = \int_{\tau_0}^{\tau_f} [f(\underline{x}) + |v|] d\tau$$

The equations of the maximum principle for

$$J = \int_{\tau_0}^{\tau_f} [f(\underline{x}) + |v|] d\tau$$

in backwards time are

$$\begin{aligned} \dot{x}_1 &= -x_2 \\ \dot{x}_2 &= a^2 x_1 - v \end{aligned} \tag{4 37}$$

$$\begin{aligned} \dot{p}_1 &= -F(x_1) - a^2 p_2 \\ \dot{p}_2 &= F(x_2) + p_1 \end{aligned} \tag{4 38}$$

$$v = N \text{ CST}(p_2) \quad (4.39)$$

As in forward time the solution of (4.37) is a parametric representation of the equation of a circle in the (x_1, x_2) -plane. The center of the circle on the x_1 -axis at $x_1 = v$ ($v = \pm N$ or zero). The trajectory proceeds in a counter-clockwise sense with increasing τ^* . The piecewise solution of (4.38) can be obtained by the method of Appendix E and is

$$\begin{aligned} p_1(\tau^*) &= p_{1e} \cos(a\Delta\tau^*) - p_{2e} a \sin(a\Delta\tau^*) - F(x_1) a^{-1} \sin(a\Delta\tau_1^*) \\ &\quad - F(x_2)[1 - \cos(a\Delta\tau_2^*)] \\ p_2(\tau^*) &= p_{2e} \cos(a\Delta\tau^*) + p_{1e} a^{-1} \sin(a\Delta\tau^*) + F(x_2) a^{-1} \sin(a\Delta\tau_2^*) \\ &\quad - F(x_1) a^{-2}[1 - \cos(a\Delta\tau_1^*)] \end{aligned} \quad (4.40)$$

Figure 4.9 shows a graph of a solution of (4.38) as obtained from (4.40). This solution corresponds to the solution of (4.37) shown in Figure 4.8a in forward time (as indicated by the arrows). As before in Part 1 and Part 2 of this section, the values of n_1 and n_2 depend on the initial values of the adjoint variables. The initial values of p_1 and p_2 used in the solution shown in Figure 4.9 are a worst case choice. Although Figure 4.9 shows a worst case, there is still some resemblance to the curve of Figure 4.8b, which is obtained from the NCES, if differences in scaling are accounted for. If the initial (backward time) value of p_1 is made more negative, the solution (4.40) of the adjoint equations which corresponds to the trajectory of (4.8a) agrees perfectly with the curve in Figure 4.8b for all except about one-fourth of the time of consideration. The difference in the curves is due to the mechanism which causes the change in the adjoint variables on encountering a boundary. For comparison purposes Figure 4.10 shows a solution obtained from (4.40) which mostly agrees with the "jump" solution.

The above example, which show excellent agreement in the solutions obtained from the NCES and from PMP with

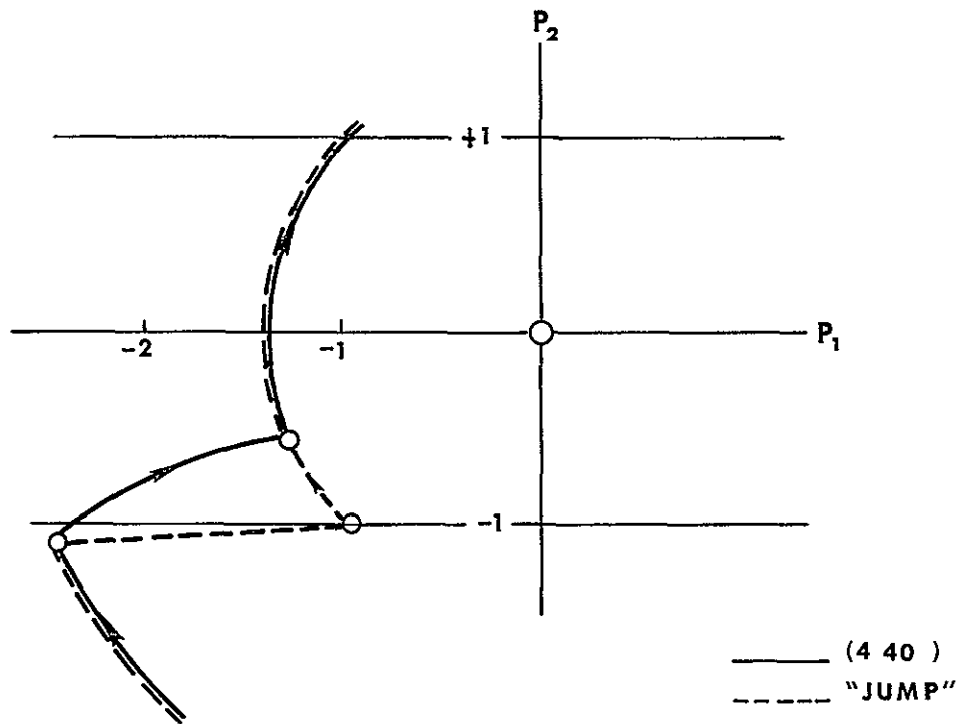


Figure 4 9 A Worst Case Adjoint Solution Corresponding to Trajectory of Figure (4 8a), $n_1 = 1.03$, $n_2 = -1$

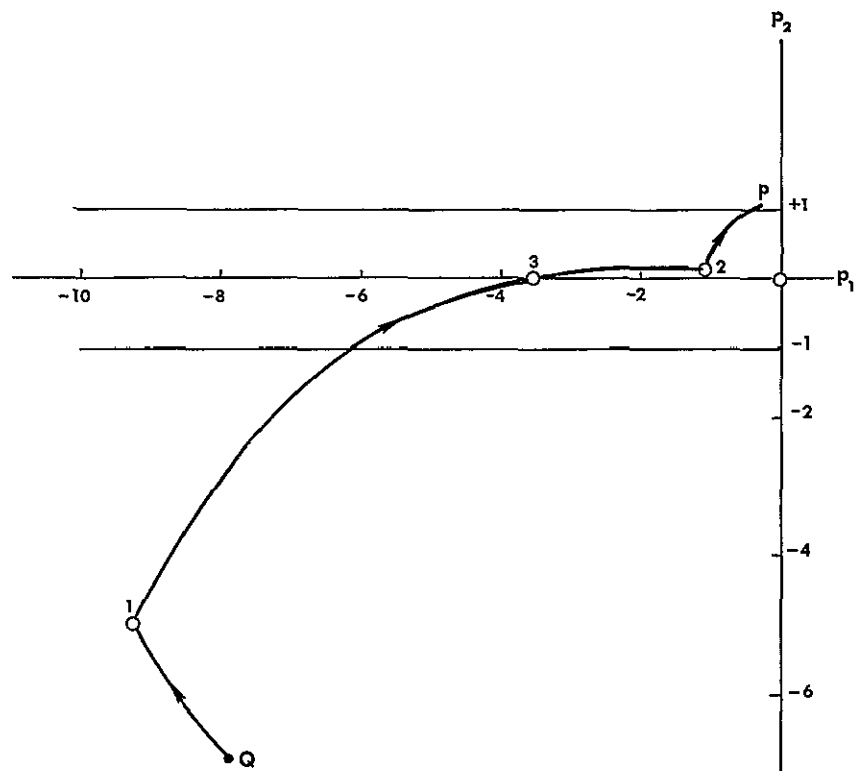


Figure 4 10 Adjoint Solutions

$$J = \int_{\tau_0}^{\tau_f} [f_1(\underline{x}) + |v|] d\tau$$

are representative of all optimal solutions which must (for a given value of N) exit the region S_Y (by more than some small allowable amount) once and only once. The main reason this generalization can be made is the fact that the parameters n_1 , n_2 and μ are freely chosen.

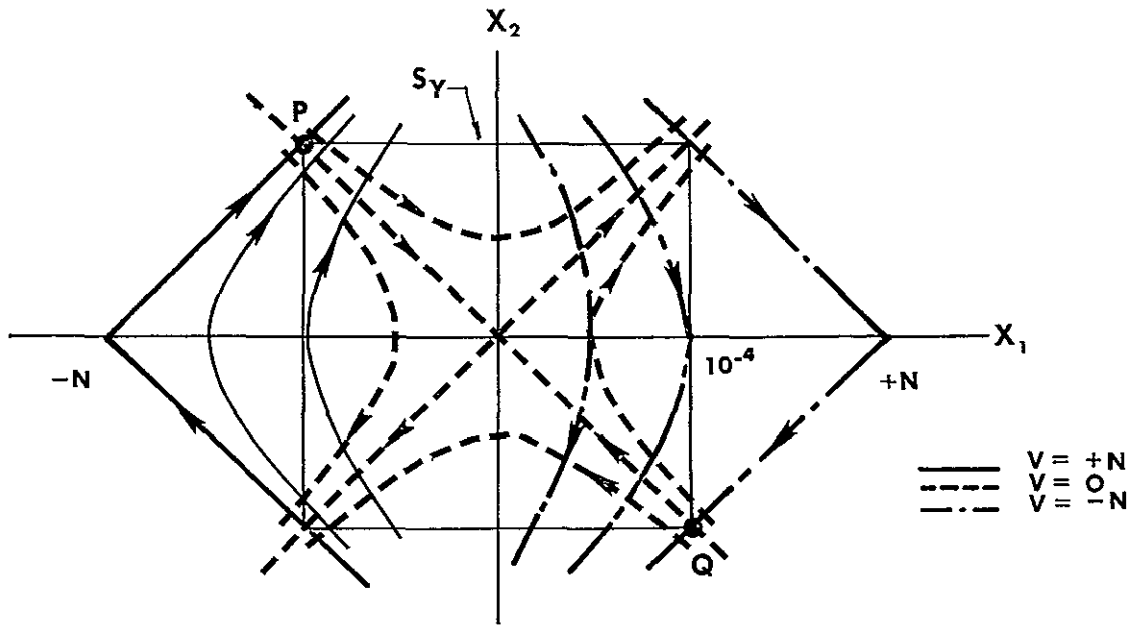
4. The Steady-State Motion Obtained From PMP for $x'' + a^2 x = v$,
 $a^2 < 0$

The equation $x'' + a^2 x = v$ with $a^2 < 0$ gives an accurate description of the yaw motion of satellite (3) for practical time intervals if the roll and pitch motions are suitably controlled. This equation also describes the pitch motion of satellite (2) near apogee and perigee if the yaw and roll motions are suitably controlled.

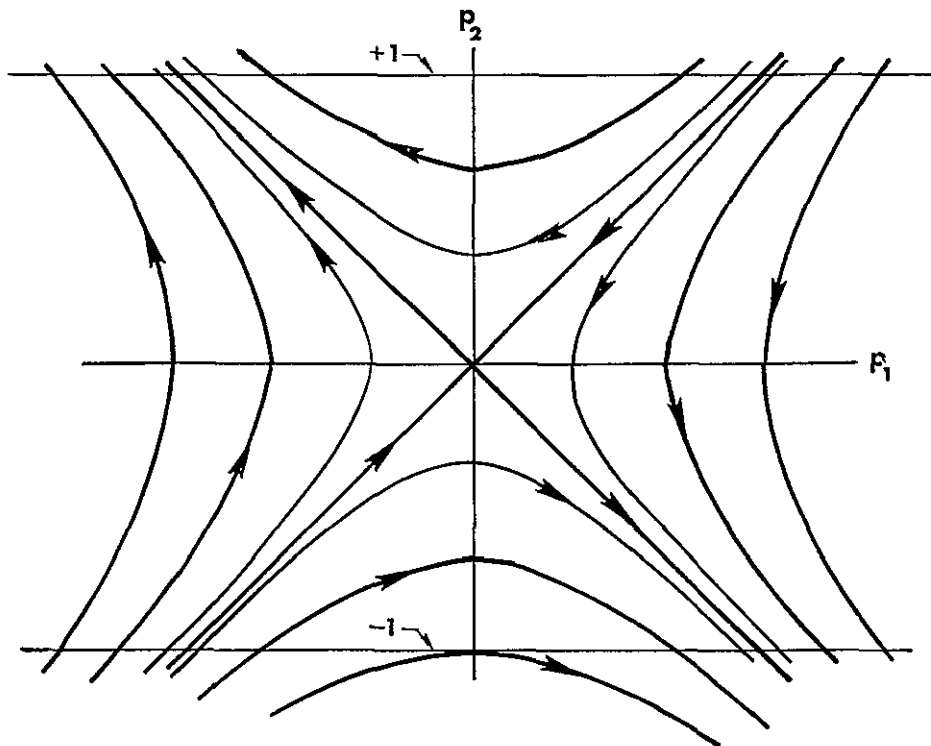
The equations of the maximum principle for this part are the same as in Part 3 except that here $a^2 < 0$ [See (4.34)-(4.36)]. Figure 4.11 shows some phase plane plots of solutions of (4.34) and (4.35) for $a^2 = -1$. The curves are hyperbolic.

Ideally, i.e., in the absence of disturbances and imperfections in the controller, the best control is the minimum-fuel control which acquires the line PQ in Figure 4.11a. (If the line PQ is acquired in this ideal case, no future control effort is required, since once PQ is acquired the trajectory moves very slowly along PQ to zero.) Since the transversality condition must hold at the final time, which is free, the minimum-fuel control which acquires the line PQ must be on $(\pm N)$ all of the time of acquisition. (See Figure 4.11b.) Therefore, in this ideal case the control must be $-N$ above PQ and must be $+N$ below PQ.

The magnitude of the control used in constructing Figure 4.11a is too small. For two reasons N should be larger. They are (1) the error in $x_1(\tau)$ grows to undesirably large values, i.e., $|x_1(\tau)| > 1.1 \times 10^{-4}$, if initially both x_1 and x_2 are near 10^{-4} or -10^{-4} , (2) for most of S_Y the cost of acquiring the line PQ decreases with increase in N until the cost is the same as for $x'' = v$ in acquiring the same line. This last reason is easily validated by considering the



a Phase Plane Trajectories of (4.34), $N = 2 \times 10^{-4}$



b Phase Plane Plots of Adjoint Variables

Figure 4.11 Some Phase Plots of Solutions of Maximum Principle Equations for $x'' + a^2 x = v$, $a^2 = -1$

time integral of the last of the system equations (equations (4 34))

$$\pm x_2 = \tilde{x}_1 \Delta\tau \pm N\Delta\tau \quad (4 41)$$

where \tilde{x}_1 is the mean value (of the integral mean value theorem) for the time interval $\Delta\tau$, $\Delta x_2 > 0$ and $N > 0$

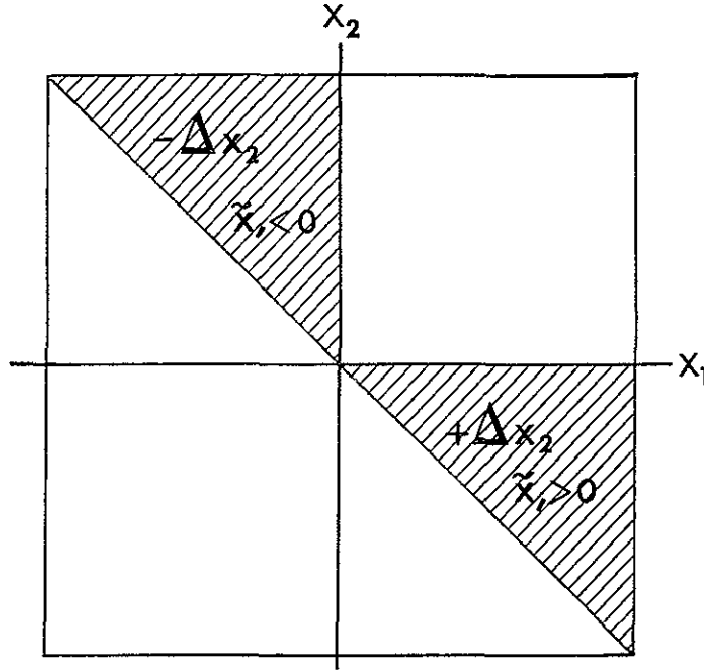


Figure 4 12 Regions of Increase in Cost With Increase in N

If (4 41) is solved for $\pm N\Delta\tau$, whose magnitude is the cost, the result is

$$\pm J = \pm N\Delta\tau = \pm \Delta x_2 - \tilde{x}_1 \Delta\tau \quad (4 42)$$

As N increases the value of \tilde{x}_1 approaches the initial value of x_1 (Even for small N , say $N = 2 \times 10^{-4}$, the change in x_1 is small compared to Δx_2 for most initial conditions and time intervals See Figure 4 11a) Since the time interval required for x_2 to change by a given amount decreases with increase in N , it is easily seen from (4 42) that the cost decreases with increase in N whenever the change in x_2 is positive or negative) and \tilde{x}_1 is negative (or positive) In the

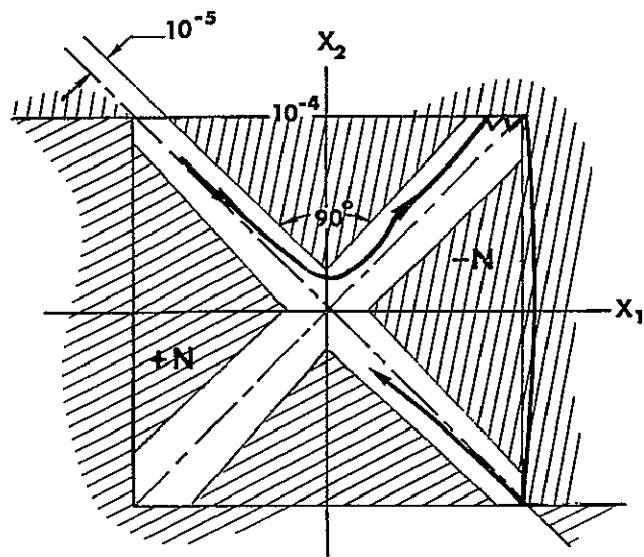
limit $J = \Delta x_2$. In the shaded regions of Figure 4 12 the cost is less than Δx_2 for bounded N and in the limit $J = \Delta x_2$.

In the more realistic case in which imperfections in the controller and disturbances of the motion are present, the line PQ cannot be precisely obtained, and, even if it could be acquired, the control effort is not exactly a minimum. The disturbances of the motion are mostly due to the coupling with the motion about other axes, the periodic oblateness part of the earth's gravitational torque and (rarely appearing) meteoroids. These disturbances can be small enough for the trajectories, which are never nearer than about 10^{-6} to the diagonal no-disturbances trajectories, to remain nearly hyperbolic. In this case the control law described by Figure 4 13a is very conservative with respect to cost. (With $N = 4 \times 10^{-4}$ the control is on only about one-seventh of the time of one orbit.) The trajectory in Figure 4 13a is realistic in the sense that a time delay of 0.1 sec is assumed in the controller and a small amplitude ($\approx 10^{-6}$) sinusoidal disturbance is assumed to affect the motion of the system described by equations (4 34) with $a^2 = -1$. The cost of the limit cycle motion of Figure 4 13b is about ten times smaller than the cost of the controlled motion of Figure 4 13a. However, the limit cycle motion requires sensors (of the state variables) which give one order of magnitude greater accuracy. If the two triangular control-on regions in S_Y which contain part of the x_1 -axis are replaced with control-off regions, the control effort is not significantly increased unless a large, but rare, disturbance causes the trajectory to acquire a point near $x_2 = 0$, $x_1 = \pm 10^{-4}$. This simplification of the control logic can result in a lower overall controller cost even though it can cause an increase in control effort (See Section B).

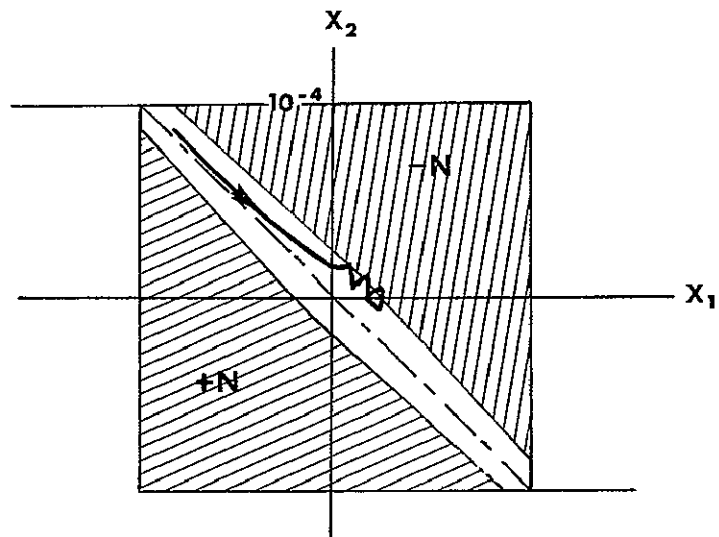
As in Part 2 and Part 3, the solution of the optimal problem with

$$J = \int_{\tau_0}^{\tau_f} [f_1(\underline{x}) + |v|] d\tau$$

is precisely the same as the solution obtained from the NCES except for the discrepancies in the adjoint variables which occur during the time when the state trajectory is outside of S_Y . The adjoint variables for



a. A Low Cost Control Law and Trajectory for a Realistic Case



b A Low Cost Control Law which Results in Limit Cycle Motion

Figure 4.13 Low Cost Control Laws and Trajectories, $N = 0.05$, Time Delay = 0.1 sec

this problem with

$$J = \int_{\tau_0}^{\tau_f} [f_1(\underline{x}) + |v|] d\tau$$

can be obtained as functions of τ^* as in Appendix E and are given by

$$\begin{aligned} p_1(\tau^*) &= p_{1e} \cosh(c\Delta\tau^*) + p_{2e} c \sinh(c\Delta\tau^*) - F(x_1) c^{-1} \sinh(c\Delta\tau_1^*) \\ &\quad + F(x_2) [\cosh(c\Delta\tau_2^*) - 1] \\ p_2(\tau^*) &= p_{2e} \cosh(c\Delta\tau^*) + p_{1e} c^{-1} \sinh(c\Delta\tau^*) + F(x_2) c^{-1} \sinh(c\Delta\tau_2^*) \\ &\quad - F(x_1) c^{-2} [\cosh(c\Delta\tau_1^*) - 1] \end{aligned} \quad (4.43)$$

where $c^2 = -a^2 > 0$ (It should be noticed that equations (4.43) are the "unstable" counterparts of equations (4.9) which are for the "stable" pitch motion)

B. THE STATION-KEEPING CONTROLS -- GENERAL ORBITS

1 Station-Keeping Control of Satellites in a Maximum Gravitational Torque Orbit

In Section A the orbits were restricted to nearly polar or nearly equatorial orbits which were of sufficient altitude that the aerodynamic torque was insignificant.

If the orbits are not nearly polar or nearly equatorial, the oblateness terms in the gravitational torque can be very significant in the case that high-accuracy earth-pointing is needed. Consider equations (2.17) with the parameters of satellites (2) and (3), for example. For all but about one-tenth of an orbit the terms which contain either c_θ or s_θ as factors are larger than the other term when $|x_1| \leq 1.1 \times 10^{-4}$, $\alpha = 1, .6$. Thus, as a limiting case the equations of steady-state motion for satellites such as (2) and (3) are

$$x_1' = x_2$$

$$x_2' = -2k_1 A_3 J(r_E/r)^2 s_\delta c_\delta c_\theta + v_1$$

$$x_3' = x_4$$

$$x_4' = 8k_2 A_3 J(r_E/r)^2 s_\delta c_\delta s_\theta + v_2$$

$$x_5' = x_6$$

$$x_6' = -A_2 + v_3 \quad (4.44)$$

Since $e = 0.01$ in these cases, A_3 and $(r_E/r)^2$ are very nearly constant so that for $\delta = 45^\circ$ equations (4.44) are closely approximated by

$$x_2' = x_2$$

$$x_2' = E_1 \cos(\tau + \theta) + v_1$$

$$x_3' = x_4$$

$$x_4' = E_2 \sin(\tau + \theta) + v_2$$

$$x_5' = x_6$$

$$x_6' = 2e \sin(\tau + \theta_0) + v_3 \quad (4.45)$$

where for satellite (2) $E_1 = -1.45 \times 10^{-3}$, $E_2 = -5.05 \times 10^{-3}$ and for satellite (3) $E_1 = 1.26 \times 10^{-3}$, $E_2 = 5.22 \times 10^{-3}$

In contradistinction to the approximate motions of Section A, no equilibrium point exists in the motion described by any one of these three pairs of equations (which in this limiting case describe the yaw, roll and pitch motions). In this case there exists no region of stability in S (which can be acquired with the aid of a minimum fuel control) which is such that no control effort is required to keep the trajectory in S for the remaining lifetime of the satellite.

Except for the equations of motion, which have a sine forcing term, the equations of the maximum principle for each pair (4.45) are the same as for $x'' = v$. The adjoint equations in the case of an integral

constraint on the state variables are (in backwards time) the same as (4.18)

Although the sine forcing terms are no longer than 0.1, their effects are most important when $|x_1| \leq 10^{-4}$ so that the optimal feedback station-keeping control law must be highly time varying. This fact and the fact that no equilibrium points and no region of stability in S exist make the determination of practical, i.e., suboptimal minimum-fuel control law improbable. However, enough of the characteristics of the optimal control law are known so that a control which performs satisfactorily can be devised.

The optimal control must be a "coast function" as given by (4.19). If the time and the states at which the control optimally switches can be found, the optimal feedback control will be known. If the NCES are applied to the problem, two characteristics of the minimum fuel control become apparent. They are (1) the initial (and final) values of the adjoint variables, as well as the jump in the adjoint variables at junction points, must be small (about one or less in p_2 and ten or less in p_1) in most applications for low fuel cost and for minimum dispersion of the trajectory, (2) the switches in low cost controls occur when the trajectory is near the boundary of the station-keeping region.

In the maximum principle is applied to the minimum-fuel problem of station-keeping via an integral constraint on the state or equivalently to the optimal problem with

$$J = \int_{\tau_0}^{\tau_f} [f_1(\underline{x}) + |v|] d\tau$$

it is found that for the "best" values of n_1 and N_1 the switches in the control occur when the trajectory is near the boundary. However, for the values of n_1 which keep $|x_1| \leq 1.1 \times 10^{-4}$, the pitch control, v_3 , is on about 95% of the time of consideration. (The time of consideration was 2π , the time of one orbit.) In this limiting case the controls of the yaw and roll motions are on about 90% of the time when the "best" values of n_1 and N_1 are used. (By reducing the values of

n_1 and allowing more error in earth-pointing the fuel cost can be reduced)

Since the solutions obtained from the optimal problem with an integral constraint and from the NCES of the minimum fuel problem all exhibit characteristic (2) given above, it is logical to ask: should successive switches in the control occur when the trajectory is near one edge of the boundary or should successive switches occur when the trajectory is alternately near two edges of the boundary? (In the case of the NCES either is possible, but, in the case of the integral constraint the latter is generally the case) The analysis which follows shows that both methods of control switching result in the same fuel cost over the lifetime of the satellite

Take, for example, the third pair of equations (4 45) The solution for $x_6(\tau)$ is

$$x_6(\tau) = x_{60} + 2e(\cos \theta_0 - \cos(\tau + \theta_0)) + v_3(\tau - \tau_0) \quad (4 46)$$

where τ_0, θ_0, x_{60} are initialized after each switch in the control Let $\Delta\tau = \tau - \tau_0$ and $\Delta x_6 = x_6(\tau) - x_{60}$. Then, since $\Delta\tau \leq 0.15$ (and is usually much less), an excellent approximation of (4 46) is

$$\pm \Delta x_6 \approx (v_3 \mp 2e \sin \theta_0) \Delta\tau \quad (4 47)$$

where the upper signs correspond to $0 \leq \theta_0 < \pi$ and the lower signs correspond to $\pi \leq \theta_0 < 2\pi$ If the control switches consistently between off and on when $x_6(\tau)$ is one of two given values (e g , both of which are near $x_6 = 1.0 \times 10^{-4}$ or $x_6 = -1.0 \times 10^{-4}$ or one of which is near $x_6 = 1.0 \times 10^{-4}$ while the other is near $x_6 = -1.0 \times 10^{-4}$), then the ratio of the time the control is on to the total time of consideration is found from (4 47) to be

$$\frac{\Delta\tau_{ON}}{\Delta\tau_{ON} + \Delta\tau_{OFF}} \approx \frac{2e}{N_3} \sin \theta_0 \quad (4 48)$$

Thus, for a given control magnitude, N_3 , the fuel cost depends only on θ_0 and e and is independent of the values of x_6 at which control switching occurs so that successive switches which occur when the

trajectory is near one edge is no more preferable than successive switches at alternate edges

A similar analysis of the dependence of the optimal switching of the control on x_5 was made. For any given value of x_6 , $|x_6| \leq 10^{-4}$, no values of x_5 , $|x_5| \leq 10^{-4}$, at which optimal switching should occur were found. The reasons for this are considered to be: (1) the rapid changes in the state due to the forcing term, (2) the absence of a preferred point or region to acquire, (3) the periodicity of the forcing terms

In summary it has been found for the limiting case of this part of Section B that at least one of any two consecutive switches in the minimum-fuel control must occur on the boundary of S and there are no preferred sets of values of $(x, x') = (x_1, x_2)$ or (x_3, x_4) or (x_5, x_6) at which the other switch in the minimum-fuel control should occur. Thus, for the motion described by any one pair of the three pair of equations (4.45) the control law given in Figure 4.14 is expected to result in satisfactory steady-state performance. The distance $d \neq 0$ is not a consequence of the theory but is an innovation which is made necessary by the very imperfection in the controller which makes the control law workable — the control time delay. For a given $d \neq 0$ ($d \leq 10^{-4}$) and a certain size time delay (or control magnitude) there is a maximum value of control magnitude (or time delay) at which chatter with no control-off intervals will occur. If the control magnitude (or time delay) is greater than this maximum value for the given value of $d \neq 0$, fuel is wasted (See Part 4 of this section.)

This control law, although simple, also results in satisfactory performance (see Part 5 and Chapter VI) when the periodic exponential forcing function of the aerodynamic torque is dominant as in the ultra high-accuracy earth-pointing of satellite (4). (In this case, as above in the case of the sine forcing term, it is not difficult to show that there are no preferred states in S at which control switches should occur.)

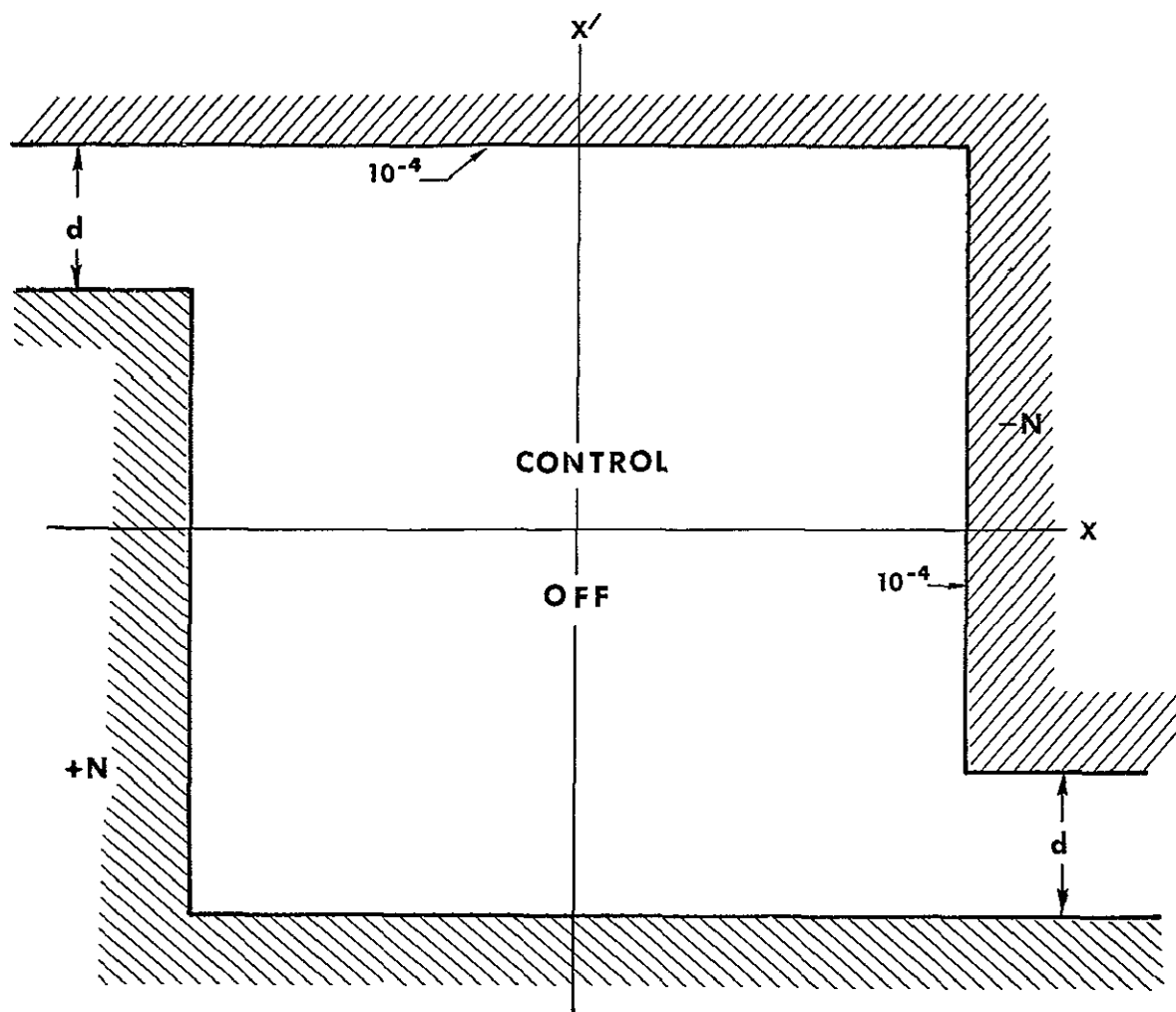


Figure 4 14. A Single-Axis Station-Keeping Control Law

2 Improvement of the Control Law of Part 1, Section A

Although the suboptimal station-keeping control law, equations (4.2) with the second and fourth of equations (4.8) and the second of equations (4.9), was derived for "stable" satellites in either polar or equatorial orbits, similar control laws can be derived for most "unstable" satellites in general orbits. All of these control laws are similar in the terms in which the derivatives of the "penalty function", $F(x_1)$, $i = 1, \dots, 6$, enter. These terms are zero when \underline{x} is in S . All other terms contain the piecewise constant variables, p_{ie} , $i = 1, \dots, 6$, whose average values over several orbits are nearly zero.

If p_{ie} , $i = 1, \dots, 6$, are taken as identically zero, the control law is greatly simplified, and, for the "best" values of n_1 and N_1 it is, in each phase plane projection, very nearly the same as in Figure 4.14 with $d = 0$. In comparison, the fuel cost in the case $p_{ie} \equiv 0$ was found to be 25% (roll-yaw) to 66% (pitch) less than when both the full system equations and the full control law was used. The largest percentage values correspond to those satellite configurations which require the greatest control effort for earth pointing.

3 The Controls - Approximate Motions

The control law for single-axis motion which is given in Figure 4.14 is expected to result in the efficient control of the approximate motions of this section and Section A of this chapter. Since the most general nearly earth-pointing motions of the satellites considered here can be approximated (in a least a piecewise sense) by the approximate motions above in this section and in Section A, the three-axes control law whose components are as in Figure 4.14 is expected to result in the efficient station-keeping control of the general motion.

If the control law given in Figure 4.14 is used in the control of the motion of $x'' + a^2 x = v$, $a^2 > 0$, and if a realistic time delay in the control is assumed, say 0.1 sec, the trajectories in Figure 4.15 are typical. These trajectories compare well with the optimal trajectories of Part 3, Section A. (See Figure 4.7.) The distance, d , was taken to be zero, the worst value. If $d = 1.0 \times 10^{-4}$, the agreement with the

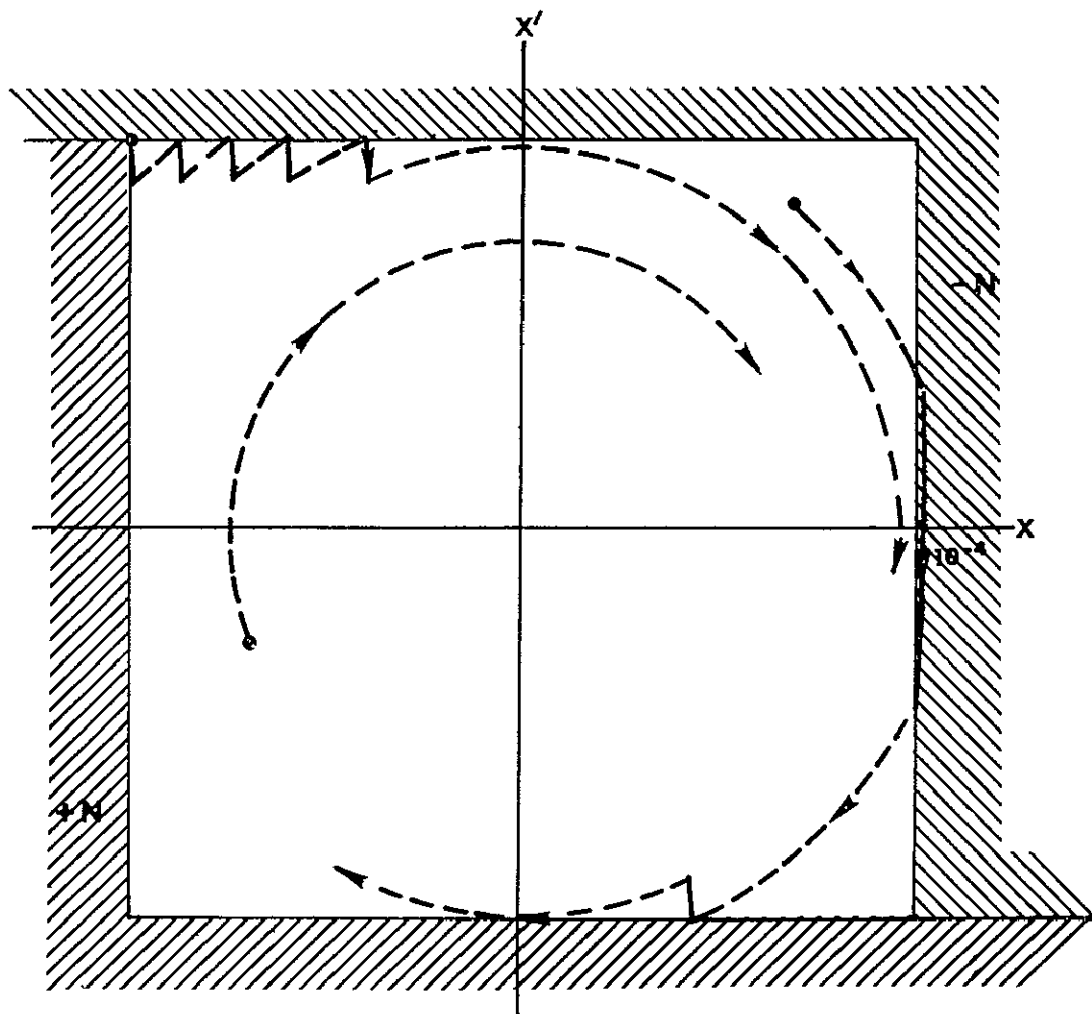


Figure 4.15. The Control of Figure 4.14 Applied to $x'' + a^2 = v$,
 $a^2 = 1.0$, $N = 0.1$, $d = 0$

optimal trajectories of Part 3, Section A is even better and the fuel cost is reduced in some cases by as much as 47%. However, if no future control effort is needed, the fuel expenditure is minute even with $d = 0$.

Consider the motion of $\ddot{x} + a^2 x = v$, $a^2 < 0$, when v is as represented in Figure 4.14. If the time delay in the control is 0.1 sec, the trajectories in Figure 4.16 are typical in the case $a^2 = -0.95$ (This value of a^2 is slightly more realistic for approximating the "unstable" yaw and pitch motions than $a^2 = -1$). The distance, d , is taken just large enough so that the control (with a time delay of 0.1 sec) is not on all of the time if chatter motion near the two corners $(x, x') = (\pm 10^{-4}, \mp 10^{-4})$ occurs. For minimum fuel cost d should be as small as possible. The fuel cost in this case with $d = 10^{-5}$ and $N = 0.05$ is about

$$J = \int_{\tau_0}^{\tau_f} |v| d\tau = 3 \times 10^{-4}$$

per orbit

4 The Controls - Station-Keeping Motions of the Satellites

The four satellites as described by equations (2.17) or equations (2.18) with the control for each axis as described in Figure 4.14 were simulated on a PACE TR-48 analog computer. (The patching diagrams are given in Appendix F.) Some of the results of the many simulation runs are shown in Figure 4.17 - Figure 4.20 as phase plane trajectories (or more precisely, the projection of trajectories into the phase planes). (The plots were made by an x-y plotter which is directly connected to the computer output.) In all figures the initial point, P_1 , is outside of S and on the boundary of a region, S^+ , which is twice the size of S (in maximum dimension). The reason P_1 is not taken in S but on the boundary of a newly defined region S^+ is given in the acquisition chapter, Chapter V. The real time (satellite time) of each run is at least the time of one orbit. When more information is obtained from a trajectory corresponding to more than one orbit (for example, the stabilization of the roll-yaw motion of satellite (2)), the

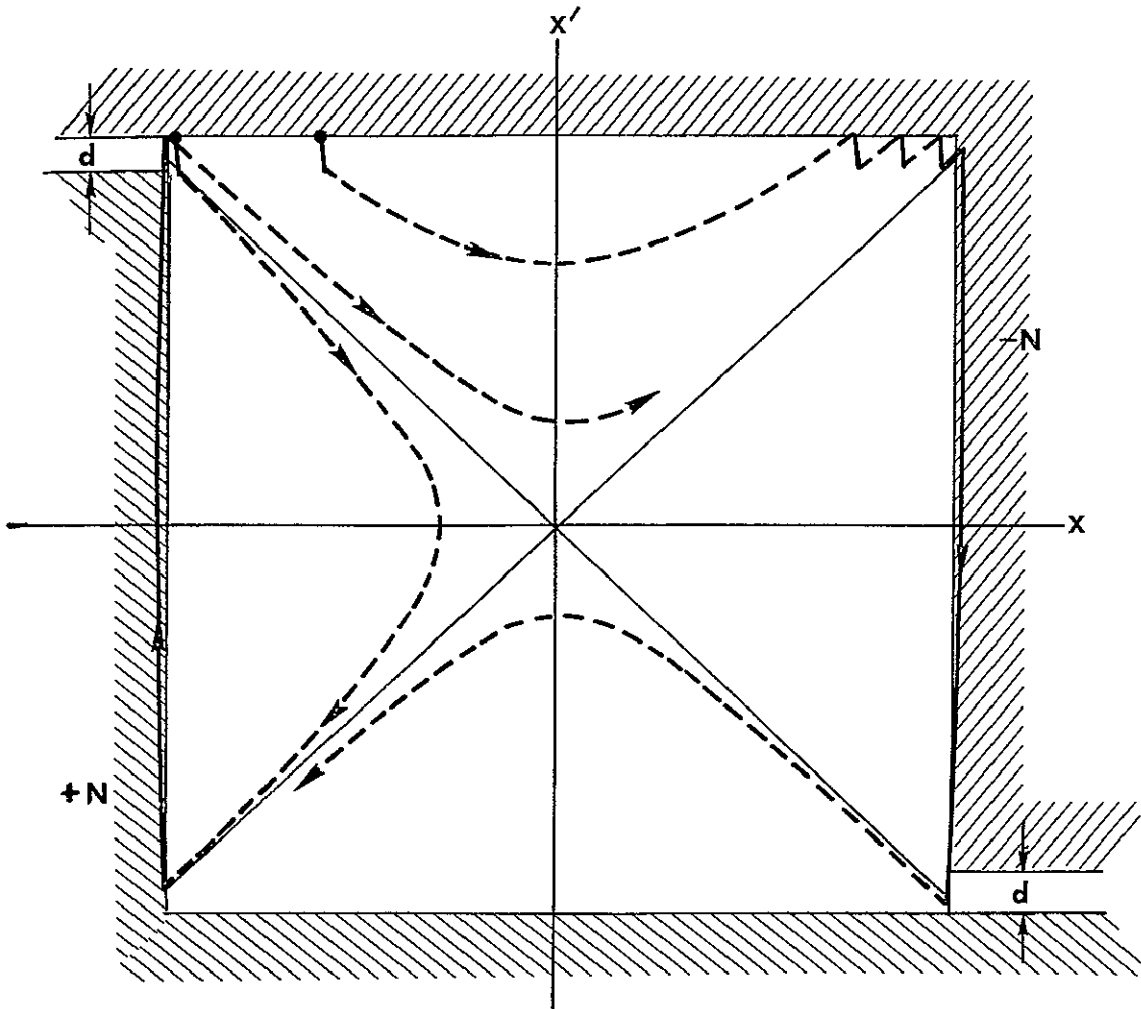
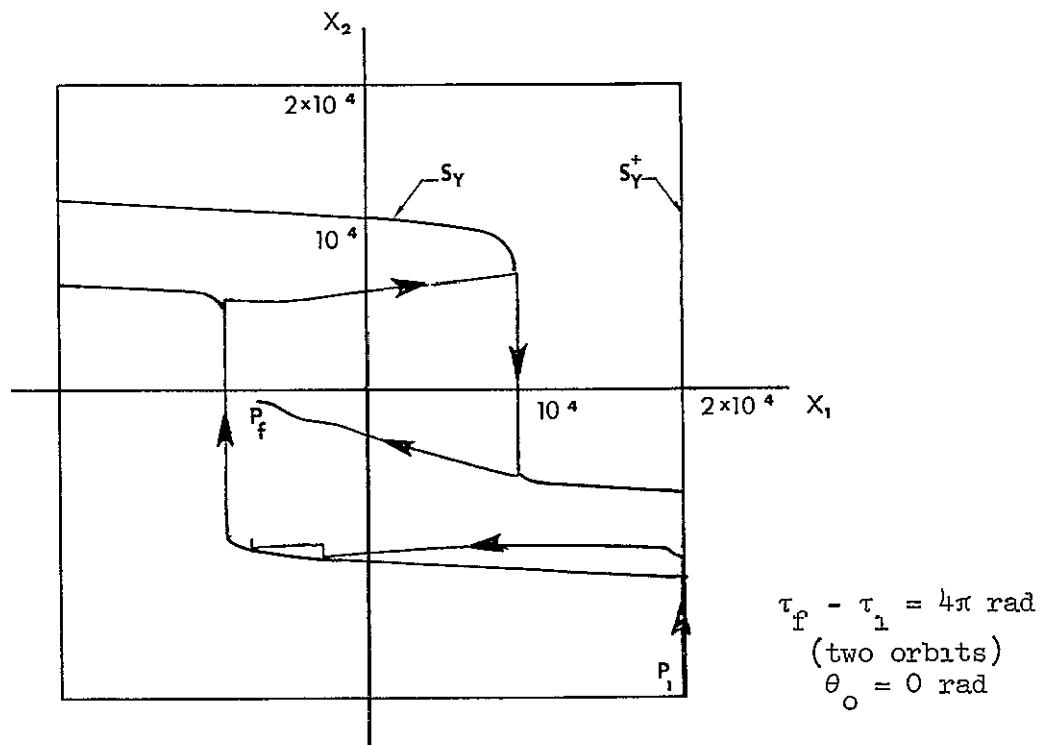
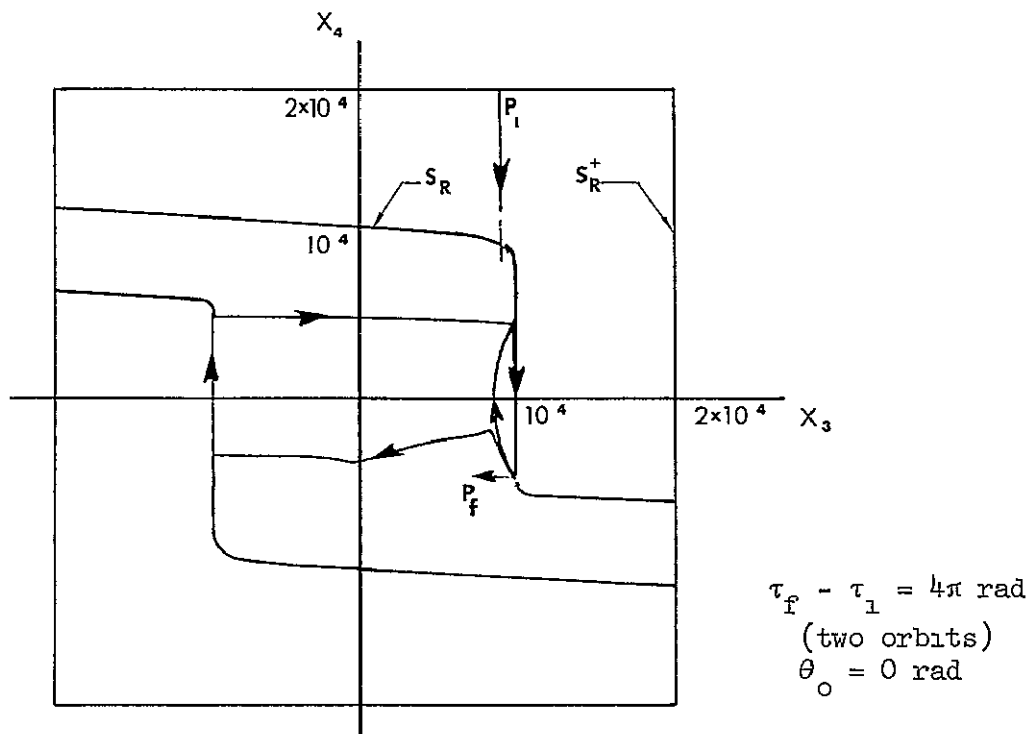


Figure 4 16 The Control of Figure 4 14 Applied to $x'' + a^2 x = v$,
 $a^2 = -0.95$, $N = 0.05$, $d = 10^{-5}$

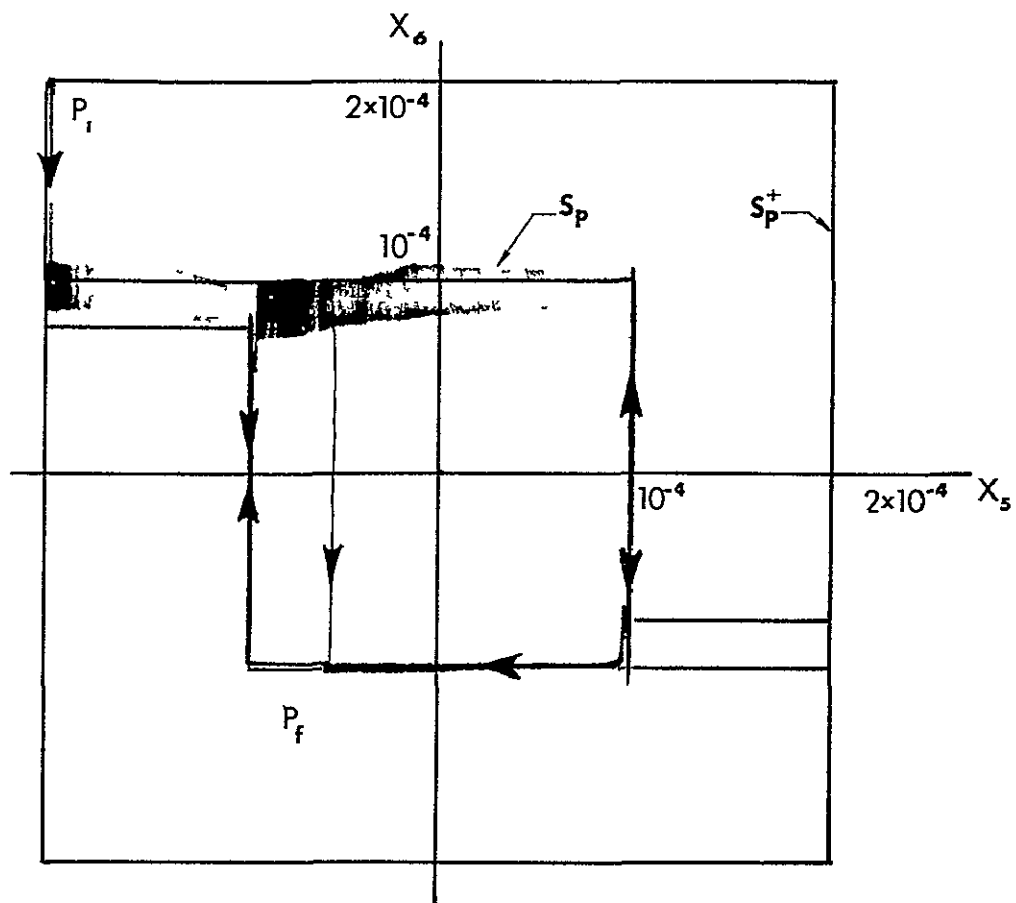


a Yaw Trajectory, $N_1 = 0.01$, $t_d^- = 0.5 \text{ sec}$, $t_d^+ = 1.25 \text{ sec}$, $d = 4 \times 10^{-5}$



b Roll Trajectory, $N_2 = 0.01$, $t_d^- = 0.5 \text{ sec}$, $t_d^+ = 1.0 \text{ sec}$, $d = 4.0 \times 10^{-5}$

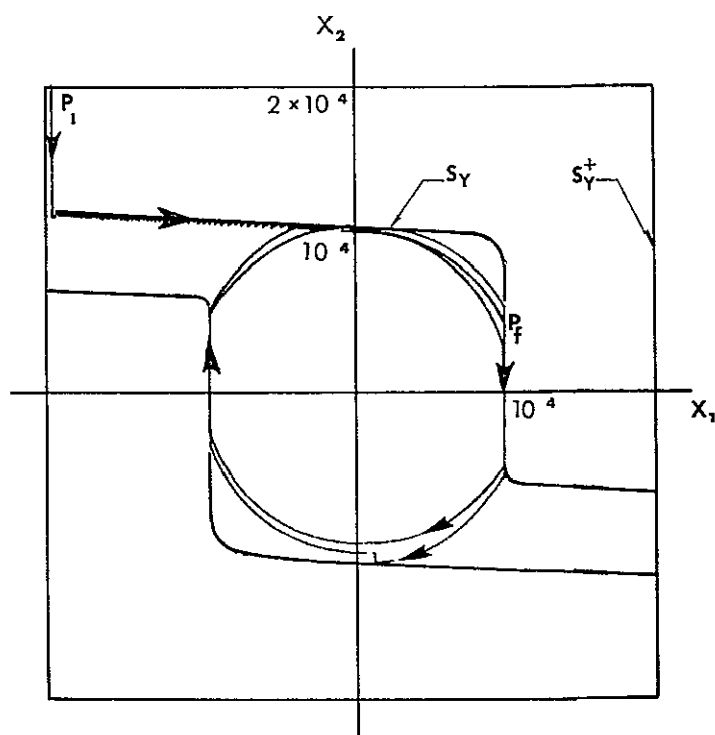
Figure 4.17 Station-Keeping Motion of Satellite (1)



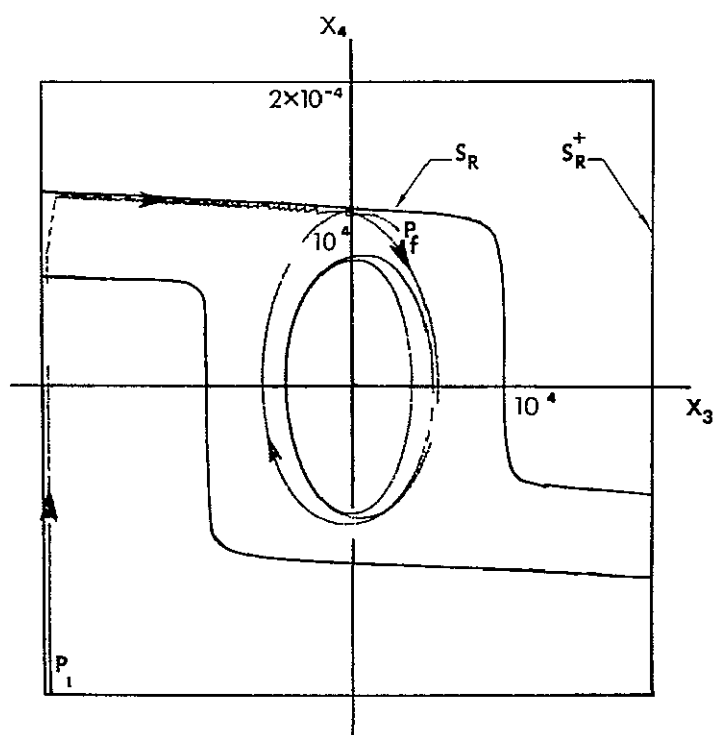
$$\begin{aligned}\tau_f - \tau_i &= 4\pi \text{ rad} \\ &(\text{two orbits}) \\ \theta_0 &= \pi/2 \text{ rad}\end{aligned}$$

c Pitch Trajectory, $N_3 = 0.2$, $t_d^- = 0.05 \text{ sec}$, $t_d^+ = 0.01 \text{ sec.}$,
 $d = 2.5 \times 10^{-5}$

Figure 4.17 Continued.

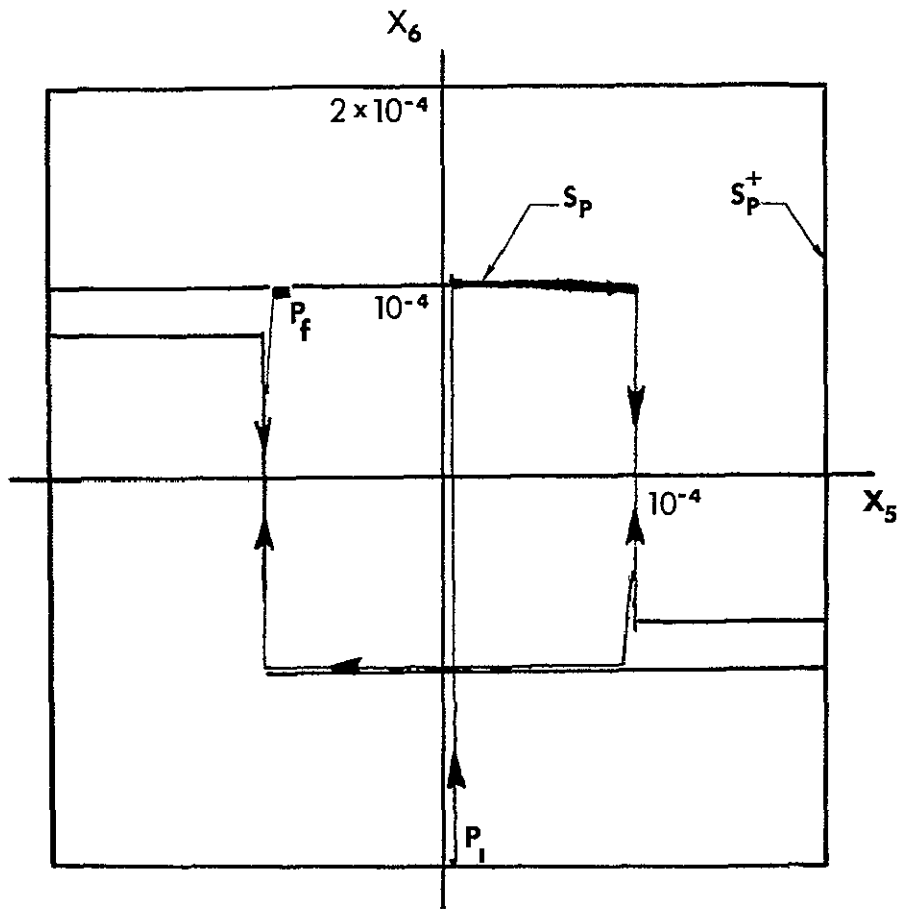


- a Yaw Trajectory, $N_1 = 0.02$, $t_d^- = 0.5 \text{ sec}$, $t_d^+ = 1.25 \text{ sec}$,
 $d = 4 \times 10^{-5}$



- b Roll Trajectory, $N_2 = 0.02$, $t_d^- = 0.5 \text{ sec}$, $t_d^+ = 1.0 \text{ sec}$,
 $d = 4 \times 10^{-5}$

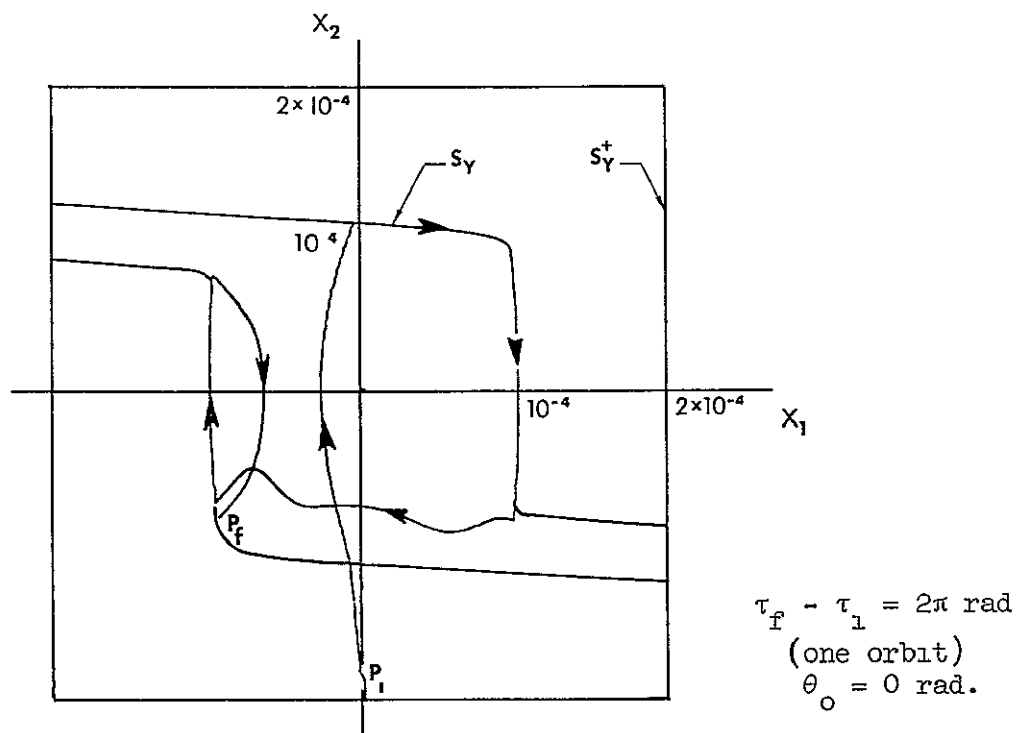
Figure 4.18 Station-Keeping Motion of Satellite (2)



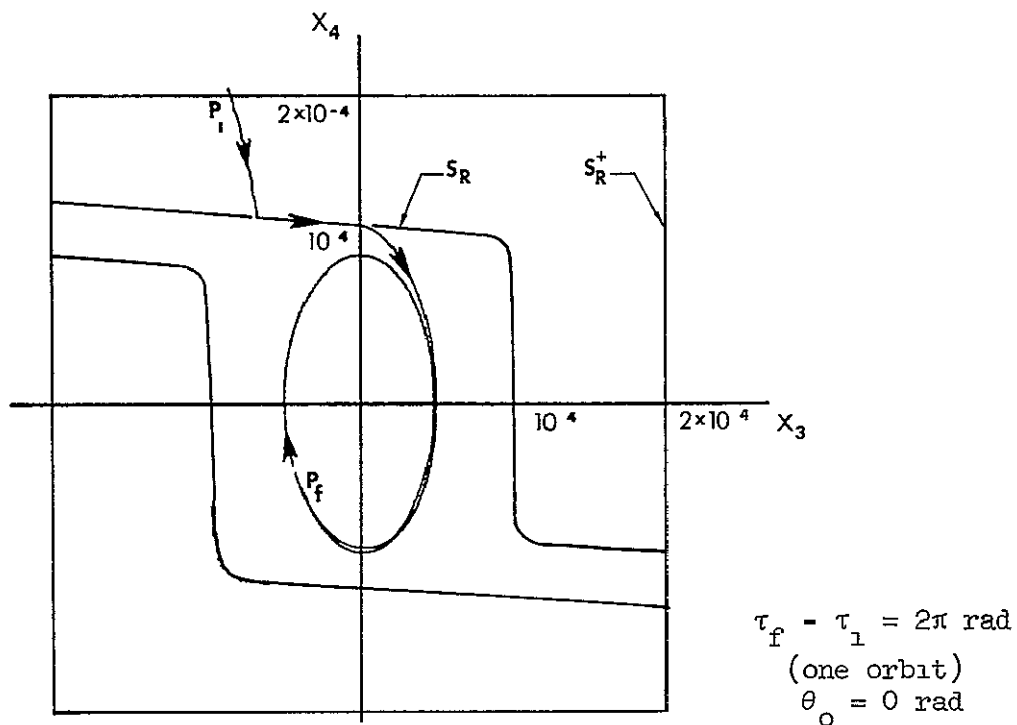
$$\begin{aligned} \tau_f - \tau_i &= 2\pi \text{ rad} \\ &(\text{one orbit}) \\ \theta_o &= 90^\circ \end{aligned}$$

- c. Pitch Trajectory, $N_3 = 0.03$, $t_d^- = 0.2 \text{ sec}$, $t_d^+ = 0.04 \text{ sec}$,
 $d = 2.5 \times 10^{-5}$

Figure 4.18 Continued.

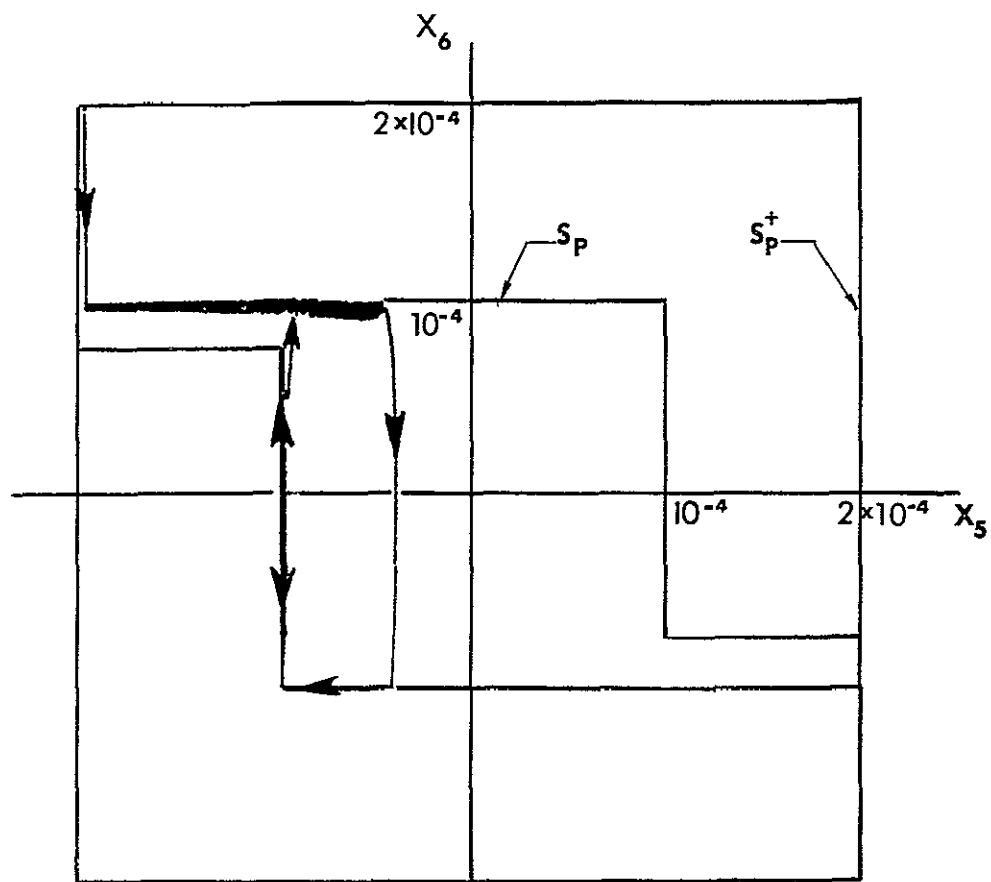


- a Yaw Trajectory, $N_1 = 0.001$, $t_d^- = 0.5 \text{ sec}$, $t_d^+ = 1.25 \text{ sec}$,
 $d = 2 \times 10^{-5}$



- b Roll Trajectory, $N_2 = 0.001$, $t_d^- = 0.5 \text{ sec}$, $t_d^+ = 1.0 \text{ sec}$,
 $d = 2 \times 10^{-5}$

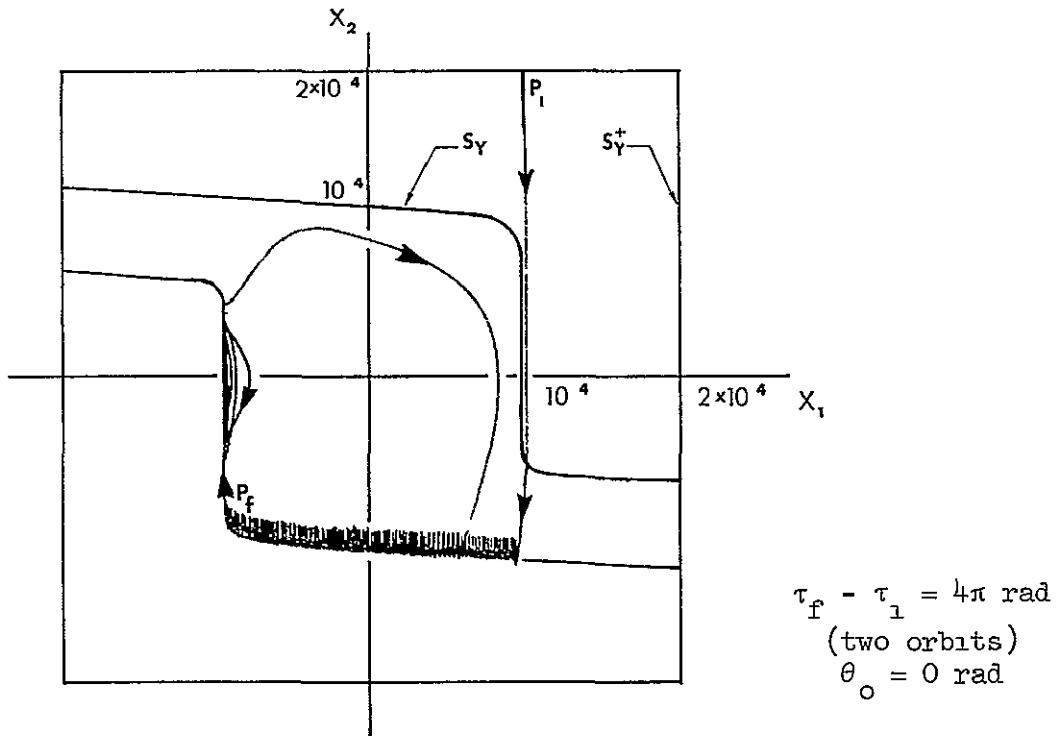
Figure 4.19 Station-Keeping Motion of Satellite (3)



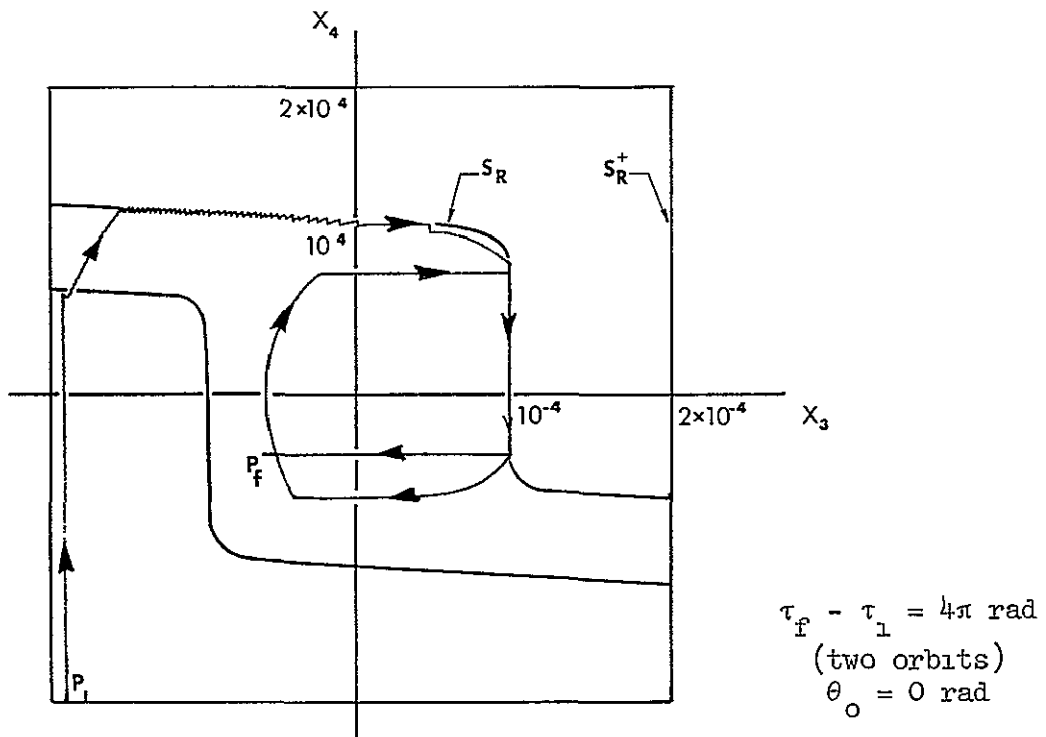
$$\begin{aligned} \tau_f - \tau_1 &= 2\pi \text{ rad.} \\ &(\text{one orbit}) \\ \theta_o &= \pi/3 \text{ rad} \end{aligned}$$

c Pitch Trajectory, $N_3 = 0.03$, $t_d^- = 0.2 \text{ sec}$, $t_d^+ = 0.04 \text{ sec}$,
 $d = 2.5 \times 10^{-5}$

Figure 4.19 Continued

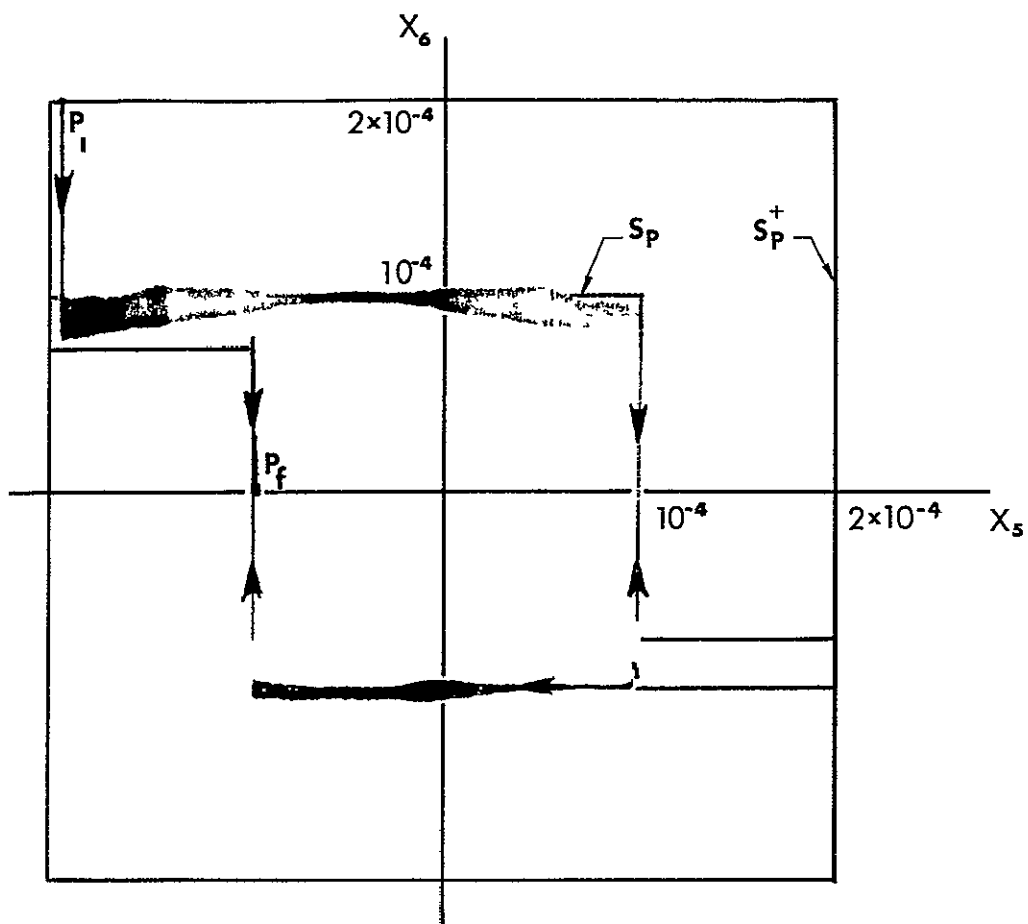


- a Yaw Trajectory, $N_1 = 0.01$, $t_d^- = 0.5 \text{ sec}$, $t_d^+ = 1.25 \text{ sec}$,
 $d = 4 \times 10^{-5}$



- b Roll Trajectory, $N_2 = 0.01$, $t_d^- = 0.5 \text{ sec}$, $t_d^+ = 1.0 \text{ sec}$,
 $d = 4 \times 10^{-5}$

Figure 4.20 Station-Keeping Motion of Satellite (4)



$$\begin{aligned} \tau_f - \tau_1 &= 2\pi \text{ rad} \\ &\text{(one orbit)} \\ \theta_o &= 0 \text{ rad} \end{aligned}$$

- c Pitch Trajectory, $N_3 = 0.12$, $t_d^- = 0.2 \text{ sec}$, $t_d^+ = 0.04 \text{ sec}$,
 $d = 2.5 \times 10^{-5}$

Figure 4.20 Continued

real time is the time of two orbits. The point in the orbit corresponding to the initial time is given by θ_0 , the angle of the satellite from perigee. The time delay in each part of the controller is given in each figure as t_d^- , which corresponds to $-N$, and t_d^+ , which corresponds to $+N$. It should be noted in reading the figures that the lightest regions of the rapid chatter parts of the pitch trajectories generally correspond to the most rapid chatter while the darker parts of the trajectory correspond to slower motion. In Figure 4 20a is shown a yaw trajectory of satellite (4) (which is greatly influenced by the aerodynamic torque) for the time of two orbits. The part of the trajectory corresponding to the second orbit overlaps part of the first orbit trajectory. However, the early rapid chatter motion, which occurs when the aerodynamic torque is near its maximum magnitude, is light enough for the later less rapid chatter motion to be seen over it. In the roll and yaw parts of Figures 4 17 - 4 20 the boundary lines of the phase plane projections of S are not perfectly straight as in Figure 4 14. These boundaries were created in the analog simulation by an electronic signum function generator which was not perfect, i.e., the characteristics of the diodes used were only nearly ideal. The large control magnitudes required in pitch resulted in chatter motion along the nearly vertical parts of the boundary unless these parts of the boundary were straightened up somewhat. Therefore, for the pitch parts of Figure 4 17 - Figure 4 20 the boundary lines were (electronically) made very straight by connecting two diode signum function generators in series.

Table 4 1 gives the fuel expenditure (nondimensional) for the simulation runs of Figure 4 17 - Figure 4 20. J_{R-Y} and J_P are the total fuel expenditures for the roll-yaw and pitch controls, respectively. $J_{R-Y,ACQ}$, for example, is the cost of acquiring the roll-yaw projection of S from the point P_1 . $J_{P,SS}$, for example, is the cost of the steady-state pitch motion. The fuel expenditure for these runs were typical of all runs of the same duration. The average (the initial points in S and the angle θ_0 were varied) steady-state fuel expenditure for one orbit differed from the steady-state values in Table 4 1 by about two or three percent. Of course, the acquisition part of the fuel expenditure depended greatly on P_1 and to a lesser extent on θ_0 .

TABLE 4 1 FUEL EXPENDITURE FOR THE SIMULATION RUNS OF FIGURE 4 17 -
FIGURE 4 20

SATELLITE	(1)	(2)	(3)	(4)
J_{R-Y}	* 7.52×10^{-3}	* 7.60×10^{-3}	3.71×10^{-3}	* 7.88×10^{-3}
J_P	* 3.05×10^{-1}	6.03×10^{-2}	7.52×10^{-2}	* 13.94×10^{-2}
$J_{R-Y, ACQ}$	2.88×10^{-3}	4.34×10^{-3}	1.25×10^{-3}	2.04×10^{-3}
$J_{P, ACQ}$	3.09×10^{-2}	3.0×10^{-4}	1.51×10^{-2}	1.03×10^{-2}
(†) $J_{R-Y, SS}$	* 4.64×10^{-3}	* 3.26×10^{-3}	2.46×10^{-3}	* 5.84×10^{-3}
(†) $J_{P, SS}$	* 2.74×10^{-1}	6.03×10^{-2}	6.01×10^{-2}	* 12.91×10^{-2}

*Denotes two orbits, otherwise one orbit

NOTE The nondimensional cost values are translated in Chapter VI into the number of pounds per orbit (or year) for the example satellites of Chapter II

(†)RECALL. Satellite (1) is "mildly stable" in all axes but the pitch motion is strongly forced, satellite (2) is "very stable" in roll-yaw but is "unstable" in pitch with forced motion; satellite (3) is "unstable" in yaw, "stable" in roll and pitch and pitch has forced motion, satellite (4) is similar to satellite (1) except that yaw and pitch are "destabilized" by the aerodynamic torque.

(Compare, for example, the value of $J_{P,ACQ}$ for satellite (2) with the value for satellite (1))

From the describing differential equations of controlled motion and the example trajectories of Figure 4 17 - Figure 4 20 it is apparent that for all initial state in S the station-keeping part of the controller can keep the state space trajectory from departing S by a significant amount (except, perhaps, when large unaccounted for disturbances overpower the station-keeping part of the controller). Since the minimum fuel expenditure of the station-keeping controller for one orbit is not known, the steady-state fuel cost per orbit obtained in the simulation runs cannot be compared with an absolute minimum. However, since from Figure 4 17 - Figure 4 20 it is clear that the single-axis satellite motions are approximated, in at least a piecewise sense, by the approximation motions of Section A and this section, (Section B) the steady-state fuel cost is considered to be nearly a minimum. Thus, the station-keeping part of the controller is considered to perform satisfactorily. (In Chapter VI cost, error and other performance measures are evaluated for particular satellites of particular weights. There it is found that the weight of fuel used in one year is very small compared to the weights of the satellites.)

V. DERIVATION OF ACQUISITION CONTROL LAWS

A. EXTENSIONS OF BUSCH'S SOLUTION

In Chapter III, Section D, Part 2 it was mentioned that Busch, using PMP and a reverse-time integration method, has found a nearly minimum-fuel optimal feedback control law which for a "stable" satellite results in acquisition to a region much larger (6.3×10^{-3} radians) than S^+ (see e.g. Figure (4.20)). The control law works well for $x_1 \leq 0.5$ radians, $i = 1, \dots, 6$, but, for some large initial angles (about 60°), the coupling between the controlled roll motion and the controlled yaw motion via the controls through the pitch angle and the large value of $\cos^{-1}\theta_2$ in the second of Equation (2.14) have a destabilizing effect. The Busch control law results in an acquisition time of about the time of one-half orbit from initial angles of about 25° . Acquisition from larger angles requires much longer acquisition times, and, in some cases when the satellite is "unstable" (e.g., satellite (3)) and the initial angles are large, acquisition takes a much longer time. (In some cases the motion can become uncontrollable so that acquisition cannot be accomplished.)

Thus, for the controllers of the satellites' motions to perform satisfactorily, the Busch control law must be modified so that (1) the region S^+ can be acquired even if large imperfections exist in the controllers, (2) the time of acquisition from $x_1 \leq 1.5$ radians, $i = 1, \dots, 6$, is the time of one-quarter orbit or less, and, (3) "unstable" satellites such as satellite (3) are controllable for large initial angles.

1. Via Phase Plane Techniques

In component form the Busch control law can be written as

$$u_1 = (-N_1'/2)(\text{SGN}(x_2|x_2| + 2x_1) + \text{SGN}(x_2 + 0.1 x_1))$$

$$u_2 = \begin{cases} -N_2'\text{SGN}(x_4) & \text{IF } x_4^2 > 1.7 \times |x_3| \\ 0 & \text{IF } x_4^2 < 1.7 \times |x_3| \end{cases}$$

$$u_3 = \begin{cases} -N'_3 \text{SGN}(x_6) & \text{IF } x_6^2 > 2 \times |x_5| \\ 0 & \text{IF } x_6^2 < 2 \times |x_5| \end{cases} \quad (5.1)$$

where u_1 , $i = 1, 2, 3$, is the nondimensional acquisition control torque measure numbers, $N'_1 = 1$, and $\text{SGN}(\)$ is the signum function. Figure (5.1) shows sketches of the two types of control switching curves in the phase planes. It should be noticed that N'_1 , $i = 1, 2, 3$, are all unity, and, therefore, the parabolic switching curves in the yaw and pitch phase planes are the same as for the minimum-fuel control of $x'' = u$ when $|u_{\max.}| = 1.0$. Thus, if the magnitude of the control components are increased to shorten the acquisition time, an obvious modification to the Busch control law is the modification of the parabolic switching curves which makes them compatible with the larger values of N'_1 , $i = 1, 2, 3$, i.e., in the equation $x'^2 = \pm ax$, the coefficient $a (=2N)$ is modified with N .

Clearly, $N'_1 = 1.0$, $i = 1, 2, 3$, are too small to give acquisition from $|x_1| = 1.5$ radians, $i = 1, \dots, 6$, in a τ -interval of 1.57 i.e., in the time of one-quarter orbit. Consider acquisition from $(x, x') = (1.5, 1.5)$ for $x'' = u$ in minimum time. It is not difficult to see that for $|u_{\max.}| = N = 10$ the acquisition time is $\tau_f - \tau_0 = 0.95$. From a study of the minimum-time acquisition of other simple systems i.e., $x'' + a^2 x = u$, $a^2 > 0$, $a^2 < 0$, it was found that minimum-time acquisition is accomplished in $\tau_f - \tau_0 = 1.57$ if N was large enough. In particular the required values of N ranged from a little larger than 2.0 to almost ten (depending on a^2). Thus, it seems that $N'_1 = 10$, $i = 1, 2, 3$, are nearly lower bounds for the magnitudes of the control components for minimum-time acquisition. For minimum-fuel acquisition $N'_1 = 10$, $i = 1, 2, 3$, seem, certainly, to be lower bounds. Since values of N'_1 , $i = 1, 2, 3$, which are much larger than ten (say, one-hundred) can result in very poor performance (such as higher cost and no acquisition to S^+) when the usual imperfections in the controller (e.g. time delays) are present, the initial value assumed for each of N'_1 , $i = 1, 2, 3$, was taken as ten. (In the next part it is seen that "spiraling in" to S^+ from $x_1 \approx 0.1$, $i = 1, \dots, 6$, should be avoided for low fuel cost. "Spiraling in" is avoided if

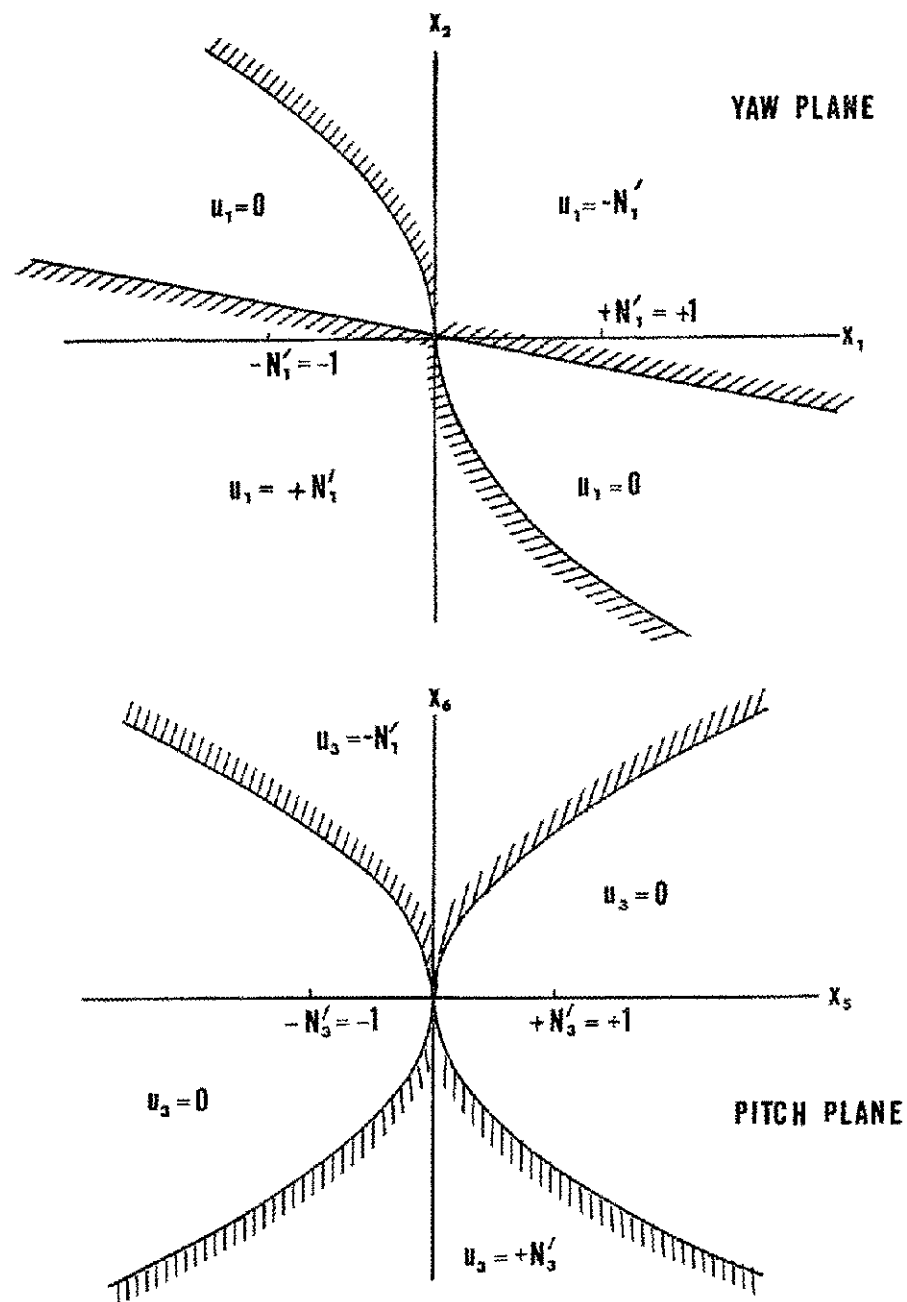


Figure 5.1 Switching Curves of the Busch Control Law in the Yaw and Pitch Planes.

N_1' , $i = 1, 2, 3$, are large enough (≥ 10), since the parabolic switching curves are nearly coincident with the "zeroing" part of a trajectory from a point on a parabolic switching curve with $|x_1| \approx 0.1$, $i = 2, 4, 6$.)

Since Busch was successful in using a straight line for the other switching curve in the phase plane of the least "stable" motion and since the switching logic for such a curve is very simple, straight lines with various slopes were studied as possible switching curves. Phase plane methods with the constraints on the time of acquisition and fuel cost were used initially in the study in the hope of saving computer time. Since the initial values of the state variables considered were no larger than 1.50 radians, the control-on part of the phase plane trajectories very nearly coincided with parts of parabolic curves such as $x_2^2 = 2N_1'x_1$ if $N_1' \geq 10$. Thus, since the behavior of the phase plane trajectories was generally known when the trajectory was in a control-on region, the phase plane analysis was limited mainly to the control-off regions.

The phase plane analysis consisted of (1) the calculation of the slopes of control-off trajectories at numerous points in the phase planes by assuming the trajectories in the other two phase planes to be various nominal points and (2) for switching lines of various slopes the estimation of the time between control-on intervals with the aid of $\Delta x_1 = (\tilde{x}_{i+1})\Delta\tau_{\text{off}}$, $i = 1, 3, 5$, where \tilde{x}_{i+1} is the (integral) mean rate value. Equations (2.14) were used for $|x_1| \approx 1.0$, $i = 1, \dots, 6$, and equations (2.17) and (2.18) were used for $|x_1| \approx 0.1$, $i = 1, \dots, 6$. The worst possible values $\delta = \pi/4$ and $\theta_0 = \pi/4$ (or $\frac{5\pi}{4}$) were used in each case for each satellite. The results of this analysis can be summarized as follows: (1) the slope of the switching line which gave a maximum control-off time interval of $\Delta\tau_{\text{off}} \approx 1.0$ also resulted in most cases in the lowest estimated fuel cost (the total control-on time for acquisition was estimated to be about 20-30% of the time of acquisition i.e., $\Delta\tau_{\text{on}} \approx 0.3-0.5$), (2) if the motion was not very "stable" (e.g. satellite (1)), some of the smaller (in magnitude) slopes tried resulted in chatter motion which was very costly and time consuming (especially for $|x_1| < 0.01$, $i = 1, 3, 5$, where the sine forcing terms are most influential), and, (3) slopes of the switching line which were much greater (about 10x) resulted in a much higher cost estimate (about 200% higher). The slopes of the

switching lines which are expected to result in a satisfactory acquisition control law are given in Table 5.1. These slopes are given in Table 5.1 for each phase plane of each satellite and are generally compromises which are arrived at by placing the greatest emphasis on fuel economy and simplicity. For example, the slope of the straight line of the type 2 switching curves is larger than was estimated as needed for large angles. The estimated values of the slope for pitch of satellites (1), (2) and (4) for large angles ranged from about -0.75 to -1.5, however, for small angles ($|x_1| < 0.01$, $i = 1, 3, 5$) the magnitudes of the slopes were estimated to be about -6.0. Thus, since pitch must be "zeroed" faster than roll and yaw to avoid detrimental coupling and since other curves which give a variable slope are not as simple, a slope of -2 is a compromise.

In the next part of this section the maximum principle is used to check and/or offer modifications to the control laws of this part.

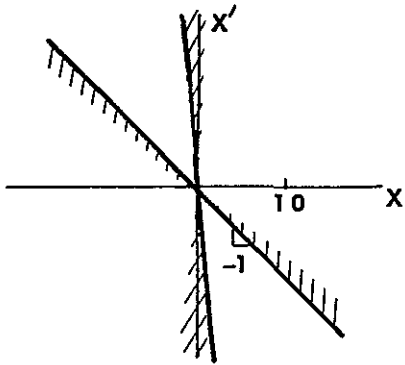
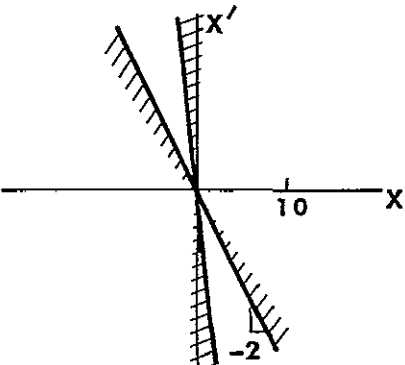
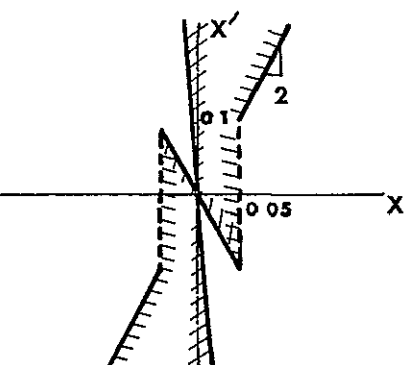
2. Via Pontryagin's Maximum Principle

Using the reverse-time integration method, the maximum principle was applied to the acquisition problem. That is, the equations of motion (with the 'coast function' optimal control) and the adjoint equations were written in backwards time and integrated with the aid of the digital computer. (For the program see Appendix F.) The solutions of the equations of motion were plotted as phase plane trajectories (i.e., projections of the trajectories) so that the control switching points in the phase planes could be easily observed.

Since S^+ is small compared to the scale used in the phase plane plots and since, by "smoothing" the corners of S^+ , the final (forward time) adjoint vector can span the six-dimensional vector space, the origin of the state space was considered to be the final goal instead of S^+ . That is, since the origin of the state space and S^+ are almost equivalent with respect to FMP and since computationally it is simpler to take $x(\tau_f) = 0$, the origin was acquired.

The linearized equations of motion [Equations (2.17) with the aerodynamic torque terms included for satellite (4)] were used in this application of the maximum principle. The reasons for using the linearized equations are (1) the linear and nonlinear optimal solutions agreed

TABLE 5 1 MODIFIED VERSIONS OF BUSCH'S SWITCHING CURVES

<p>TYPE 1</p> 	<p><u>PLANES</u></p> <p>YAW-ALL SATELLITES</p> <p>ROLL-SATELLITES (1), (2) AND (4)</p> <p>(slopes for roll, yaw of satellites (1) and (4) could be as large as 15)</p>
<p>TYPE 2</p> 	<p><u>PLANES</u></p> <p>PITCH - SATELLITES (1), (2) AND (4)</p>
<p>TYPE 3</p> 	<p><u>PLANES</u></p> <p>ROLL-SATELLITE (3)</p> <p>PITCH-SATELLITE (3)</p>

very well for $|x_1| < 0.1$, $i = 1, 3, 5$, in the cases tested*, (2) for $|x_1| > 0.1$, $i = 1, 3, 5$, the nonlinear equations are highly coupled and result in erratic control switching points (since control switching for one axis depends on the motions of the other axes), and (3) the computer time for each solution run of the nonlinear system of equations was too great (about ten minutes) to be practicable (since many solutions were needed).

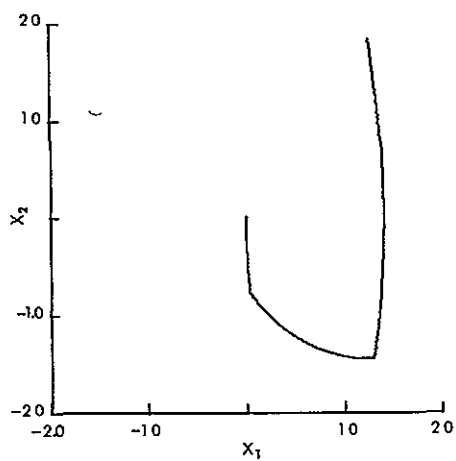
Some typical solutions of the linear optimal acquisition equations are given in graphical form in Figure 5.2. It should be noted that no trajectories "spiral in" toward the origin. "Spiraling in" is not a characteristic of an optimal trajectory in the case $N_1 \geq 10$, $i = 1, 2, 3$. Indeed, for such large values on N_1 three switches in each control component is generally a maximum number in the time interval of $\tau_f - \tau_0 = 1.57$ since the adjoint variables on which the switches depend generally give (in backward time) a short control-on interval followed by a long control-off interval or with a short control-off interval and then a long control-on interval).

In Table 5.2 are given some of the data obtained from the thirty-two backward time solutions. In particular Table 5.2 presents the range of values for the slopes of the switching lines which pass through the origin and the point at which the control switches from off to on. Also presented are the consensus values (for lines drawn through the greatest number of switching points) of the slopes and the best values for stabilization of the motion.

In the next section, Section B, the final states of the backward time runs are used as the initial states in the solutions of the full nonlinear equations of suboptimally controlled motion. These forward time solutions of the nonlinear equations of suboptimal controlled motion and their fuel costs are compared with optimal linear solutions and their costs in the performance evaluation chapter, Chapter VI.

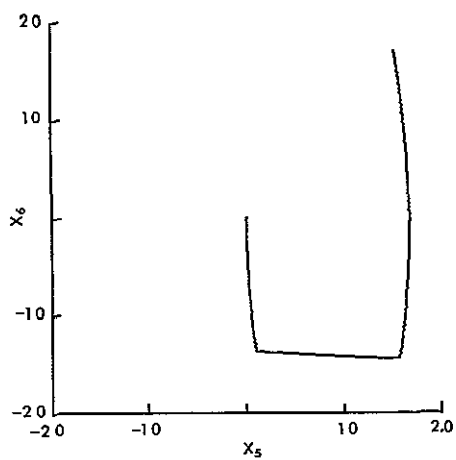
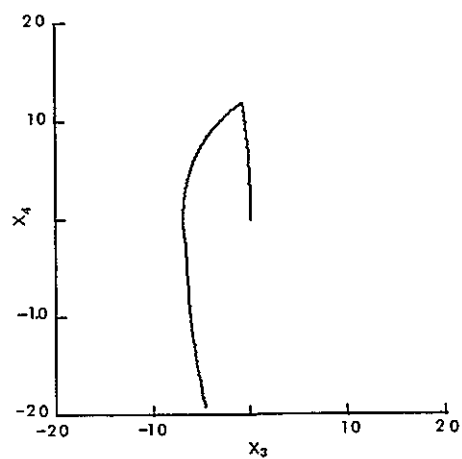
B. ACQUISITION CONTROL LAWS WHICH PERFORM SATISFACTORILY

*Also, Busch found very good agreement in many comparisons



YAW

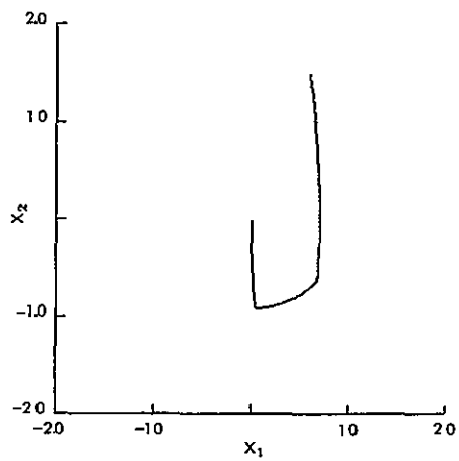
ROLL



PITCH

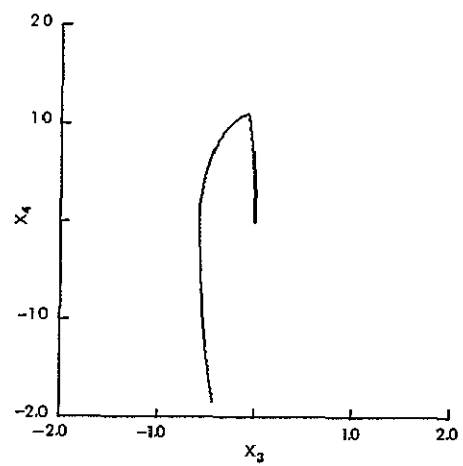
a Satellite (1), $J = 8.19$, $\tau_f - \tau_o = 1.42$, $\theta_o = \pi/4$.

Figure 5.2 Optimal (Linear) Acquisition Solutions

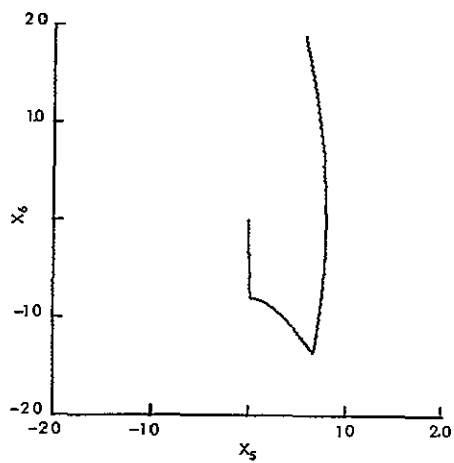


YAW

ROLL

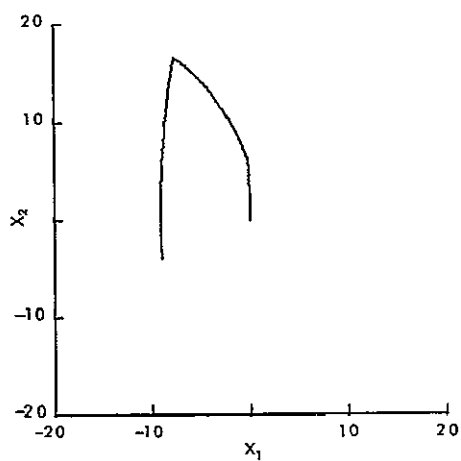


PITCH



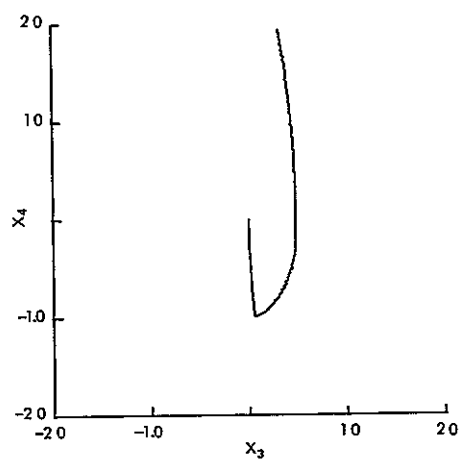
b. Satellite (2), $J = 8.92$, $\tau_f - \tau_o = 1.32$, $\theta_o = \pi/4$.

Figure 5.2 Continued

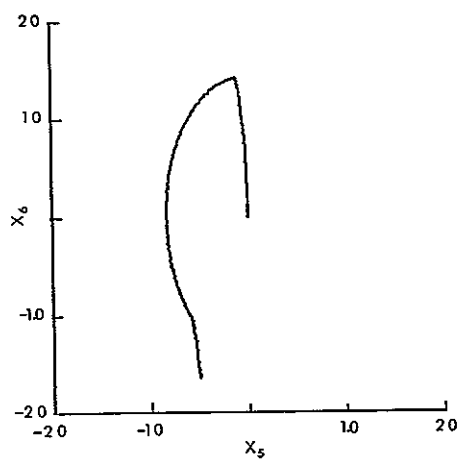


YAW

ROLL

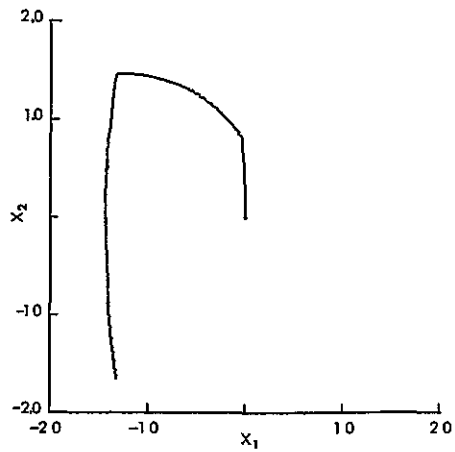


PITCH



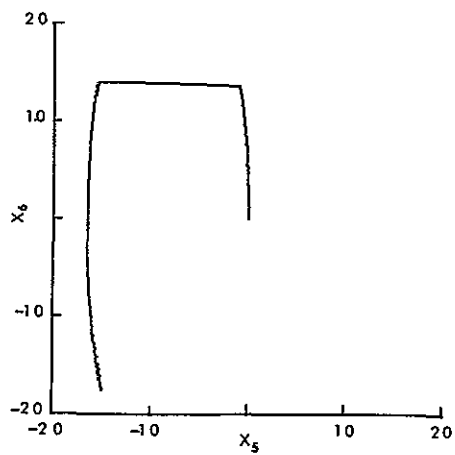
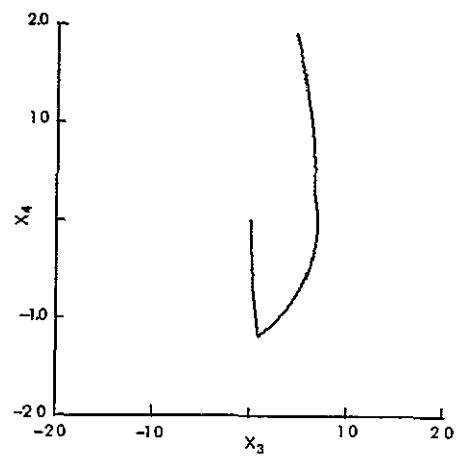
c Satellite (3), $J = 6.03$, $\tau_f - \tau_o = 1.46$, $\theta_o = \pi/4$

Figure 5.2 Continued



YAW

ROLL



PITCH

d. Satellite (4), $J = 8.73$, $\tau_f - \tau_o = 1.42$, $\theta_o = 5\pi/4$

Figure 5 2. (Continued)

TABLE 5 2 SLOPES FOR THE STRAIGHT LINE SWITCHING CURVES AS OBTAINED FROM THE OPTIMAL (LINEAR) SOLUTIONS				
SATELLITE	AXIS	RANGE OF SLOPES	CONSENSUS	BEST FOR STABILIZATION
(1) "STABLE"	YAW	-1 01 → + ∞*	-1 00 (OR +0 41)	-1 01
	ROLL	-1 28 → + ∞*	+0 33 (OR -1 13)	-1 28
	PITCH	-1 01 → -0 89	-0 92	-1 01
(2) VERY "STABLE" IN ROLL AND YAW, "UN- STABLE" IN PITCH	YAW	-0 77 → -0 59	-0 69	-0 77
	ROLL	-0 38 → -0 19	-0 35	-0 38
	PITCH	-2 1 → -1 63	-1 81	-2 1
(3) "UNSTABLE" IN YAW, "STABLE" IN ROLL AND PITCH	YAW	-0 86 → + ∞*	+0 42 (OR -0.67)	-0 86
	ROLL	-0.91 → + ∞*	-0 61 (OR +0.40)	-0 91
	PITCH	+1 03 → +1 5	+1 25	+1 03
(4) "STABLE" BUT GREATLY AFFECTED BY AERO TORQUE	YAW	-0 94 → + ∞*	-0 77 (OR +0 39)	-0 94
	ROLL	-0 85 → + ∞*	+0 42 (OR -0 84)	-0 85
	PITCH	-1 33 → -0 89	-1 02	-1 33

* Depends on initial condition of adjoint variables, but, generally if
yaw ~ -∞, then roll ~ 1 0 and vice versa

In Section A, Part 1 three types of phase plane switching curves (Table 5.1) were suggested by the phase plane analysis as possible "improvements"* of the Busch switching curves. In Part 2 of the last section the linear equations for an optimal acquisition solution were integrated in backward time. Some of the data obtained from these integrations are presented in Table 5.2.

If the consensus values for the slopes of the switching lines (Table 5.2) are compared to the slopes given in the sketches in Table 5.1, good agreement is found in about half of the cases. The exceptions are pitch-satellite (1), roll-satellite (2) pitch-satellite (4), which are each off by nearly a factor of two, and roll or yaw of satellites (1), (3) and (4), which are mostly off by a sign. If the best values for stabilization (the greatest slopes obtained from the optimal solutions) are compared to the slopes of Table 5.1, the agreement is found to be good in every case.

Of the two types of switching curves, the parabolic curves have the smallest deviation from the optimal. This is, of course, expected for control magnitudes of ten or greater. From Figure 5.2 it is clear that the parabolic switching curves will work very well when $|x_1|$, $i = 1, \dots, 6$, are small, however, for large angles and rates it is possible that some modifications will be needed.

The following control law was used in the initial tests of acquisition of the satellites from large angles [using the nonlinear equations of motion, (2.14) - (2.16)]

$$u_1 = (-N'_1/2)\{\text{SGN}(x_{1+1}|x_{1+1}| + 20x_1) + \text{SGN}(x_{1+1} + M_1x_1 \text{SGN}(Q_1 - |x_1|))\}, \quad i = 1, 2, 3 \quad (5.2)$$

where M_1 , the negative of the slopes, and the "change-in-slope" factor Q_1 , $i = 1, 2, 3$, were as given in Table 5.3 (If Q_1 is large, $\text{SGN}(Q_1 - |x_1|)$ is positive for all x_1 and has essentially no effect)




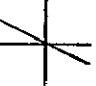
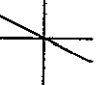



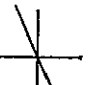



Using some of the final conditions (backward time) of the optimal

*Busch considered only one "stable" satellite. Here, consistent acquisition to a smaller region from larger angles is obtained for four ("stable" and "unstable") satellites.

(linear) solutions for initial conditions, the full nonlinear equations with the control given by (5.2) and Table 5.3 were integrated with the aid of the digital computer. Since some chatter motion was expected along the straight switching lines in some planes, a time delay was built into the control. The time delay was initially simulated by making the control a function of the value of the state at the end of the previous step of integration. The integration and the plotting (by the Stanford Cal-Comp Plotter) were carried out in two steps so that the small details of the phase plane plots could be observed. First, the digital computer integration proceeded from $|x_1| \approx 1.5$, $i = 1, \dots, 6$, down to $|x_1| \leq 0.02$, $i = 1, 3, 5$. Then, using the final values of the first run, the second digital computer run was made down to $|x_1| \leq 2.0 \times 10^{-4}$, $i = 1, \dots, 6$. (Acquisition from S^+ to S^- was simulated on the analog computer. See Figures (4.17) - (4.20).)

The initial runs (for the four satellites) were quite time consuming and only seven out of the twelve phase plane curves of each run appeared as expected. The trajectories in the phase planes of satellite (1) did not proceed toward the origin as directly as those trajectories of Figure (5.2). The reasons for this were considered to be (1) the slope of the switching line in pitch was too small (in magnitude) and caused the acquisition in the pitch plane to be too slow, and, (2) the slow acquisition in pitch resulted in harmful cross-coupling between the roll control and yaw and the yaw control and roll. The fuel cost for this run was $J = 15.87$ and the time $(\tau_f - \tau_0)$ of acquisition was greater than 2.0. The initial integration run of satellite (3) gave an unstable solution i.e., after a short time the state space trajectory began moving away from the origin and continued until there was no hope of acquisition. This unstable behavior proved to depend somewhat on the initial conditions, however, the main reasons for this bad performance are considered to be the same as the reasons for the poor performance in the initial run of satellite (1). The initial integration run of satellite (2) showed that early chatter motion in roll and yaw occurred. This early chatter motion appeared to be the reason for the cost and acquisition time being greater than expected. The (nondimensional) cost was $J = 9.91$ and the (nondimensional) time was 1.74. The initial solution for satellite (4) was

TABLE 5 3 THE PARAMETERS OF THE CONTROL LAW FOR THE INITIAL TEST

SATELLITE	AXIS	M_1	Q_1	SKETCH OF SWITCHING LINES
(1)	YAW	1.0	10 0	 TYPE 1
	ROLL	1.0	10 0	 TYPE 1
	PITCH	1 0	10 0	 TYPE 1
(2)	YAW	0.5	10 0	 MODIFIED TYPE 1 OR 2
	ROLL	0 5	10 0	 MODIFIED TYPE 1 OR 2
	PITCH	2 0	10 0	 TYPE 2
(3)	YAW	1 0	10 0	 TYPE 1
	ROLL	2 0	0 05	 TYPE 3
	PITCH	2 0	0 05	 TYPE 3
(4)	YAW	1 0	10 0	 TYPE 1
	ROLL	1.0	10 0	 TYPE 1
	PITCH	2 0	10 0	 TYPE 2

generally as expected except for a little early chatter motion in roll and yaw. The cost and time of acquisition compared very well with the optimal (linear) acquisition cost and time. In all of the initial runs (except the run for satellite (3) which did not result in acquisition) the parabolic control switching curves gave good results with only a slight amount of chatter motion to S^+ when in one case a "zeroing" part of a trajectory missed S^+ .

The following changes were made in the phase plane switching lines of satellites (1), (2) and (3), in the hope of improving the performance of their acquisition controls. (The initial run for satellite (4) indicated that its control resulted in satisfactory performance so that no changes in the control for satellite (4) were made.) The slope of the switching line for pitch-satellite (1) was decreased from -1.0 to -2.0 in the hope of achieving quicker acquisition in pitch so that the detrimental cross coupling between roll and yaw would be eliminated. The slopes of the switching lines in roll and yaw for satellite (2) were decreased from -0.5 to -1.0 in an attempt to alleviate the early chatter motion in roll and yaw and, thus, reduce the fuel cost and time of acquisition. The slope of the switching line in roll-satellite (3) was reversed in sign for $|x_3| \geq 0.05$ (by changing Q_2 to 10.0) and was increased in slope from -2.0 to -1.0. This modification was made in an attempt to acquire [for the unstable satellite (3)] the region S^+ (Since pitch for satellite (3) is so highly "stable", the negative slope of the switching line in pitch was retained.) In the remaining simulation runs of the suboptimally controlled nonlinear system the computation time was shortened by removing the fixed time delay and introducing a more natural but slightly varying time delay. This was accomplished by introducing the stepsize cutting limiter of Part I, Section A, Chapter IV. For a stepsize of $\Delta\tau = 0.002$, a time delay of about $t_d = 0.125$ sec was built into the control by limiting the number of cuts to four.* The accuracy was not significantly affected by this limit. The step size was taken as $\Delta\tau = 0.0002$ for the second part of each run. This gave an effective time delay of about $t_d = 0.01$ sec during this part. The smaller

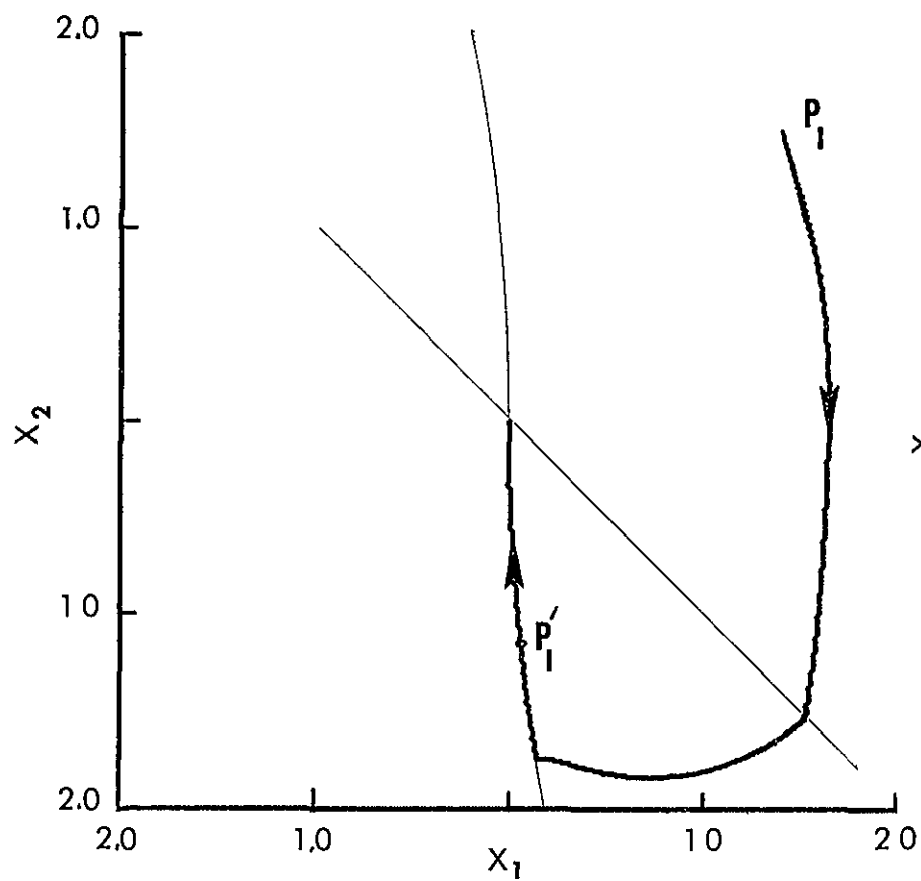
*Recall that τ , the nondimensional time (in radians) is equal to nt where n is the average orbital rate and t is the real time in seconds

time delay was required when the trajectory encountered the region S^+ , since much larger time delays resulted in the overshooting of S^+ . The larger time delay was used during the first part of each run to save computer time. The large time delay was considered a worst case.

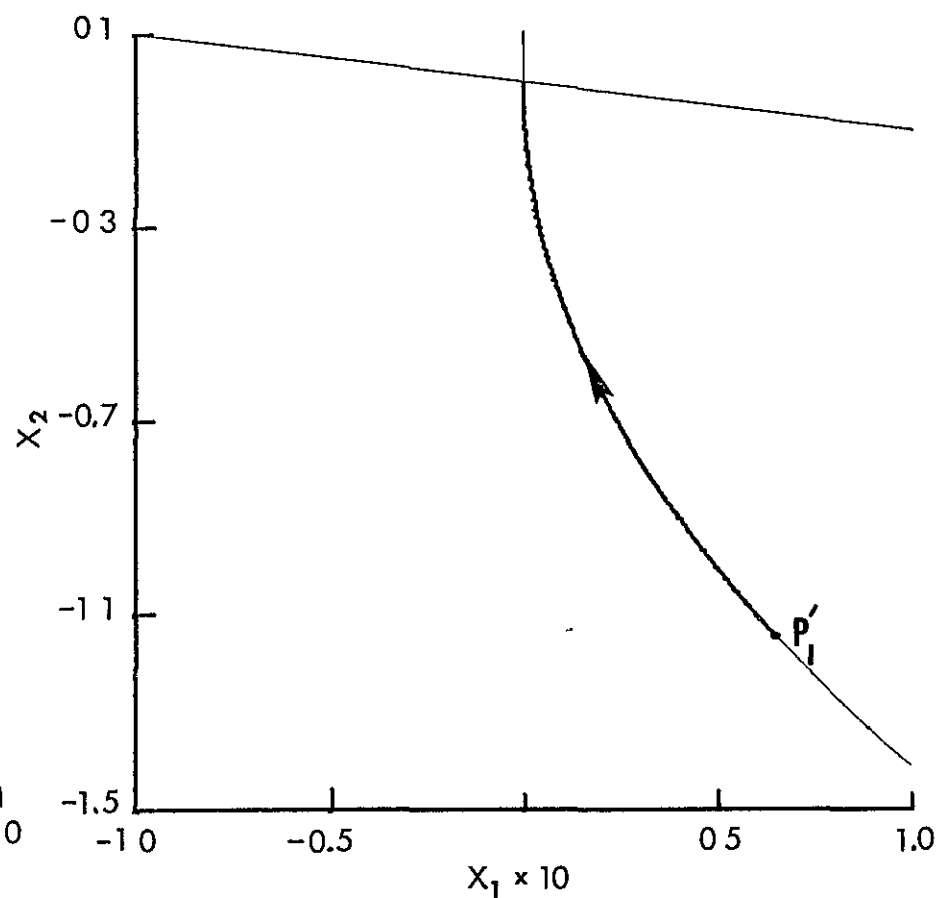
The results of the second set of digital computer simulation runs for the four satellites with the new control laws [same as in Table 5.1 except for roll-satellite (3)] and the new time delays showed definite improvements. Satellite (1) acquired the region S^+ within the time of one-quarter orbit and the fuel cost was reduced by about 25%. The results for satellite (2) showed an improvement of about 10% in the fuel cost and a slight improvement in the acquisition time. Satellite (3) was again uncontrollable but this time it took longer for the trajectory to begin moving away from S^+ . New initial conditions (final conditions of an optimal (linear) solution) were used in the test of the acquisition control of satellite (4). Again, the results for satellite (4) were satisfactory. The fuel cost and time of acquisition compared very well with that of the optimal (linear).

The pitch control of satellite (3) was again modified. The positive slope of the switching line (when $|x_5| > 0.05$) was changed to a negative slope in the hope of reducing the large angle coupling between the yaw control and roll and the roll control and yaw by rapidly reducing the pitch angle. Simulation of the acquisition of satellite (3) with the newly modified control was made for several initial conditions. These simulation runs gave satisfactory results although the fuel costs were 35-67% greater than the optimal (linear) fuel costs.

In Figure (5.3) - Figure (5.6) are shown phase plane plots of the phase plane projections of one of the worst case acquisition trajectories for each satellite. These are worst case trajectories since they show more chatter than others and since the fuel costs and/or times of acquisition are generally greater. The right plot on each page of Figures (5.3) - (5.6) is an enlargement of the origin. Of course, these plots do not show all of the acquisition. Once a phase plane projection of S^+ [see Figure (4 17) - Figure(4 20)] is acquired by the phase plane projection of the acquisition trajectory, the station-keeping part of the controller [see Figure (6.1)] takes over and performs the acquisition form near the

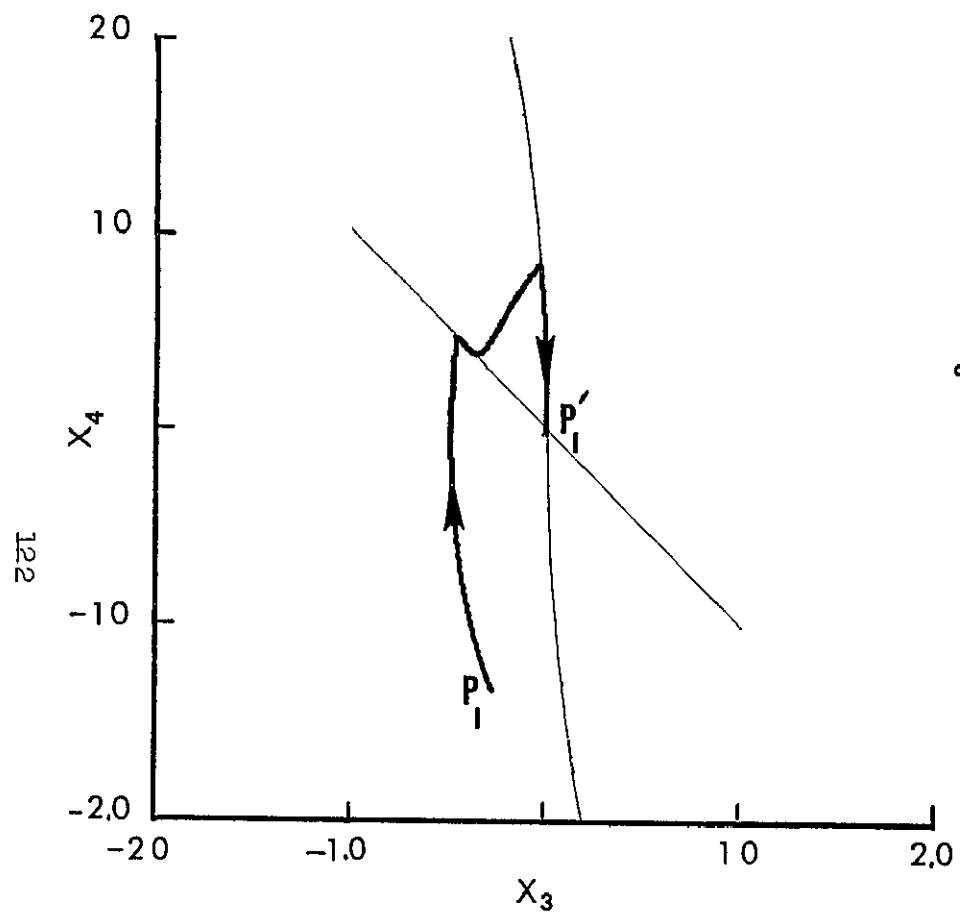


a. Large Yaw Angles

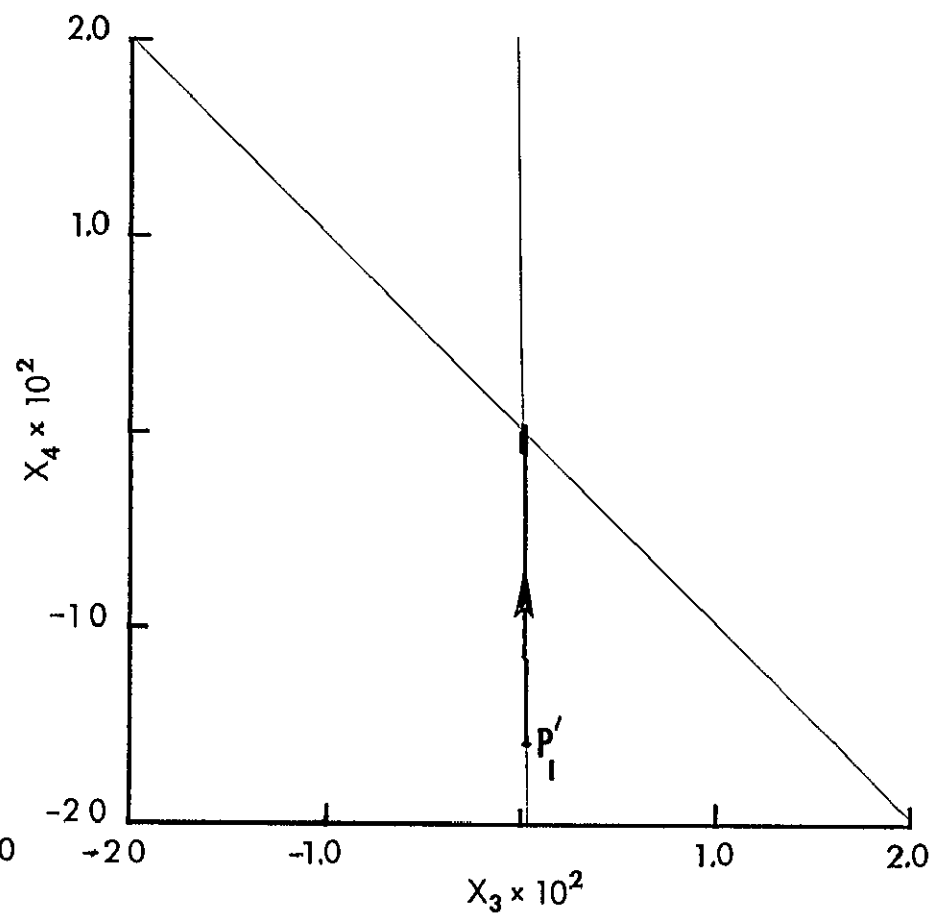


b Small Yaw Angles

Figure 5.3 Suboptimally Controlled Acquisition Motion of Satellite (1),
 $J = 12.66$, $\tau_F - \tau_O = 1.42$, $\theta_O = \pi/4$

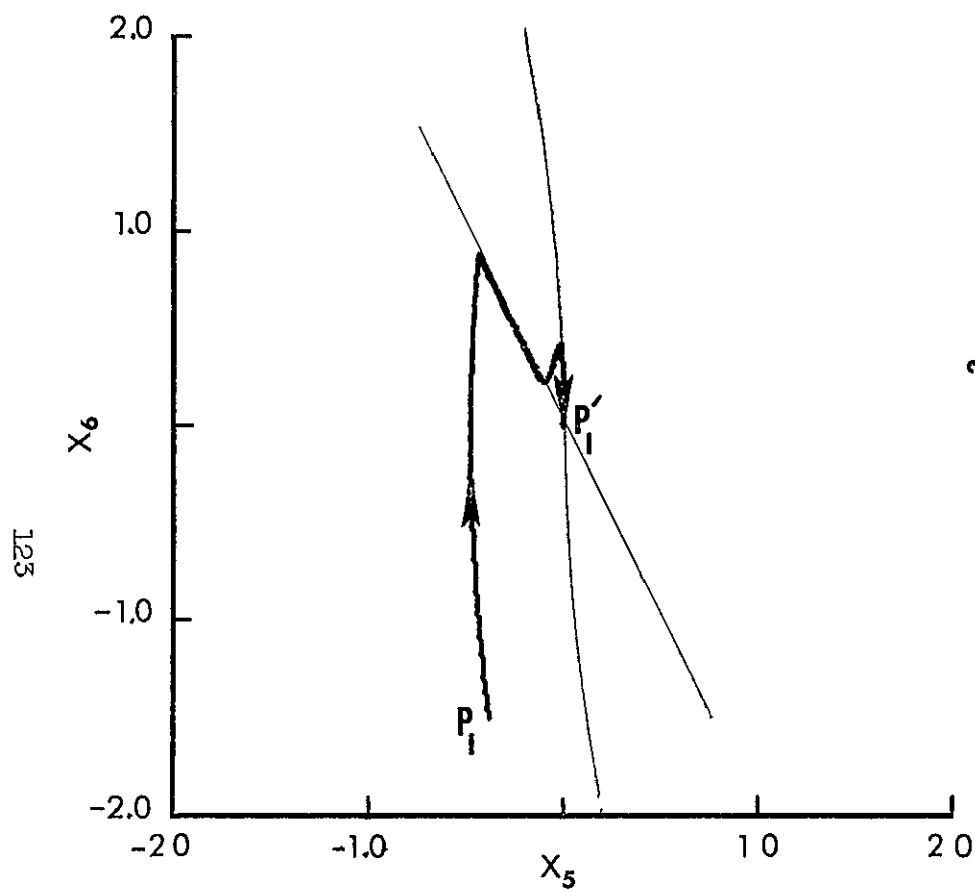


c Large Roll Angles

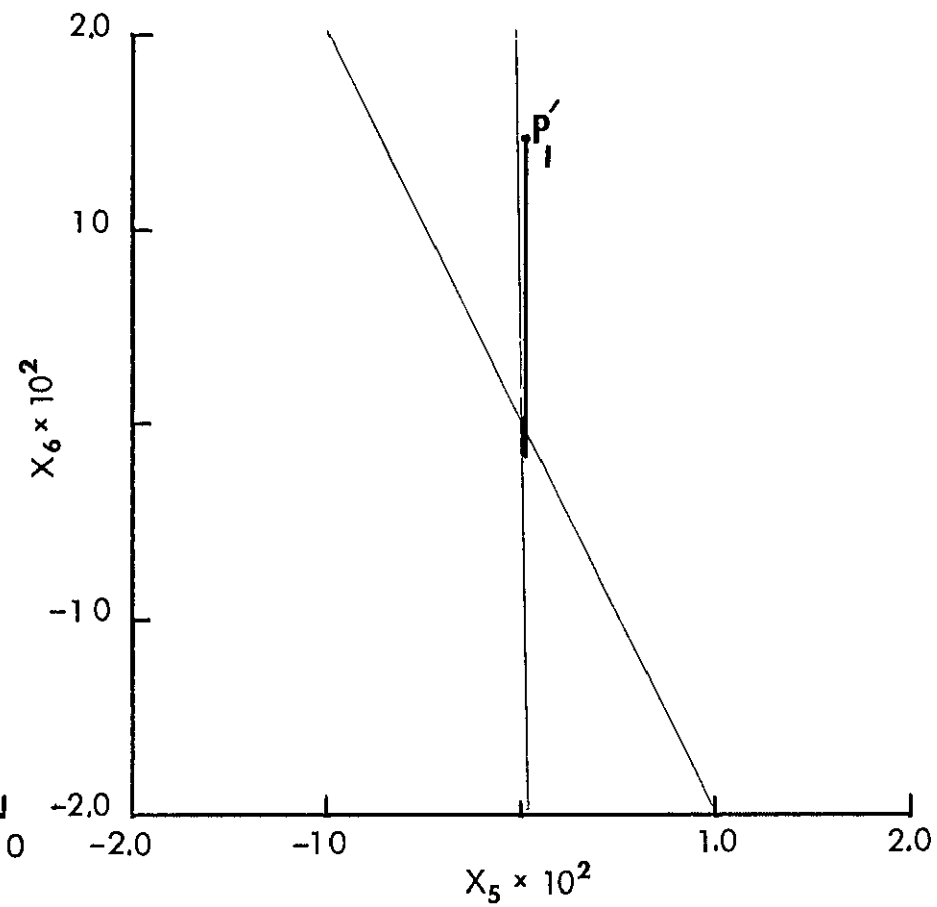


d Small Roll Angles

Figure 5 3. Continued

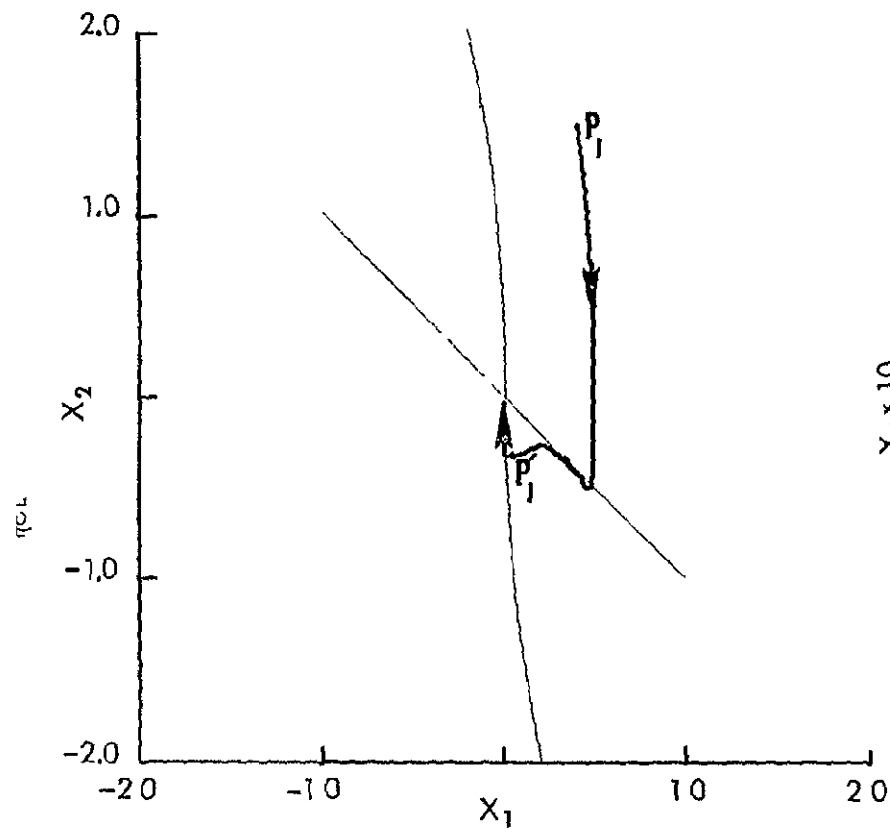


e Large Pitch Angles

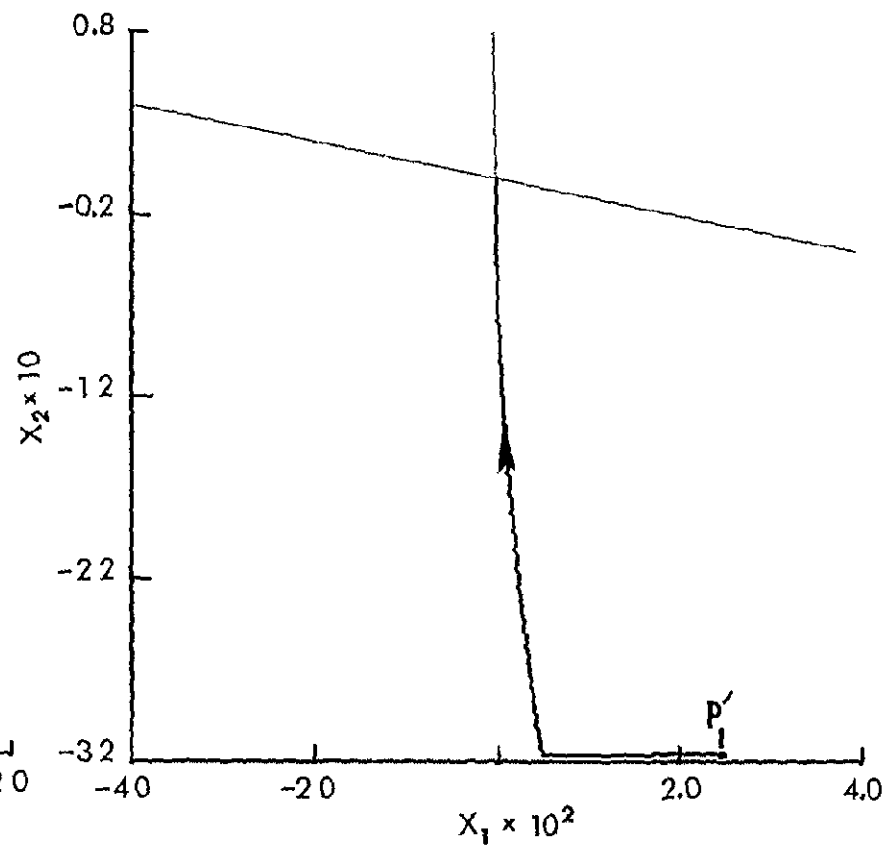


f Small Pitch Angles

Figure 5.3. Continued

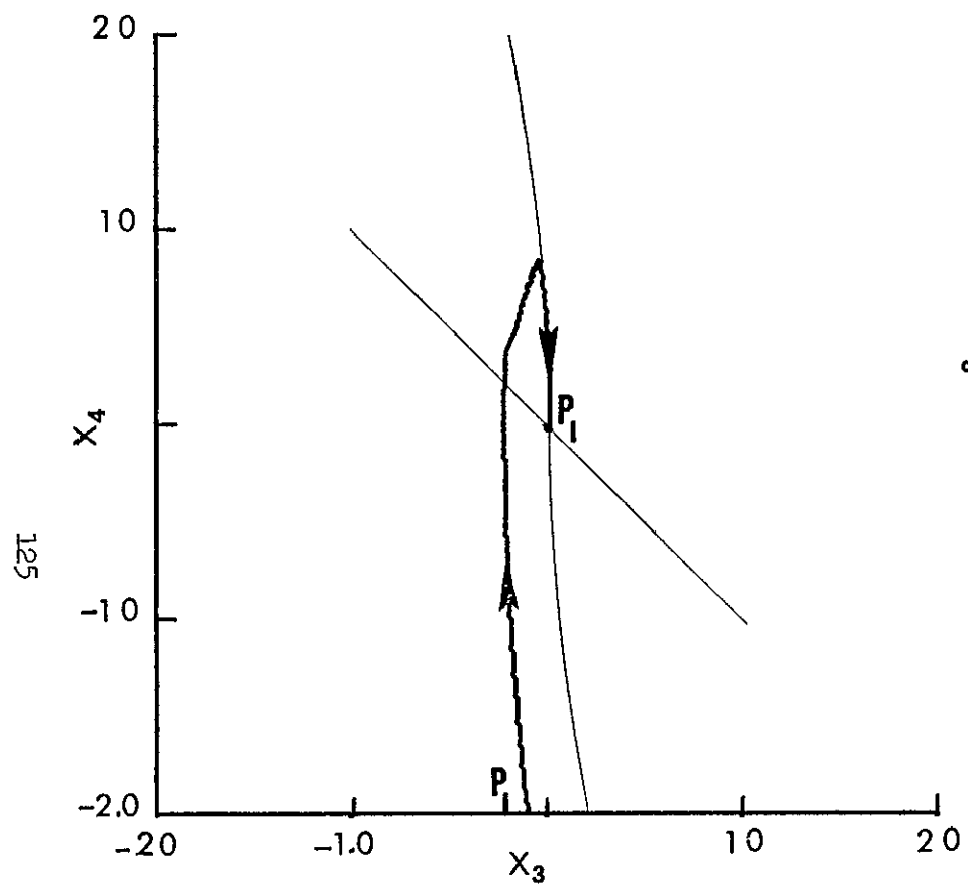


a. Large Yaw Angles

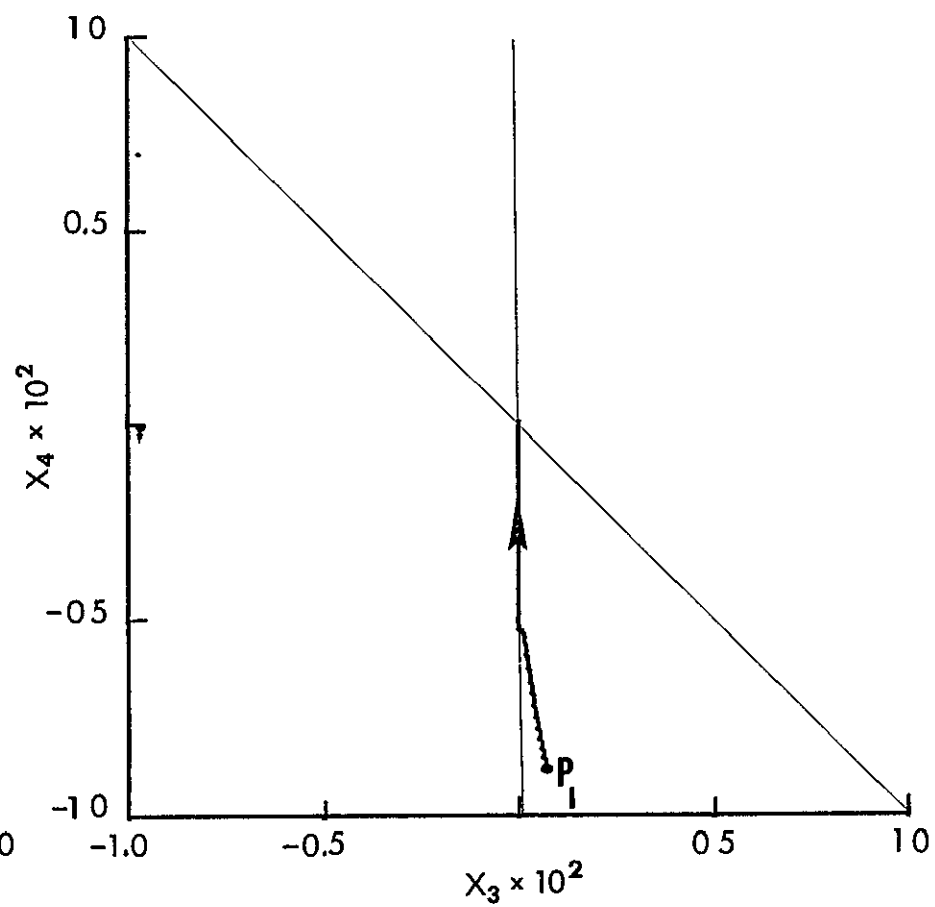


b Small Yaw Angles

Figure 5.4 Suboptimally Controlled Acquisition Motion of Satellite (2),
 $J = 9.07$, $\tau_f - \tau_o = 1.69$, $\theta_o = \pi/4$.

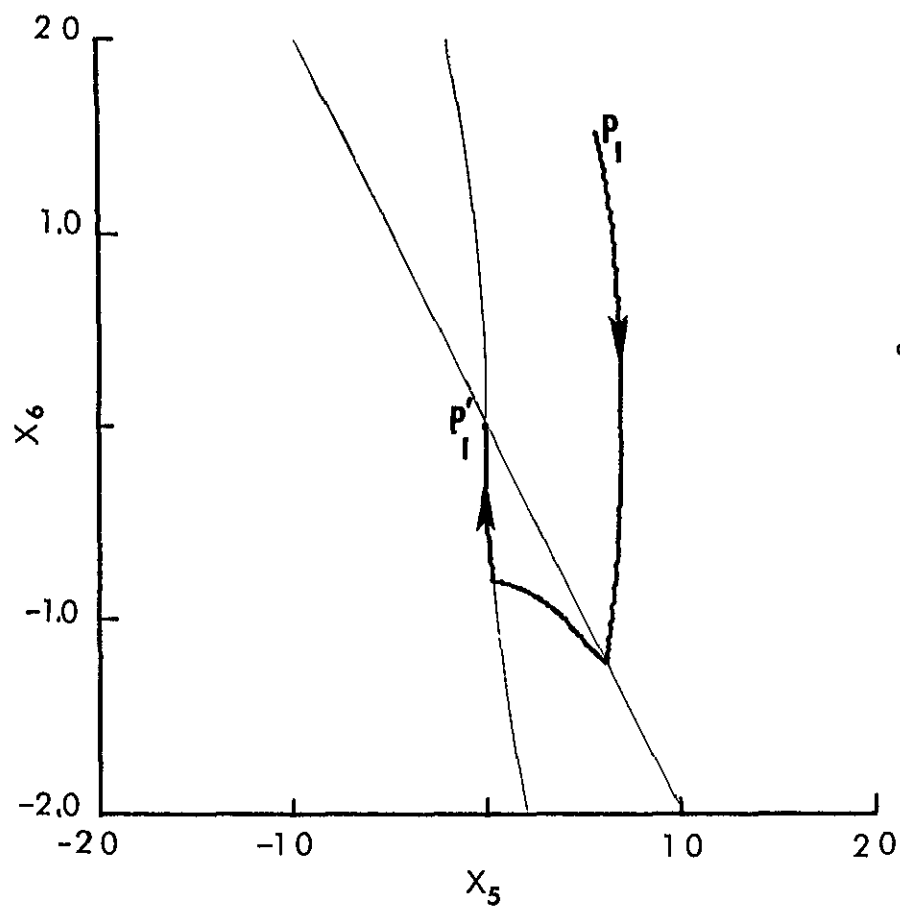


c. Large Roll Angles

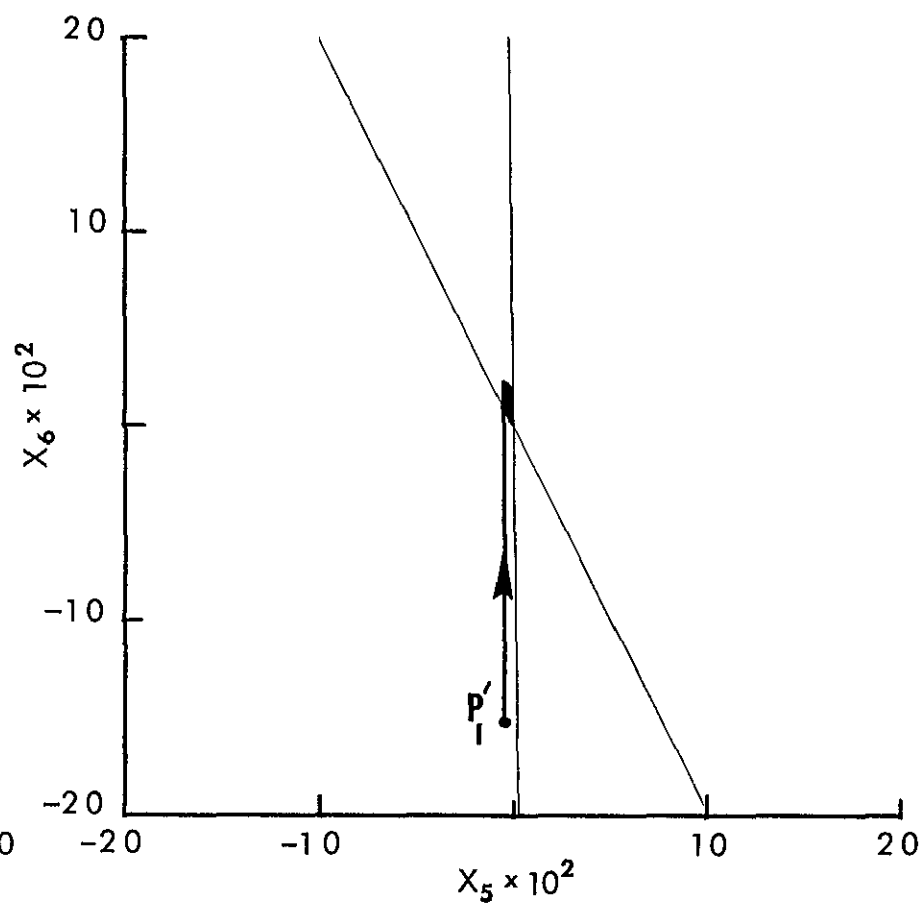


d. Small Roll Angles

Figure 5 4 Continued.

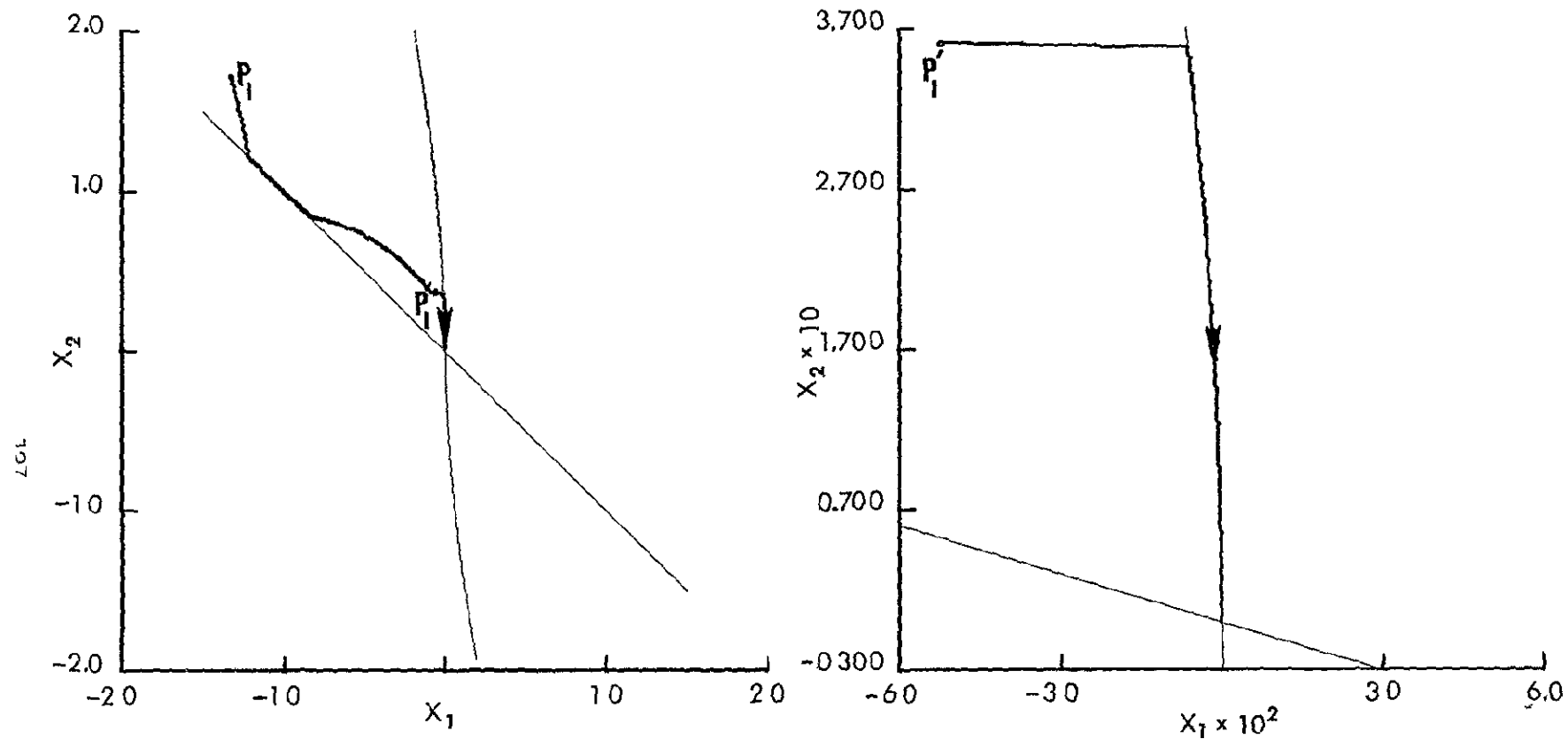


e Large Pitch Angles



f Small Pitch Angles

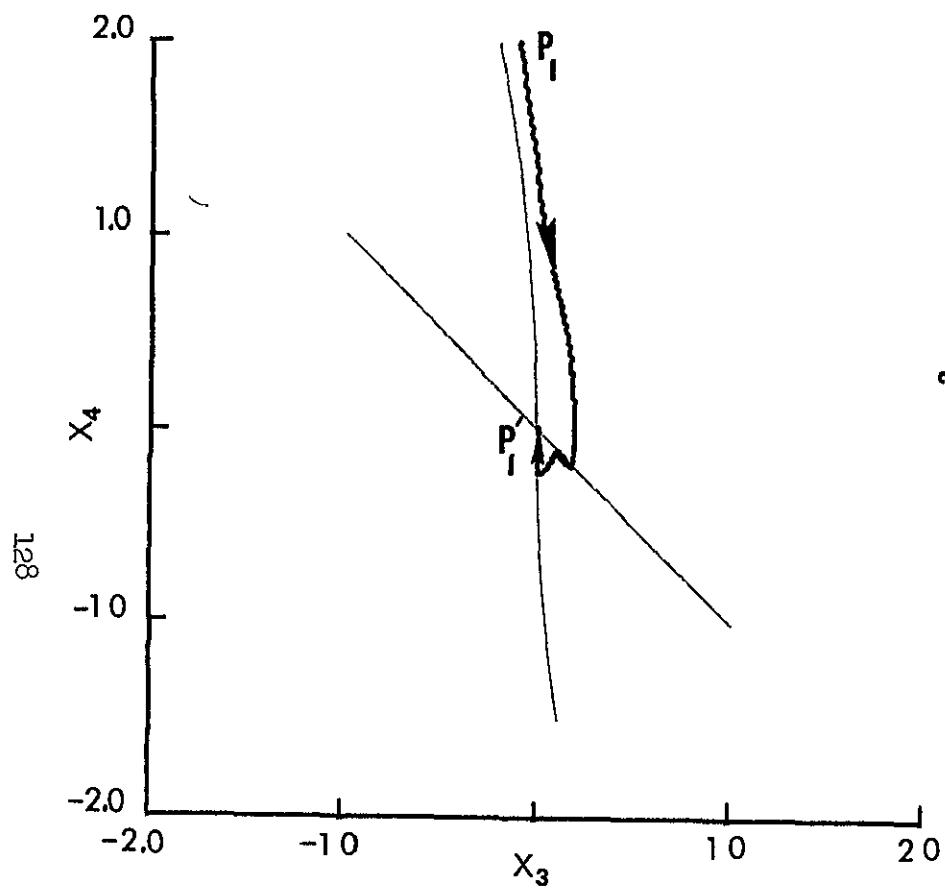
Figure 5 4 Continued



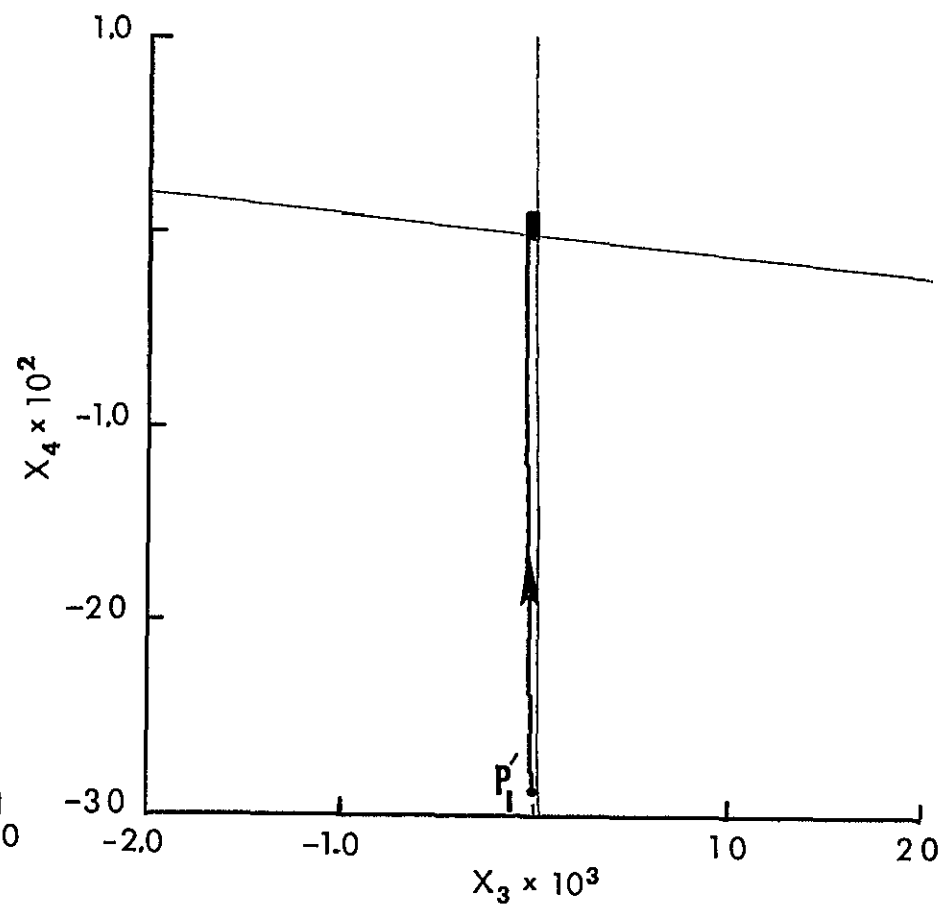
a. Large Yaw Angles

b Small Yaw Angles

Figure 5.5 Suboptimally Controlled Acquisition Motion of Satellite (3),
 $J = 9.75$, $\tau_a - \tau_- = 1.63$, $\theta_- = \pi/4$

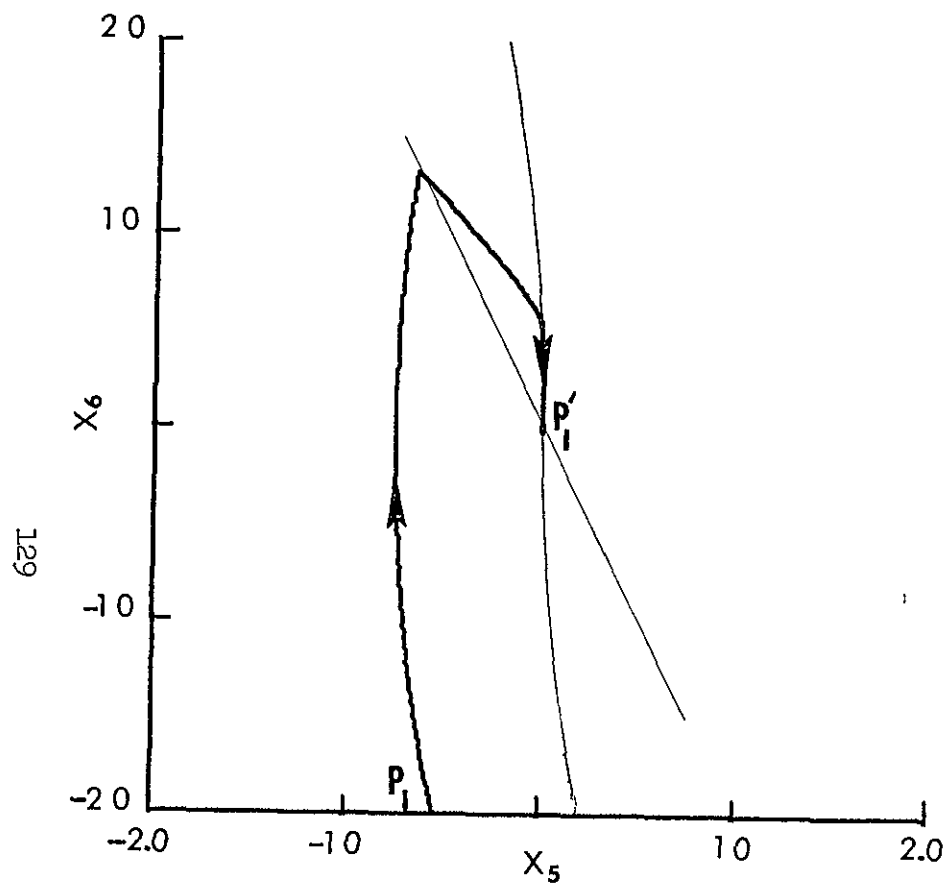


c. Large Roll Angles

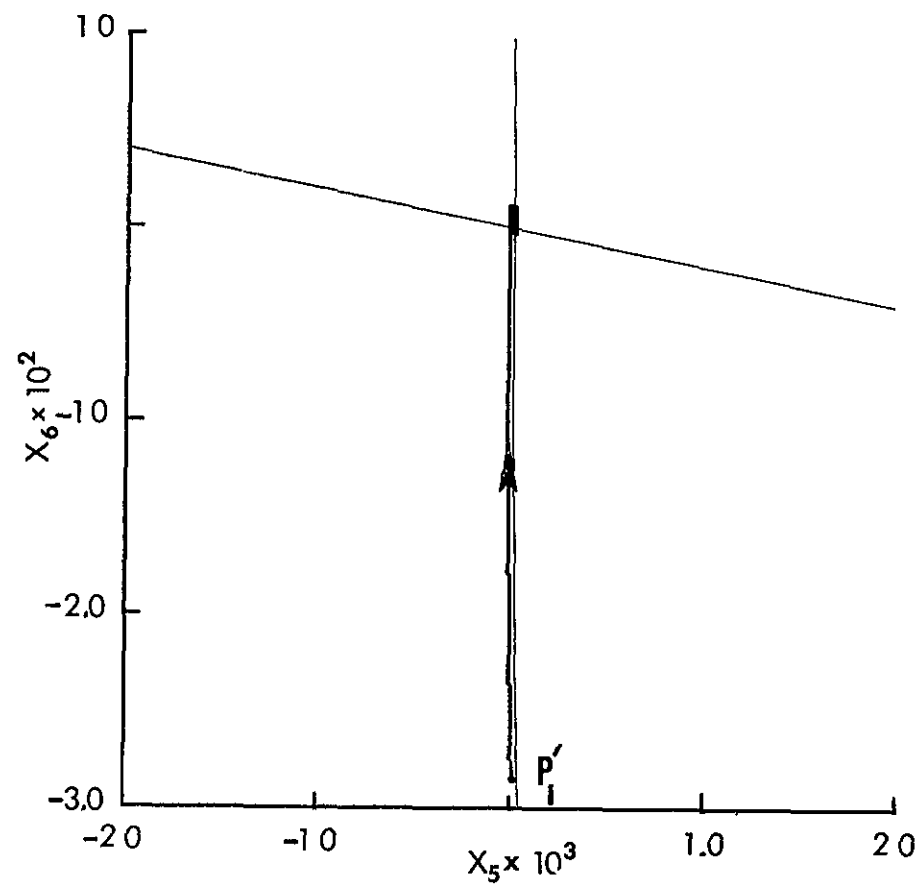


d. Small Roll Angles

Figure 5 5. Continued.

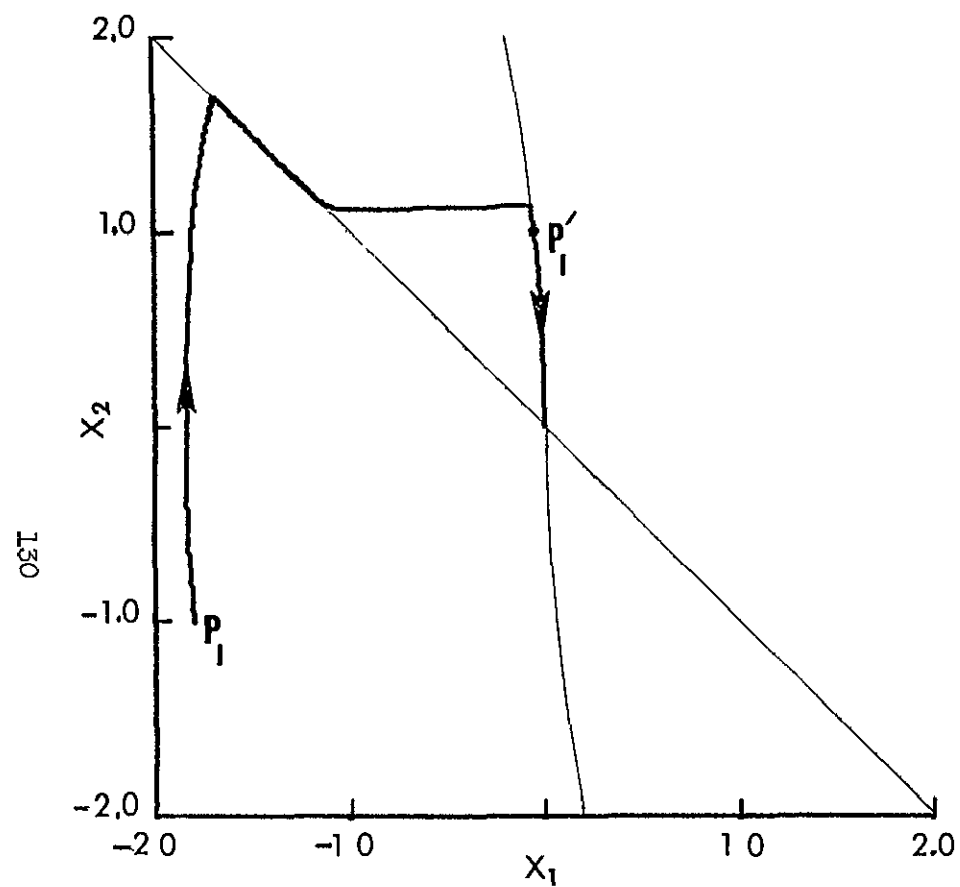


e Large Pitch Angles

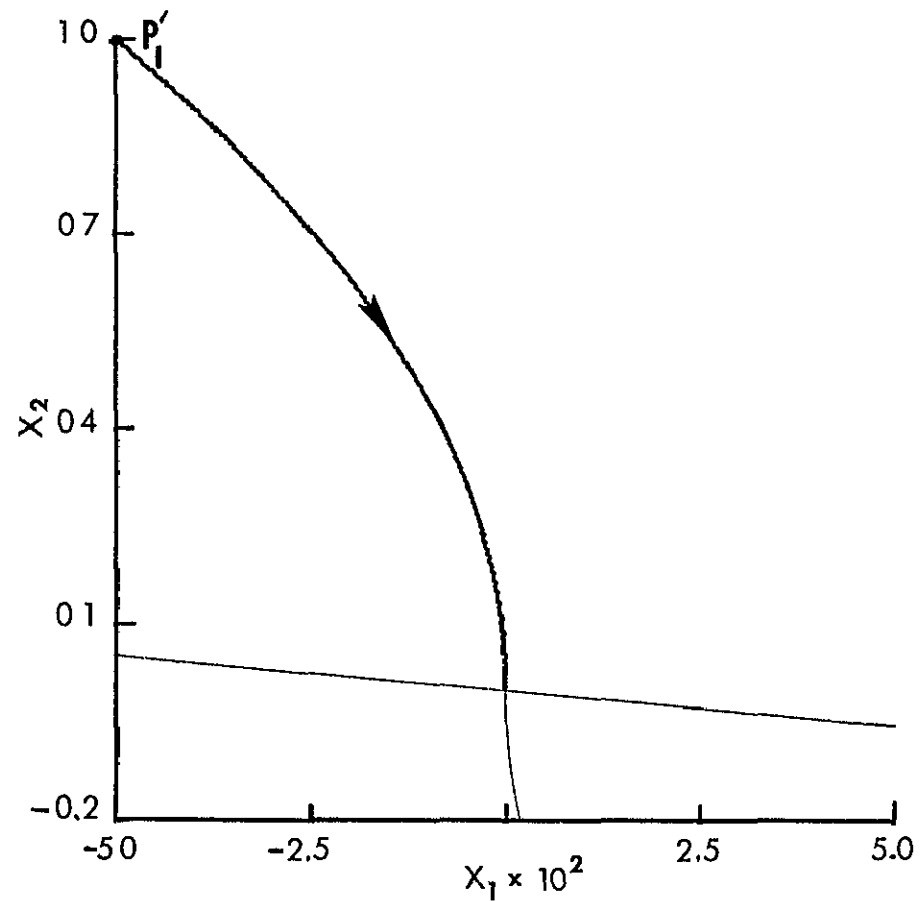


f Small Pitch Angles

Figure 5 5 Continued

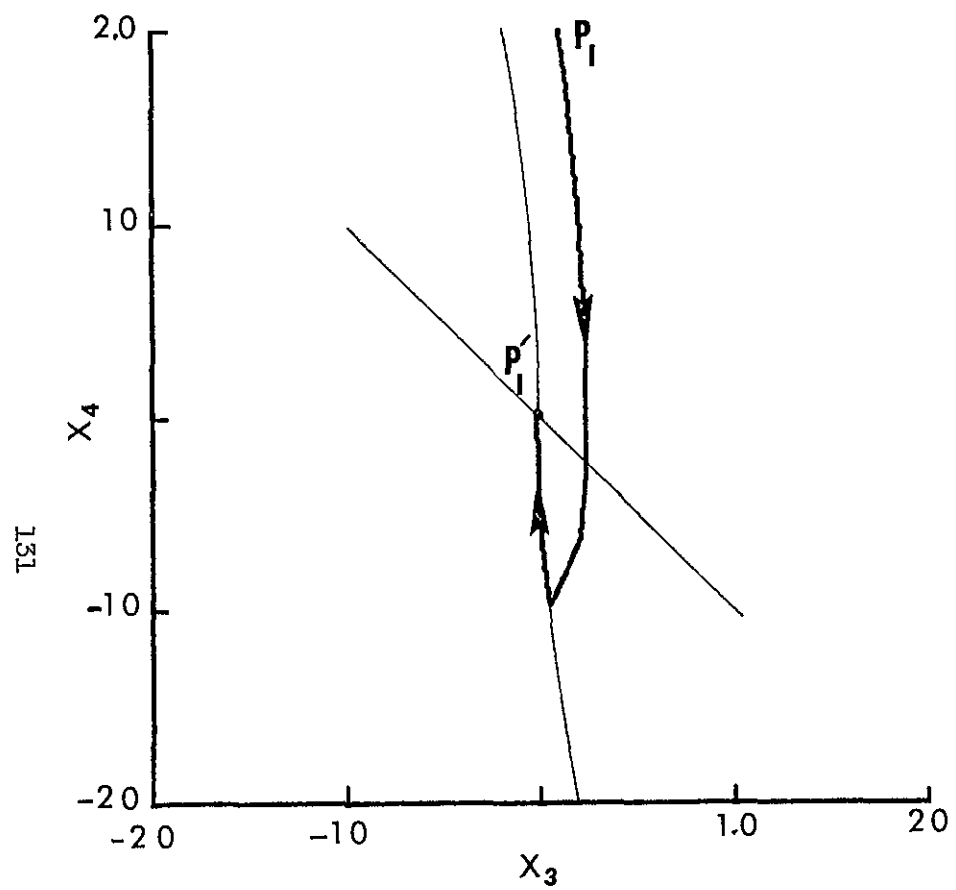


a. Large Yaw Angles

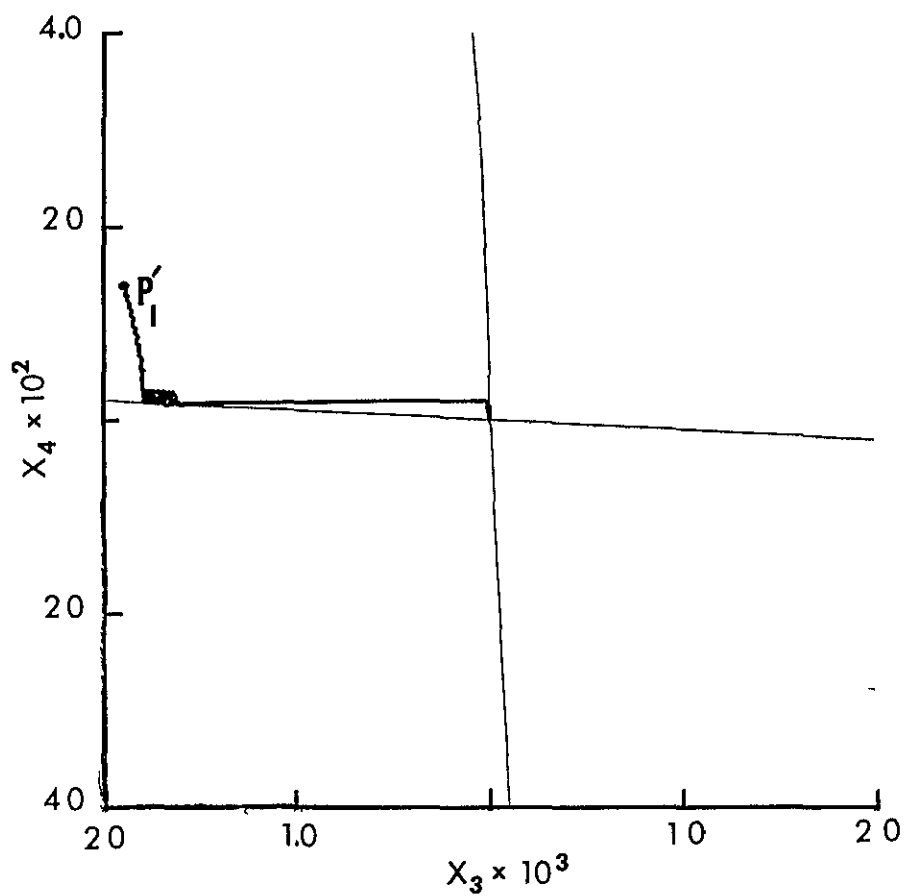


b Small Yaw Angles

Figure 5 6. Suboptimally Controlled Acquisition Motion of Satellite (4),
 $J = 8.37$, $\tau_f - \tau_o = 1.69$, $\theta_o = 7\pi/4$

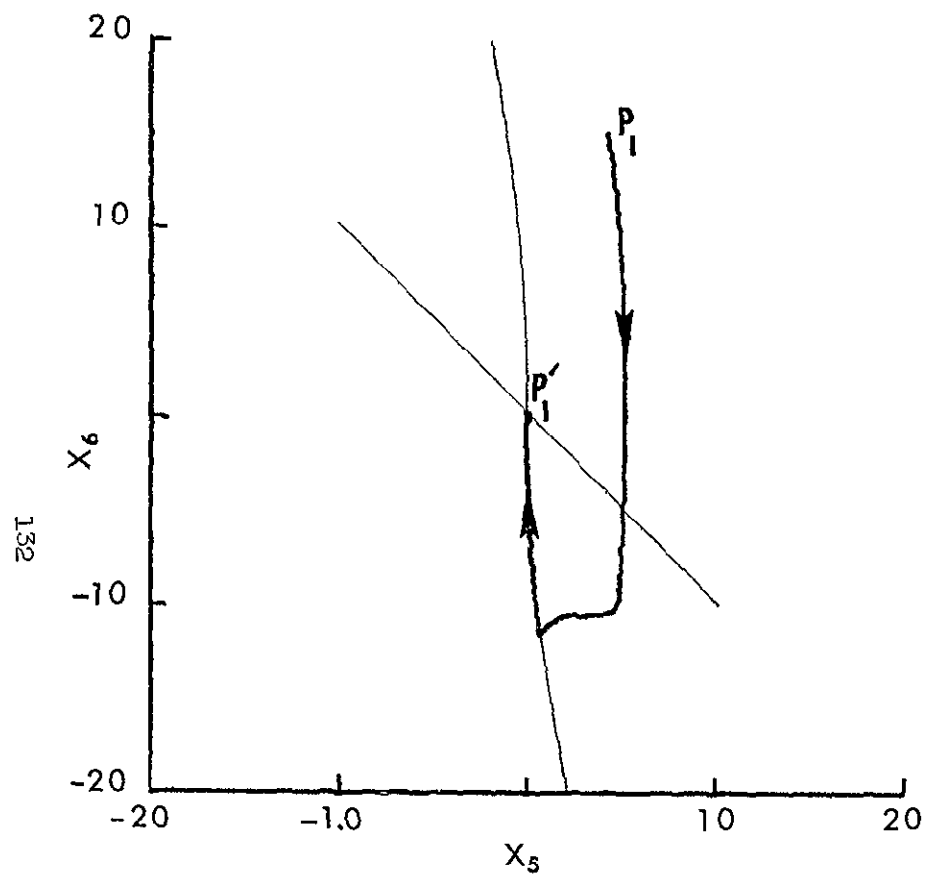


c Large Roll Angles

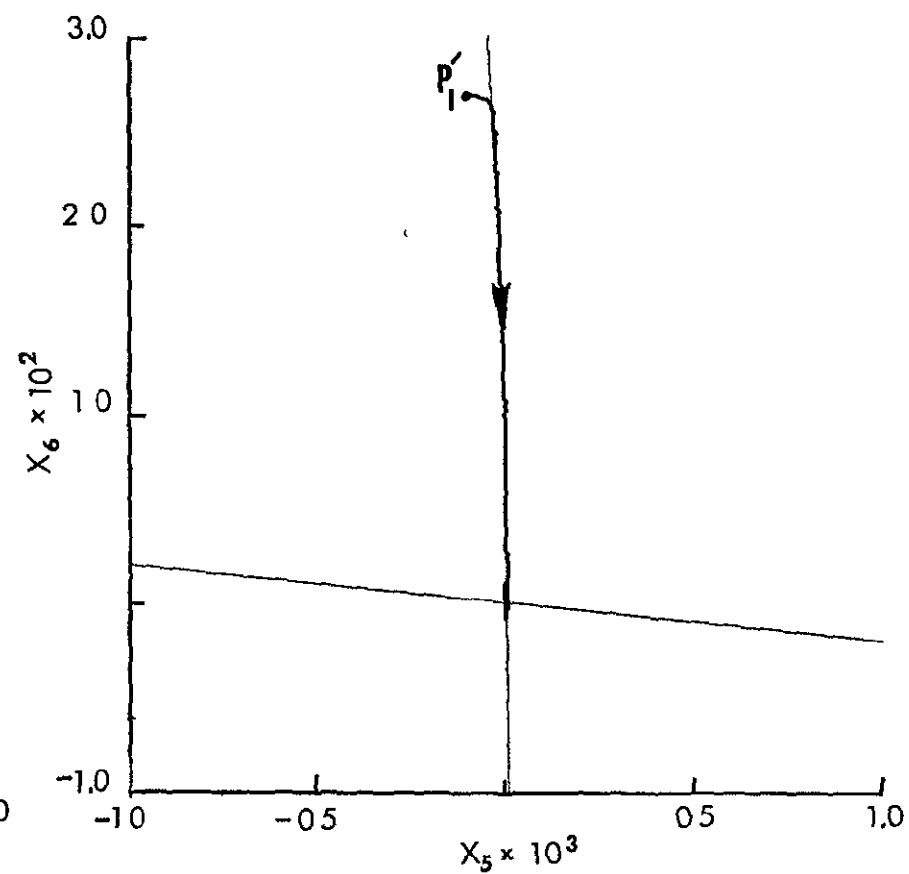


d. Small Roll Angles

Figure 5.6 Continued.



e. Large Pitch Angles



f Small Pitch Angles

Figure 5 6. Continued.

projected boundary of S^+ to the projection of S . (Since two widely different levels of control torque are needed for satisfactory performance in acquisition and station-keeping, the region S^+ was acquired by the acquisition part of the controller. Otherwise, rapid chatter motion and wasted control effort result from the control torque being too large for the region of station-keeping. See the data of Chapter VI on the fuel cost versus the size of N_1 , $1 = 1, 2, 3$, and the size of S .)

VI. COMPLETE ATTITUDE CONTROL AND PERFORMANCE EVALUATION

The complete attitude control system consisting of the station-keeping controls derived in Chapter IV and the acquisition controls derived in Chapter V are considered to give satisfactory performance. A block diagram of this complete attitude control system is given in Figure (6.1).

In the remainder of this chapter the performances of the two parts of the complete control system are evaluated in terms of the performances of other systems and in terms of the weight of fuel required for a year of control as compared to the weight of the satellite. Also, presented here are performance limitations imposed by imperfections.

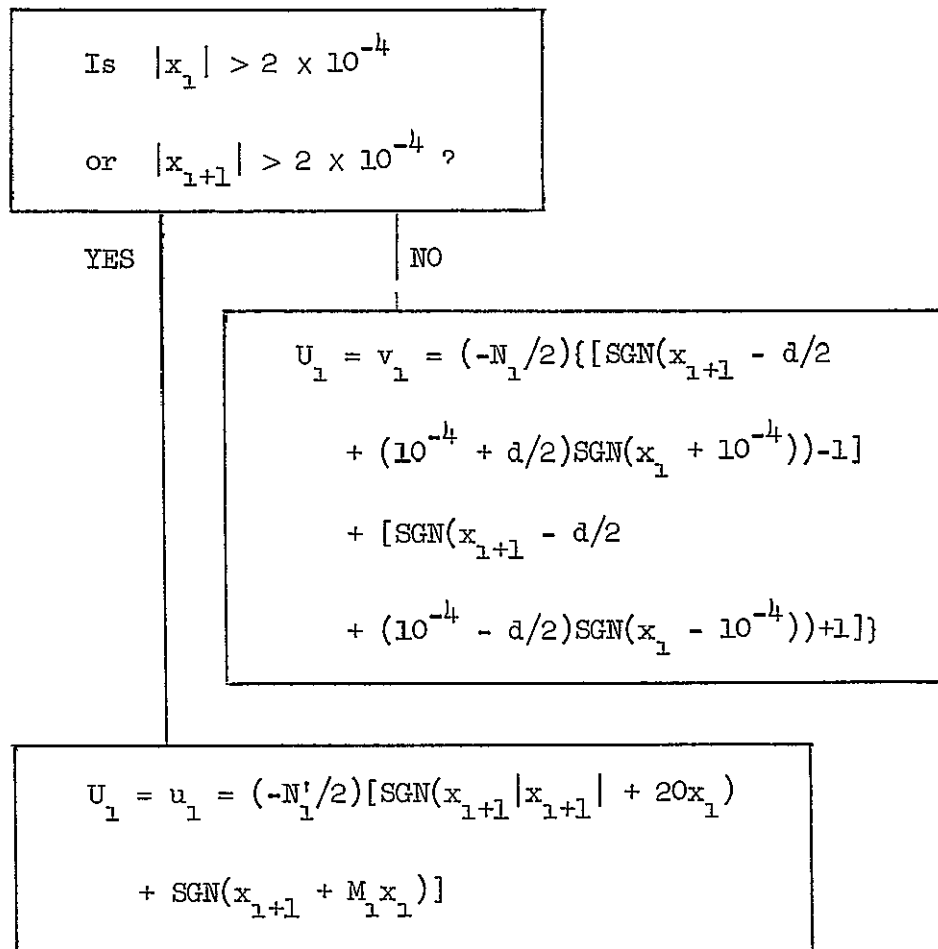
A. ACQUISITION CONTROL COMPARED TO OPTIMAL (LINEAR) ACQUISITION CONTROL

In Section B of Chapter V, the selected acquisition control system was tested and found to perform satisfactorily, however, a thorough comparison of the fuel costs found in the test runs with the optimal (linear) fuel costs was not made. Although the optimal (linear) fuel costs are probably very conservative, they are considered to be a lower bound which is large enough for the comparison to be meaningful.

The average nondimensional fuel cost for the acquisition simulation runs of satellite (1) was $J = 12.4$. For satellites (2), (3) and (4) the average fuel costs were 10.2, 14.1 and 13.2, respectively. These average costs differed from the average optimal (linear) fuel cost by 34%, 15%, 43% and 36% for satellites (1), (2), (3) and (4), respectively. The percent differences of the average costs seem quite high, however, considering the strong cross coupling which occurs when the angles are large ($\geq 60^\circ$), the fact that a simple fixed switching logic control is used and the fact that the optimal (linear) cost is not a greatest lower bound, these percent differences are not unsatisfactory.

Several simulation runs of the nonlinear acquisition system were made for small angles ($\approx 5^\circ$) from the final conditions (backward time) of optimal (linear) runs. The percent differences for the small cases were about 15%.

The variation in the percent difference for each individual run was



- NOTES:
- (1) The index $i = 1, 2, 3$ for yaw, roll and pitch, respectively
 - (2) $M_1 = 1.0$, $M_2 = 1.0$ and $M_3 = 2.0$
 - (3) The distance d (see Section B, Chapter 4) depends on the satellite, the strength of station-keeping control and on the controllers time delay
 - (4) U_i , $i = 1, 2, 3$, are the nondimensional control components (either acquisition or steady-state)

Figure 6.1 Block Diagram of the Complete Attitude Control System

from -4.1% to +62%. The extreme percent differences belonged to the large angle runs. The suboptimal system had an advantage of 4.1% over the optimal system in one of the runs for satellite (4), however, the time of acquisition for the suboptimal was almost 20% greater than that of the optimal. The maximum percent difference of 62% was for the run of satellite (3) which was given in Figure (5.5).

One of the main reasons for the greater fuel cost of the suboptimal system is the chatter motion which occurs during acquisition from some initial conditions. This chatter motion can be avoided, even with a fixed switching logic control, by increasing the values of M_1 (the negative values of the slopes of the straight line switching curves). If the values of M_1 are increased until no (or little) chatter motion occurs, the time of acquisition generally decreases, but, the fuel cost increases. However, unless the slopes are increased until no (or little) chatter motion occurs (about a factor of ten), the costs do not generally increase by more than 100%.

The nondimensional fuel cost values can be translated for particular satellites into the weight of fuel used in, say, pounds. If, while a gas jet is on, it is assumed that the gas flow rate and exhaust velocity are constant, the weight-flow for a gas jet couple is given by

$$\dot{w}_1 = \frac{N'_1 I_1 n^2}{2\ell_1} \frac{g}{v}, \quad 1 = 1, 2, 3, \quad (6.1)$$

where $2\ell_1$ is the moment arm distance, g is the acceleration of gravity and v is the magnitude of the exhaust velocity. If both sides of (6.1) are multiplied by $n^{-1}\Delta\tau$ (recall that $\tau = nt$), the result is

$$w_1 = \dot{w}_1 \Delta t = N'_1 \Delta\tau \frac{I_1 n}{2\ell_1} \frac{g}{v} = J_1 \frac{I_1}{2\ell_1} n \frac{g}{v} \quad (6.2)$$

which is the weight of fuel used in the time interval, Δt , that the gas jet couple is on.

The ratio v/g , whose reciprocal is a factor in (6.2), is usually referred to as the specific impulse, I_{sp} . A realistic value for v is 1500 ft./sec. so that a reasonable specific impulse is $I_{sp} = 46.5$ sec.

In this case $g/v = 2.15 \times 10^{-2} \text{ sec.}^{-1}$. The values of n for the satellites considered in this investigation range from 0.95×10^{-3} to 1.13×10^{-3} . In the following calculations of the weight of fuel used, the worst case value of $n = 1.13 \times 10^{-3}$ is used. The typical satellites referred to are those of Section D, Chapter II. Since the typical satellites are spherical or cylindrical and since the lever arm distance, $2\ell_1$, is usually half the length of an axis, the ratio $I_1/2\ell_1$ can be approximated by $1/5 m\ell_1$, if the satellite is spherical, by $1/4 m\ell_1$ for the longitudinal axis and by $1/6 m\ell_1$ for the transverse axis, if the satellite is cylindrical. (m is the satellite's mass. For satellite (1) $m = 1,860$ slugs. For satellites (2), (3) and (4) m is 1550 slugs, 1550 slugs and 310 slugs, respectively.)

Now the nondimensional average acquisition fuel cost for each satellite can be translated into pounds weight. The values of J (given earlier in this section) for satellites (1), (2), (3) and (4) are 12.4, 10.2, 14.1 and 13.2, respectively. Therefore, the approximate (worst) weights of fuel used on the average for acquisition by satellites (1), (2), (3) and (4) are 0.88 lbs. ($\ell_1 = 7$ ft.), 1.28 lbs. ($\ell_1 = 15$ ft.), 1.78 lbs. ($\ell_1 = 15$ ft.) and 0.10 lbs. ($\ell_1 = 4.5$ ft.), respectively

B. STATION-KEEPING CONTROL

In Part 4, Section B of Chapter IV the station-keeping control system was simulated on the analog computer and found to perform satisfactorily. In this section the performance of the station-keeping control is evaluated by comparing it to the hybrid station-keeping control system of Busch (which contains a reaction wheel) and by evaluating fuel costs changes with various parameters of the system.

1. Comparison with Busch's Solution

Busch obtained station-keeping control in roll and yaw simply by leaving small (6.3×10^{-3} radians) circular regions of no control about the origin in the roll and yaw phase planes of the acquisition phase plane switching logic. This performed well for the "stable" satellite considered by Busch. (The steady-state cost per orbit for roll and yaw was about $J = 10^{-3}$.)

Since the pitch motion was forced by a sinusoidally varying term and since neither of the switching curves were of a "stabilizing" type, Busch's pitch acquisition control could only achieve complete acquisition in pitch periodically and the error in pitch grew periodically to about 0.1 radians. The fuel cost for this periodic reacquisition in pitch was high. To gain greater accuracy in pitch and to reduce the weight of the fuel used, Busch supplemented the pitch part of the control system with a reaction wheel.

If the environmental torques acting on the satellite are nearly sinusoidal, the power required for "pushing" against the reaction wheel is nearly zero, so that, except for the weight of the reaction wheel and supporting components the weight of the pitch part of the controller is negligible. However, since the environmental torques are not sinusoidal but have the character of a nearly constant forcing term with some periodic variations, the reaction wheel must be continuously "pushed" against in such a way that the wheel speed is continuously increased. Since Busch used gas jets to produce the torque to hold the satellite steady while slowing the reaction wheel once it reached its saturation speed, his steady-state fuel consumption was increased by 21.9%. (This increase was due to slowing the reaction wheel when only cross coupling caused the wheel speed saturation i.e , all forcing terms were considered as purely sinusoidal.)

The weight of the fuel used for station-keeping can be compared (for the same size satellite) to the weight required by Busch's system for station-keeping control. Consider the "stable" satellite (2) Busch suggests a reaction wheel moment of inertia of $I_w = 10^{-5} \times I_3 = 1.21$ slugs-ft.². If the reaction wheel is a brass cylinder with a diameter of 1.5 ft. and a height of one foot, the weight of the reaction wheel is 138 lbs. From Table 4.1 it is found that the cost of the steady-state pitch control for satellite (2) is $J_{p,ss} = 6.03 \times 10^{-2}$ per orbit. The cost for a year (about 5.6×10^3 orbits) of pitch steady state control is $J = 337$. From Equation (6.2) the weight of fuel used in pitch for a year of station-keeping is found to be 8.47 lbs. ($\ell_1 = 3$ ft.). In the same manner the weight of the fuel used for roll-yaw station-keeping is found to be 113 lbs. ($\ell_1 = 15$ ft.) per year which is about the same as

Busch's roll-yaw control used for the 50,000 lb. satellite.

Clearly, the weight of the fuel used for station-keeping by the control of Section B, Chapter IV is much less (about 94%) than the weight required by Busch's station-keeping control system.

2. Fuel Expenditure Per Orbit For Values of Various Parameters

The fuel cost for station-keeping varies with the values of parameters such as eccentricity (e), inertia parameters (k_1), strength of the control (N_1), size of $S(s_1)$ and the peak voltage of sensor noise. Simulation runs (as in Section B, Chapter IV) were made to determine the effect of the variation of these parameters on the fuel cost. (The results of the runs also offer a check on the behavior predicted for the satellites by the analysis of the simple motions of Chapter IV.)

To test the effect of eccentricity on the fuel cost, simulation runs were made for the inertia parameters of satellite (3) which is "unstable" in yaw but "stable" in roll and pitch. From these runs it was found that the roll-yaw fuel cost varied by only 3% for a variation in e from 0.0 to 0.05, however, the pitch fuel cost varied directly as the eccentricity. Figure (6.2) shows the pitch fuel cost as a function of eccentricity.

To test the effect of the inertia parameters on the fuel cost per orbit, five sets of values of k_1 , $i = 1, 2, 3$, (which correspond to five satellites whose earth-pointing motions range from highly "unstable" to highly "stable") were used in the simulation runs. The change in the pitch fuel cost was negligible when $e = 0.05$ was used. A second set of runs was made with $e = 0.01$ in the hope that the reduction of the size of the relatively large forcing term would result in noticeable changes in the pitch fuel cost with changes in k_3 , however, the results were the same for this set of runs. The changes in the roll-yaw fuel cost with changes in k_1 and k_2 were quite significant (a maximum increase of 172%) These changes are represented in the chart of Figure (6.3) for $N_1 = N_2 = 0.01$, $e = 0.05$ and $d = 3 \times 10^{-5}$.

Satellites (2) and (3) were simulated in the investigation of the effect of the strength of control on the fuel cost. (These two satellites were chosen for this investigation since satellite (2) is

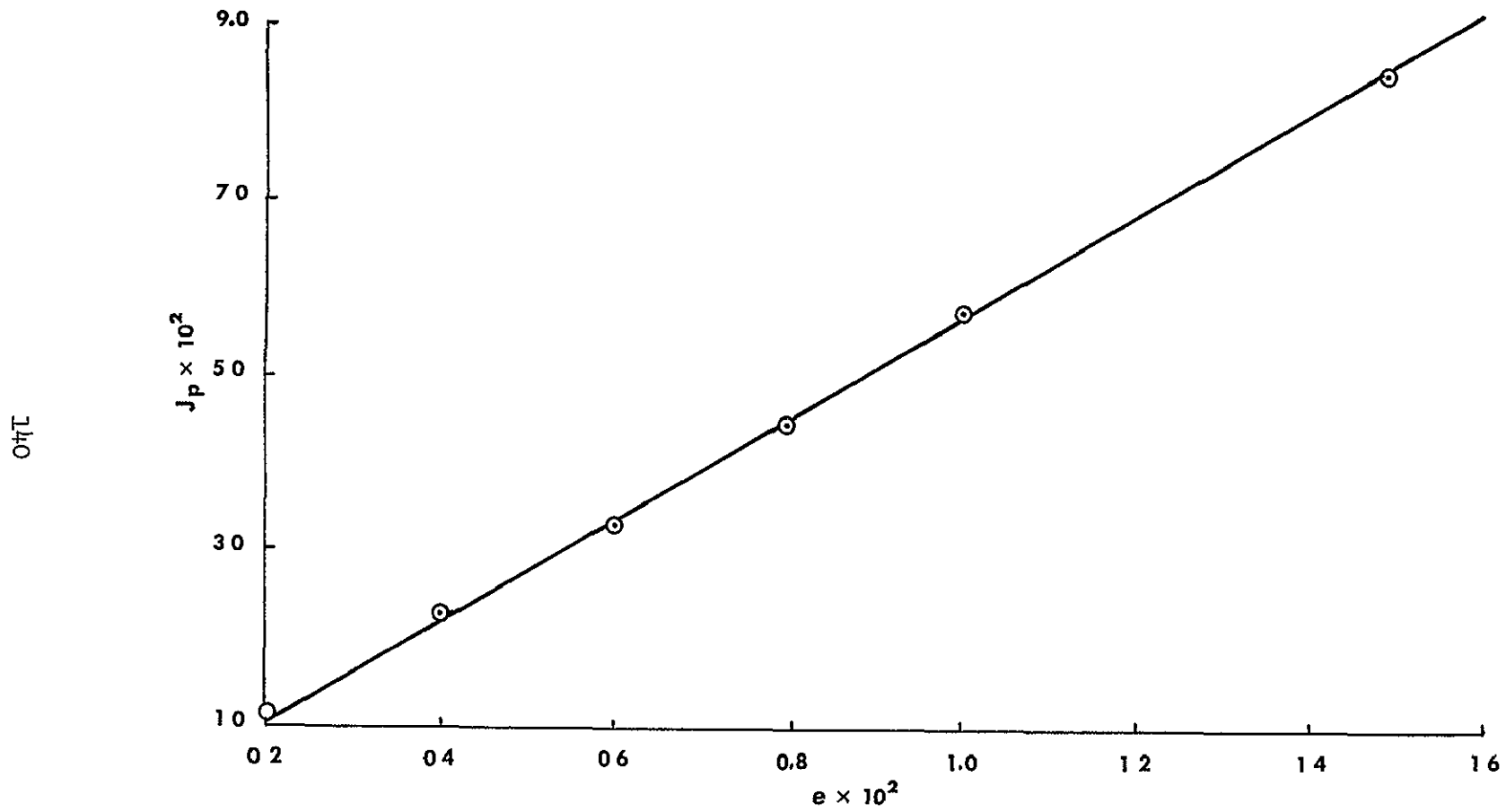


Figure 6.2 Pitch Fuel Cost Per Orbit vs. Eccentricity, $N_3 = 0.035$, $k_3 = 0.99$, $d = 0$

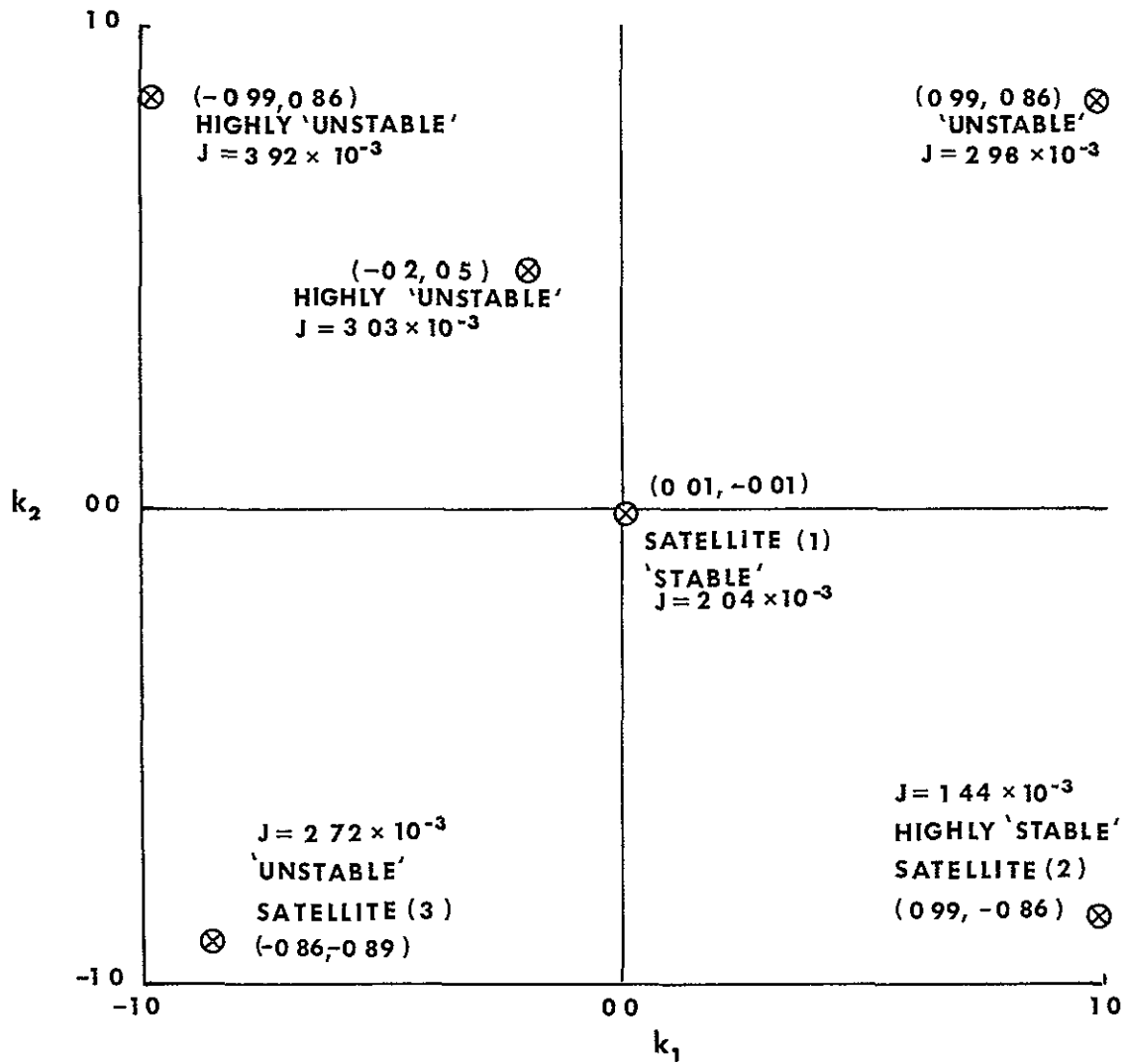


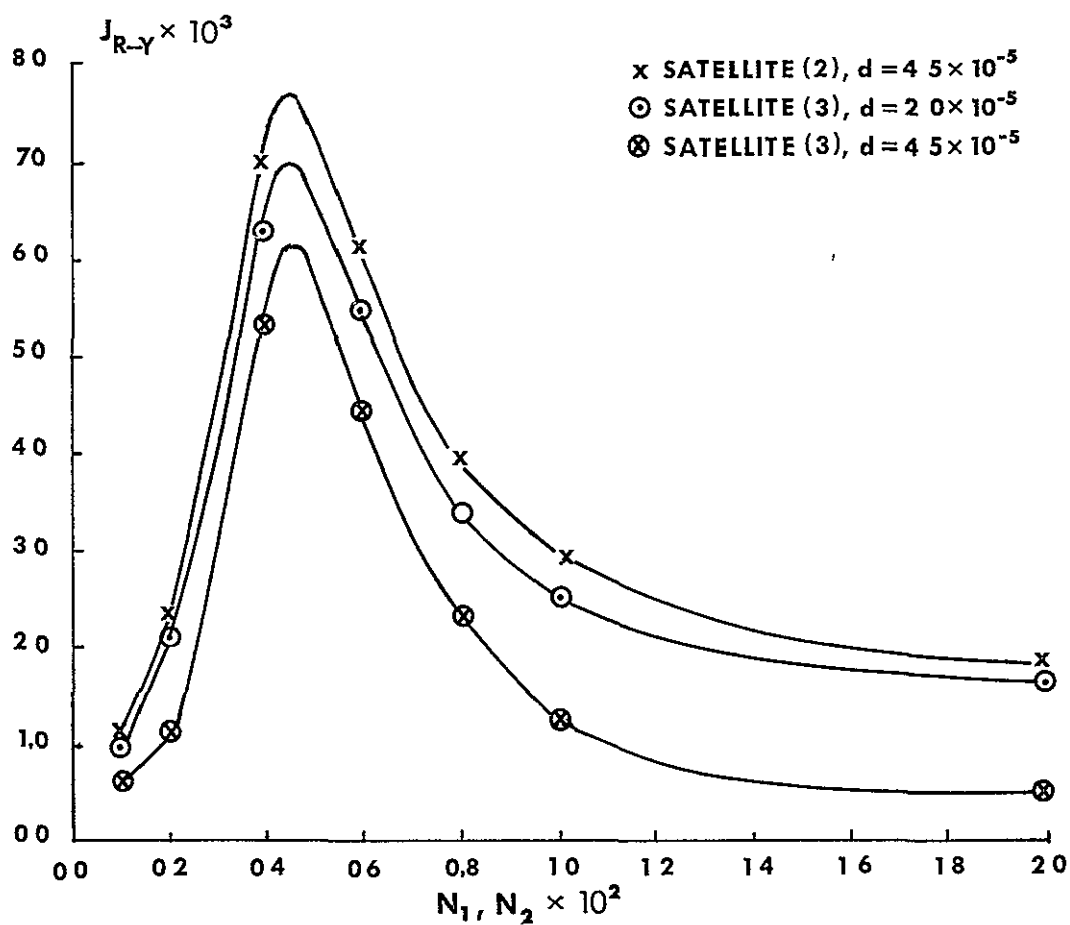
Figure 6.3. Roll-Yaw Fuel Cost for Various Values of k_1 and k_2 ,
 $N_1 = N_2 = 0.01$, $e = 0.05$, $d = 3 \times 10^{-5}$.

"unstable" in pitch and satellite (3) is "unstable" in yaw.) The distance d was taken as 2.0×10^{-5} , 2.5×10^{-5} in the pitch control and as 2×10^{-5} and 4.5×10^{-5} in both the roll and yaw controls. Recall from Chapter IV that in pitch, when the sinusoidal forcing term is most significant, the distance d should be large enough to insure a control-off interval in any interval which contains two consecutive control switches to $\pm N_3$. Also, recall that for "stable" single-axis motions (e.g. those of $x'' + a^2 x = v$) the fuel cost should decrease with increases in d ($\leq 10^{-4}$). For "unstable" single-axis motions (e.g. those of $x'' + a^2 x = v$, $a^2 < 0$) the fuel cost should increase with d ($\leq 10^{-4}$), however, d must be just large enough to insure a control-off interval in any interval which contains two consecutive control switches to $\pm N$.

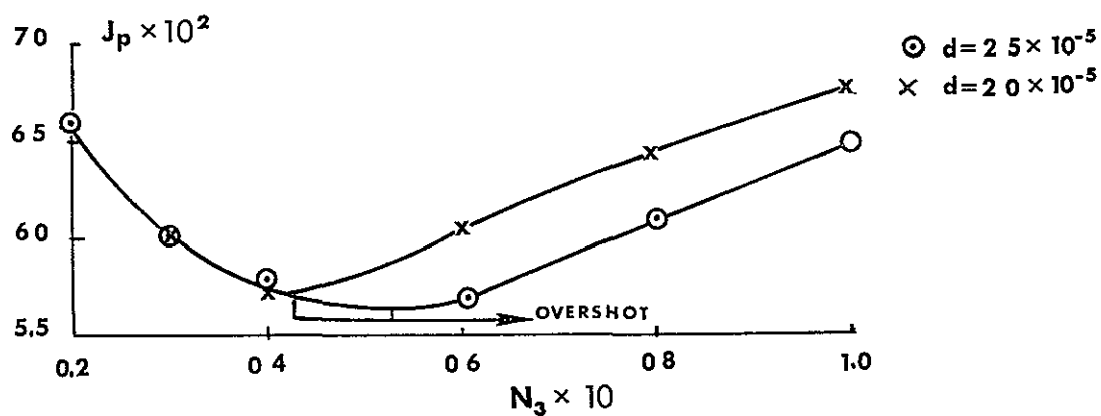
Figure (6.4a) shows the roll-yaw fuel cost per orbit of satellites (2) and (3) plotted as a function of the control strength for the various values of d . Since the pitch fuel cost varies insignificantly with the inertia parameters, only the pitch fuel cost per orbit of satellite (3) is shown plotted in Figure 6.4b. The points on the curves of Figure 6.4b marked "overshoot" correspond to the values of N_3 (for a time delay of about 0.5 sec.) for which control-on pitch trajectories overshoot the small strips (of width d) in the pitch phase plane. For N_3 greater than these values the values of d are not large enough to insure a control-off interval in any interval which contains two consecutive control switches to $\pm N_3$.

The effect of the size of the region S on the fuel cost per orbit was investigated for satellite (2). The results of this investigation are given in Figure 6.5. The point (0.0,0.0) aided in the construction of the curve for roll-yaw. (This was possible since the origin of the roll-yaw state space is an equilibrium point.)

To test the effect of sensor noise on the error and fuel cost per orbit a low frequency (100 cps) Gaussian noise generation was used. The noise was added to the state variables as they entered the controller. Runs were made for satellite (3) with $N_1 = 0.04$ and $d = 2.5 \times 10^{-4}$. The peak noise voltages used were 0.05, 0.1 and 0.2 times the peak state variable voltage of 1.0 volt. The error and fuel cost of each run with noise were compared to the error and fuel cost of the noiseless run.



a. Roll-Yaw of Satellites (2) and (3)



b Pitch of Satellite (3)

Figure 6.4 Fuel Cost Per Orbit vs Control Strength.

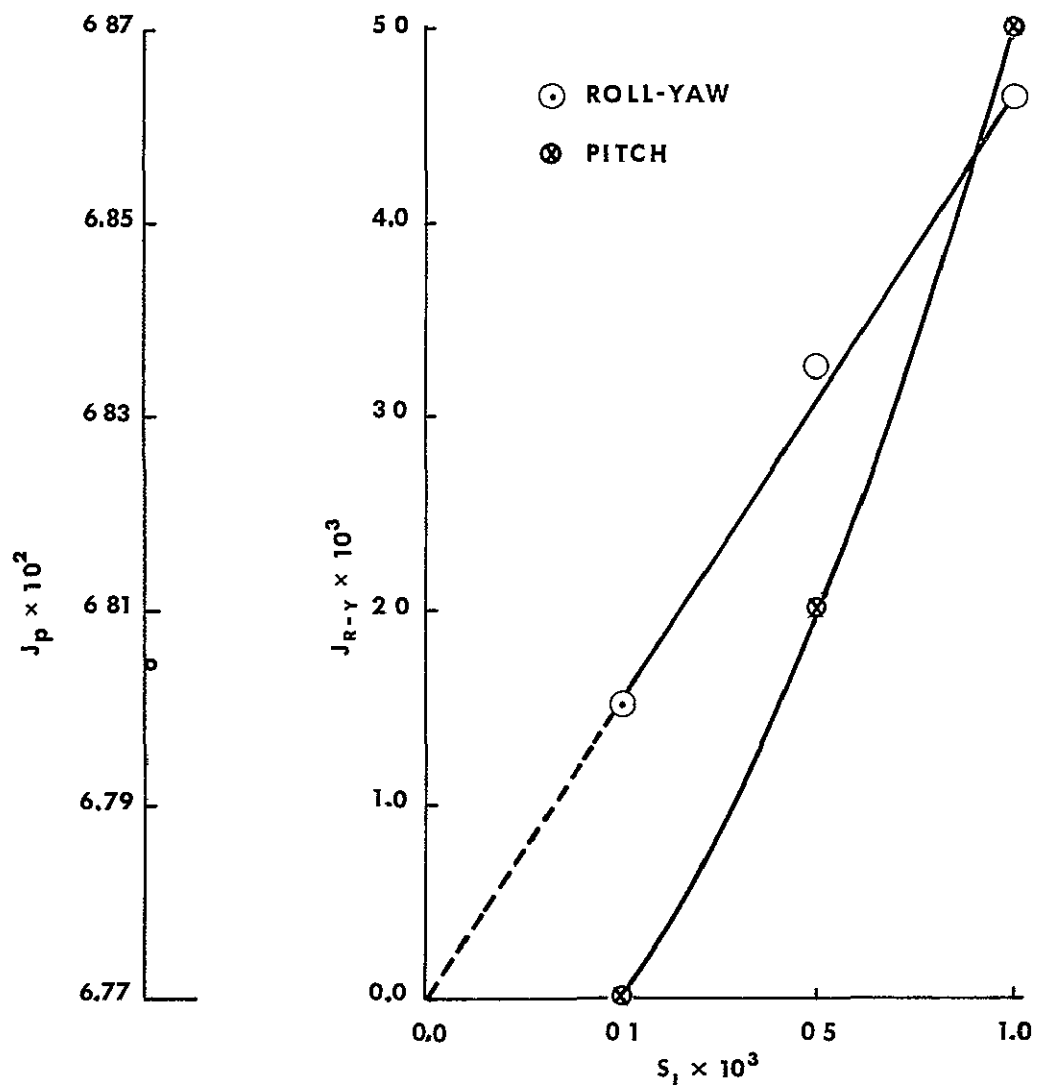


Figure 6.5. Fuel Cost Per Orbit vs Size of the Region S - Satellite (2),
 $d = 2.0 \times 10^{-5}$, $N_1 = N_2 = 0.01$, $N_3 = 0.1$

The fuel cost was found to increase slightly (less than 2%) while the error was at most 0.5×10^{-5} radians or 5%.

C. IMPERFECTIONS IN THE MODEL AND THE ULTIMATE ABILITY TO EARTH-POINT

1. Nonrigidity of the Satellites

The mathematical satellite models were made on the assumption that the satellites are rigid. This, of course, is not precisely the case, however, for the satellite configurations considered in this investigation, the effects of the various causes of nonrigidity can be made acceptably small. Contributors to nonrigidity include the slight deformation of the satellite structure in the small force environment (The largest gas jet required for acquisition gives only 0.17 lbs. of thrust.), the motion of the valves of the gas jets and the gaseous fuel

In the steady-state mode, the deformation of the satellites should be insignificant when, for example, an attached camera is to be aligned very accurately for earth-pointing to within 10^{-4} radians. For the satellites considered here the deformation is generally much smaller than the best machining tolerance available today and is, therefore, insignificant

The motion of the gas jet valves is very rapid so that the valves are opened or closed in just a few milliseconds. Thus, the gas valve must attain a speed of the order of 100 in./sec from rest (with respect to the satellite). After attaining this speed the valve must again be brought to rest. The forces required to accelerate the valves and to bring them to rest can cause a significant torque (about 0.1 ft.-lbs.) unless care is taken in their design.

Since the pressure due to a completely gaseous fuel is (for all practical purposes) uniformly distributed over the inner surface of the fuel container, the torque due to the pressure forces is essentially zero (regardless on the containers shape or its position in the satellite). Therefore, the third contributor to the satellite's state of nonrigidity has an insignificant effect on the satellite's earth-pointing performance.

2. Gas Jet Misalignment

Each gas jet pair was assumed to be aligned such that the torque

of the couple was "about" a principal axis of inertia for the mass center. In practice the orientations of the principal axes are known to within only about 0.01 radians. Hence, when a gas jet pair is on, it is probable that a torque with a magnitude of about 0.01 of the gas jet pair's torque is applied about the other principal axes. It is most likely that these misalignment torques will not improve the control systems performance, however, their effects on the accuracy are considered to be insignificant but they can result in as much as a 12% increase in the fuel cost.

3. Sensors and Error

In this investigation it is assumed that the state of the attitude motion is available from sensors. In the last section, Section B, it was found that low frequency (100 cps) noise added to the state variable signals from the sensors has almost no effect on the performance (even if its peak voltage is 0.2 of the sensor's output voltage). However, if there is a bias error of 10%, say from the misalignment of the sensors, the earth-pointing accuracy will suffer by 10% at times and the fuel cost will generally increase.

4. Others

The mathematical satellite models used in this investigation do not account for very large forces such as those due to the motion of a man on board and the collision of the satellite with a very high momentum, but "non-fatal" meteoroid.

Calculations based on $\Delta x_{i+1} \approx Nm_i \Delta \tau$, $i = 1, 2, 3$, and on $n^2 I_i Nm_i \Delta \tau \approx l_i m \Delta v$, $i = 1, 2, 3$, where Nm_i is the effective value of the i th component of the nondimensional meteoroid torque, m is the meteoroid's mass, l_i is the moment arm for the i th axis and Δv is the change in the magnitude of the meteoroid's velocity, showed that (for Δv between 20,000 ft./sec. and 60,000 ft./sec. and for l_i between 1.0 ft. and 15 ft.) the station-keeping control should be able to easily accommodate meteoroids with masses up to about 5×10^{-5} lbs. several times per orbit. (Accommodation of meteoroids of this size is considered to occur rarely. See Section F, Chapter II.) The acquisition control, which acts like a back-up station-keeping control with some decrease in accuracy,

should be able to accommodate meteoroids up to about 0.05 lbs. (with little loss of accuracy).

A man in motion aboard the satellite can exert forces on the satellite which cannot be compensated for by the station-keeping control. (The force on the satellite due simply to the man casually raising his arm above his head is about 10 lbs.) The acquisition control cannot compensate for these forces unless (for the satellites considered in this investigation) the nondimensional control magnitudes, N_1 , $i = 1, 2, 3$, are increased to about 10,000 and the time delays are reduced to about 10 microseconds. (Of course, if the satellites are much more massive than those considered here, say about 1000 tons, the values of N_1 and of the time delays do not need to be so extreme.)

VII. CONCLUSION

A feedback control system for efficiently controlling the attitude motions of satellites in elliptic orbits about an oblate earth with an atmosphere was devised. The criteria used for efficient (or "satisfactory") performance were (1) high-accuracy (10^{-4} radians) in earth-pointing after the acquisition of the earth-pointing mode has been accomplished within the time of one-quarter orbit from large angles ($\geq 60^\circ$), (2) minimum fuel expenditure, and, (3) practicality of the system. Although four particular satellite configurations ("stable" and "unstable") were assumed in the derivation, the devised control system performed well for a wide variety of satellite shapes, orbits and parameters of the control. (See Chapter VI.)

The derivation of the control system proceeded in two steps. First, in Chapter IV the station-keeping part of the controller was devised. Pontryagin's maximum principle, the "jump conditions" and the guidelines obtained from the minimum-fuel station-keeping controls devised for single-axis systems were used in this derivation. The maximum principle was applied to (1) the minimum-fuel problem which was considered as a problem in the theory of optimal processes with bounded phase coordinates and (2) the minimum-fuel problem with an integral constraint on the state (of the attitude) for maintaining high-accuracy earth-pointing.

In Chapter V the acquisition part of the controller was devised. Pontryagin's maximum principle and phase plane methods were used to extend the Busch acquisition control to give (1) acquisition for a wider range of satellites (including "unstable" satellites), (2) higher accuracy and (3) acquisition from larger angles in the more realistic time of one-quarter orbit.

Two avenues of future research related to this investigation are considered to be (1) the theory (sufficiency conditions) for the long-time optimal control of highly forced systems with bounded phase coordinates and (2) the high-accuracy and efficient control of the attitude motion of a manned satellite (by, perhaps, devices other than gas jets).

REFERENCES

1. Athans, M , "Fuel-Optimal Control of a Double Integral Plant with Response Time Constraints", IEEE Transactions on Applications and Industry, Vol. 83, July 1964.
2. Bandeen, W. R., and Manger, W. P., "Angular Motion of the Spin Axis of the Tiros I Meteorological Satellite Due to Magnetic and Gravitational Torques", J. of Geophysical Research, Vol. 65, No. 9, September 1960
3. Breakwell, J V., "The Optimization of Trajectories", J. Soc Ind Appl. Math., Vol. 7, No. 2, June 1959.
- 4 Breakwell, J V., and Koehler, L., "Elliptic Orbits Lifetimes", Advances in Astronautical Sciences, Plenum Press, New York, 1962.
- 5 Bryson, A. E., Denham, W. F., and Dreyfus, S. E., "Optimal Programming Problems with Inequality Constraints", AIAA Journal, Vol. 1, No 11, November 1963.
6. Busch, R., "The Attitude Control of a Satellite in an Elliptic Orbit", Stanford University Ph.D Thesis, 1966, SUDAAR No. 261.
7. Chang, S. S. L., "Optimal Control in Bounded Phase Space", Automatica, Vol. 1, 1962.
8. Christman, D. R., and McMillan, A. R., Journal of Environmental Sciences, Vol. 9, February 1966.
9. Cloutier, G J., "Attitude Perturbation of Space Vehicles by Meteoroid Impact", Journal of Spacecraft and Rockets, Vol. 3, April 1966.
10. Craig, A., and Flügge-Lotz, I., "Investigation of Optimal Control with a Minimum-Fuel Consumption Criterion for a Fourth-Order Plant with Two Control Inputs, Synthesis of an Efficient Suboptimal Control", ASME Journal of Basic Engineering, Vol. 87, Series D, No 1, March 1965

11. DeBra, D. B., "The Large Attitude Motions and Stability Due to Gravity, of a Satellite with Passive Damping in a Orbit of Arbitrary Eccentricity About an Oblate Body", Stanford University Ph D. Thesis, May 1962, SUDAER Report No. 126.
12. Flügge-Lotz, I., Discontinuous and Optimal Control, McGraw-Hill Book Co , New York (New book to appear spring, 1968).
13. Flügge-Lotz, I , and Marbach, H., "The Optimal Control of Some Attitude Control Systems for Different Performance Criteria", ASME Journal of Basic Engineering, Vol. 85, Series D, June 1963.
14. Foy, W. H., "Fuel Minimization in Flight Vehicle Attitude Control", IEEE Transactions on Automatic Control, Vol. AC-8, April 1963.
15. Haefner, K. B., "Attitude Control and Stabilization System for an Orbiting Vehicle", AFFDL-TR-64-165, May 1965
16. Hales, K. A., "Minimum-Fuel Control of a Sixth-Order Nonlinear Plant by an Extended Method of Steepest Descent", Stanford University Ph.D. Thesis, January 1966, SUDAAR No 257
- 17 Halkin, H., "On the Necessary Condition for Optimal Control of Non-linear Systems", Technical Report No. 116, Applied Mathematics and Statistics Laboratory, Stanford University, June 13, 1963.
18. Hayes, W. D., and Probst, R. F., Hypersonic Flow Theory, Academic Press, New York, 1959.
19. Horwitz, H. P., and Lanning, W. C., "Precision Attitude Control Using Pulse Width Modulation", Control Engineering, Vol. 13, June 1966.
20. Huston, R. L., "Twin-Gyro Attitude Control System", Journal of Spacecraft and Rockets, Vol. 3, July 1966.
- 21 Johnson, F. S., "Atmospheric Structure", Satellite Environment Handbook, Stanford University Press, Stanford, California, 1961.
22. Kane, T. R., Force and Energy (The second of three parts of a preliminary edition from a forthcoming text on dynamics), Holt, Rinehart and Winston, New York, 1966

23. King-Hele, D , Theory of Satellite Orbits in an Atmosphere, Butterworth, London, 1964.
24. Lee, E. B., "An Approximation to Linear Bounded Phase Coordinate Control Problems", Journal of Mathematical Analysis and Application, Vol. 13, 1966
25. Marbach, H , "The Optimal Control of Linear Systems for a Minimum Control-Effort Performance Criterion", Stanford University Ph.D. Thesis, 1963, SUDAER Report No. 153.
26. McElvain, R. J., "Effects of Solar Radiation Pressure on Satellite Attitude Control", Guidance and Control (Progress in Astronautics and Rocketry), Vol. 8, Academic Press, New York, 1962.
27. Meditch, J. S., "On Minimal-Fuel Satellite Attitude Control", IEEE Transactions on Applications and Industry, Vol. 83, No 71, March 1964
28. Nichol, K. C., "Research and Investigation on Satellite Attitude Control, Parts I and II", AFFDL-TR-64-168, June 1965.
29. Pontryagin, L. S., et al., The Mathematical Theory of Optimal Processes, Edited by L. W. Neustadt, Interscience Publishers, New York, 1962.
30. Rozonoer, L. I., "Pontryagin's Maximum Principle in the Theory of Optimal Systems - Parts I and II", Avtomatika i Telemekhanika, Vol. 20, 1962.
31. Russell, D L., "Penalty Functions and Bounded Phase Coordinate Control", Honeywell MPG-Report 1541-TR7, 16 January 1964.
32. Schwartz, L., "On Minimum-Energy Attitude Acquisition Using Reaction Wheel Control", Journal of Spacecraft and Rockets, Vol. 3, July 1966.
33. Sterne, T. E., An Introduction to Celestial Mechanics, Interscience Publishers, Inc., New York, 1960.

34. Wheeler, P. C., "Magnetic Attitude Control of Rigid Axially Symmetric Spinning Satellites in Circular Earth Orbits", Stanford University Ph.D. Thesis, April 1965, SUDAER Report No. 224.
35. Whipple, F. L., "Environment in Space-Dust and Meteorites", *Astronautics*, Vol. 7, No. 8, August 1962.

APPENDIX A. THE GRAVITATIONAL TORQUE

DeBra [11] has shown that the gravitational torque for B^* (the c m of the satellite) due to an oblate earth is suitably given by

$$\begin{aligned} \underline{T}_g = & (3\mu/r^3) \underline{n}_{R_1} \times \underline{I}_{R_1} \\ & + (5\mu J r_E^2/r^5) \underline{n}_{R_1} \times \underline{I}_{R_1} (1 - 7 \cos^2 \gamma) \\ & - (2\mu J r_E^2/r^5) \underline{N} \times \underline{I}_N \\ & + (10\mu J r_E^2/r^5) \cos \gamma (\underline{n}_{R_1} \times \underline{I}_N + \underline{N} \times \underline{I}_{R_1}) \end{aligned} \quad (A.1)$$

where $J = 3/2 (I_p - I_E)/m_E r_E^2 = 1.63 \times 10^{-3}$, $\mu = m_E G$, I_p and I_E are the polar and equatorial principal moment of inertia for E^* (the c m of the earth) m_E is the earth's mass, r_E is the earth's equatorial radius, G is the universal gravitation constant, \underline{n}_{R_1} is a unit vector directed from E^* to B^* , \underline{N} is a unit vector which is parallel to the earth's axis, γ is the angle between \underline{N} and \underline{n}_{R_1} , and \underline{I}_{R_1} and \underline{I}_N are second moment vectors of the satellite, B , relative to B^* for \underline{n}_{R_1} and \underline{N} , respectively Kane [22] shows that \underline{I}_N , for example, can be written as

$$\underline{I}_N = \sum_{i=1}^3 \sum_{j=1}^3 b_{ij} I_{ij} \underline{n}_j \quad (A.2)$$

where \underline{n}_i , $i = 1, 2, 3$, are mutually perpendicular unit vectors, $b_{ij} = \underline{N} \cdot \underline{n}_i \underline{n}_j$, $i = 1, 2, 3$, and I_{ij} , $i, j = 1, 2, 3$, are moments and products of inertia of B relative to B^* for \underline{n}_i and \underline{n}_j

Suppose \underline{n}_i , $i = 1, 2, 3$ are parallel to principal axes of inertia of B for B^* (see Figure 2.1) Then $I_{ij} = 0$ for $i \neq j$. If \underline{n}_i , $i = 1, 2, 3$, are right handed unit vectors and $a_i = \underline{n}_{R_1} \cdot \underline{n}_i$, $i = 1, 2, 3$, then with the aid of A.2 and a similar relation for \underline{I}_{R_1} the terms which appear as vector products in A.1 can be written as

$$\begin{aligned}\underline{n}_{R_1} \times \underline{I}_{R_1} &= a_3 a_2 (I_3 - I_2) \underline{n}_1 + a_1 a_3 (I_1 - I_3) \underline{n}_2 \\ &+ a_2 a_1 (I_2 - I_1) \underline{n}_3\end{aligned}$$

$$\begin{aligned}\underline{N} \times \underline{I}_N &= b_3 b_2 (I_3 - I_2) \underline{n}_1 + b_1 b_3 (I_1 - I_3) \underline{n}_2 \\ &+ b_2 b_1 (I_2 - I_1) \underline{n}_3\end{aligned}$$

$$\begin{aligned}\underline{n}_{R_1} \times \underline{I}_N &= (a_2 b_3 I_3 - a_3 b_2 I_2) \underline{n}_1 + (a_3 b_1 I_1 - a_1 b_3 I_3) \underline{n}_2 \\ &+ (a_1 b_2 I_2 - a_2 b_1 I_1) \underline{n}_3\end{aligned}$$

$$\begin{aligned}\underline{N} \times \underline{I}_{R_1} &= (b_2 a_3 I_3 - b_3 a_2 I_2) \underline{n}_1 + (b_3 a_1 I_1 - b_1 a_3 I_3) \underline{n}_2 \\ &+ (b_1 a_2 I_2 - b_2 a_1 I_1) \underline{n}_3\end{aligned}\tag{A 3}$$

where $I_{1j} = I_{j1}$, $i = j = 1, 2, 3$

Now the gravitational torque as given by A.1 can be written with the aid of equations A.3 in the desired component form. A more useful expression for the torque is obtained if a_i , and b_i , $i = 1, 2, 3$, are written as functions of the attitude angles θ_i , $i = 1, 2, 3$, and of the parameters of the orbit of the satellite, δ , θ , θ_p (see Figure A.1). This will be done before equations A.3 are substituted into A.1.

It is not difficult to conclude with the aid of Figure A.1 and trigonometry that

$$\underline{N} = \sin \delta [\sin (\theta + \theta_p) \underline{n}_{R_1} + \cos (\theta + \theta_p) \underline{n}_{R_2}] + \cos \delta \underline{n}_{R_3}\tag{A 4}$$

where \underline{n}_{R_1} is the unit vector given above, \underline{n}_{R_3} is a unit vector which is normal to the orbit plane with its sense given by the right hand rule for increasing θ , \underline{n}_{R_2} is a unit vector which together with \underline{n}_{R_1} and \underline{n}_{R_3} form a set of right-handed mutually perpendicular unit

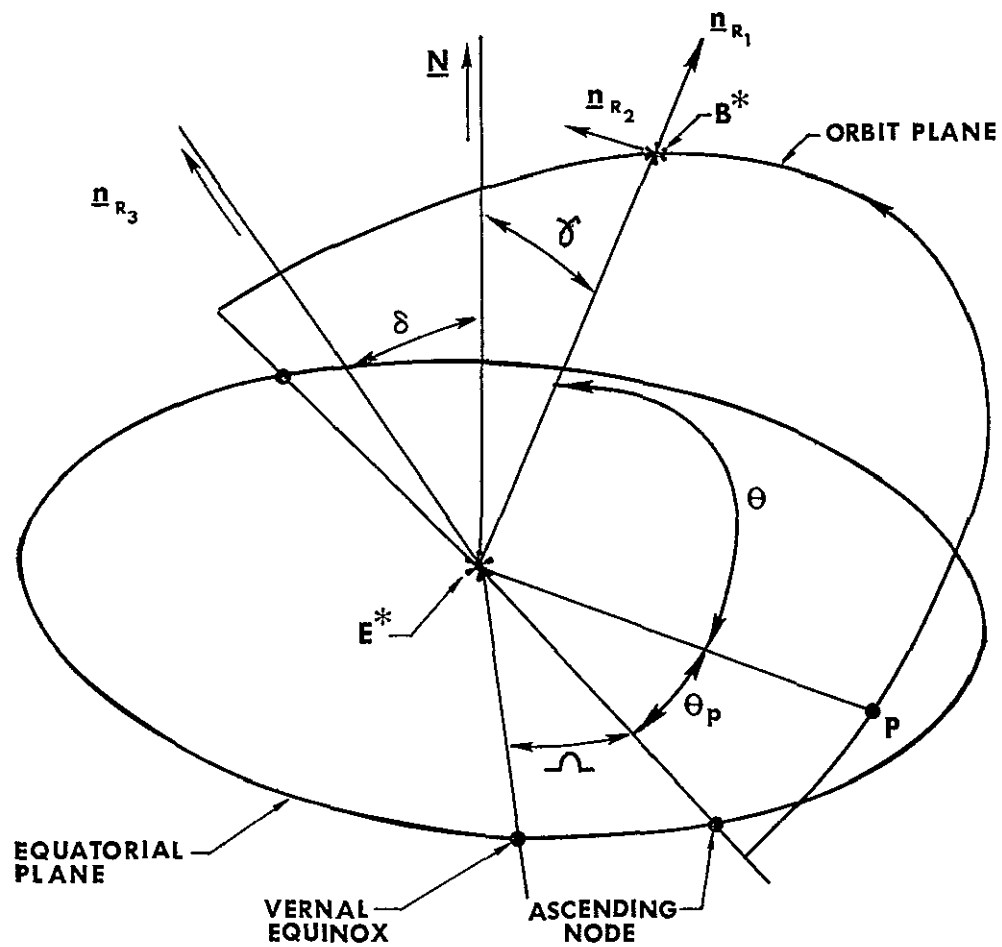


Figure A 1 Unit Vectors and Parameters of the Orbit

vectors and θ_p is the angle between the ascending line of nodes and the line between E^* and the perigee point of the orbit.

Now, if \underline{n}_{R_1} , $i = 1, 2, 3$, are written in terms of \underline{n}_1 , $i = 1, 2, 3$, and if these expressions are substituted into A 4, then the coefficients of \underline{n}_1 , $i = 1, 2, 3$, in the resulting expression will be b_1 , $i = 1, 2, 3$, respectively. The coefficients of \underline{n}_1 , $i = 1, 2, 3$, in the expression for \underline{n}_{R_1} are a_1 , $i = 1, 2, 3$, respectively.

If the three-axes Euler angles, $\theta_1, \theta_2, \theta_3$, are used as in Busch [6], it can be concluded that

$$\begin{aligned}\underline{n}_{R_1} &= c_2 c_3 \underline{n}_1 - c_2 s_3 \underline{n}_2 + s_2 \underline{n}_3 \\ \underline{n}_{R_2} &= (s_1 s_2 c_3 + c_1 s_3) \underline{n}_1 + (c_1 c_3 - s_1 s_2 s_3) \underline{n}_2 - s_1 c_2 \underline{n}_3 \\ \underline{n}_{R_3} &= (s_1 s_3 - c_1 s_2 c_3) \underline{n}_1 + (s_1 c_3 + c_1 s_2 s_3) \underline{n}_2 + c_1 c_2 \underline{n}_3\end{aligned}\quad (A\ 5)$$

where $c_i = \cos \theta_i$, $s_i = \sin \theta_i$, $i = 1, 2, 3$

From the first of A 5 it is observed that

$$a_1 = c_2 c_3, \quad a_2 = -c_2 s_3, \quad a_3 = s_2 \quad (A\ 6)$$

and from A 4 and A 5 it is observed that

$$\begin{aligned}b_1 &= s_\delta s_\theta c_2 c_3 + s_\delta c_\theta c_1 s_3 - c_\delta c_1 s_2 c_3 + s_\delta c_\theta s_1 s_2 c_3 + c_\delta s_1 s_3 \\ b_2 &= s_\delta c_\theta c_1 c_3 + c_\delta s_1 c_3 - s_\delta s_\theta c_2 s_3 + c_\delta c_1 s_2 s_3 - s_\delta c_\theta s_1 s_2 s_3 \\ b_3 &= c_\delta c_1 c_2 + s_\delta s_\theta s_2 - s_\delta c_\theta s_1 c_2\end{aligned}\quad (A\ 7)$$

where, for example, $c_\delta = \cos \delta$ and $s_\theta = \sin (\theta + \theta_p)$

Now with A.3, A 6 and A 7 the gravitational torque, which is given by A.1, can be expressed in a form which is convenient for studying its effect on the attitude motion of earth-pointing satellites. The sub-

stitution of A.3 into A.7 results in $T_g = T_{g1} \underline{n}_1 + T_{g2} \underline{n}_2 + T_{g3} \underline{n}_3$
where

$$\begin{aligned}
T_{g1} &= (\mu/r^3) (I_3 - I_2) \{3a_3a_2 + 5J [r_E/r]^2 [1 - 7 \cos^2\gamma] a_3a_2 \\
&\quad - 2J [r_E/r]^2 b_3b_2 + 10J [r_E/r]^2 \cos\gamma [a_2b_3 + a_3b_2]\} \\
T_{g2} &= (\mu/r^3) (I_1 - I_3) \{3a_1a_3 + 5J [r_E/r]^2 [1 - 7 \cos^2\gamma] a_1a_3 \\
&\quad - 2J [r_E/r]^2 b_1b_3 + 10J [r_E/r]^2 \cos\gamma [a_3b_1 + a_1b_3]\} \\
T_{g3} &= (\mu/r^3) (I_2 - I_1) \{3a_2a_1 + 5J [r_E/r]^2 [1 - 7 \cos^2\gamma] a_2a_1 \\
&\quad - 2J [r_E/r]^2 b_2b_1 + 10J [r_E/r]^2 \cos\gamma [a_1b_2 + a_2b_1]\} \quad (A.8)
\end{aligned}$$

In the terms of equations A.8 the factors which involve only a_1
and b_1 , $i = 1, 2, 3$, are given by

$$\begin{aligned}
a_3a_2 &= -c_2s_2s_3, \quad a_1a_3 = c_2s_2c_3, \quad a_2a_1 = -c_2^2c_3s_3 \\
b_3b_2 &= s_\delta c_\delta c_\theta c_1^2 c_2 c_3 + s_\delta^2 c_\theta s_\theta c_1 s_2 c_3 - s_\delta^2 c_\theta^2 c_1 s_1 c_2 c_3 \\
&\quad + c_\delta^2 c_1 s_1 c_2 c_3 - c_\delta s_\delta s_\theta c_1 c_2^2 s_3 + (\text{terms in } s_1^2, \dots, s_1^4) \\
b_1b_3 &= s_\delta c_\delta s_\theta c_1 c_2^2 c_3 + s_\delta^2 s_\theta^2 c_2 s_2 c_3 - s_\delta^2 s_\theta c_\theta s_1 c_2^2 c_3 \\
&\quad + s_\delta c_\delta c_\theta c_1^2 c_2 s_3 - c_\delta^2 c_1^2 c_2 s_2 c_3 + (\text{terms in } s_1^2, s_1^3)
\end{aligned}$$

$$b_2 b_1 = s_\delta^2 s_\theta^2 c_1^2 c_2^2 c_3^2 + s_\delta c_\delta s_\theta s_1 c_2 c_3^2 - s_\delta^2 s_\theta^2 c_2^3 c_3 s_3 \\ + s_\delta^2 c_\theta^2 c_1^2 c_3 s_3 - s_\delta c_\delta c_\theta c_1^2 s_2 c_3^2 + (\text{terms in } s_1^2, \dots, s_1^5)$$

$$a_2 b_3 + a_3 b_2 = c_\delta c_1 c_2 (s_2 - c_2 s_3) + (\text{terms in } s_1^2, \dots, s_1^4)$$

$$a_3 b_1 + a_1 b_3 = c_\delta c_1 c_2^2 c_3 + 2 s_\delta s_\theta c_2 s_2 c_3 - s_\delta c_\theta s_1 c_2^2 c_3 \\ + (\text{terms in } s_1^2, s_1^3)$$

$$a_1 b_2 + a_2 b_1 = s_\delta c_\theta c_1 c_2 c_3^2 - 2 s_\delta s_\theta c_2^2 c_3 s_3 + c_\delta s_1 c_2 c_3^2 \\ + (\text{terms in } s_1^2, s_1^3) \quad (\text{A.9})$$

From A.4 it is found that $\cos \gamma = \underline{N} \cdot \underline{n}_{R_1}$ is given by

$$\cos \gamma = s_\delta s_\theta \quad (\text{A.10})$$

APPENDIX B. THE AERODYNAMIC TORQUE

If a satellite is in orbit 100 miles or more above the earth's surface, then the ratio of the speed of B^* to the most probable random speed of the air molecules is of the order of 10^3 . At these altitudes the mean free path of the molecules greatly exceed the maximum linear dimension of the satellite. Hayes and Probstein [18] have shown for bodies in such free molecular flow that the pressure and shear is given by

$$p = (2 - f_n) \rho V^2 \cos \psi$$

$$\tau = f_t \rho V^2 \sin \psi \cos \psi$$

where f_n and f_t are the normal and tangential accommodation coefficients, ρ is the density of the air, $V = |\underline{v}^{p/a}|$ where $\underline{v}^{p/a}$ is the velocity of a point P of the element of surface area of B relative to the free-stream velocity of the air near the satellite and ψ is the angle between the vector $\underline{v}^{p/a}$ and a line normal to the surface element.

For the satellite attitude motions considered in this thesis the angular velocity of B in inertial space is such that error in taking $\underline{v}^{p/a} = \underline{v}^{B^*/a}$ is at most 0.0001%. In the following derivation V will be assumed to be $|\underline{v}^{B^*/a}|$.

The accommodation coefficients are defined by $f_t = (\tau_i - \tau_r)/\tau_i$ and $f_n = (p_i - p_r)/(p_i - p_b)$ where, for example, p_b is the normal momentum component of the molecules which are re-emitted from the surface with a Maxwellian distribution at the surface temperature T_b and the subscripts i and r denote incident and reflected. Hayes and Probstein conclude from the results obtained by experimentalists that f_t lies in the range between 0.8 and 1.0 and f_n is about unity.

If \underline{n} denotes a unit vector normal to the element of surface area, say ds , and is directed out of B and if \underline{n} is such that $\underline{v}^{B^*/a} = V \underline{n}$, then the force on ds is given by

$$d\underline{F} = -\rho V^2 \cos \psi [(2-f_n) \cos \psi \underline{n} - f_t \sin \psi \underline{n}_t] ds \quad (B 1)$$

where \underline{n}_t is a unit vector in the direction of the projection of $-\underline{n}$ onto ds .

For a spherical satellite the integration of (B.1) over the half of the surface in the flow gives

$$\underline{F} = -C_D S \rho V^2 / 2 \underline{n} \quad (B.2)$$

where $C_D = 2 - f_n - f_t$ and S is the projected area so that the force vector is parallel to \underline{v}^{B^*}/a and is a drag force.

If $f_n = f_t = 1$ in (B.1), then $d\underline{F}$ is parallel to \underline{v}^{B^*} for an element of a satellite of arbitrary shape. Thus, the sum \underline{F} will be a drag force only for any satellite if $f_n = f_t = 1$.

If $f_n = 1$ and $f_t = 0.80$, the lowest value given above, then in (B.1), the term in parentheses can be written as

$$\underline{n} + 0.2 \sin \psi (\cos \psi \underline{n}_\ell - \sin \psi \underline{n})$$

where \underline{n}_ℓ is perpendicular to \underline{n} and is directed maximally away from ds . Examination of this term shows that a "lift" component of the force is possible for some orientations of some satellites. For a cylindrical satellite with either circular or elliptic cross section in a nearly earth-pointing orientation, say 10^{-3} radians, the term which contributes to the lift is smaller than 10^{-3} times the drag component for both lateral and end surfaces so that the "lift" component of the resultant force will be insignificantly small. For all other orientations of any satellite the ratio of "lift" to "drag" is still less than 0.12.

The aerodynamic force used in the calculation of the aerodynamic torque for B^* will be that given by (B.2).

King-Hele [23] considers the error to be less than 5% when C_D is taken to be 2.2 for both spheres and cylinders ($\ell/d > 1$) if C_D is based on the mean area, S , perpendicular to the direction of motion.

The atmospheric density ρ has been determined experimentally and theoretically in recent years for altitudes above 100 miles. It has been found (see King-Hele [23] and Johnson [21]) that ρ decreases almost logarithmically with altitude between about 150 miles and about 500 miles. If this be the case then

$$\rho = \rho_p \exp[-K(r-r_p)] \quad (\text{B } 3)$$

where the subscript p denotes perigee, K is a constant to be determined from the data and r is the distance from E^* to B^* . The atmospheric density data is usually plotted on semi-log graph paper so that K can be read from the plots directly. From these plots it is observed that K should be about 0.02 miles^{-1} from an altitude of 200 miles and should be about 0.01 miles^{-1} from an altitude of 500 miles. Also, it is observed that due to changes in the sun's influence between day-time and night-time, the density changes by a factor of about two at an altitude of 200 miles and by a factor of about ten at an altitude of 500 miles. The maximum values occur in the daytime. If it is desired to fix ρ_p and K for any one orbit without regard to day and night, then for the most nearly correct values of ρ over the range of altitudes of the orbit and over the time interval of days it is best to pick the day-time value of ρ_p and the value of K which corresponds to day-time values of ρ near perigee. This is done in the thesis for a height of perigee of 200 miles. In this case the density, ρ , as given by (B 3) is considered to be too large during night-time by a factor of two at 200 miles and by a factor of ten at 500 miles. It is considered to be too small by a factor of 0.7 during day-time at 500 miles and to be correct during day-time at 200 miles.

The torque of the aerodynamic forces acting on the elements of surface area of a spherical or high-accuracy earth-pointing cylindrical satellite is given by

$$\underline{T}_a = \underline{\ell} \times \underline{F} \quad (\text{B } 4)$$

where $\underline{\ell}$ is the distance vector from B^* to the geometrical centroid (GC) of the satellite.

In Appendix A, Figure A 1, the orbiting reference axes with unit vectors $\underline{n}_{R1}, \underline{n}_{R2}, \underline{n}_{R3}$ were defined. The unit vectors $\underline{n}_i, i = 1, 2, 3$, are defined in Section A of Chapter II (see Figure (2.1)).

Since the GC is fixed in B, it is convenient to write

$$\underline{\ell} = \ell_1 \underline{n}_1 + \ell_2 \underline{n}_2 + \ell_3 \underline{n}_3 \quad (\text{B.5})$$

where $\ell_1 = \underline{\ell} \cdot \underline{n}_1$, $1 = 1, 2, 3$. If \underline{n} is written in terms of \underline{n}_1 , $1 = 1, 2, 3$, then with the use of (B 5) \underline{T}_a will be in terms of \underline{n}_1 , $1 = 1, 2, 3$, as desired.

Since $\underline{v}^{B^*/a} = \underline{v}^{B^*} - \underline{v}^a = V\underline{n}$ and since $\underline{v}^{B^*} = \dot{r}\underline{n}_{R_1} + r\dot{\theta}\underline{n}_{R_2}$ and $\underline{v}^a = \underline{\omega}^E \times r\underline{n}_{R_1} = \dot{\theta}_E r(\underline{N} \times \underline{n}_{R_1})$ where θ_E is the angular speed of the earth and \underline{N} is given in Appendix A, then

$$\underline{n} = \frac{\dot{r}}{v} \underline{n}_{R_1} + \frac{r(\dot{\theta} - \theta_E c_\delta)}{v} \underline{n}_{R_2} + \frac{r\dot{\theta}_E s_\delta c_\theta}{v} \underline{n}_{R_3} \quad (B 6)$$

where s_δ, c_θ are defined in Appendix A.

From (B.6) it is seen that

$$V^2 = \dot{r}^2 + r^2\dot{\theta}^2 + r^2[\dot{\theta}_E^2(c_\delta^2 + s_\delta^2 c_\theta^2) - 2\theta_E \dot{\theta} c_\delta] \quad (B 7)$$

With the aid of (C 7)-(C 9) equation (B 7) can be written as

$$V^2 = \frac{h^2(1+e^2 + 2ec\theta)}{a^2(1-e^2)^2} - 2h\theta_E c_\delta + r^2\dot{\theta}_E^2(c_\delta^2 + s_\delta^2 c_\theta^2)$$

where $c\theta = \cos \theta$.

If $e \leq 0.05$, then the expression for v differs from

$$V = (h/a)(1 + 2ec\theta)^{1/2} = r\dot{\theta} \quad (B 8)$$

only in the third significant figure.

The substitution of (A.5) into (B 6) and the results of this substitution into (B 2) produces an expression for the force, \underline{F} , which is in terms \underline{n}_1 , $1 = 1, 2, 3$. If this expression for the force is substituted into (B 4) with (B 5) and if the vector product is carried out, the result is $\underline{T}_a = T_{a1}\underline{n}_1 + T_{a2}\underline{n}_2 + T_{a3}\underline{n}_3$ where

$$T_{a1} = -\frac{C_D S \rho V}{2} \{ \dot{r}(\ell_2 s_2 + \ell_3 c_2 s_3) - r(\theta - \theta_E c_\delta)[\ell_2 s_1 c_2 + \ell_3(c_1 c_3 - s_1 s_2 s_3)] + r\dot{\theta}_E c_\theta s_\delta[\ell_2 c_1 c_3 - \ell_3(s_1 c_3 + c_1 s_2 s_3)] \}$$

$$T_{a2} = -\frac{C_D S \rho V}{2} \{ \dot{r}(\ell_3 c_2 c_3 - \ell_1 s_2) + r(\theta - \theta_E c_\delta)[\ell_3(s_1 s_2 c_3 + c_1 s_3) + \ell_1 s_1 c_2] \}$$

$$\begin{aligned}
& + r\dot{\theta}_E c_{\theta} s_{\delta} [\ell_3 (s_1 s_3 - c_1 s_2 c_3) - \ell_1 c_1 c_2] \} \\
T_{a3} = & - \frac{C_D S \rho V}{2} \{ -r(\ell_1 c_2 s_3 + \ell_2 c_2 c_3) + r(\theta - \dot{\theta}_E c_{\delta}) [\ell_1 (c_1 c_3 - s_1 s_2 s_3) \\
& - \ell_2 (s_1 s_2 c_3 + c_1 s_3)] + r\dot{\theta}_E c_{\theta} s_{\delta} [\ell_1 (s_1 c_3 + c_1 s_2 s_3) \\
& - \ell_2 (s_1 s_3 - c_1 s_2 c_3)] \} \quad (B 9)
\end{aligned}$$

The quantities ρ and v in (B.9) are assumed to be suitably given by (B.3) and (B 8). The quantities r, \dot{r} , and $\dot{\theta}$ are given as functions of time in Appendix C. The quantities $C_D, S, \ell_1, 1 = 1, 2, 3$, pertain to a given satellite, and, the quantities $h, a, c_{\delta}, s_{\delta}, \theta_p, r_p, K$ and ρ_p pertain to a given orbit. Except for C_D , which is taken as $C_D = 2.2$, given values of these quantities were chosen in Chapter II. The angular speed of the earth is $\theta_E = 7.3 \times 10^{-5}$ rad/sec.

The error in the torque components, (B 9), are considered to be caused primarily by the error in ρ and the error in the product $C_D S$. These errors were discussed above. The total error in each of T_{a1} , $1 = 1, 2, 3$, is considered to be between 2000% to large (night-time at 500 miles) and 50% too small (day-time at 500 miles). Generally, this means that the magnitudes of the components of \underline{T}_a are between 1/2 and 20 times the correct values.

For the purpose of determining a feedback control law which will result in suitable attitude motion, when this motion is influenced by the atmosphere, this inaccuracy is insignificant. Of course, performance measures such as fuel cost can be in error as much as T_{a1} , $1 = 1, 2, 3$, are in error, but, generally, this depends on the magnitudes of the components of the other torques which influence the attitude motion.

APPENDIX C THE PARAMETERS OF THE ORBIT AS FUNCTIONS OF TIME

King-Hele [23] and Sterne [33] have derived expressions for the rates of change of a , e , Ω , δ and θ_p of a Kepler orbit due to the primary perturbing sources which are the earth's oblateness and the earth's atmosphere. For the orbits considered in this investigation the changes are less than 10 miles per day in a , 2×10^{-4} per day in e , 7° per day in Ω , 1° per day in δ and 10° per day in θ_p . For any one orbit these changes cause only an insignificant change in the terms in the attitude equations of motion. Thus, since the equations of motion are periodically time varying, they need to be integrated for a single orbit only so that for any one integration a , e , Ω , δ and θ_p can be assumed constant.

The angle θ varies from zero to 2π radians. For a Kepler orbit θ is related to r by

$$r = (h^2/\mu) (1 + e\cos\theta)^{-1} \quad (C.1)$$

where $\mu = m_E G$, $c\theta = \cos\theta$ and h is a constant such that $r^2\dot{\theta} = h$. Thus,

$$\frac{\mu}{r^3} = n^2 (1 + e\cos\theta)^3 \quad (C.2)$$

$$\dot{\theta} = n (1 + e\cos\theta)^2 \quad (C.3)$$

and

$$\frac{1}{r^2} = \frac{(1 + e\cos\theta)^2}{a^2 (1 - e^2)^2} \quad (C.4)$$

* For convenience $c\theta = \cos\theta$, but generally $c\theta = \cos(\theta + \theta_0)$.

where $n = \mu^2/h^3$ and $a(1 - e^2) = h^2/\mu$

The differentiation of C.3 with respect to time and the substitution of C 3 into the differentiated expression gives

$$\dot{\theta} = -2n^2 e s_{\theta} (1 + ec\theta)^3 \quad (C.5)$$

The angle θ can be written as an approximate function of t so that the right hand sides of equations C 1 - C 5 can be written as approximate functions of t

In the thesis e is assumed to be less than or equal to 0.05. In this case the function $(1 + ec\theta)^{-2}$ can be expanded in a rapidly converging power series in e so that the integral of C 3 can be written as

$$\int_0^{\theta} (1 - 2ec\theta + 3e^2 c^2 \theta - [\text{REMAINDER}]) d\theta = n \int_0^t dt$$

where $(\text{REMAINDER}) = 4e^3[(c\theta + ec^2\theta)^3/(1 + ec\theta)^8]_{e=x}$ for $0 \leq x \leq 0.05$. If the maximum absolute value of the REMAINDER is used, then

$$\left| \int_0^{\theta} (\text{REMAINDER}) d\theta \right| < 6.5 \times 10^{-4} \theta$$

so that

$$nt = \theta(1 + 3/2e^2) - 2e \sin\theta + 3/4e^2 \sin 2\theta$$

with an error less than 0.06% or

$$nt = \theta - 2e \sin\theta \quad (C.6)$$

with an error only in the third significant figure (except at $\theta = 0$ where the error is zero)

Equations C 1 - C.5 are approximately given by

$$r = (h^2/\mu) (1 - ec\theta) \quad (C 7)$$

$$\frac{\mu}{r^3} = n^2 (1 + 3ec\theta) \quad (C 8)$$

$$\theta = n (1 + 2ec\theta) \quad (C 9)$$

$$r^{-2} = a^{-2} (1 + 2ec\theta) \quad (C 10)$$

$$\dot{\theta} = -2n^2 es\theta (1 + 3ec\theta) \quad (C 11)$$

with the approximation only in the third significant figure

The use of C.6 and trigonometric identities results in

$$c\theta = \cos nt \cos (2e \sin\theta) - \sin nt \sin (2e \sin\theta) \quad (C 12)$$

and

$$s\theta = \sin nt \cos (2e \sin\theta) + \cos nt \sin (2e \sin\theta) \quad (C 13)$$

The expressions for $c\theta$ and $s\theta$ given in C 12 and C.13 differ from exact values by less than 0.01. (This is easily seen by plotting $[\cos\theta - \cos(\theta \pm \epsilon)]$ and $[\sin\theta - \sin(\theta \pm \epsilon)]$ as a function of the error, $\epsilon \leq 0.01$ ($\epsilon > 0$), for various values of θ) Thus, if C 12 and C 13 are substituted into C.7 - C 11, then C.7 - C 10 will be in error only in the fourth significant figure and C 11 will be in error by less than 1% for most of the orbit. In C 7 - C 11 the factors $(1 - ec\theta)$, $(1 + 2ec\theta)$, $(1 + 3ec\theta)$ and $s\theta (1 + 3ec\theta)$ can be written with the aid of C 12 and C 13 as

$$\begin{aligned}
(1 - ec\theta) &= 1 - e \cos nt \cos (2e \sin\theta) \\
&\quad + e \sin nt \sin (2e \sin\theta)
\end{aligned} \tag{C.14}$$

$$\begin{aligned}
(1 + 2ec\theta) &= 1 + 2e \cos nt \cos (2e \sin\theta) \\
&\quad - 2e \sin nt \sin (2e \sin\theta)
\end{aligned} \tag{C.15}$$

$$\begin{aligned}
(1 + 3ec\theta) &= 1 + 3e \cos nt \cos (2e \sin\theta) \\
&\quad - 3e \sin nt \sin (2e \sin\theta)
\end{aligned} \tag{C.16}$$

$$\begin{aligned}
s\theta (1 + 3ec\theta) &= \sin nt \cos (2e \sin\theta) + \cos nt \sin (2e \sin\theta) \\
&\quad + 3e \cos nt \sin nt [\cos^2 (2e \sin\theta) - \sin^2 (2e \sin\theta)] \\
&\quad + 3e (\cos^2 nt - \sin^2 nt) \sin (2e \sin\theta) \cos (2e \sin\theta)
\end{aligned} \tag{C.17}$$

Since $e \leq 0.05$, then $|\sin (2e \sin\theta)| \leq 2e \leq 0.1$ and $|\cos (2e \sin\theta)| = 1.00$. Thus, C.14 - C.16 can differ from

$$(1 - ec\theta) = 1 - e \cos nt \tag{C.18}$$

$$(1 + 2ec\theta) = 1 + 2e \cos nt \tag{C.19}$$

$$(1 + 3ec\theta) = 1 + 3e \cos nt \tag{C.20}$$

only in the third significant figure and

$$\begin{aligned}
s\theta (1 + 3ec\theta) &= \sin nt + \cos nt \cdot 2e \sin\theta + 3 e \cos nt \sin nt \\
&\quad + 3e (\cos^2 nt - \sin^2 nt) \cdot 2e \sin\theta
\end{aligned} \tag{C.21}$$

is in error by less than 1%. Since $\sin\theta = \sin nt + 2e \sin\theta \cos nt$ (from C.13) with less than 1% error for most of the orbit, then C.21 can be written as

$$s\theta (1 + 3e\cos\theta) = \sin nt + 5e \cos nt \sin nt$$

or

$$s\theta^4(1 + 3e\cos\theta) = \sin nt + 5/2 e \sin 2nt \quad (C.22)$$

with a total error of less than 1% for most of the orbit. (Actually, the difference in the exact values and the values given by C.22 is less than 0.01 for the entire orbit, but the percent error becomes unbounded as the exact value approaches zero).

Now the substitution of C.18 - C.20 and C.22 into C.7 - C.11 results in

$$r = r_p [1 - e(\cos nt - 1)] \quad (C.23)$$

$$\frac{\mu}{r^3} = n^2 (1 + 3e \cos nt) \quad (C.24)$$

$$\dot{\theta} = n (1 + 2e \cos nt) \quad (C.25)$$

$$r^{-2} = a^{-2} (1 + 2e \cos nt) \quad (C.26)$$

$$\ddot{\theta} = -2n^2 e (\sin nt + 5/2 e \sin 2nt) \quad (C.27)$$

where in C.7 h^2/μ has been replaced by $a(1 - e^2) = r_p(1 + e)$ and terms in e^2 omitted. The results in equations C.23 - C.26 differ from the exact values in the third or higher significant figure, and, the values for $\ddot{\theta}$ which are given by C.27 are in error by less than 0.01 parts in one for most of the orbit.

If C.6 is used, then $s\theta$ and $c\theta$ can be written approximately as

$$\begin{aligned}\sin (\theta + \theta_0) &= \sin (nt + \theta_0) \\ &+ 2e \cos (nt + \theta_0) \sin nt (1 + 2e \cos nt)\end{aligned}\quad (C.28)$$

$$\begin{aligned}\cos (\theta + \theta_0) &= \cos (nt + \theta_0) \\ &- 2e \sin (nt + \theta_0) \sin nt (1 + 2e \cos nt)\end{aligned}\quad (C.29)$$

The order of approximation in C.28 and C.29 is the same as in C.12 and C.13.

APPENDIX D THE STATE-SPACE REGION OF STATION-KEEPING

The region of station-keeping, S , was defined in Section A of Chapter III. Since it is clear that at least parts of the boundary of S must be switching surfaces for a feedback control law, the choice of the region S from possible station-keeping regions should be a best choice. The criteria used for a best choice are small error, a minimum fuel expenditure and simplicity.

If the angle, φ , between the local vertical and the satellite-fixed line L_1 [see Figure (2.1)] and its rate, $\dot{\varphi}$, are required to be small, say $|\varphi| \leq s$, $|\dot{\varphi}| \leq r$, then the requirements on θ_1 , $1 = 2, 3$, and their rates are

$$|\varphi| \approx \sqrt{\theta_2^2 + \theta_3^2} = \sqrt{x_3^2 + x_5^2} \leq s$$

$$|\dot{\varphi}| \approx \frac{|\theta_2 \dot{\theta}_2 + \theta_3 \dot{\theta}_3|}{\sqrt{\theta_2^2 + \theta_3^2}} = \frac{|x_3 x_4 + x_5 x_6|}{\sqrt{x_3^2 + x_5^2}} \leq r$$

For near earth-pointing, the yaw angle and its rate must also be restricted to small values so that the requirements on θ_1 and $\dot{\theta}_1$ are $|\theta_1| \leq s_1$, $|\dot{\theta}_1| \leq s_2$. This region of station-keeping is not sufficient to avoid exceedingly large values in either $\dot{\theta}_2$ or $\dot{\theta}_3$. Also, the switching logic for a controller based on such a region is not simple.

Generally, the station-keeping region should be closed region of the state-space which encloses the origin. Thus, in any phase-plane projection of the region, the projection of its boundary should be a closed curve which encircles the origin. Circles, ellipses, parts of parabolas, parts of straight lines, etc. can be used for constructing the closed curves. However, if parts of curves such as circles, parabolas, etc., which are analytically described with squares of the state variables, are used, the error in the state variable signal from the sensors is compounded. Thus, the region which encloses the origin should be constructed with linear functions unless such a region results

in a significant fuel cost increase. The region S , as given, is one such region. The dependence of the size of the region on fuel cost is discussed in Section B, Chapter VI.

APPENDIX E. AN APPROXIMATE SOLUTION OF THE ADJOINT EQUATIONS

For satellites which are "stable" in roll-yaw, the approximate solution of the adjoint equations for

$$J = \int_{\tau_0}^{\tau_f} [f_1(\underline{x}) + \sum_{i=1}^3 |v_i|] d\tau$$

which is derived below is in excellent agreement with the digital computer solutions.

Let τ_e , $\tau_0^* \leq \tau_e \leq \tau_f^*$, denote the time at which the roll-yaw (pitch) trajectory re-enters the roll-yaw (pitch) projection of S if the trajectory has departed the projection of S . Otherwise, let $\tau_e = \tau_0^*$. With this fixed (after each encounter with the boundary of S) time, the piecewise linear equations, (4.4) and (4.6) with (4.7), can be approximated by piecewise constant equations by replacing τ^* with τ_e in A_1 , A_2 and A_3 .

Let τ_1 , $\tau_0^* \leq \tau_1 \leq \tau_f^*$, $i = 1, \dots, 6$, Denote the time at which the projected trajectory, $x_1(\tau^*)$, exits the x_1 -projection of S . Then, since $F(x_1)$ is 10^{n_1} , -10^{n_1} or zero and since A_1 , A_2 and A_3 are now constants, equations (4.4) and (4.6) can be laplace transformed as follows

yaw-roll

$$\begin{aligned} sP_1 - p_{1e} &= \frac{-F(x_1)}{s} \exp(-\tau_1 s) - k_1 A_1^2 P_2 + A_2 P_4 \\ sP_2 - p_{2e} &= \frac{F(x_2)}{s} \exp(-\tau_2 s) + P_1 - K_2 A_1 P_4 \\ sP_3 - p_{3e} &= \frac{-F(x_3)}{s} \exp(-\tau_3 s) - A_2 P_2 + k_2 (3A_3 + A_1^2) P_4 \\ sP_4 - p_{4e} &= \frac{F(x_4)}{s} \exp(-\tau_4 s) + K_1 A_1 P_2 + P_3 \end{aligned} \quad (E.1)$$

Pitch

$$\begin{aligned} sP_5 - p_{5e} &= \frac{-F(x_5)}{s} \exp(-\tau_5 s) - 3k_3 A_3 P_6 \\ sP_6 - p_{6e} &= \frac{F(x_6)}{s} \exp(-\tau_6 s) + P_5 \end{aligned} \quad (E.2)$$

where $p_{1e} = p_1(\tau_e)$, $1 = 1, \dots, 6$, and $P_1 = P_1(s)$ is the Laplace transform of the variable $p_1(\tau^*)$, $1 = 1, \dots, 6$.

If equations (E.1) are solved for P_1 , $1 = 1, \dots, 4$, and equations (E.2) are solved for P_1 , $1 = 5, 6$, the results are

$$\begin{aligned} P_1 &= \{p_{1e}s^3 - (T_1 + p_{2e}B_1 + p_{4e}B_5)s^2 + [p_{1e}(B_4 - B_3) - p_{2e}B_4B_5 \\ &\quad - p_{3e}B_5 + p_{4e}B_1B_2 - B_1T_2 - B_5T_4]s + p_{1e}B_2B_5 + p_{2e}(B_1B_3 - B_5^2) \\ &\quad + p_{3e}B_1B_2 + (B_3 - B_2B_4)T_1 - B_4B_5T_2 + B_5T_3 + B_2T_4 \\ &\quad - [B_5B_2T_1 + (B_1B_3 - B_5^2)T_2 - B_1B_2T_3]s^{-1}\}/\Delta \\ P_2 &= \{p_{2e}s^3 + (p_{1e} - B_2p_{4e} + T_2)s^2 - (p_{2e}B_3 + p_{3e}B_2 + p_{4e}B_5 \\ &\quad + T_1 + B_2T_4)s - (p_{1e}B_3 + p_{3e}B_5 + B_3T_2 - B_2T_3 + B_5T_4) \\ &\quad + (B_3T_1 + B_5T_3)s^{-1}\}/\Delta \\ P_3 &= \{p_{3e}s^3 + (B_5p_{2e} - B_3p_{4e} - T_3)s^2 + [p_{1e}B_5 + p_{2e}B_3B_4 \\ &\quad + p_{3e}(B_1 + B_2) + p_{4e}B_5B_2 + B_5T_2 - B_3T_4]s + p_{1e}B_3B_4 \\ &\quad + p_{3e}B_4B_5 + p_{4e}(B_1B_3 + B_5^2) - B_5T_1 + B_3B_4T_2 - (B_1 + B_2B_4)T_3 \\ &\quad - B_2B_5T_4] - [B_3B_4T_1 - B_4B_5T_3 + (B_5^2 - B_1B_3)T_4]s^{-1}\}/\Delta \\ P_4 &= \{p_{4e}s^3 + (p_{2e}B_4 + p_{3e} + T_4)s^2 + (p_{1e}B_4 + p_{2e}B_5 + p_{4e}B_1 \\ &\quad + B_4T_2 - T_3)s + p_{1e}B_5 + p_{3e}B_1 - B_4T_1 + B_5T_2 + B_1T_4 \\ &\quad - (B_5T_1 + B_1T_3)s^{-1}\}/\Delta \end{aligned} \quad (E.3)$$

$$P_5 = (p_{5e}s - p_{6e}B_6 - T_5 - B_6T_6s^{-1})/(s^2 + B_6)$$

$$P_6 = (p_{6e}s + p_{5e} + T_6 - T_5s^{-1})/(s^2 + B_6) \quad (E.4)$$

where $T_1 = F(x_1)\exp(-\tau_1 s)$, $1 = 1, \dots, 6$, $\Delta = s^4 + (B_1 - B_3 + B_2B_4)s^2 + B_5(B_2 - B_4)s + B_5^2 - B_1B_3$ and $B_1 = k_1A_1^2$, $B_2 = K_2A_1$, $B_3 = k_2(A_1^2 + 3A_5)$, $B_4 = K_1A_1$, $B_5 = -A_2$ and $B_6 = 3k_3A_3$ with A_1 , $1 = 1, 2, 3$, evaluated at $\tau^* = \tau_e$.

Let $B_1 - B_3 + B_2B_4 = 2a$, $B_2 - B_4 = b$ and $B_5^2 - B_1B_3 = c$. Then Δ can be written as

$$\Delta = s^4 + 2as^2 + B_5bs + c \quad (E.5)$$

If the characteristic equation, (E.5), has roots which do not change type, e.g., from type imaginary to type complex, with time, then equations (E.3) and (E.4) can be inverted once-and-for-all to give the approximate solution of (4.4) and (4.6) for the entire time of one orbit. This is the case if B_5b is zero or very small.

For satellites (1) and (2) B_5b varies periodically from about 10^{-4} to -10^{-4} and the roots of (E.5) have real parts less than 0.1 in magnitude. Thus, the exponential factors in the solution due to these real parts are nearly unity for solution times i.e., the time intervals between two successive encounters with the boundary of S, less than unity (In Chapter IV it is seen that dozens of encounters occur in the time of one orbit, which takes about six time units to complete.)

If the term in (E.5) with B_5b as a factor is omitted, then (E.5) can be written as $\Delta = (s^2 + \omega_1^2)(s^2 + \omega_2^2)$ where $\omega_1^2 = a + \sqrt{a^2 - c}$ and $\omega_2^2 = a - \sqrt{a^2 - c}$. If this expression of Δ is substituted into equations (E.3) and if, on inverting (E.3) and (E.4) for positive and real values of ω_1, ω_2 and B_6 , the functions $\sin y$ and $\cos y$ are replaced by y and $1 - y^2$, respectively, then the approximate solution of equations (4.4) and (4.6) is

$$\begin{aligned}
p_1 &= p_{1e} \{1 - [(B_3 - B_4) + (\omega_1^2 + \omega_2^2)](\Delta\tau^*)^2\} - p_{2e} [B_1 \Delta\tau^* \\
&\quad + B_4 B_5 (\Delta\tau^*)^2] - p_{3e} B_5 (\Delta\tau^*)^2 - p_{4e} [B_5 \Delta\tau^* - B_1 B_2 (\Delta\tau^*)^2] \\
&\quad - F(x_4) B_5 (\Delta\tau_4^*)^2 - F(x_1) \Delta\tau_1^* - F(x_2) B_1 \Delta\tau_2^{*2} \\
p_2 &= p_{1e} \Delta\tau^* + p_{2e} \{1 - [(\omega_1^2 + \omega_2^2) + B_3](\Delta\tau^*)^2\} - p_{3e} B_2 (\Delta\tau^*)^2 \\
&\quad - p_{4e} (B_2 \Delta\tau^* + B_5 \Delta\tau^{*2}) + F(x_2) \Delta\tau_2^* - F(x_1) (\Delta\tau_1^*)^2 - F(x_4) B_2 (\Delta\tau_4^*)^2 \\
p_3 &= p_{1e} B_5 (\Delta\tau^*)^2 + p_{2e} [B_5 \Delta\tau^* + B_3 B_4 (\Delta\tau^*)^2] + p_{3e} \{1 - [(\omega_1^2 - \omega_2^2) \\
&\quad + (B_1 + B_2)](\Delta\tau^*)^2\} - p_{4e} (B_3 \Delta\tau^* + B_2 B_5 (\Delta\tau^*)^2 + F(x_2) B_5 (\Delta\tau_2^*)^2 \\
&\quad - F(x_3) \Delta\tau_3^* - F(x_4) B_3 (\Delta\tau_4^*)^2 \\
p_4 &= p_{1e} B_4 (\Delta\tau^*)^2 + p_{2e} [B_4 \Delta\tau^* + B_5 (\Delta\tau^*)^2] + p_{3e} \Delta\tau^* \\
&\quad + p_{4e} \{1 - [(\omega_1^2 + \omega_2^2) + B_1](\Delta\tau^*)^2\} + F(x_4) \Delta\tau_4^* - F(x_3) (\Delta\tau_3^*)^2 \\
&\quad + F(x_2) B_4 (\Delta\tau_2^*)^2
\end{aligned} \tag{E 6}$$

$$\begin{aligned}
p_5 &= p_{5e} [1 - B_6 (\Delta\tau^*)^2] - p_{6e} B_6 (\Delta\tau^*)^2 - F(x_5) \Delta\tau_5^* - F(x_6) B_6 (\Delta\tau_6^*)^2 \\
p_6 &= p_{5e} \Delta\tau^* + p_{6e} [1 - B_6 (\Delta\tau^*)^2] + F(x_6) \Delta\tau_6^* - F(x_5) (\Delta\tau_5^*)^2
\end{aligned} \tag{E 7}$$

where $\Delta\tau^* = \tau^* - \tau_e$ and $\Delta\tau_l^* = \tau^* - \tau_l$, $l = 1, \dots, 6$

An approximate solution of the adjoint equations for "unstable" satellites can be derived in a similar manner. However, instead of sine and cosine functions (which can be replaced by simpler functions) appearing in the equations, the equations contain the exponential function and are much more complicated in yaw-roll. In Section A, Part 3 of Chapter IV an approximate solution is presented for "unstable" pitch motion

APPENDIX F. DIGITAL AND ANALOG COMPUTER PROGRAMS

In Figures F 1, F 2, F 5 and F 6 are given listings of the digital computer programs. These are given in the order in which they are used in the text. The word "clock" which appears in the digital computer program is an ALGOL procedure. This procedure was used to determine the elapsed time required for the execution of certain parts of the programs so that measures could be taken to reduce excessive computation times. The symbols used in the differential equations (DE) procedures are not the same as in the differential equations in the text since these symbols were reserved for the plot routine. However, the equivalences are given in the comments.

In Figures F 3 and F 4 are given simplified analog computer programs which were used to simulate the acquisition motions from S^+ to S and the steady-state motion for the suboptimal steady-state control. The time delays required in these simulations were obtained from the time delays in the comparators by time scaling.


```

PROCEDURE KUTTAMERSON(N, X, HH, Y, F, EPS, AB, ERROR, STEPSIZE);
  VALUE N, HH, EPS, AB, STEPSIZE; INTEGER N; REAL X, HH, EPS, AB;
  REAL ARRAY Y[0]; PROCEDURE F; BOOLEAN ERROR, STEPSIZE;
COMMENT: VERSION OF 660518 660722
  EPS AND AB ARE THE RELATIVE AND ABSOLUTE ERROR BOUNDS RESP.
  STEPSIZE TRUE TO WRITE STEPSIZE WHEN CHANGED
  STEPSIZE FALSE FOR NO OUTPUT
  ERROR IS SET TRUE IF STEPSIZE BECOMES TOO SMALL ELSE FALSE;
BEGIN COMMENT KUTTA MERSON INTEGRATES A SYSTEM OF N FIRST ORDER
  ORDINARY DIFFERENTIAL EQUATIONS. SEE L. FOX, "NUMERICAL
  SOLUTION OF ORDINARY AND PARTIAL DIFFERENTIAL
  EQUATIONS", P. 24, PERMAGON PRESS, 1962;
  OWN REAL HC, FINAL, H2, H3, H6, H8, ERR, TEST, T, H;
  OWN INTEGER I, CU, CUT; OWN BOOLEAN DBL; LABEL L, KM, RETURN;
  OWN REAL ARRAY Y1, Y2, F0, F1, F2[0:30];
COMMENT EXCEPT FOR HC, THE OWN VARIABLES ARE FOR SPEED ONLY;
  FORMAT MSSG("THE STEP SIZE IS NOW", R12.5, " AT T=", R12.5);
  DEFINE FORI = FOR I+1 STEP 1 UNTIL N DO #,
    CONSTANTS = H2+H/2.0; H3+H/3.0; H6+H/6.0; H8+H/8.0 #;
COMMENT CHECK FOR INITIAL ENTRY AND ADJUST H IF NECESSARY;
  ERROR ← FALSE;
  H ← HH;
  IF N=0 THEN BEGIN HC ← H; GO TO RETURN END;
  IF H=0 THEN GO TO RETURN; FINAL ← X+H;
  IF HC=0 THEN HC ← H;
  IF EPS≠0 AND ABS(H) > ABS(HC) THEN
    IF SIGN(H) ≠ SIGN(HC) THEN H ← HC ← -HC ELSE H ← HC;
COMMENT: CUT IS THE NUMBER OF TIMES THAT THE STEP SIZE IS ALLOWED TO
  HALVE ITSELF IN SUCCESSION;
  CUT ← 4;
  CU ← CUT;
  T ← X+H; X ← FINAL; CONSTANTS;
COMMENT MAIN KUTTA-MERSON STEP LOOP;
  L:FOR T+1 STEP H UNTIL FINAL DO
    BEGIN KM: F(T=H, Y, F0);
      FORI Y1[I] ← F0[I]×H3+Y[I]; F(T=2×H3, Y1, F1);
      FORI Y1[I] ← (F0[I]+F1[I])×H6+Y[I]; F(T=2×H3, Y1, F1);
      FORI Y1[I] ← (F1[I]×3.0+F0[I])×H8+Y[I]; F(T=H2, Y1, F2);
      FORI Y1[I] ← (F2[I]×4.0-F1[I]×3.0+F0[I])×H2+Y[I]; F(T, Y1, F1);
      FORI Y2[I] ← (F2[I]×4.0+F1[I]+F0[I])×H6+Y[I];
COMMENT DOES THE STEP SIZE H NEED TO BE CHANGED;
      IF EPS≠0 THEN
        BEGIN DBL ← TRUE;
          FORI BEGIN ERR←ABS(Y1[I]-Y2[I])×0.2; TEST←ABS(Y1[I])×EPS;
            IF ERR>TEST AND ERR>AB THEN COMMENT HALF H;
              BEGIN H ← H2; T+T=H2;
                IF (CU+CU=1) < 0 THEN BEGIN ERROR ← TRUE; EPS←0;
                  GO TO KM; END;
                IF STEPSIZE THEN WRITE(MSSG, H, T);
                IF T+H=T THEN BEGIN X←T; ERROR ← TRUE; GO TO RETURN;
                  END;
                CONSTANTS; GO TO KM;
              END,
            IF 64.0×ERR>TEST THEN DBL ← FALSE;
          END;
        END;

```

Figure F 1. Solution of Approximate, Minimum-Fuel Optimal, Station-Keeping Equations [(4 3) and (4 4)] for Roll-Yaw.

```

PROCEDURE DE(TAU,Y,DY);
  VALUE TAU;
  REAL TAU;
  ARRAY Y,DY[0];
BEGIN
  REAL A1,A2,A3,A4;
  COMMENT Y[1]=1000×X1, Y[2]=1000×X2, Y[3]=1000×X3, Y[4]=1000×X4,
    Y[5]=0.01×P1, Y[6]=0.01×P2, Y[7]=0.01×P3, Y[8]=0.01×P4,
    Y[9]=J,ROLL=YAW=JRY;
  Y1← Y[1]; Y2← Y[2]; Y3← Y[3]; Y4← Y[4];
  Y5← Y[5]; Y6← Y[6]; Y7← Y[7]; Y8← Y[8];
  RG←0.1;
  FX1← IF ABS(Y1)≤RG      THEN 0.0 ELSE IF Y1>RG      THEN PR1
    ELSE -PR1;
  FX2← IF ABS(Y2)≤RG      THEN 0.0 ELSE IF Y2>RG      THEN PR2
    ELSE -PR2;
  FX3← IF ABS(Y3)≤RG      THEN 0.0 ELSE IF Y3>RG      THEN PR3
    ELSE -PR3;
  FX4← IF ABS(Y4)≤RG      THEN 0.0 ELSE IF Y4>RG      THEN PR4
    ELSE -PR4;
  COMMENT W1=V1, W2=V2;
  W1← IF ABS(Y6)>0.01 THEN N1×SIGN(Y6) ELSE 0.0;
  W2← IF ABS(Y8)>0.01 THEN N2×SIGN(Y8) ELSE 0.0;
  CT←COS(TAU); ST←SIN(TAU);
  A1←1+4×E×CT, A2←2×E×(ST+5×E×ST×CT);
  A3←1+2×E×CT; A4←4+13×E×CT;
  DY[1]← -Y2;
  DY[2]← K1×A1×Y1-A2×Y3-K3×A3×Y4-1000×W1;
  DY[3]← -Y4;
  DY[4]← A2×Y1+K4×A3×Y2-K2×A4×Y3-1000×W2;
  DY[5]← -0.01×FX1-K1×A1×Y6-A2×Y8;
  DY[6]← 0.01×FX2+Y5-K4×A3×Y8;
  DY[7]← -0.01×FX3+A2×Y6+K2×A4×Y8;
  DY[8]← 0.01×FX4+K3×A3×Y6+Y7;
  DY[9]← ABS(W1)+ABS(W2);
  END DE;
COMMENT INITIAL(FINAL) CONDITIONS;
  START: READ(E,N1,N2,K1,K2,K3,K4,PR1,PR2,PR3,PR4,X10,X20,X30,X40,
    MU){FINISH};
  TAU←T[0]←0;
  Y[1]←1000×X10; X1[0]←X10;
  Y[2]←1000×X20; X2[0]←X20;
  Y[3]←1000×X30; X3[0]←X30;
  Y[4]←1000×X40; X4[0]←X40;
  Y[5]← IF ABS(X10)=RG      THEN -MU×SIGN(X10) ELSE 0.0;
  Y[6]← IF ABS(X20)=RG      THEN -MU×SIGN(X20) ELSE 0.0;
  P2[0]←Y[6]; P1[0]←Y[5];
  Y[7]← IF ABS(X30)=RG      THEN -MU×SIGN(X30) ELSE 0.0;
  Y[8]← IF ABS(X40)=RG      THEN -MU×SIGN(X40) ELSE 0.0;
  P4[0]←Y[8]; P3[0]←Y[7];
  Y[9]←0;
  WRITE(LABL),
  WRITE(RESL,TAU,X10,X20,X30,X40,Y[6],Y[8],W1,W2);
COMMENT CALCULATING USING KUTTAMERSON AND LOADING ARRAYS;
  FOR L← 1 STEP 1 UNTIL 628 DO BEGIN

```

Figure F.1 Continued.

```

KUTTAMERSON(9,TAU,0.01,Y,DE,@=4,@=5,FINISH,FALSE);
T[L]←L;
X1[L]←0.001×Y[1]; X2[L]←0.001×Y[2]; X3[L]←0.001×Y[3];
X4[L]←0.001×Y[4];
P2[L]←100×Y[6]; P4[L]←100×Y[8]; P1[L]←100×Y[5]; P3[L]←100×Y[7];
PRINT←1;
IF L MOD PRINT = 0 THEN
WRITE(RESL,T[L],Y[1],Y[2],Y[3],Y[4],Y[6],Y[8],W1,W2);
END KUTTAMERSON LOOP;
JRY←Y[9];
WRITE(PARM,E,K1,K2,K3,K4,JRY);
WRITE([PAGE],PARMT,PR1,PR2,PR3,PR4,N1,N2,MU);

```

Figure F 1 Continued.

```

PROCEDURE KUTTAMERSONCN, X, HH, Y, F, EPS, AB, ERROR, STEPSIZE);
  VALUE N, HH, EPS, AB, STEPSIZE; INTEGER N; REAL X, HH, EPS, AB;
  REAL ARRAY Y(0); PROCEDURE F; BOOLEAN ERROR, STEPSIZE;
COMMENT: VERSION OF 660518 660722
  EPS AND AB ARE THE RELATIVE AND ABSOLUTE ERROR BOUNDS RESP.
  STEPSIZE TRUE TO WRITE STEPSIZE WHEN CHANGED
  STEPSIZE FALSE FOR NO OUTPUT
  ERROR IS SET TRUE IF STEPSIZE BECOMES TOO SMALL ELSE FALSE;
BEGIN COMMENT KUTTA MERSON INTEGRATES A SYSTEM OF N FIRST ORDER
  ORDINARY DIFFERENTIAL EQUATIONS. SEE L. FOX, "NUMERICAL
  SOLUTION OF ORDINARY AND PARTIAL DIFFERENTIAL
  EQUATIONS", P. 24, PERMAGON PRESS, 1962;
  OWN REAL HC, FINAL, H2, H3, H6, H8, ERR, TEST, T, H,
  OWN INTEGER I, CU, CUT; OWN BOOLEAN DBL; LABEL L, KM, RETURN;
  OWN REAL ARRAY Y1, Y2, F0, F1, F2(0:30);
COMMENT EXCEPT FOR HC, THE OWN VARIABLES ARE FOR SPEED ONLY;
  FORMAT MSSG("THE STEP SIZE IS NOW", R12.5, " AT T=", R12.5);
  DEFINE FORI = FOR I+1 STEP 1 UNTIL N DO #,
  CONSTANTS = H2+H/2.0; H3+H/3.0; H6+H/6.0; H8+H/8.0 #;
COMMENT CHECK FOR INITIAL ENTRY AND ADJUST H IF NECESSARY,
  ERROR + FALSE;
  H + HH,
  IF N=0 THEN BEGIN HC + H, GO TO RETURN END;
  IF H=0 THEN GO TO RETURN; FINAL + X+H;
  IF HC=0 THEN HC + H;
  IF EPS#0 AND ABS(H)>ABS(HC) THEN
    IF SIGN(H)#SIGN(HC) THEN H + HC + -HC ELSE H + HC;
COMMENT: CUT IS THE NUMBER OF TIMES THAT THE STEP SIZE IS ALLOWED TO
  HALVE ITSELF IN SUCCESSION;
  CUT + 10;
  CU + CUT;
  T + X+H; X + FINAL; CONSTANTS;
COMMENT MAIN KUTTA-MERSON STEP LOOP;
  L:FOR T+T STEP H UNTIL FINAL DO
    BEGIN KM; F(T=H, Y, F0);
      FORI Y1(I) + F0(I)*H3+Y(I); F(T=2*H3, Y1, F1);
      FORI Y1(I) + (F0(I)+F1(I))*H6+Y(I); F(T=2*H3, Y1, F1);
      FORI Y1(I) + (F1(I)*3.0+F0(I))*H8+Y(I); F(T=H2, Y1, F2);
      FORI Y1(I) + (F2(I)*4.0-F1(I)*3.0+F0(I))*H2+Y(I); F(T, Y1, F1);
      FORI Y2(I) + (F2(I)*4.0+F1(I)+F0(I))*H6+Y(I);
COMMENT DOES THE STEP SIZE H NEED TO BE CHANGED;
      IF EPS#0 THEN
        BEGIN DBL + TRUE;
          FORI BEGIN ERR+ABS(Y1(I)-Y2(I))*0.2; TEST+ABS(Y1(I))*EPS;
            IF ERR>TEST AND ERR>AB THEN COMMENT HALF H;
              BEGIN H + H2; T+T=H2;
                IF (CU+CU=1)<0 THEN ERROR + TRUE;
                IF STEPSIZE THEN WRITE(MSSG, H, T);
                IF T+H=T THEN BEGIN X+T; ERROR + TRUE; GO TO RETURN;
                END;
                CONSTANTS; GO TO KM;
              END;
            IF 64.0*ERR>TEST THEN DBL + FALSE;
          END;
          IF DBL AND H < HH THEN BEGIN H + 2.0*H;

```

Figure F 2 Solution of Approximate, Minimum-Fuel Optimal, Station-Keeping Equations [(4.5) and (4.6)] for Pitch

```

        IF STEPSIZE THEN WRITE(MSSG,H,T);
        CU ← CUT;
        CONSTANTS END DOUBLE H;
    END;
    FORI Y[I] ← Y2[I];
END KUTTA MERSON LOOP;
IF EPS=0 THEN GO TO RETURN;
COMMENT NOW BE SURE TO HAVE T = FINAL ;
HC ← H; H ← FINAL-(T-H);
IF ABS(H)>ABS(FINAL)*1.4551915228@-11 THEN
    BEGIN T ← FINAL; EPS ← 0; CONSTANTS; GO TO L END;
RETURN; END KUTTA MERSON;
PROCEDURE DE(TAU,Y,DY);
    VALUE TAU; REAL TAU;
    ARRAY Y,DY[0];
BEGIN
    REAL A,B;
    CT←COS(TAU); ST←SIN(TAU);
    A←2×E×(ST+5×E×ST×CT);
    B←1+3×E×CT;
COMMENT Y[1]=1000×X5, Y[2]=1000×X6, Y[3]=0.01×P5, Y[4]=0.01×P6, Y[5]=
    J,PITCH=JP;
    Y1← Y[1], Y2← Y[2], Y3← Y[3], Y4← Y[4];
    RG5←0.1, RG6←0.1;
    FX5← IF ABS(Y1)≤RG5 THEN 0 ELSE
        IF Y1>RG5 THEN PR5 ELSE -PR5;
    FX6← IF ABS(Y2)≤RG6 THEN 0 ELSE
        IF Y2>RG6 THEN PR6 ELSE -PR6;
COMMENT W3=W3;
    W3← IF ABS(Y4)>0.01 THEN N3×SIGN(Y4) ELSE 0;
    DY[1]← -Y2;
    DY[2]← 3×K3×B×Y1+1000×(A-W3);
    DY[3]← -0.01×FX5-3×K3×B×Y4;
    DY[4]←0.01×FX6+Y3;
    DY[5]← ABS(W3);
END DE ;
COMMENT INITIAL(FINAL) CONDITIONS;
START: READ(E,K3,N3,PR5,PR6,X50,X60,Y[3],Y[4],Y[5])[FINISH];
TAU←0.0; I[0]←0.0;
    Y[1]←1000×X50;
    X5[0]←X50;
    Y[2]←1000×X60;
    X6[0]←X60;
    Y[3]← IF ABS(X50)=RG5 THEN -MU×SIGN(X50) ELSE 0.0;
    Y[4]← IF ABS(X60)=RG6 THEN -MU×SIGN(X60) ELSE 0.0;
    P5[0]←Y[3];
    P6[0]←Y[4];
WRITE(LABL);
WRITE(RESL,TAU,X50,X60,Y[3],Y[4],W3);
COMMENT CALCULATING WITH KUTTAMERSON AND LOADING ARRAYS;
FOR L ← 1 STEP 1 UNTIL 628 DO BEGIN
    KUTTAMERSON(5,TAU,0.01,Y,DE,@=4,@=5,NUTS,FALSE);
    IF NUTS THEN
        WRITE(<"STEPSIZE WAS CUT FOUR TIMES AND KMC CONTINUED,T=",
        F6.3,>>,TAU);

```

Figure F.2. Continued.

```

X5[L]*0.001*Y[1]; X6[L]*0.001*Y[2];
P5[L]*100*Y[3]; P6[L]*100*Y[4];
T[L]*L;
PRINT*1;
IF L MOD PRINT = 0 THEN
WRITE(RESL,T[L],Y[1],Y[2],Y[3],Y[4],W3);
                                END CALCULATING AND LOADING LOOP;
JP*Y[5];
WRITE([PAGE],PARM,E,K3,N3,PR5,PR6,MU,JP);

```

Figure F 2 Continued.

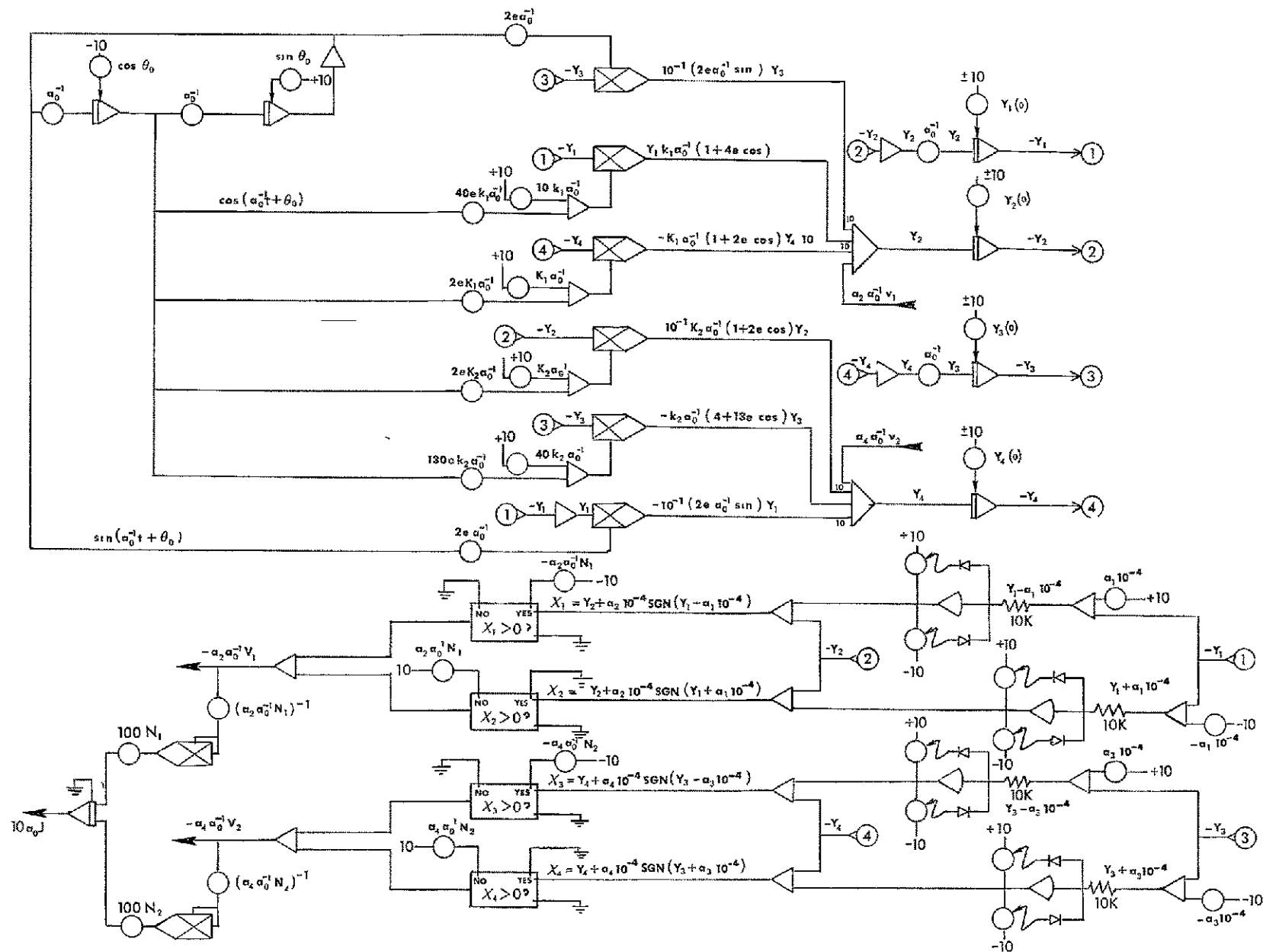


Figure P 3 Analog Computer Program for Roll-Yaw (Generator of Aero-dynamic Torque Terms Not Shown)

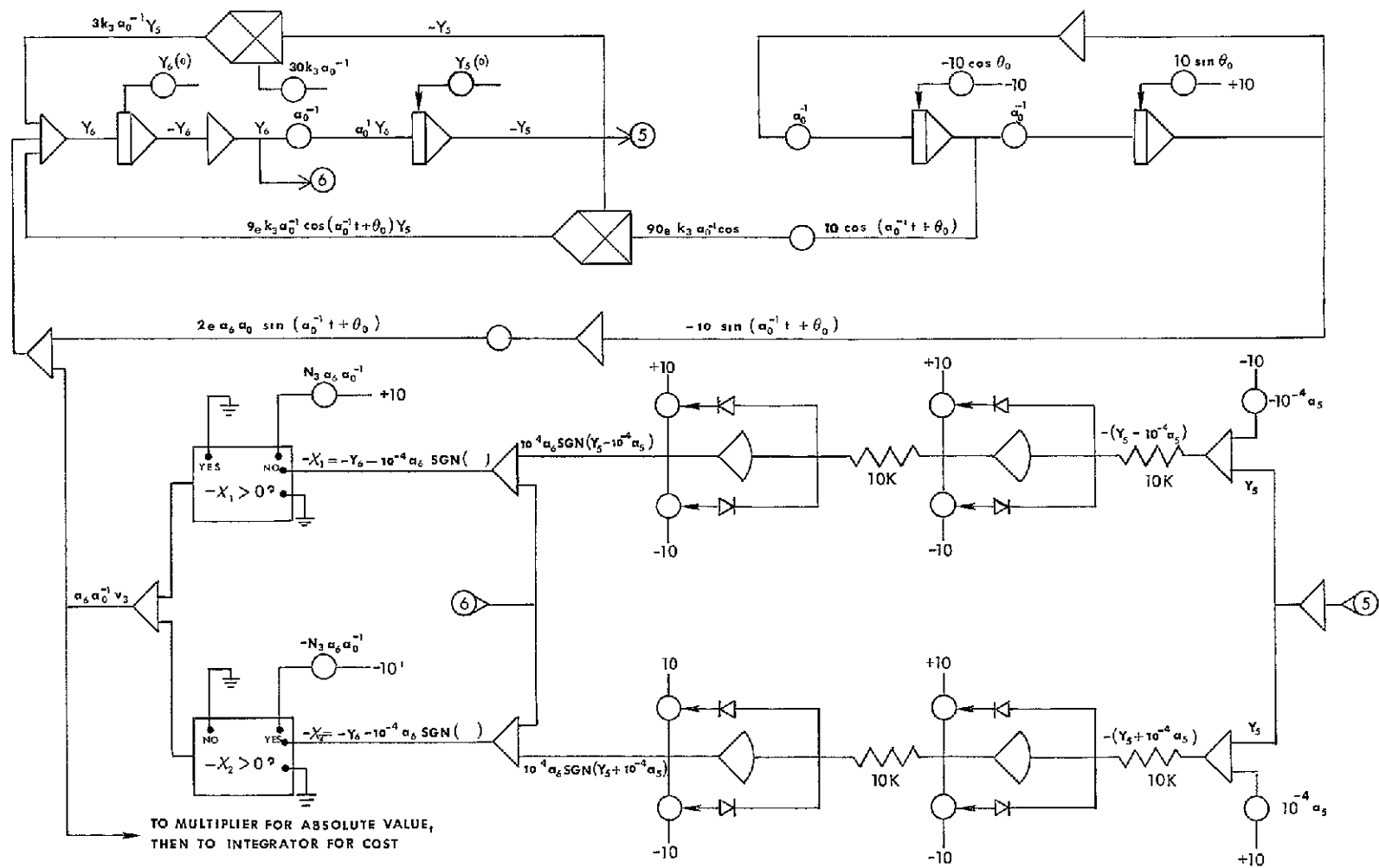


Figure F 4 Analog Computer Program for Pitch (Generator of Aerodynamic Torque Term Not Shown)


```

PROCEDURE KUTTAMERSON(N, X, H, Y, F, EPS, AB, ERROR, STEPSIZE);
  VALUE N, H, EPS, AB, STEPSIZE; INTEGER N; REAL X, H, EPS, AB;
  REAL ARRAY Y[0]; PROCEDURE F; LABEL ERROR; BOOLEAN STEPSIZE;
  COMMENT EPS AND AB ARE THE RELATIVE AND ABSOLUTE ERROR BOUNDS RESP.
  STEPSIZE TRUE TO WRITE STEPSIZE WHEN CHANGED, FALSE FOR NO OUTPUT;
  BEGIN COMMENT KUTTA MERSON INTEGRATES A SYSTEM OF N FIRST ORDER
    ORDINARY DIFFERENTIAL EQUATIONS. SEE L. FOX, "NUMERICAL
    SOLUTION OF ORDINARY AND PARTIAL DIFFERENTIAL
    EQUATIONS", P. 24, PERMAGON PRESS, 1962;
    OWN REAL HC, FINAL, H2, H3, H6, H8, ERR, TEST, T;
    OWN INTEGER I; OWN BOOLEAN DBL, LABEL L, KM, RETURN;
    OWN REAL ARRAY Y1, Y2, F0, F1, F2[0:30];
  COMMENT EXCEPT FOR HC, THE OWN VARIABLES ARE FOR SPEED ONLY;
  FORMAT MSSG("THE STEP SIZE IS NOW", E18.11);
  DEFINE FORI = FOR I+1 STEP 1 UNTIL N DO #,
    CONSTANTS = H2+H/2.0; H3+H/3.0; H6+H/6.0; H8+H/8.0 #;
  COMMENT CHECK FOR INITIAL ENTRY AND ADJUST H IF NECESSARY;
  IF N=0 THEN BEGIN HC ← H; GO TO RETURN END;
  IF H=0 THEN GO TO RETURN; FINAL ← X+H;
  IF HC=0 THEN HC ← H;
  IF EPS≠0 AND ABS(H)>ABS(HC) THEN
    IF SIGN(H)≠SIGN(HC) THEN H ← HC ← -HC ELSE H ← HC;
  T ← X+H; X ← FINAL; CONSTANTS;
  COMMENT MAIN KUTTA-MERSON STEP LOOP;
  L:FOR T←T STEP H UNTIL FINAL DO
    BEGIN KM: F(T-H, Y, F0);
      FORI Y1[I] ← F0[I]×H3+Y[I]; F(T-2×H3, Y1, F1);
      FORI Y1[I] ← (F0[I]+F1[I])×H6+Y[I]; F(T-2×H3, Y1, F1);
      FORI Y1[I] ← (F1[I]×3.0+F0[I])×H8+Y[I]; F(T-H2, Y1, F2);
      FORI Y1[I] ← (F2[I]×4.0-F1[I]×3.0+F0[I])×H2+Y[I]; F(T, Y1, F1);
      FORI Y2[I] ← (F2[I]×4.0+F1[I]+F0[I])×H6+Y[I];
  COMMENT DOES THE STEP SIZE H NEED TO BE CHANGED;
  IF EPS≠0 THEN
    BEGIN DBL ← TRUE;
      FORI BEGIN ERR←ABS(Y1[I]-Y2[I])×0.2; TEST←ABS(Y1[I])×EPS;
        IF ERR>TEST AND ERR>AB THEN COMMENT HALF H;
        BEGIN H ← H2; T←T-H2;
          IF STEPSIZE THEN WRITE([DBL], MSSG, H);
          IF T+H=T THEN BEGIN X←T; GO TO ERROR END;
          CONSTANTS; GO TO KM;
        END;
        IF 64.0×ERR>TEST THEN DBL ← FALSE;
      END;
      IF DBL THEN BEGIN H ← 2×H;
        IF STEPSIZE THEN WRITE([DBL], MSSG, H);
        CONSTANTS END DOUBLE H;
    END;
    FORI Y[I] ← Y2[I];
  END KUTTA MERSON LOOP;
  IF EPS=0 THEN GO TO RETURN;
  COMMENT NOW BE SURE TO HAVE T = FINAL;
  HC ← H; H ← FINAL-(T-H);
  IF ABS(H)>ABS(FINAL)×1.4551915228×10-11 THEN
    BEGIN T ← FINAL; EPS ← 0; CONSTANTS; GO TO L END;
  RETURN; END KUTTA MERSON;

```

Figure F.5 Solution of Nonlinear, Suboptimal Acquisition Equations
 $[(2\ 14)-(2\ 16)\text{ and } (5\ 2)]$

```

        IF DBL AND H < HH THEN BEGIN H ← 2.0×H;
        IF STEPSIZE THEN WRITE(MSSG,H,T);
        CU ← CUT;
        CONSTANTS END DOUBLE H;
    END;
    FOR I Y[1] ← Y2[I];
    END KUTTA MERSON LOOP;
    IF EPS=0 THEN GO TO RETURN;
    COMMENT NOW BE SURE TO HAVE T = FINAL ;
    HC ← H; H ← FINAL-(T-H);
    IF ABS(H)>ABS(FINAL)×1.45519152280-11 THEN
        BEGIN T ← FINAL; EPS ← 0; CONSTANTS; GO TO L END;
    RETURN; END KUTTA MERSON;
    PROCEDURE DE(TAU,Y,DY);
    VALUE TAU; REAL TAU;
    ARRAY Y,DY[0];
    BEGIN
    REAL A1,A2,A3,A4,TA,C1,C2,C3,S1,S2,S3,CT,ST;
    TA← TAU+THETA0; CT← COS(TA); ST← SIN(TA);
    A1← 1+2×E×CT; A2←-2×E×ST; A3←1+3×E×CT; A4← C×A1×EXP(K×E×(CT-1));
    COMMENT Y[1]=X1, Y[2]=X2, Y[3]=X3, Y[4]=X4, Y[5]=X5, Y[6]=X6, Y[7]=J;
    Y1←Y[1]; Y2←Y[2]; Y3←Y[3]; Y4←Y[4]; Y5←Y[5]; Y6←Y[6];
    C1←COS(Y1); C2←COS(Y3); C3←COS(Y5);
    S1←SIN(Y1); S2←SIN(Y3); S3←SIN(Y5);
    V1← IF ABS(Y1)<0.0002 AND ABS(Y2)<0.0002 THEN 0 ELSE
        -(N1/2)×(SIGN(Y2×ABS(Y2))+20×Y1)+SIGN(Y2+M1×Y1×SIGN(Q1=ABS(Y1))));
    V2← IF ABS(Y3)<0.0002 AND ABS(Y4)<0.0002 THEN 0 ELSE
        -(N2/2)×(SIGN(Y4×ABS(Y4))+20×Y3)+SIGN(Y4+M2×Y3×SIGN(Q2=ABS(Y3))));
    V3← IF ABS(Y5)<0.0002 AND ABS(Y6)<0.0002 THEN 0 ELSE
        -(N3/2)×(SIGN(Y6×ABS(Y6))+20×Y5)+SIGN(Y6+M3×Y5×SIGN(Q3=ABS(Y5))));
    W1← Y2×C2×C3+Y4×S3+A1×(S1×S3-C1×S2×C3);
    W2← Y4×C3-Y2×C2×S3+A1×(S1×C3+C1×S2×S3);
    W3← Y6+Y2×S2+A1×C1×C2;
    DY[1]← Y2;
    DY[2]←(Y2×Y4×S2-Y4×Y6+A1×(Y4×C1×C2-Y2×S1×S2-Y6×S1)+A2×C1×S2+K2×S3×W3×W1
        -K1×C3×W2×W3-3×A3×(K1+K2)×C2×S2×C3×S3+A4×C3×(S1×C2+C1×C3)
        +C3×V1-S3×V2)/C2;
    DY[3]← Y4;
    DY[4]← Y2×Y6×C2-A1×C1×(Y2+Y6×S2)-A2×S1-W3×(K1×W2×S3+K2×W1×C3)
        +3×A3×(K2×C3×C3-K1×S3×S3)×C2×S2+C3×V2-S3×V1;
    DY[5]← Y6;
    DY[6]←-Y2×Y4×C2-DY[2]×S2+A1×(Y2×S1×C2+Y4×C1×S2)-K3×W1×W3-3×K3×A3×C2×C2×
        C3×S3-A2×C1×C2+A4×C1×(S3-C3)+V3;
    DY[7]← ABS(V1)+ABS(V2)+ABS(V3);
    END DE;
    COMMENT INITIAL CONDITIONS;
    START: READ(E,K1,K2,K3,N1,N2,N3,X10,X20,X30,X40,X50,X60,M1,Q1,M2,Q2,
        M3,Q3,C,D,K,THETA0,X1L,X2L,X3L,X4L,X5L,X6L,X1R,X2R,X3R,X4R,X5R,X6R)
    [FINISH];
    TAU← Y[7]← T[0]← 0;
    X1[0]← Y[1]← X10;
    X2[0]← Y[2]← X20;
    X3[0]← Y[3]← X30;
    X4[0]← Y[4]← X40;
    X5[0]← Y[5]← X50;

```

Figure F 5 Continued.

```

X6[0]← Y[6]← X60;
WRITE(LABL);
WRITE(RESL,TAU,X10,X20,X30,X40,X50,X60);
COMMENT CALCULATING WITH KUTTAMERSON AND LOADING ARRAYS;
FOR L← 1 STEP 1 WHILE L≤1000 AND (ABS(Y[2])≥D OR ABS(Y[4])≥D OR
                                ABS(Y[6])≥D) DO
    BEGIN
    KUTTAMERSON(7,TAU,0.002,Y,DE,θ=4,θ=5,NUTS,FALSE);
    IF NUTS THEN WRITE(<"STEP SIZE WAS CUT FOUR TIMES BUT KMC CONTINUED,
    T=",F6.3,>,TAU);
    X1[L]← Y[1];
    X2[L]← Y[2];
    X3[L]← Y[3];
    X4[L]← Y[4];
    X5[L]← Y[5];
    X6[L]← Y[6];
    T[L]←0.002×L;
    PRINT +1;
    IF L MOD PRINT=0 THEN WRITE(RESL,T[L],Y[1],Y[2],Y[3],Y[4],Y[5],Y[6]);
    END CALCULATING AND LOADING LOOP;
    J← Y[7];
    WRITE([PAGE],PARM,E,K1,K2,K3,C,D,J);
                                CLOCK;

```

Figure F.5. Continued

```

PROCEDURE KUTTAMERSON(N, X, HH, Y, F, EPS, AB, ERROR, STEPSIZE),
  VALUE N, HH, EPS, AB, STEPSIZE, INTEGER N; REAL X, HH, EPS, AB,
  REAL ARRAY Y(0), PROCEDURE F, BOOLEAN ERROR, STEPSIZE,
COMMENT. VERSION OF 660518 660722
  EPS AND AB ARE THE RELATIVE AND ABSOLUTE ERROR BOUNDS RESP.
  STEPSIZE TRUE TO WRITE STEPSIZE WHEN CHANGED
  STEPSIZE FALSE FOR NO OUTPUT
  ERROR IS SET TRUE IF STEPSIZE BECOMES TOO SMALL ELSE FALSE;
BEGIN COMMENT KUTTA MERSON INTEGRATES A SYSTEM OF N FIRST ORDER
  ORDINARY DIFFERENTIAL EQUATIONS. SEE L. FOX, "NUMERICAL
  SOLUTION OF ORDINARY AND PARTIAL DIFFERENTIAL
  EQUATIONS", P. 24, PERMAGON PRESS, 1962,
  OWN REAL HC, FINAL, H2, H3, H6, H8, ERR, TEST, T, H,
  OWN INTEGER I, CU, CUT, OWN BOOLEAN DBL, LABEL L, KM, RETURN,
  OWN REAL ARRAY Y1, Y2, F0, F1, F2(0.30);
COMMENT EXCEPT FOR HC, THE OWN VARIABLES ARE FOR SPEED ONLY;
  FORMAT MSSG("THE STEP SIZE IS NOW", R12.5, " AT T=", R12.5);
  DEFINE F0(I) = FOR I+1 STEP 1 UNTIL N DO #,
    CONSTANTS = H2+H/2.0, H3+H/3.0, H6+H/6.0, H8+H/8.0 #,
COMMENT CHECK FOR INITIAL ENTRY AND ADJUST H IF NECESSARY ;
  ERROR ← FALSE,
  H ← HH,
  IF N=0 THEN BEGIN HC ← H, GO TO RETURN END,
  IF H=0 THEN GO TO RETURN; FINAL ← X+H,
  IF HC=0 THEN HC ← H,
  IF EPS≠0 AND ABS(H)>ABS(HC) THEN
    IF SIGN(H)≠SIGN(HC) THEN H ← HC ← -HC ELSE H ← HC;
COMMENT: CUT IS THE NUMBER OF TIMES THAT THE STEP SIZE IS ALLOWED TO
  HALVE ITSELF IN SUCCESSION;
  CUT ← 10,
  CL ← CUT,
  T ← X+H, X ← FINAL, CONSTANTS;
COMMENT MAIN KUTTA-MERSON STEP LOOP,
  L:FOR T+1 STEP H UNTIL FINAL DO
    BEGIN KM: F(T=H, Y, F0);
      FOR I Y1(I) ← F0(I)*H3+Y(I), F(T=2*H3, Y1, F1),
      FOR I Y1(I) ← (F0(I)+F1(I))*H6+Y(I), F(T=2*H3, Y1, F1);
      FOR I Y1(I) ← (F1(I)*3.0+F0(I))*H8+Y(I); F(T=H2, Y1, F2),
      FOR I Y1(I) ← (F2(I)*4.0-F1(I)*3.0+F0(I))*H2+Y(I), F(T, Y1, F1),
      FOR I Y2(I) ← (F2(I)*4.0+F1(I)+F0(I))*H6+Y(I);
COMMENT DOES THE STEP SIZE H NEED TO BE CHANGED ;
      IF EPS≠0 THEN
        BEGIN DBL ← TRUE,
          FOR I BEGIN ERR←ABS(Y1(I)-Y2(I))*0.2; TEST←ABS(Y1(I))*EPS;
            IF ERR>TEST AND ERR>AB THEN COMMENT HALF H,
              BEGIN H ← H2, T←T-H2;
                IF (CU+CU-1)<0 THEN ERROR ← TRUE,
                  IF STEPSIZE THEN WRITE(MSSG, H, T),
                  IF T+H=T THEN BEGIN X←T, ERROR ← TRUE; GO TO RETURN;
                END,
                CONSTANTS; GO TO KM;
              END,
              IF 64.0*ERR>TEST THEN DBL ← FALSE;
            END,
            IF DBL AND H < HH THEN BEGIN H ← 2.0*H;

```

a Roll-Yaw

Figure F 6. Solution of Optimal Linear Acquisition Equations in Backward Time

```

        IF STEPSIZE THEN WRITE(MSSG,H,T);
        CU ← CUT;
        CONSTANTS END DOUBLE H;
    END;
    FOR I Y[1] ← Y2[I];
    END KUTTA MERSON LOOP;
    IF EPS=0 THEN GO TO RETURN;
    COMMENT NOW BE SURE TO HAVE T = FINAL ;
    HC ← H, H ← FINAL-(T-H);
    IF ABS(H)>ABS(FINAL)*1.4551915228e-11 THEN
        BEGIN T ← FINAL; EPS ← 0; CONSTANTS; GO TO L END;
    RETURN; END KUTTA MERSON;
    PROCEDURE DE(TAU,Y,DY);
    VALUE TAU, REAL TAU;
    ARRAY Y,DY[0];
    BEGIN
    REAL A1,A2,A3,A4,TAUB;
    TAUB← TAU-IF-THETA0, CT← COS(TAUB); ST← SIN(TAUB);
    A1← 1+2*EXCT, A2← 2*EXST, A3← 4+13*EXCT; A4← 1+4*EXCT,
    COMMENT Y1=X1, Y2=X2, Y3=X3, Y4=X4, Y5=P1, Y6=P2, Y7=P3, Y8=P4,
    Y1← Y[1]; Y2← Y[2], Y3← Y[3], Y4← Y[4], Y5← Y[5], Y6← Y[6], Y7← Y[7];
    Y8← Y[8];
    V1← IF ABS(Y6)>1.0 THEN N1*SIGN(Y6) ELSE 0;
    V2← IF ABS(Y8)>1.0 THEN N2*SIGN(Y8) ELSE 0;
    DY[1]←-Y2;
    DY[2]← K1*A4*Y1-A2*Y3-K3*A1*Y4-C*A1*EXP(K*EX(CT-1))-V1;
    DY[3]←-Y4;
    DY[4]← A2*Y1+K4*A1*Y2-K2*A3*Y3-V2;
    DY[5]←-K1*A4*Y6-A2*Y8;
    DY[6]← Y5-K4*A1*Y8;
    DY[7]← A2*Y6+K2*A3*Y8;
    DY[8]← K3*A1*Y6+Y7;
    DY[9]← ABS(V1)+ABS(V2);
    END DE;
    COMMENT INITIAL (FINAL) CONDITIONS ;
    START, READ(E,K1,K2,K3,K4,N1,N2,X10,X20,X30,X40,P10,P20,P30,P40,C,K,
    TF,THETA0)[FINISH];
    TAU← T[0]← Y[9]← 0;
    Y[1]← X1[0]← X10;
    Y[2]← X2[0]← X20;
    Y[3]← X3[0]← X30;
    Y[4]← X4[0]← X40;
    Y[5]← P10;
    Y[6]← P20;
    Y[7]← P30;
    Y[8]← P40;
    WRITE (LABEL);
    WRITE(RESL,TAU,X10,X20,X30,X40,P10,P20,P30,P40);
    COMMENT CALCULATING WITH KUTTAMERSON AND LOADING ARRAYS;
    FOR L← 1 STEP 1 WHILE L≤150 AND ABS(Y[2])≤1.850 AND ABS(Y[4])≤1.850 DO
        BEGIN
        KUTTAMERSON(C,TAU,0.01,Y,DE,@=4,@=5,NUTS,FALSE);
        IF NUTS THEN WRITE(<"STEPSIZE WAS CUT AT LEAST TEN TIMES BUT KUTTAMERSON
        CONTINUED,T=",F6.3,>,TAU);
        X1[L]← Y[1];

```

Figure F 6. Continued.

```

X2[L]← Y[2];
X3[L]← Y[3];
X4[L]← Y[4];
T[L] ← L;
PRINT ← 1;
IF L MOD PRINT =0 THEN WRITE(RESL,T[L],Y[1],Y[2],Y[3],Y[4],Y[5],Y[6],
                             Y[7],Y[8]);
    END CALCULATING AND LOADING LOOP;
J← Y[9];
WRITE([PAGE],PARM,E,K1,K2,K3,K4,C,J);

```

Figure F.6 Continued.


```

PROCEDURE AXIS(X,Y,BCD,NC,SIZE,THETA,YMIN,DY),VALUE X,Y,NC,SIZE,THETA,YM
IN,DY;REAL X,Y,SIZE,THETA,YMIN,DY;INTEGER NC,ALPHA ARRAY BCD[0],BEGIN RE
AL TH,CTH,STH,I,XB,YB,XA,YA,ICTH,ISTH,YMAX,ABSV,EXPP;LABEL L50;TH+THETA*
0.017455;ICTH+CTH+COS(TH),ISTH+STH+SIN(TH),XB+X,YB+Y,IF THETA<0 THEN BEGI
N ICTH=-ICTH;ISTH=-ISTH END,PLOT(XA+X-.1*ISTH,YA+Y+.1*ICTH,3);FOR I+1STE
P 1 UNTIL SIZE DO BEGIN PLOT(XB,YB,2);PLOT(XB+XB+CTH,YB+YB+STH,2),PLOT(XA
+XA+CTH,YA+YA+STH,2),END,IF NC<0 THEN GO TO L50,YMAX+YMIN+SIZE*DY;IF ABSV
+ABS(YMIN)<ABS(YMAX) THEN ABSV+ABS(YMAX),EXPP+0;I+1;WHILE ABSV>9999.999DO
BEGIN ABSV+ABSV*.1,I+I*.1;EXPP+EXPP-1END,WHILE ABSV<0.999DO BEGIN ABSV+
ABSV*10.0,I+I*10.0;EXPP+EXPP+1END,DY+DY*I;YMAX+YMAX*I,XA+XB-.15*ISTH-.53
*CTH,YA+YB+.15*ICTH-.53*STH,FOR I+SIZE STEP-1 UNTIL 0DO BEGIN IF ABS(YMAX
)>0.001 THEN NUMBER(XA,YA,0.1,YMAX,THETA,3);YMAX+YMAX-DY;XA+XA-CTH,YA+YA-
STH END,I+1;IF EXPP=0 THEN NC ELSE NC+7;YA+((SIZE+SIZE*.5)-.06*I)*STH+.33*I
CTH+Y;XA+(SIZE-.06*I)*CTH-.33*ISTH+X;SYMBOL(XA,YA,.14,BCD,THETA,NC),IF E
XPP=0 THEN GO TO L50,I+((I-6)*.12,XA+I*CTH+XA,YA+I*STH+YA);ABCD[0]+ "x 10 "
;SYMBOL(XA,YA,.14,ABCD,THETA,6),IF EXPP=1 THEN GO TO L50;XA+XA+.25*CTH-.0
7*STH,YA+YA+.25*STH+.07*CTH;NUMBER(XA,YA,.07,EXPP,THETA,0);L50:END;

```

```

PROCEDURE LINE(X,Y,N,K),VALUE N,INTEGER N;BOOLEAN K;ARRAY X,Y[0];BEGIN I
NTEGER I,I3,A,B,C,IF K THEN BEGIN A+0,B+1,C+N-1,END ELSE BEGIN A+N-1;B+
1;C+0,END;I3+3;FOR I+A STEP B UNTIL C DO BEGIN PLOT(X[I],Y[I],I3);I3+2EN
D,K+NOT K,END;

```

```

PROCEDURE SCALE(A,N,K,L,YMIN,DY);VALUE N,L,K,INTEGER N,K,REAL L,DY,YMIN;
REAL ARRAY A[0],BEGIN REAL YMAX,INTEGER I,NMK,YMIN+YMAX+A[K-1],NMK+N-K,F
OR I+K+K-1 STEP K UNTIL NMK DO IF A[I]>YMAX THEN YMAX+A[I] ELSE IF A[I]<Y
MIN THEN YMIN+A[I],DY+(YMAX-YMIN)/L,FOR I+K-1 STEP K UNTIL NMK DO A[I]+(A[
I]-YMIN)/DY,END;

```

```

PROCEDURE SETPLOTTER,BEGIN PLOT(0.0,0.0,-1019),ABCD[0]+ "START ",ABCD[1]+
"CALIBR";ABCD[2]+ "ATION ",SYMBOL(0.0,5.0,0.28,ABCD,-90.0,18);ABCD[0]+ "Y=
0 ",SYMBOL(0.0,-0.14,0.28,ABCD,0.0,3),PLOT(0.8,0.0,3),PLOT(7.0,0.0,2),
ABCD[0]+ "SET X ",SYMBOL(6.7,0.5,0.28,ABCD,90.0,5),PLOT(7.0,0.0,3),PLOT(7
.0,28.0,2);PLOT(1.0,28.0,2),ABCD[0]+ "Y=28 ",SYMBOL(0.0,27.84,0.28,ABCD,
0.0,4),PLOT(10.0,0.0,-3),END;

```

```

FILL C[*] WITH OCT040404040404,OCT040404040405,OCT040404040406,OCT0404040
40407,OCT040404040504,OCT040404040505,OCT040404040506,OCT040404040507,OCT
040404040604,OCT040404040605,FILL A2[0,*] WITH OCT50500,OCT50600,OCT5070
0,FILL A2[1,*] WITH OCT60500,OCT60600,OCT60700,FILL A2[2,*] WITH OCT70500,
OCT70600,OCT70700,FILL SYMA[*] WITH OCT10304146371706,OCT11000000000000,OCT
110302027160000,OCT40000144463717,OCT60500000000000,OCT01103041433414,OCT
34454637170600,OCT43033730204000,OCT00000000000000,OCT01103041433404,OCT
74700000000000,OCT03143443413010,OCT1061737460000,OCT06074721200000,OCT34
434130100103,OCT14344546371706,OCT05140000000000,OCT01103041463717,OCT60
41333440000,OCT11151404141202,OCT42323135344404,OCT40100105164655,OCT514
24435251412,OCT21314200000000,OCT10112120107022,OCT23454637170600,OCT111
22221117014,OCT15252414000000,OCT02440600000000,OCT01417006440200,OCT212
52303430000,OCT00034346371706,OCT34340000000000,OCT04073746453404,OCT0304
143340000,OCT42413010010617,OCT37464500000000,OCT00073746413000,OCT47070
434040040,OCT47070434040000,OCT33434130100106,OCT17374645000000,OCT00070
444474000,OCT10302027173700,OCT00011110000000,OCT40202747000000,OCT36271
706054031,OCT42201001031400,OCT40312324364700,OCT45034100000000,OCT44041
513040000,OCT01452305410000,OCT01103041470000,OCT00070347254000,OCT07004
000000000,OCT00072347400000,OCT00074047000000,OCT10304146377036,OCT47703

```

Figure F 6. Continued


```

717060110, OCT00073746453404, OCT10010617374641, OCT30107022400000, OCT00073
746453404, OCT34434000000000, OCT02324334140516, OCT46262720000000, OCT01452
305412303, OCT43232521000000, OCT03430000000000, OCT00112324160700, OCT10212
212112170, OCT24251514240000, OCT01417042044600, OCT00000000000000, OCT00470
000000000, OCT01103041433414, OCT05061737460000, OCT20270747000000, OCT07011
030414700, OCT07204700000000, OCT07002440470000, OCT00477007400000, OCT07244
724200000, OCT07470040701434, OCT00000000000000, OCT10212313122200, OCT00477
016060717, OCT16704131304041, OCT02463545053513, OCT34300000000000, OCT024270
04440000, OCT07272000000000, OCT14167036340000, OCT00404404000424, OCT220000
00000000, OCT00442204402200, OCT00400044044422, OCT00400444002200, OCT243443
41301001, OCT3142422000000, OCT24422002242200, OCT20224422042200, OCT2224220
0000000, OCT24014124220000, OCT24024224202200, OCT44331304131100, OCT1131403
1332200, OCT10365004641070, OCT22200000000000, OCT0242220242200, OCT0044044
0220000, OCT00442224202204, OCT40220242200000, FILL SYMB[*]WITH OCT30157, OC
T12156, OCT14155, OCT22153, OCT32151, OCT14150, OCT12147, OCT06146, OCT14145, OC
T14144, OCT26142, OCT14141, OCT16140, OCT14137, OCT20135, OCT22000, OCT12002, OC
T22003, OCT32005, OCT14007, OCT22011, OCT30013, OCT12015, OCT40016, OCT30021, OC
T34023, OCT42025, OCT32030, OCT26032, OCT06034, OCT14035, OCT12036, OCT24037, OC
T30041, OCT24043, OCT16045, OCT16046, OCT14047, OCT26050, OCT14052, OCT14053, OC
T12054, OCT10055, OCT32056, OCT14060, OCT06061, OCT12062, OCT12063, OCT12064, OC
T14065, OCT06066, OCT12067, OCT10070, OCT34071, OCT16073, OCT30074, OCT24076, OC
T26100, OCT26102, OCT04104, OCT14105, OCT30106, OCT14110, OCT00111, OCT04112, OC
T30113, OCT10115, OCT14116, OCT06117, OCT12120, OCT12121, OCT12122, OCT16123, OC
T14125, OCT34126, OCT22130, OCT12132, OCT10133, OCT12134; OLTH+@10;
PLOT(0,0,1019);
BEGIN
REAL CT, ST, X, TAU, TF, THETA0, E, K3, N3, V3, X50, X60, P50, P60, J, C, K,
Y1, Y2, Y3, Y4, X5MIN, X6MIN, DX5, DX6,
INTEGER L, PRINT,
ARRAY Y[0:51], T, X5, X6[0:500],
BOOLEAN NUTS;
LABEL START, FINISH,
ALPHA ARRAY HOZ, VER[0:1];
FORMAT LABL("TAU", X3, "X5", X5, "X6", X5, "P5", X5, "P6");
FORMAT RESL(I3, 4(X2, F5.2));
FORMAT PARM("E=", F5.2, X2, "K3=", F6.3, X2, "C=", E10.2, X2, "J=", F5.2);
PROCEDURE KUTTAMERSON(N, X, HH, Y, F, EPS, AR, ERROR, STEPSIZE);
VALUE N, HH, EPS, AB, STEPSIZE; INTEGER N; REAL X, HH, EPS, AB;
REAL ARRAY Y[0]; PROCEDURE F; BOOLEAN ERROR, STEPSIZE;
COMMENT: VERSION OF 660518 660722
EPS AND AB ARE THE RELATIVE AND ABSOLUTE ERROR BOUNDS RESP.
STEPSIZE TRUE TO WRITE STEPSIZE WHEN CHANGED
STEPSIZE FALSE FOR NO OUTPUT
ERROR IS SET TRUE IF STEPSIZE BECOMES TOO SMALL ELSE FALSE;
BEGIN COMMENT KUTTA MERSON INTEGRATES A SYSTEM OF N FIRST ORDER
ORDINARY DIFFERENTIAL EQUATIONS. SEE L. FOX, "NUMERICAL
SOLUTION OF ORDINARY AND PARTIAL DIFFERENTIAL
EQUATIONS", P. 24, PERMAGON PRESS, 1962;
OWN REAL HC, FINAL, H2, H3, H6, H8, ERR, TEST, T, H;
OWN INTEGER I, CU, CUT; OWN BOOLEAN DBL; LABEL L, KM, RETURN;
OWN REAL ARRAY Y1, Y2, F0, F1, F2[0:30];
COMMENT EXCEPT FOR HC, THE OWN VARIABLES ARE FOR SPEED ONLY;
FORMAT MSSG("THE STEP SIZE IS NOW", R12.5, " AT T=", R12.5);
DEFINE FORI = FOR I=1 STEP 1 UNTIL N DO #,
CONSTANTS = H2+H/2.0, H3+H/3.0, H6+H/6.0, H8+H/8.0 #;

```

Figure F 6 (Continued)

```

COMMENT CHECK FOR INITIAL ENTRY AND ADJUST H IF NECESSARY ,
ERROR ← FALSE,
H ← HH ,
IF N=0 THEN BEGIN HC ← H, GO TO RETURN END;
IF H=0 THEN GO TO RETURN, FINAL ← X+H;
IF HC=0 THEN HC ← H,
IF EPS≠0 AND ABS(H) > ABS(HC) THEN
    IF SIGN(H)≠SIGN(HC) THEN H ← HC ← -HC ELSE H ← HC,
COMMENT: CUT IS THE NUMBER OF TIMES THAT THE STEP SIZE IS ALLOWED TO
        HALVE ITSELF IN SUCCESSION;
CUT ← 10;
CU ← CUT;
T ← X+H; X ← FINAL, CONSTANTS;
COMMENT MAIN KUTTA-MERSON STEP LOOP ;
L:FOR T←T STEP H UNTIL FINAL DO
    BEGIN KM: F(T-H,Y,F0);
        FORI Y1[I] ← F0[I]×H3+Y[I]; F(T-2×H3, Y1, F1),
        FORI Y1[I] ← (F0[I]+F1[I])×H6+Y[I], F(T-2×H3, Y1, F1);
        FORI Y1[I] ← (F1[I]×3.0+F0[I])×H8+Y[I], F(T-H2, Y1, F2);
        FORI Y1[I] ← (F2[I]×4.0-F1[I]×3.0+F0[I])×H2+Y[I], F(T, Y1, F1),
        FORI Y2[I] ← (F2[I]×4.0+F1[I]+F0[I])×H6+Y[I],
COMMENT DOES THE STEP SIZE H NEED TO BE CHANGED ;
        IF EPS≠0 THEN
            BEGIN DBL ← TRUE,
                FORI BEGIN ERR←ABS(Y1[I]-Y2[I])×0.2, TEST←ABS(Y1[I])×EPS;
                    IF ERR>TEST AND ERR>AB THEN COMMENT HALF H;
                        BEGIN H ← H2; T←T-H2,
                            IF (CU+CU-1) < 0 THEN ERROR ← TRUE;
                                IF STEPSIZE THEN WRITE(MSSG,H,T),
                                    IF T+H=T THEN BEGIN X←T, ERROR ← TRUE, GO TO RETURN,
                                        END,
                                        CONSTANTS, GO TO KM;
                                END,
                                IF 64.0×ERR>TEST THEN DBL ← FALSE,
                                END;
                                IF DBL AND H < HH THEN BEGIN H ← 2.0×H,
                                    IF STEPSIZE THEN WRITE(MSSG,H,T),
                                    CU ← CUT;
                                    CONSTANTS END DOUBLE H;
                                END;
                                FORI Y[I] ← Y2[I],
                                END KUTTA MERSON LOOP;
                                IF EPS=0 THEN GO TO RETURN,
                                COMMENT NOW BE SURE TO HAVE T = FINAL ;
                                HC ← H, H ← FINAL-(T-H),
                                IF ABS(H) > ABS(FINAL)×1.4551915228e-11 THEN
                                    BEGIN T ← FINAL; EPS ← 0, CONSTANTS; GO TO L END;
                                RETURN: END KUTTA MERSON,
                                PROCEDURE CLOCK;BEGIN OWN INTEGER TEMPUS,TEMPUS1,
                                    FORMAT FMT1(X97, "DATE: ", A2,A2,A2), FMT2(6 (
                                        "- - - - -"), "ELAPSED TIME WAS", F7.3, " SECONDS - - - "
                                        " TOTAL TIME WAS", F8.3, " SECONDS."),
                                    IF TEMPUS ≠ 0 THEN WRITE(FMT2, -(TEMPUS -(TEMPUS + TIME(2))) / 60.0
                                        ,-(TEMPUS1 - TEMPUS) / 60.0)
                                ELSE BEGIN WRITE(FMT1,(TEMPUS+TIME(5)).[36:12],TEMPUS.[24:12],

```

Figure F 6 Continued,

```

TEMPUS.(12:12)), TEMPUS+TEMPUS1+TIME(2); END;END CLOCK;
PROCEDURE DE(TAU,Y,DY);
VALUE TAU; REAL TAU;
ARRAY Y,DY[0];
BEGIN
REAL A3,TAUB;
TAUB← TAU-TF-THETA0; CT← COS(TAUB); ST← SIN(TAUB); A3←1+3×EX×CT,Y1+Y[1],
Y2+Y[2];Y3+Y[3],Y4+Y[4], V3←IF ABS(Y4)>1.0 THEN N3×SIGN(Y4) ELSE 0,
DY[1]←-Y2,
DY[2]← 3×K3×A3×Y1+2×EX×ST+C×(1+2×EX×CT)×EXP(K×EX×(CT-1))-V3;
DY[3]←-3×K3×A3×Y4;
DY[4]← Y3;
DY[5]← ABS(V3);
END DE;
COMMENT INITIAL (FINAL) CONDITIONS;                                CLOCK;
START: READ(E,K3,N3,X50,X60,P50,P60,C,K,TF,THETA0){FINISH};
TAU←T[0]←Y[5]←0,
Y[1]← X5[0]← X50;
Y[2]← X6[0]← X60;
Y[3]← P50,
Y[4]← P60;
WRITE (LABL),
WRITE (RESL,TAU,X50,X60,P50,P60),
COMMENT CALCULATING WITH KUTTAMERSON AND LOADING ARRAYS;
FOR L← 1 STEP 1 WHILE L≤150 AND ABS(Y[2])≤1.850 DO
BEGIN
KUTTAMERSON(5,TAU,0.01,Y,DE,e=4,e=5,NUTS,FALSE);
IF NUTS THEN WRITE(<"STEP SIZE WAS CUT AT LEAST TEN TIMES BUT KUTTAMERSON
CONTINUED,T=",F6.3,>,TAU);
X5[L]← Y[1];
X6[L]← Y[2];
T[L] ← L;
PRINT +1,
IF L MOD PRINT =0 THEN WRITE(RESL,T[L],Y[1],Y[2],Y[3],Y[4]);
END CALCULATING AND LOADING LOOP;
J ← Y[5];
WRITE([PAGE],PARM,E,K3,C,J);
COMMENT PLOTTING X6 VS X5 ;                                CLOCK;
X5[L]←X6[L]←-2, X5[L+1]←X6[L+1]←2;
SCALE(X5,L+2,1,4,X5MIN,DX5),
SCALE(X6,L+2,1,4,X6MIN,DX6);
H0Z[0]← " X5 ";
VER[0]← " X6 ";
PLOT(0,1,-3);
AXIS(0,0,H0Z,4,4,0,X5MIN,DX5);
AXIS(0,0,VER,4,4,90,X6MIN,DX6);
LINE(X5,X6,L,TRUE),
PLOT(10,-1,-3);                                CLOCK;
COMMENT IF MORE DATA CARDS ARE TO BE READ THEN;
GO TO START;
FINISH:
END;
PLOT(0,0,1019);
END.

```

Figure F 6 Continued